Degree Ph.D. Year 2007 Name of Author COLLINS, C.R.

Functional studies of the *Plasmodium falciparum* Apical Membrane Antigen 1

Christine Rosemary Collins

Division of Parasitology

National Institute for Medical Research

London, NW7 1AA

A Thesis submitted in part fulfilment of the requirements of University College London for the degree of Doctor of Philosophy

2005

ProQuest LLC
789 East Eisenhower Parkway
P.O. Box 1346
Ann Arbor, MI 48106-1346

Abstract

Host cell invasion by apicomplexan parasites involves multiple molecular interactions at the parasite-host cell interface, many of which provide likely targets for drug or vaccine-mediated intervention. Apical membrane antigen-1 (AMA-1) is an essential, widely conserved type I integral membrane protein which is mobilised onto the parasite surface from micronemes just prior to invasion. Antibodies to AMA-1 can prevent invasion. In the case of the malaria parasite, antibodies to AMA-1 can also protect against blood-stage infection *in vivo* and *Plasmodium falciparum* AMA-1 (PfAMA-1) is a prime candidate for inclusion in a blood-stage malaria vaccine. Rational vaccine design would benefit from a clearer understanding of PfAMA-1 function and the delineation of functionally important domains of the protein. A COS-7 cell-surface expression system, combined with a mutagenesis-based screen, was used to identify a series of residues critical for the binding of a monoclonal antibody that interferes with PfAMA-1 function. Most of these residues lie in a single disulfide-constrained domain of the molecule. Our data indicate that this domain is of particular functional and immunological significance.

In contrast to studies of AMA1 from other species of *Plasmodium*, we have been unable to identify a role for PfAMA1 in erythrocyte binding using this system. This result may be due to the absence of essential parasite factors in this heterologous system. Furthermore, it has not been possible to identify any associated parasite proteins. Thus, the role of AMA1 in invasion is still unclear.

Much of this work has relied on use of the *Pfama1* synthetic gene (*sgPfama1*). To validate the use of this gene sequence and show functionality of the gene product in the parasite, transfection studies were carried out. Attempts are underway to replace the endogenous gene sequence with a haemagglutinin (HA) tagged version of the synthetic gene. Expression of the *sgPfama1* gene product has been confirmed by immunofluorescence assay, as well as correct localisation to the apical end of the parasite. Disruption of the endogenous gene sequence remains to be confirmed.

Acknowledgements

I would like to express my gratitude to my supervisor Mike Blackman for his invaluable guidance and support throughout the whole of my project. I would particularly like to thank Fiona Hackett for her help with automated DNA sequencing (among many other things) and Chrislaine Withers-Martinez for her encouragement, ideas and advice throughout my PhD. I would like to thank Rebecca O'Donnell for help, her technical advice and for patiently reading much of my thesis! She is a great friend and will be sorely missed. I cannot ignore the rest of the Blackman lab who have been very encouraging and helpful during my time at Mill Hill. They have patiently tolerated my occasional (ice bucket lid) outbursts without apparently holding it against me. Thanks guys! My thanks also go to Muni Granger for her initial guidance with parasite culture.

This work was carried out at the NIMR with the financial support of the Medical Research Council, for which I am grateful. I would also like to thank Chetan E. Chitnis (Malaria Research Group, International Centre for Genetic Engineering and Biotechnology, New Delhi, India) and Julie Healer (The Walter and Eliza Hall Institute, Melbourne, Australia) for the kind gifts of the plasmids pRE4 and pHAM-ACPGFP, respectively. My thanks also go to Adrian Bachelor for the kind gift of the PfAMA1 structure figure and allowing its reproduction and modification.

I must also thank my family, particularly my parents, who have provided encouragement throughout my prolonged and somewhat circuitous route through academia.

These acknowledgements would be incomplete if I did not finish by thanking Bill "really useful" Jarra for all his help and support. The last four years have at times been very difficult and I wouldn't have made it without him.

Abbreviations

A

ABRA:	Acidic basic repeat antigen,
ACPGFP:	Acyl carrier protein-green fluorescent protein
adsN1:	N1 anti-AMA1 sera adsorbed out against reduced and alkylated rPfAMA1
ama1:	Apical membrane antigen 1 - gene
AMA1:	Apical membrane antigen 1

B

BbAMA1:	*Babasia. bovis* AMA1
B-cell:	(Antibody forming) lymphocyte

C

CD3:	Cluster determinant 3
CD36:	Cluster determinant 36
$CD4^+$ T-cells:	Helper T-cells – expressing Cluster determinant 4
CHAPS:	3-[(3cholamidopropyl)-dimethylammonio] propanesulfonate
CSP:	Circumsporozoite protein
CR1:	Complement-receptor 1
CDPK:	Calcium dependent protein kinase)

D

DAPI:	4,6-diamidino-2-phenylindole
dATP:	Adénine triphosphate
DBL-EBP:	Duffy binding-like erythrocyte binding protein
DBP:	Duffy binding protein
DBs:	Disulphide bonds
DHFR-TS:	DHFR-thymidylate synthase (PbDT3')
DOC:	Sodium deoxycholate
DI-III:	Domains of PfAMA1ectodomain
DTSS:	P3,3'–dithiobis [sulfosuccinimidyl] propionate
DTT:	α-dithiothreitol,
DI – DIII:	Sub-domains of the ectodomain of *P.falciparum* AMA1

E

EBA-175:	Erythrocyte binding antigen-175
eba-175:	Erythrocyte binding antigen-175 - gene
EBL:	Erythrocyte binding-like (proteins)
ebl:	erythrocyte binding-like (proteins) - gene family

EBPs:	Erythrocyte binding proteins
ECL:	Enhanced Chemiluminescence solution
EGTA:	Ethylene glycol-bis(β-aminoethyl ether)-N,N,N'-tetraacetic acid
EGF:	Epidermal growth factor
ERKs:	Extracellular regulated kinases

F

FCS:	Foetal calf serum
Fab:	Univalent antigen binding fragment (antibody)
$F(ab)_2$:	Bivalent antigen binding fragment (antibody)

G

GPI:	Glycosylphosphatidylinositol

H

Hdhfr::	Human dihydrofolate reductase - gene
HPLC:	High performance liquid chromatography
hRBCs:	Human red blood cells
HVR :	Hyper-variable region (within DI of the PfAMA1 ectodomain)

I

ICAM:	Intercellular adhesion molecule
IEM:	Immuno-electron microscopy
IFA:	Immunofluorescence assays/ Indirect immunofluorescence
IgG, IgM:	Immunoglobulin G, M, etc.
IMP:	Intra-membrane particles
ITAMs:	Immunoreceptor tyrosine activation motifs

L

LSA1:	Liver stage antigen1

M

mAb:	Monoclonal antibody
Maebl:	Merozoite antigen erythrocyte binding ligand - gene
MAEBL:	Merozoite antigen erythrocyte binding ligand
MAPK:	Mitogen-activation protein kinase
MAPKKK:	MAPK kinase kinase
MBP:	Myelin basic protein
MESH:	Merozoite-surface sheddase

MIC2:	Microneme protein 2 - *T. gondii* tachyzoite
MSP1:	Merozoite surface protein 1

N

N1:	Mouse polyclonal antisera against "native" (i.e. non-reduced) PfAMA1

P

PAN:	Plasminogen Apple Nematode motifs
PBS:	Phospahate buffered saline
PcAMA1:	*P. chabaudi* AMA1
PCR:	Polymerase chain reactions
Pfama1:	*P.falciparum* AMA1 - gene
PfAMA1:	*P.falciparum* AMA1
PfEMP-1:	*P. falciparum* Erythrocyte membrane protein 1
PfMAEBL:	*P. falciparum* MAEBL
Pfmap-1 &2:	*P. falciparum* homologues of MAPKs
PfMSP1:	*P. falciparum* merozoite surface protein 1
$PfMSP1_{42}$:	PfMSP1 42 kDa proteolytic processing fragment
Pfmyo-A:	*P. falciparum* myosin A
PfRESA:	*P.falciparum* Ring associated erythrocyte surface antigen
PH:	Pleckstrin homology
PK:	Protein kinases
PP:	Phosphatases
PMSF:	Phenylmethyl sulphonyl fluoride
p-Ser:	Phosphoserine
PfSSP2:	*P. falciparum* sporozoite surface protein 2
Pfs25:	25 kDa sexual stage antigen (*P.falciparum*)
p-Thr:	Phosphothreonine
p-Tyr:	Phosphotyrosine
PvAMA1:	*P. vivax* AMA1
PV:	Parasitophorous vacuole
PVM:	Parasitophorous vacuole membrane
PvSSP2:	*P. vivax* sporozoite surface protein 2
Py235:	*P. yoelii* 235 kDa protein

R

RBC:	Red blood cells
rPfAMA1:	Recombinant PfAMA1
RFLP:	Restriction fragment length polymorphisms
R1:	Polyclonal antisera to reduced and alkylated) recombinant PfAMA1

S

SDM:	Site directed mutagenesis
SDS:	Sodium dodecyl sulphate
SDS PAGE:	SDS polyacrylamide gel electrophoresis
SERA:	Serine repeat antigen
SH:	Src homology
SRB:	Superdex running buffer
SUB2:	Subtilisin-like serine protease

T

TCR:	T-cell antigen receptor
TE:	Tris-EDTA buffer
Tgama1:	*T. gondii ama1* - gene
TgAMA1:	*T. gondii* AMA1
TgMIC3:	*T. gondii* microneme protein (MIC3)
Tk:	Thymidine kinase – gene
TLCK:	Tosyl-lysine chloromethyl ketone
TMD:	Transmembrane domain
TSP:	Thrombospondin
TRAP:	Thrombospondin-related anonymous protein

U

UTR:	Untranslated region.

Index of Contents

Chapter 1

Introduction

Chapter 2

Materials and methods

Chapter 3

Analysis of the RBC binding properties of PfAMA1

Chapter 5

Function of PfAMA1 in signal transduction

Chapter 6

Functionality of sgPfAMA1 in *P. falciparum*

Chapter 7

Discussion

Index of Figures

Chapter 1

Chapter 2

Chapter 3

Chapter 4

Chapter 5

Chapter 6

Chapter 7

Index of Tables

Chapter 1

Chapter 2

Chapter 4

Chapter 1

Introduction

1.1: Parasites of the phylum Apicomplexa

Apicomplexan parasites are obligate intracellular protozoa, responsible for numerous diseases of medical and veterinary importance. Parasites of this phylum infect a variety of intermediate hosts, such as humans (in the case of *Plasmodium*, *Toxoplasma*, and *Cryptosporidium*), cattle (*Theileria* and *Babesia*) and poultry (*Eimeria*) and most require more than one host to complete their complex life cycles (Blackman and Bannister, 2001). Many of these parasites are initially transmitted to a vertebrate host by an insect vector, where they undergo cycles of asexual and sexual differentiation respectively. *Toxoplasma* is unusual in that the entire life cycle occurs in vertebrate host species, the sexual cycle occurring in the intestine of the feline host. Typically these parasites are adapted to invasion of a single host-cell type by a specific cell-invasive life-cycle stage, or zoite. *Toxoplasma* is again exceptional in that the asexual stage has evolved the ability to invade and develop within a range of cell types in diverse host species (Smith, 1995).

Despite clear differences between parasites of this phylum there are many common features shared by them. During the asexual cycle, zoites actively invade host cells where they undergo nuclear division and replication, generating multiple daughter zoites (Kappe et al., 1999). The parasitised cell is lysed, the parasites released are able to invade new host cells and the cycle repeats in this ordered manner, regulated by the circadiam rhythm of the parasite. The sexual cycle typically does not involve repeating cycles of nuclear division and replication to generate daughter zoites of the same type but involves the progression from one developmental stage to another, each stage undergoing an amplification step.

1.1.1: Host cell invasion by Apicomplexa

The sole function of apicomplexan zoites is to invade new host cells (Fig 1.1.). Despite the diverse range of host cell types invaded by parasites of this phylum, the zoite stages share considerable morphological similarity. In addition, the organellar arrangement within these cells is highly polarised, reflecting the directionality of the invasion process. Invasion of the host cell involves a rapid and highly complex cascade of molecular interactions and physiological events (Preiser et al., 2000; Dubremetz et al., 1998). On first contacting the host cell an initial weak interaction occurs. This is followed by zoite re-orientation, which brings its apical region into direct contact with the host cell surface. A tight junction forms between the zoite surface and the host cell plasma membrane, the surface of which subsequently invaginates. The tight junction moves around the parasite surface, from anterior to posterior, maintaining contact with both

membranes at the point of entry as the parasite is internalised by a parasite driven process. The host cell membrane then seals, enclosing the zoite within a parasitophorous vacuole (PV).

1.1.2: Secretory organelles of apicomplexan parasites

As already discussed, apicomplexan parasites invade a wide range of different host cell types. Despite this, the overall mechanism and many of the molecules involved are probably common to all members of the phylum. Apicomplexan zoites also share morphological features diagnostic of the phylum. At the anterior end there is a specialised collection of organelles, known collectively as the apical complex (Dubremetz et al., 1998). This is composed of three types of secretory organelle (rhoptries, micronemes and dense granules) as well as an apical polar ring and, in some apicomplexa, a conoid (Soldati et al., 2004). The presence of the apical complex in all invasive stages of apicomplexan parasites suggests that the organelles of which it is composed play a role in host cell invasion by these parasites. These organelles release their contents in a tightly regulated manner during red blood cells (RBC) invasion. Micronemal proteins are thought to be involved primarily in host cell recognition and binding as well as parasite motility, rhoptry proteins in PV formation, and dense granule proteins in restructuring of the PV membrane (PVM) at and following invasion (Dubremetz et al., 1998).

1.2: Malaria, the challenge facing the global community

Over 50% of the world's population is exposed to malaria, representing an increase of nearly 10% in the last decade (Hay et al., 2004). In developing countries, malaria affects 300 – 500 million people yearly with up to 3 million, largely children, dying from the severe forms of the disease (WHO, Roll Back Malaria). Until recently malaria was controlled in, or eradicated from, several areas of the world. However, the disruptive effects of political or civil unrest, together with the emergence of insecticide resistant mosquito vectors and multi-drug resistant parasites have contributed to resurgences of the disease, which in some cases has resulted in near catastrophic epidemics. Snow *et al.* (2004) have suggested that the burden of malaria not only increases malaria specific mortality but contributes to "all-cause" mortality. As an example of this, at least 10% of paediatric HIV infection in sub-Saharan Africa is thought to result from unsafe blood transfusion (Lackritz, 1998). As severe childhood anaemia resulting from malaria is often treated by blood transfusion, children with malaria are therefore often at increased risk of exposure to HIV from contaminated blood (Ekvall, 2003).

1.2.1: *Plasmodium*; guilt by association

Human malaria is caused by four species of protozoan parasites, *Plasmodium falciparum*, *P. vivax*, *P. ovale* and *P. malariae*. *P. falciparum* is associated with the most severe forms of the disease, leading to high levels of morbidity and mortality. A number of other *Plasmodium*

species that infect simians, rodents and birds, are important experimental models. The *Plasmodium* life cycle requires vertebrate and invertebrate host species (Fig 1.1), and the parasite is transmitted to the vertebrate host by the female Anopheline mosquito during a blood meal.

The most characteristic symptom of the disease is cyclical fever occurring every 12, 24 or 72 hours (Medical Parasitology (1999), 8th edition). Cycle length is dependent on parasite species. In more severe forms of the disease, characteristic of falciparum malaria, cerebral malaria, anaemia and organ dysfunction may also occur. Continuous exposure to the disease results in a large degree of clinical immunity but this is rapidly lost if exposure is interrupted (WHO).

1.2.2: The life cycle of the *Plasmodium* parasite

The life cycle of *Plasmodium* parasites, as for all apicomplexans, is complex (see Fig 1.2). The sexual stage of the cycle begins in the vertebrate host with gametocytogenesis and continues in the mosquito vector. The drop in temperature along with other factors in the mosquito mid-gut stimulate the maturation of male (micro-) and female (macro-) gametocytes into micro- and macrogametes respectively. Fertilisation results in the formation of zygotes (ookinetes) that penetrate the mid-gut wall and form oocysts. Development of the oocyst results in the production of large numbers of haploid sporozoites. These migrate to the mosquito salivary glands from where they are injected into the blood stream of the vertebrate host at the next blood meal. This invasive parasite stage migrates to the host liver and invades hepatocytes. Here a rapid cycle of asexual replication occurs, generating up to 10^4 infective merozoites per exo-erythrocytic schizont that are eventually released to invade circulating RBCs. The intra-erythrocytic parasite cycle involves cyclical asexual replication and nuclear division (schizogony). The mature schizont ruptures, releasing 8 – 32 daughter merozoites (depending on the parasite species; Garnham, 1966). These merozoites immediately infect new RBCs and the cycle repeats until adaptive immune responses or chemotherapy controls it or the host dies. Destruction of RBCs by intra-erythrocytic parasite replication is responsible for the manifestations of the uncomplicated disease. The erythrocytic cycle of *P. falciparum* (but not of most other *Plasmodium* species) can be maintained *in vitro* (Trager and Jensen, 1976). This important development enabled a range of experimental studies investigating the processes of merozoite invasion of, and growth within, RBCs and how this can be inhibited or blocked.

1.3: Tackling the disease

Despite great advances in basic scientific and medical research, malaria is still a global problem affecting many of the world's poorest nations. The implementation and maintenance of preventative measures continues to be a problem. Two main strategies exist for the control of malaria, namely vector control or eradication, aiming at the disruption of malaria transmission,

and parasite control in the form of chemotherapy and vaccination. The transmission of malaria is affected by climate, the incidence of disease increasing in the rainy season, coinciding with the mosquito's breeding season. Vector control involves personal preventative measures such as the use of insect repellents and bed nets as well as community based preventative measures such as insecticides or environmental control of transmission. The use of insecticide treated bed nets has in fact proven to be one of the simplest, cheapest and most effective measures for the prevention of morbidity and mortality resulting from malaria in Africa and Asia (Whitty *et al.* 2005).

1.3.1: Chemotherapy

Anti-malarial drugs are amongst the most commonly used drugs in the tropics (White, 2004). Their misuse is widespread and is considered largely to be responsible for the evolution of drug resistance in *Plasmodium*. Korenromp et al. (2003) argue that drug resistance is likely to be the cause of the doubling in child mortality attributed to malaria in eastern and southern Africa. Chloroquine and sulfadoxine pyrimethamine resistance are widespread (Roper et al., 2003) (Takechi et al., 2001). In addition, resistance to the drug mefloquine has also been reported. A distinct class of antimalarials, the artemisinins are more effective at reducing parasitaemia (by about 10^4 parasites per asexual cycle) than any other anti-malarial. In addition, they inhibit gametocyte production, thus potentially reducing transmission (Price et al., 1996). It has increasingly been accepted that drug combination therapy is the best way to delay the inevitable development of drug resistance, particularly where an artemisinin derivative is included as one of the partners (White, 1999; WHO 2001). Used as part of a combination therapy artemesin need only be taken for a short period (three days) increasing the likelihood of the drug being taken at a sufficient dose for a sufficient duration, while decreasing the likelihood of resistance being developed to it (Nosten, 1994; Yeung et al., 2004). More accurate diagnostic procedures are required to reduce the inappropriate use of anti-malarials and prevent drug resistance. This is however expensive and requires implementation at the community level where the majority of childhood fever is managed (Bjorkman and Bhattarai, 2005).

1.3.2: Vaccine design

The need for a cheap, effective anti-malarial vaccine has never been more pressing. However, consistent with much earlier data, Jeffrey *et al.* (1966) demonstrated that while the course of an infection could be considerably altered by previous exposure to homologous and heterologous strains of *Plasmodium*, "solid" immunity did not develop in humans. Furthermore, naturally acquired immunity develops slowly and requires the persistence of low-density parasitaemia for maintenance of immune memory and effective immunity to "disease" (Struik and Riley, 2004). This suggests that a successful malaria vaccine will require repeated boosts or parasite infections to maintain its efficacy (Carvalho et al., 2002).

A classical approach to vaccine design has been the use of inactivated or attenuated pathogens. This approach has proven effective at inducing immunity to a number of pathogens, and similar approaches have been explored in malaria vaccine development. (Nussenzweig et al., 1967) demonstrated that mice immunised with radiation-attenuated *P. bergei* sporozoites were protected against subsequent challenge with infectious sporozoites. It was subsequently shown that immunisation of human volunteers with irradiated *P. falciparum* or *P. vivax* sporozoites similarly protects against subsequent challenge with fully infectious sporozoites of the same species (Clyde, 1975; McCarthy and Clyde, 1977; Hoffman et al., 2002; Luke and Hoffman, 2003). However, the sporozoites must be delivered alive by intravenous injection or by the bite of an infected mosquito (Hoffman et al., 2002). The logistic and ethical implications of this have led to this approach being generally abandoned in favour of subunit vaccines.

The choice of component(s) of a subunit vaccine is not straightforward. As for chemotherapeutic targets, a vaccine candidate must be parasite specific. Furthermore, it must be accessible to the host immune system. The complexity of the parasite life cycle raises the issue of which stage it is best to target. Several approaches to subunit vaccines have been considered including single component vaccines, designed to specifically target a single parasite stage, as well as multi-component vaccines, usually directed against several stages. The high-level replication rate of the parasite, particularly in the liver stage, may overwhelm vaccine induced humoural immune responses. It follows therefore that a vaccine designed to target a single parasite stage must be extremely efficient, as any parasites escaping the vaccine induced immune response will result in a full infection. For this reason several groups have taken a multi-component, multi-stage approach (D'Alessandro et al., 1995; Doolan et al., 1997), while others have suggested a need for vaccine induction of cellular as well as humoural immune responses (Pombo et al., 2002; Ballou et al., 2004). A further approach to vaccine design is that of transmission-blocking vaccines (Williamson et al., 1996; Shahabuddin et al., 1998; Tsuboi et al., 2003). These are designed to target the sexual stages of the parasite in the mosquito and would therefore not affect the progress of disease in the infected individual. This approach would require the continued control of disease by chemotherapeutic means. Alternatively, transmission-blocking components could be used in conjunction with antigens from other parasite stages in a multi-component, multi-stage approach.

Subunit vaccine candidates from different stages of the *Plasmodium* life cycle have been identified, usually on the basis of evidence indicating that an antibody response against these proteins can inhibit parasite replication *in vitro* or protect against natural or experimental challenge *in vivo*. These include the major sporozoite surface protein circumsporozoite protein (CSP), the major surface antigen of merozoites, merozoite surface protein 1 (MSP1) and the microneme protein apical membrane antigen 1 (AMA1) among others. The CSP based vaccine RTS,S/AS02 has been shown to provide reproducible short-term immunity (Stoute et al., 1997; Bojang et al., 2001). However, vaccine efficacy was estimated at only 34% overall, falling to 0%

in the last 6 weeks of surveillance (Bojang *et al.* 2001). In an attempt to extend this protection further, the Walter Reed Army Institute for Research (WRAIR) plan to develop a RTS,S/AS02 based multi-stage multi-component vaccine that includes the blood stage antigens AMA1 and MSP1 and the liver stage antigen-1 (LSA1). Phase 2 trials to determine the efficacy of these antigens alone are planned before combining them with RTS,S (Heppner et al., 2005).

These studies, among many others, demonstrate the difficulties associated with devising effective subunit vaccines. Over the last 25 years, attempts to identify vaccine candidate antigens and develop a subunit vaccine against malaria have produced mixed results. Furthermore, no subunit vaccine has been produced that possesses an efficacy anywhere near the levels identified for attenuated sporozoite vaccines, prompting some investigators to suggest a return to the more traditional approach of attenuated sporozoite vaccines (Luke and Hoffman, 2003; Hoffman et al., 2002). In a 10 year study, Hoffman *et al.* (2002) demonstrated that immunity resulting from immunization of human volunteers with attenuated sporozoites, administered via the bites of irradiated mosquitoes, was not strain-specific and lasted over 42 weeks. Furthermore, protective immunity was dose dependent, reaching 94% in volunteers immunised by over 1000 infective bites compared with 33% in those immunised with between 200 and 1000 infective bites. The development of *in vitro* culture methods for *P. falciparum* (Trager and Jensen, 1976) and reports of the routine, reliable production of mosquitoes carrying infectious sporozoites (McConkey et al., 2003) have been used in support of this idea. Nevertheless, the difficulties associated with producing sufficient viable attenuated sporozoites and devising a suitable method for administering them - particularly to indigenous populations of malaria-endemic countries - still stands in the way of such a vaccine. As the bite of an infected mosquito delivers 10 - 100 sporozoites, then 10^4 - 10^5 sporozoites would be required to complete each immunisation program. Attempts are in progress to improve the efficiency of sporozoite yield per mosquito (Luke and Hoffman, 2003) and to determine whether attenuated sporozoites can be effectively administered by some means other than intravenously (Luke and Hoffman, 2003).

In summary, despite a considerable amount of effort in this direction, a human vaccine against malaria is clearly some way from production.

1.4: Erythrocyte invasion by *Plasmodium* merozoites

The erythrocytic stage of the malaria parasite life cycle is the stage responsible for the symptoms of disease. If this cycle could be blocked or regulated, the morbidity associated with it would be reduced. For this reason a considerable amount of research has been directed at understanding the mechanisms of erythrocyte invasion by *Plasmodium* merozoites.

Like the invasive stages of other apicomplexan parasites, *Plasmodium* merozoites possess the characteristic apical complex at their anterior end (Fig 1.3.). Immuno-electron microscopy data indicate that the organelles within this complex form during the final round of nuclear division in schizont development (Bannister et al., 2000a). The apical complex is comprised of two pear-shaped rhoptries, up to 40 micronemes, and numerous dense granules, as well as three polar rings (Bannister et al., 2000a; Bannister and Mitchell, 2003; Bannister and Mitchell, 2003). Unlike some apicomplexan parasites there is no conoid (Bannister et al., 2000a).

Mature merozoites exit from the parasitised erythrocyte by a two-step protease dependent egress (Salmon et al., 2001; Wickham et al., 2003). The free merozoites make an initial weak interaction with circulating erythrocytes (Mitchell et al., 2004). This interaction is random, occurs between any point on the parasite surface and the RBC surface and is reversible. Invasion only occurs if the parasite then reorientates such that its apical tip contacts the erythrocyte surface. Attachment at this point induces deformation and rapid transient oscillation of the RBC membrane (Dvorak et al., 1975; Miller et al., 1979a), although this can also occur in the absence of apical orientation (Mitchell et al., 2004). These oscillations may assist in reorientation of the parasite. As with other apicomplexans, apical contact with the erythrocyte results in formation of an electron-dense tight junction between the two membranes (Aikawa et al., 1978). Junction formation appears to commit the parasite to the invasion pathway (Sinnis and Sim, 1997). The RBC membrane then undergoes invagination to form the PV, into which the parasite moves. During invasion the uniform surface coat of the merozoite is excluded from the internalised portion of the parasite (Aikawa et al., 1978). Similarly, the intra-membrane particles (IMP) found in the RBC membrane are largely absent from the PVM (Aikawa et al., 1981). Internalisation of the merozoite is an active, parasite driven process that can be inhibited by the actin capping and depolymerising agent cytochalasin B (Miller et al., 1979a). Furthermore, *P. falciparum* myosin A (Pfmyo-A) has been identified between the plasma membrane and cisternal membrane of the merozoites within very late schizonts and is thought to be a principal component of the *P. falciparum* invasion motility machinery (Pinder et al., 1998; Pinder et al., 2000). As the parasite enters the deepening invagination in the RBC surface, the tight junction maintains a circumferential interaction between the two membranes at the entrance (Aikawa et al., 1978). Thus, the junction traverses the parasite surface from anterior to posterior before finally closing the entrance to engulf the parasite in the PVM (Aikawa et al., 1978).

1.5: Apical organelles of *Plasmodium* merozoites

The initial weak interaction between the parasite and the RBC can occur at any point of the parasite surface and resident merozoite surface proteins, such as MSP1, are evenly distributed across the merozoite surface. It is therefore likely that such proteins mediate these initial interactions (Hall et al., 1984; Nikodem and Davidson, 2000; Goel et al., 2003). Throughout

RBC invasion the contents of the apical organelles are secreted in a tightly regulated manner and it is thought that these are involved in steps subsequent to the initial binding. Micronemes develop after the fourth round of mitotic division, while the merozoites are budding from the schizont surface (Margos et al., 2004). Proteins secreted from these organelles are thought to contribute to the specificity of the invasion process (Triglia et al., 2000), the reorientation of the parasite (Mitchell et al., 2004) and may irreversibly commit the cell to invasion by mediating tight junction formation (Miller et al., 1979a). Rhoptries are the first of the secretory organelles to develop, forming at the periphery of the schizont during the second nuclear division (Bannister et al., 2000b; Margos et al., 2004). Immuno-electron microscopy (IEM) data indicate that the rhoptry contents are segregated into basal or apical duct regions of the organelle (Bannister et al., 2000b). These organelles secrete their contents at the time of tight junction formation and merozoite internalisation (Dubremetz et al., 1998). Rhoptry proteins have been shown to modify the PVM and the erythrocyte membrane in newly invaded rings (Sam-Yellowe et al., 1988; Sam-Yellowe et al., 2004). The last of the secretory organelles to develop are the dense granules. These appear close to the nucleus when the parasite has nearly completed budding but is still attached to the residual body (Margos et al., 2004). As the merozoite enters the host cell the dense granules move to the periphery of the parasite and release their contents into the PV (Torii et al., 1989; Atkinson and Aikawa, 1990; Culvenor et al., 1991). Here they are believed to elicit further expansion of the PVM or interact with the cytoskeleton of the erythrocyte membrane (Foley et al., 1991; Da Silva et al., 1994). Table 1.1 summarises the current understanding of some the key apical organelle proteins.

Proteins found on the surface of the invasive merozoite (resident surface proteins as well as those originating from the apical organelles) are considered valuable tools for vaccine development. Not only are these proteins believed to be involved in host cell invasion, they are also accessible to the immune system. One challenge faced by those attempting to develop an effective vaccine against malaria is that many malaria antigens possess multiple polymorphic amino acid residues, resulting in considerable immunological heterogeneity. Non-synonymous polymorphisms are considered to be the result of immune selection pressure. Escalante *et al.* (1998) demonstrated that antigens expressed on the surface of *P. falciparum* infected RBCs were more polymorphic than those localised internally or expressed during the sexual stages of the parasite life cycle. This phenomenon is attributed to the strong selection pressure upon such antigens, forcing them to develop mutations, thus enabling evasion of the host immune system (Hughes and Hughes, 1995). Antigens currently being considered for a potential blood stage vaccine are resident merozoite surface proteins and components of the apical organelles, such as MSP1 and AMA1 respectively. The prevalence of polymorphic residues in such antigens suggests that an effective immune response can be induced against them (Conway and Polley 2002). However, such diversity poses problems for vaccine design based on these antigens.

1.6: The Duffy binding-like erythrocyte binding protein (DBL-EBP) super family of *Plasmodium*

Adams *et al.* (1992) identified the prototypic members of a superfamily of erythrocyte binding proteins (EBPs) also referred to as the erythrocyte binding-like (EBL) family, characterised by the presence of two types of cysteine rich domain in the extracellular region of the protein: a DBL domain (known as region II) and a highly conserved carboxy-terminal c-cys domain, of unknown function (known as region VI) (Chitnis and Miller, 1994). Greater conservation exists among the c-cys domains than is seen among the amino-terminal DBL domains (Adams et al., 1992). The function of the c-cys domain is unknown, but the degree of conservation perhaps indicates a conserved function within the different EBPs. These two regions are separated by a non-homologous hydrophilic stretch (regions III-V) (Fang et al., 1991; Adams et al., 1992). The *ebl* gene family encode two groups of proteins, differing according to whether they have a single or tandem (designated F1 and F2) DBL domain. The Duffy binding proteins of *P. knowlesi* and *P. vivax* have a single DBL domain, whereas the *P. falciparum* erythrocyte binding protein EBA-175 and other erythrocyte binding proteins (named JESEBL, BAEBL, PEBL, and EBL1) have tandem DBL domains. Proteins from this family are all type I integral membrane proteins, having an N-terminal extracellular domain and C-terminal cytoplasmic tail, separated by a putative transmembrane domain (TMD) (Adams et al., 1992).

A striking feature of this family is the conserved intron/exon structure of their genes. For most *ebl* genes a single exon encodes the signal peptide and extracellular domain, a second exon encodes the transmembrane region and two exons encode the cytoplasmic domain. The *maebl* genes and the *P. vivax* and *P. knowlesi dbp-ebl* genes have an additional intron between the coding sequence for the signal peptide and that for the extracellular domain (Kappe et al., 1998c; Adams et al., 1992).

Genes encoding members of the EBP family are usually single copy. *Plasmodium* species clearly utilise different receptor molecules depending on their host cell of preference, allowing them to invade mature RBCs in the case of *P. falciparum* and reticulocytes in the case of *P vivax*. There may also be a need for the parasite to be able to recognise the RBCs of phenotypically diverse hosts whose RBC membranes may reflect this diversity. These organisms therefore deploy a family of related proteins to mediate erythrocyte binding during invasion, rather than products of a multigene family. The distinction between a protein superfamily and multigene family is somewhat arbitrary. It could be argued that the difference between a family of related proteins and proteins encoded by a multigene family is that the former mediate similar processes but display different functional specificities and variable levels of homology to other members of the superfamily. By comparison, the latter exhibit the same specificities but different antigenicity, their function being protected by differential expression of family members in which homology is retained within the family. In agreement with this,

members of the DBL-EBP superfamily of proteins that participate in erythrocyte invasion by merozoites do so by mediating erythrocyte binding. These proteins exhibit different receptor specificities. The erythrocyte membrane protein 1 family of *P. falciparum* (PfEMP-1) encoded by a multi-gene family (the *var* gene family) are variant surface antigens that also contain a DBL domain and are therefore members of the DBL-EBP superfamily. PfEMP1 is implicated in cytoadherence of trophozoite and schizont stage parasites to the host endothelium in the brain and placenta as well as resetting (Leech et al., 1984; Chen et al., 1998). PfEMP1 mediates these processes by interacting with CD36, Thrombospondin (TSP) and intercellular adhesion molecule (ICAM) on the endothelial surface (Pasloske et al., 1994) and complement-receptor 1 (CR1) on the erythrocyte surface (Rowe et al., 1997). By contrast, the 235 kDa protein-family of *P. yoelii* (Py235), encoded by 35 genes in the *P. yoelii* genome, is implicated in erythrocyte invasion by *P. yoelii* merozoites (Oka et al., 1984; Holder and Freeman, 1984). However, Preiser *et al.* (2002) demonstrated that distinct (seemingly stage specific) subsets of *py235* genes are transcribed in *P. yoelii* oocysts, sporozoites, liver-stage and erythrocytic merozoites. Clearly, oocyst expressed Py235 mediates different receptor binding specificities in the mosquito host than do proteins expressed in asexual stage parasites in the vertebrate host. It is unclear whether Py235 variants expressed in the asexual stages of the parasite life cycle are able to mediate the interactions required for oocyst-sporozoite migration to the salivary glands. In addition, Smith *et al.* (1995) suggest that expression of different *var* genes correlates with alterations in cytoadherent phenotypes. However, this study looked at the correlation between ICAM1 binding potential by *P. falciparum* clones and the presence of a specific *var* transcript. This does not rule out the possibility that switches in PfEMP1 expression merely alter the affinity of binding rather than the specificity of binding. Chen *et al.* (2000) identified three independent binding domains within the PfEMP1 ectodomain that mediate binding to different host receptors. It is possible that different combinations of variants of these domains confer different binding phenotypes and also possibly the virulence phenotype on the parasite. Therefore the question still remains whether subsets of PfEMP-1 proteins provide the adhesive properties required by the parasite in different scenarios such as cerebral or placental sequestration, and rosetting? These findings highlight the potential problem associated with drawing a distinction between members of a multigene family and structural/functional protein families. Nevertheless, the presence of multiple EBPs within a parasites genome may allow the utilisation of different host cell receptors, adding to the redundancy of the invasion process. In summary, this single DBL-containing superfamily therefore provides the parasite with two distinct survival mechanisms: one that provides invasion pathway redundancy and the other that results in a variant antigen repertoire (Michon et al., 2002; Mayer et al., 2004).

1.6.1: The Duffy blood group binding antigen of *P. knowlesi* and *P. vivax*

During invasion, *P. knowlesi* and *P. vivax* merozoites depend on recognition of an epitope on the Duffy blood group antigen (a chemokine receptor) on the erythrocyte surface (Miller et al., 1975; Miller and Carter, 1976; Haynes et al., 1988; Wertheimer and Barnwell, 1989; Horuk et al., 1993). The chymotrypsin sensitive motif recognised by these parasites lies within a 35 amino acid stretch at the N-terminus of the extracellular domain of the human and rhesus monkey Duffy antigen (Ranjan and Chitnis, 1999). They therefore invade only Duffy-positive erythrocytes. In the absence of this antigen, they form the initial attachment with the host RBC and undergo reorientation, but are unable to complete tight junction formation and invasion (Miller et al., 1979b). This observation provided some of the earliest evidence indicating that invasion comprises a series of mechanistically distinct steps, involving a cascade of different molecules.

The *P. knowlesi* genome encodes three Duffy binding-like proteins (α, β and γ) (Adams et al., 1990). The *P. knowlesi* β and γ proteins bind Duffy-independent receptors (sialic acid and some unidentified determinant respectively) on rhesus monkey erythrocytes (Chitnis and Miller, 1994; Ranjan and Chitnis, 1999). The α protein binds the Duffy blood group antigen on human erythrocytes. *P. knowlesi* parasites invade trypsin treated Duffy-negative human RBC and rhesus erythrocytes rendered Duffy-negative by chymotrypsin treatment (Haynes et al., 1988). This finding suggests that, under certain circumstances, invasion by these parasites can continue via an alternative pathway, or bypass certain Duffy antigen dependent steps in the pathway.

Mild proteolysis with trypsin demonstrated that region II of the *P. knowlesi* α-gene product consists of two structurally distinct modules (major and minor), linked by a protease susceptible linker region (Singh et al., 2003). The major module, from cysteines 5 to 8 of this domain, encompasses the erythrocyte binding domain. The equivalent region of the *P. vivax* protein showed similar binding properties. The non-functional surrounding region may however contribute to the affinity and specificity of binding (Ranjan and Chitnis, 1999).

1.6.2: The erythrocyte binding antigen 175 (EBA-175) of *P. falciparum*

Different clones of *P. falciparum* have been shown to use alternative receptors and pathways (Mitchell et al., 1986; Perkins and Holt, 1988; Dolan et al., 1994). The well characterised EBA-175 of *P. falciparum* binds trypsin sensitive terminal sialic acid (Neu5Ac(α2-3)Gal) on O-linked oligosaccharides of glycophorin A on the RBC surface (Orlandi et al., 1992; Sim et al., 1994a). Neuraminidase treatment of erythrocytes, which results in removal of sialic acid from the erythrocyte surface, reduces invasion by *P. falciparum*. However, the parasite is still able to infect En(a-) cells that lack glycophorin A, indicating that this molecule alone cannot be the sole

receptor for *P. falciparum* (Miller et al., 1977). The existence of a sialic acid independent pathway has been demonstrated (Dolan et al., 1990), as has the use, by invasive merozoites, of glycophorins B and C as erythrocyte receptors (Dolan et al., 1994; Maier et al., 2003). Furthermore, partial disruption of the *eba-175* gene in *P. falciparum* did not abrogate invasion as parasites switched to a sialic acid independent invasion pathway (Reed et al., 2000; Kaneko et al., 2000).

Antibodies recognising region II of EBA-175 blocked invasion of sialic acid dependent (FVO) and independent (3D7) strains of *P. falciparum* parasites, leading to the suggestion that this parasite receptor may utilise alternative pathways (Narum et al., 2000). Alternatively, invasion-inhibition of 3D7 parasites by these antibodies may result from steric hindrance of some other parasite receptor molecule. In support of this, disruption of the *eba-175* locus in 3D7 parasites had no effect on merozoite invasion efficiency, indicating that the sialic acid independent nature of 3D7 parasites is not a result of EBA-175 utilising an alternative pathway (Duraisingh et al., 2003b). However, loss of EBA-175 function severely reduced the invasion efficiency of merozoites into chymotrypsin treated erythrocytes (glycophorin A is the predominant chymotrypsin resistant receptor), compared to wild type 3D7 parasites. This finding suggests that the EBA-175 gene product is functional in wild type 3D7 parasites and is a component of the dominant chymotrypsin resistant invasion pathway. This supports the existence of multiple invasion pathways, relying on different/unique erythrocyte binding-like (*ebl*) gene products and variable RBC receptors/ligands (Chitnis and Blackman, 2000).

1.6.3: The 140 kDa erythrocyte binding protein of *Plasmodium*

An additional *ebl* gene has been identified on chromosome 13 of the *P. falciparum* (3D7 strain) genome sequence (Mayer et al., 2001). The gene sequence predicts a structure typical of DBL-EBP, namely two cysteine rich domains, regions II and VI, a TMD and a cytoplasmic domain. The exon/intron structure of the corresponding gene from Dd2/Nm parasites is identical to that of EBA-175. The 140 kDa protein encoded by this gene (known as BAEBL, see table 1.1), immunoprecipitated from *P. falciparum* culture supernatants, binds normal, but not neuraminidase treated, human erythrocytes (Thompson et al., 2004; Narum et al., 2002). Narum *et al.* (2002) identified a 50% reduction in the ability of BAEBL to bind trypsin treated human erythrocytes, while Thompson *et al.* (2001) observed no such effect. Under these conditions binding of EBA-175 to human erythrocytes is completely abrogated. Thus, these related DBL-EBPs have different receptor specificities. Mayer *et al.* (2001) suggested that unlike EBA-175, the receptor for BAEBL on human erythrocyte is glycophorin C/D. Furthermore, Maier *et al.* (2003) identified the receptor as glycophorin C. By comparison, Thompson *et al.* (2001) suggest a protease resistant receptor on the host erythrocyte for BAEBL, which is inconsistent with it being glycophorin C. In a second study, Mayer *et al.* (2002) suggested that four polymorphic sites found in the erythrocyte binding domain of BAEBL (region II) enabled this molecule, from

different parasite strains, to utilise alternative host erythrocyte receptors. Thompson *et al.* (2002) identified a parasite line that lacked BAEBL, showing that this gene product in not essential for parasite survival and confirming the redundancy of these invasion pathways.

1.6.4: The merozoite antigen erythrocyte binding ligand (MAEBL)

Kappe *et al.* (1997) initially identified a sub-family of erythrocyte binding proteins in the rodent parasites *P. yoelii* and *P. berghei*, however, homologues are present and highly conserved throughout the genus (Kappe et al., 1998). The intron/exon structure of the *maebl* gene, as well as the homology in the predicted protein sequence for its carboxy-terminal cysteine rich domain, transmembrane region and cytoplasmic tail, identify it as a member of the DBL family. However, MAEBL is unique in that it shows more sequence homology in its amino-terminal cysteine rich region to AMA1 than it does to the corresponding region of other *ebl* gene products (Kappe et al., 1998). This region is comprised of two cysteine rich domains M1 and M2, each bearing considerable deduced amino acid similarity to the cysteine rich domains I and II (DI-II) of AMA1 (see below) (Kappe *et al.* 1998). Homology with AMA1 derives mainly from the conservation of cysteine residues. The MI and M2 domains of MAEBL share 40% sequence homology, each containing 16 cysteines of which 10 are conserved in AMA1 DI-II.

Analysis of *P. yoelii* mixed stage parasites by indirect immunofluorescence (IFA) analysis, using antibodies raised against M2 of MAEBL, has shown co-localisation with AMA1 and the 235 kDa rhoptry protein (Noe and Adams, 1998). These findings, along with other studies (Noe et al., 2000; Ghai et al., 2002), seem to suggest that MAEBL localises to the rhoptries of developing merozoites. However, IEM studies have localised *P. falciparum* AMA1 to the micronemes (Bannister *et al.* 2003). This indicates that either the localisation of MAEBL in *P. yoelii* and *P. falciparum* is different or, possibly, the mixed-stage nature of the *P. yoelii* parasites used confused the issue. Further IEM is required to fully resolve this matter. Rhoptry localisation is however supported by the finding that the *maebl* transcript pattern peaks in mid to late trophozoites, and is absent in late schizonts (Blair et al., 2002). By comparison, transcripts for other *ebl* genes (*eba-175*, *baebl*, *pebl* and *jesebl*) are most abundant in late schizogony. These findings are consistent with the timing of rhoptry (4 nuclei stage) and microneme (16 nuclei stage) development (Margos et al., 2004). In mature *P. yoelii* merozoites, MAEBL and AMA1 localise to the merozoite surface (Peterson et al., 1989; Kappe et al., 1997). This has never been observed for other DBL-EBPs. However, as for EBA-175 (Sim et al., 1990) and AMA1 (Margos et al., 2004; Howell et al., 2005), the extracellular domain was not detectable in ring or trophozoite stage parasites using anti-M2 antibodies (Ghai et al., 2002). Targeted disruption of the *maebl* gene locus indicates that, like BAEBL, this gene product is not essential for parasite survival in blood stages (Fu et al., 2005).

Expression of the *P. yoelii* MAEBL domains M1 and M2 in membrane bound form on the surface of COS-7 cells has been used to show that M1 and M2 bind murine, but not human, erythrocytes; however, M2 binds with higher efficiency (Kappe et al., 1998c). Similarly, a soluble recombinant form of *P. falciparum* MAEBL (PfMAEBL) M2 domain exhibited high affinity binding for human erythrocytes (Ghai et al., 2002). Papain treatment of human erythrocytes completely abrogated PfMAEBL binding, whereas trypsin treatment merely reduced it (Ghai et al., 2002). Neuraminidase on the other hand slightly increased binding. Thus, PfMAEBL recognises a peptide-based determinant on the erythrocyte surface that is distinct from the receptor recognised by EBA-175.

1.7: Merozoite surface protein 1 (MSP1)

Many resident merozoite surface proteins have been identified, several of which could potentially be involved in making the initial interaction between the parasite and host cell. One example, and the most comprehensively studied in *P. falciparum*, is MSP1 which gene disruption experiments suggest is functionally important, if not essential, in the erythrocytic stage of the parasite life cycle (O'Donnell et al., 2000).

Like many merozoite stage antigens, MSP1 is proteolytically processed. This generates a complex of polypeptides that are linked to the merozoite surface via a glycosylphosphatidylinositol (GPI) anchor (Holder and Freeman, 1982; Lyon et al., 1986; McBride and Heidrich, 1987). Subsequent to schizont rupture, a further processing step occurs within the 42kDa membrane bound fragment (Blackman et al., 1991b; Miller et al., 1993). A 33kDa amino-terminal fragment ($MSP1_{33}$) is released, exposing a carboxyl-terminal 19kDa fragment ($MSP1_{19}$) at the merozoite surface, consisting of two epidermal growth factor (EGF)-like domains (Blackman et al., 1990; Blackman et al., 1996; Morgan et al., 1999; Chitarra et al., 1999). This 19kDa fragment is carried into the erythrocyte on invasion and can be detected in a circumferential localisation in ring stage parasites (Blackman, 1994). Antibodies found to block this secondary processing also block erythrocyte invasion (Blackman, 1994). This processing step goes rapidly to completion during the invasion process, suggesting it is of functional significance (Blackman et al., 1996).

Whether the release of $MSP1_{33}$ is required to break some parasite-host interaction, or to expose the functional $MSP1_{19}$ fragment is unknown. However, invasion-inhibitory monoclonal and polyclonal antibodies exist that recognise epitopes in the EGF domains of $MSP1_{19}$ (Blackman et al., 1990; Chang et al., 1992; Spencer Valero et al., 1998; O'Donnell et al., 2000). Studies to assess the role of antibodies acquired against $MSP1_{19}$ in immune or semi-immune individuals in malaria endemic areas indicate a protective role for this antigen (Egan et al., 1995; Egan et al., 1996; de Koning-Ward et al., 2003; O'Donnell et al., 2001). In other systems EGF-like domains have been shown to play a role in adhesion, suggesting that $MSP1_{19}$ might have an adhesive

function in invasion. However, initial reports of the erythrocyte binding activity of MSP1 were inconclusive (Perkins et al., 1998; Nikodem and Davidson, 2000; Rodriguez et al., 2002). $MSP1_{19}$ is functionally constrained across distantly related species of *Plasmodium* (O'Donnell et al., 2002) suggesting that it plays a highly conserved role. Two recent studies identify Band 3 as the host cell receptor for MSP1 (Goel et al., 2003; Li et al., 2004b). Li *et al.* (2004b) suggested that MSP1 and MSP9 form a complex that interacts with a Band 3 homo-dimer on the RBC surface. Whatever the precise role of MSP1, its circumferential localisation on the surface of the merozoite suggests that if it does play an erythrocyte-binding role in invasion, it does so by facilitating the initial interaction with the host cell.

1.8: Apical membrane antigen 1 (AMA1)

Apical membrane antigen 1 (AMA1) is widely regarded as a leading candidate for inclusion in a blood stage malaria vaccine (Waters et al., 1991). Identified initially in *P. knowlesi*, homologues of AMA1 have been found in all species of *Plasmodium* (Deans et al., 1982; Marshall et al., 1989; Peterson et al., 1990; Waters et al., 1990; Waters et al., 1991; Cheng and Saul, 1994; Dutta et al., 1995; Kappe and Adams, 1996; Marshall et al., 1996; Kocken et al., 2000) Therefore it is possible that vaccine development involving AMA1 may have broad applications.

In *Plasmodium*, AMA1 is the product of a single copy gene. However, apparently two additional, less well conserved homologous are present in the genome of *T. gondii*. Expressed towards the end of the fourth nuclear division in developing *Plasmodium* schizonts (Margos et al., 2004) AMA1 is a type I integral membrane protein comprising an N-terminal ectodomain, a 21 amino acid transmembrane region and a 55 amino acid, C-terminal cytoplasmic tail (Fig 1.4) (Peterson et al., 1989). Upon synthesis, AMA1 is targeted to the micronemes of developing merozoites (Healer et al., 2002; Bannister et al., 2003). Around the time of schizont rupture, AMA1 is released, via the apical prominence, onto the surface of the merozoite (Peterson et al., 1989). Surface localisation of AMA1 can be occasionally detected in merozoites within schizonts, following budding (Peterson et al., 1989; Margos et al., 2004). This indicates that interaction with a new host cell is not a prerequisite for AMA1 release from the micronemes.

Attempts to disrupt the *ama1* gene locus in *P. falciparum* (Triglia et al., 2000) and *T. gondii* (Hehl et al., 2000) have proven unsuccessful using traditional reverse genetics approaches. However, the recent development of a conditional knock-out system for *T. gondii*, has allowed the controlled disruption of the *ama1* gene locus in this parasite (Mital et al., 2005). The inability to disrupt the gene locus completely in earlier studies had led to the suggestion that this gene product was essential for apicomplexan parasite survival. Mital *et al.* (2005) disrupted the endogenous *T. gondii ama1* (*Tgama1*) gene in parasites expressing a myc-tagged version of TgAMA1 under the control of a tetracycline-sensitive conditional promoter. When fully active, expression of myc-tagged TgAMA1 from this promoter was only 10% the level of TgAMA1 in

wild type parasites; invasion efficiency for these parasites was indistinguishable from that of wild type parasites. Down-regulation of promoter activity resulted in a decrease in myc-tagged TgAMA1 expression to 0.5% the level of TgAMA1 in wild type parasites. This being the average figure, some parasites must have expressed myc-tagged TgAMA1 at a level between 0.5 and 10%, perhaps above the critical threshold required for invasion. Alternatively, the two homologues of AMA1 identified in the *T. gondii* genome may function in some alternative invasion pathway. Such homologues have not been identified in any *Plasmodium* genome. Downregulation of the conditional *Tgama1* gene resulted in an 85% decrease in invasion efficiency. Taken together, these results suggest that, at least in *Plasmodium* and probably also in *Toxoplasma*, AMA1 is an essential gene product that plays a critical role in invasion.

1.8.1: Structure of AMA1

At the amino acid level, AMA1 is highly conserved among *Plasmodium* species, having at least 50% identity in pair-wise comparison of known sequences (Marshall et al., 1989). Furthermore, structurally important residues are positionally conserved (Waters et al., 1990). Most notably, the AMA1 ectodomain from all species of *Plasmodium* contains 16 absolutely conserved cysteine residues all of which participate in intra-molecular disulphide bonds (Hodder et al., 1996; Nair et al., 2002). That these bonds constrain the molecule to form three sub-domains (DI, DII and DIII) has been confirmed by the solution of the *P. vivax* AMA1 (PvAMA1) crystal structure (Pizarro et al., 2005). Figure 1.4 shows a schematic representation of the domain structure of *P.falciparum* AMA1 (PfAMA1). That the first 10 of these cysteine residues, found in DI and DII, are conserved in the AMA1 orthologues of the apicomplexans *T. gondii* (Hehl et al., 2000; Donahue et al., 2000) and *Babesia bovis* (Gaffar et al., 2004) suggests that the disulphide bonding pattern observed in these domains, and thus possibly the domain structure, is conserved in these phyla.

The core structure of both DI and DII comprise so-called Plasminogen Apple Nematode (PAN) motifs (Pizarro *et al.* 2005), a family of protein domains that include N domains of members of the plasminogen/hepatocyte growth factor family, A- or apple domains or the plasma predallikrein/coagulation factor XI and domains found in various nematode proteins (Tordai *et al.* 1999). Present in functionally diverse molecules, PAN domains can generally be described as mediating adhesion, via protein-protein or protein-carbohydrate interactions. In AMA1, these domains have been extensively modified. PAN domains are normally characterised by the presence of six cysteine residues, all involved in disulphide bonding. Domain I of AMA1 has three disulphide bonds and DII has only two; however, only the disulphide bond linking cysteines 2 and 5 in each of these domains is consistent with those found in the normal PAN module (Bai et al., 2005; Pizarro *et al.* 2005). The central five-stranded, anti-parallel β-sheet is packed against a twelve residue α-helix on one face and a double stranded β-sheet on the other (Bai et al., 2005; Chesne-Seck *et al.* in press) and these conform well to previously published

structures. In addition, about 50% of DI lacks secondary structure, with multiple ordered but flexible loops that extend from the core PAN structure. By contrast, DII has a more closely packed secondary structure, with a single long loop (denoted the DII loop) extending from its surface (Bai et al., 2005). The DII loop interacts with a hydrophobic pocket in DI, contributing two of the nine amino acid residues that line the pocket (Bai et al., 2005). The DII loop is invariant in length in different *Plasmodium* orthologues; however, it has low sequence identity (21%) (Chesne-Seck *et al.* in press). This loop is slightly longer in AMA1 from *Babasia bovis* AMA1 (BbAMA1), and about half the length in TgAMA1 (Chesne-Seck *et al.* in press).

By comparison, domain III shows no homology to any known polypeptide fold (Pizzaro *et al.* 2005). Sequence identity between orthologues in *Plasmodium* in this domain is 33%, compared to 39% overall. This domain in AMA1 shows the least homology in orthologues from parasites of different phyla. In BbAMA1 only four cysteine residues exist in DIII, however, these align with four of those in *Plasmodium* sequences and possibly form disulphide bonds corresponding to Cys443-Cys502 and Cys490-Cys507 in PfAMA1 (Chesne-Seck *et al.* in press). In contrast, TgAMA1 has six cysteine residues in DIII, only two of which align with cysteines in DIII of *Plasmodium* sequences (Chesne-Seck *et al.* in press). However, in *Plasmodium* AMA1, these cysteines do not interact to form a disulphide bond. Thus, none of the disulphide bonds in DIII of TgAMA1 align with those of orthologues from *Plasmodium*. It is possible therefore that DIII of BbAMA1 bears some structural similarity to that of *Plasmodium* orthologues, however, TgAMA1 is likely to be structurally distinct. Like *Plasmodium*, merozoites of *B. bovis* merozoites invade and develop within erythrocytes, while *T. gondii* tachyzoites invades nucleated cells. It is possible that differences observed in the structure of these AMA1 orthologues may reflect differences in host cell specificity.

1.8.2: Proteolytic processing of AMA1

A schematic representation of AMA1 processing can be found in figure 1.5. PfAMA1 is synthesized as an 83 kDa precursor containing a N-terminal prodomain, which is absent in AMA1 from all other *Plasmodium* species studied, except the chimpanzee parasite, *P. reichenowi*. Around the time of schizont rupture, PfAMA1 is proteolytically processed, the prodomain being removed, leaving a 66 kDa membrane-bound fragment which is released from the micronemes and redistributed across the merozoite surface (Peterson et al., 1989, Narum and Thomas, 1994). After further proteolytic processing the molecule is shed from the merozoite surface as a 48 kDa fragment, known as $PfAMA1_{48}$ (Howell et al., 2001). About 30% of the 48 kDa fragment undergoes an additional cleavage within DIII, producing two fragments held together by a disulphide bond, the larger of which is known as $PfAMA1_{44}$ (Howell et al., 2003). Once PfAMA1 is shed from the parasite surface, no further processing occurs, suggesting that this internal cleavage is mediated by a parasite protease. This internal cleavage is possibly conserved in AMA1 from other species of *Plasmodium*, since in *P. knowlesi* AMA1 (PkAMA1)

two fragments, of 44 kDa and 42 kDa, were identified in Western blot analysis of parasite culture supernatants and free merozoites, under reducing conditions (Deans, 1984). Similar to the ratio of $PfAMA1_{44}$ to $PfAMA1_{48}$ in *P. falciparum*, the 42 kDa PkAMA1 species appear to be about half the intensity of the 44 kDa form (Deans, 1984). If this situation is analogous to that in *P. falciparum*, under non-reducing conditions these should be observed as a single band, the 42 kDa fragment being disulphide bonded to the C-terminus of the 44 kDa fragment; however, this has not been investigated. The functional significance of this internal cleavage is unknown. In *T. gondii* a similar shedding process occurs, but here the shed TgAMA1 fragment migrates as a single band of 54 kDa under reducing conditions in Western blot analysis suggesting that the additional internal cleavage within TgAMA1 DIII does not occur to any significant extent (Hehl et al., 2000); however, as noted above DIII in TgAMA1 is probably structurally distinct from that in *Plasmodium* AMA1. After shedding of the ectodomain, the TMD region and cytoplasmic tail are carried into the RBC with the invading parasite (Howell et al., 2005). Dutta *et al.* (2003) demonstrated that invasion inhibitory Abs raised against PfAMA1 functioned by blocking shedding. This raises the possibility that, as for MSP1 in *Plasmodium* (Blackman *et al.*, 1994) and the microneme protein MIC2 in *Toxoplasma* (Brossier et al., 2003), processing of AMA1 is essential for invasion. The development of a system for conditional gene expression in *P. falciparum* will allow a thorough analysis of the functional significance of AMA1 processing and shedding in invasion (Meissner and Soldati, 2005).

Evidence from protease inhibitor studies suggests that a single calcium-dependent, serine protease mediates shedding of both PfAMA1 and MSP1 (Howell et al., 2003). This was an unexpected finding since the cleavage sites of these two proteins lies within structurally quite different motifs; these are RAEVT517-518SNNEV for PfAMA1 (Howell et al., 2003) and LQGML286-287NISQH for MSP1 (Blackman et al., 1991a). Previously identified "sheddases" appear to be dependent on the presence of conformationally unrestrained peptides surrounding the cleavage bond and its distance from the membrane, and – unusual among proteases - their recognition of these motifs is often apparently not dependent on the precise amino acid sequence within them (Schwager et al., 2001). The Thr517-Ser518 site at which the PfAMA1 ectodomain is cleaved lies 29 amino acid residues from the membrane, an appropriate distance for cleavage by a sheddase, and the membrane bound parasite protease responsible has therefore been named merozoite-surface sheddase or MESH (Howell *et al.* 2005). As discussed above, the C-terminal 19 kDa fragment of PfMSP1 is comprised of two EGF domains that form an inverted U-shaped structure (Morgan et al., 1999) thus bringing the cleavage site into close proximity to the membrane and making it readily accessible to MESH. The subtilisin-like serine protease SUB2, released from micronemes onto the surface of the merozoite around the time of schizont rupture, has been identified as the *Plasmodium* MESH responsible for shedding of AMA1 and MSP1 (Harris *et al.* submitted). SUB2 has no homologue in *T. gondii* and, consistent with this, shedding of TgAMA1 occurs at an intra-membrane location and is mediated by a member of the serine protease family known as rhomboids (Howell et al., 2005). These seven-

pass transmembrane proteins cleave their substrates within the membrane. Microneme proteins of *Plasmodium*, such as EBA-175, are also quite probably shed at intra-membrane sites, presumably also by rhomboids (Blackman, unpublished data). Inhibition of normal PfAMA1 processing results in an alternative shed form of 52 kDa. Identification of the shedding site that results in this aberrant form suggests that it lies within the membrane (Howell et al., 2003a). Why some microneme proteins of *Plasmodium* are shed at intra-membrane sites while others, such as AMA1, are processed at sites outside the membrane is unclear.

1.8.3: Polymorphisms within the AMA1 ectodomain

1.8.3.1: Selection pressure on the PfAMA1 ectodomain

Unlike a number of other malarial antigens, AMA1 does not possess any of the tandem repeat motifs thought to act as a "smoke screen" to "distract" the immune system (Peterson et al., 1989, Waters et al., 1991). However, several studies have highlighted the presence of polymorphic residues in the AMA1 ectodomain (Thomas et al., 1990; Oliveira et al., 1996). Most of these are the result of non-synonymous substitutions, meaning that mutations in the gene sequence give rise to amino acid residues that are different from those found in the original sequence. While the prevalence of non-synonymous substitutions in the sequence encoding the PfAMA1 ectodomain indicates positive diversifying selection, the low abundance of synonymous substitutions may result instead from the limited availability of synonymous substitutions due to the biased codon usage observed in *P. falciparum* (Escalante et al., 1998b; Endo *et al.* 1996). However, the codon bias observed in *P. reichenowi* is comparable to that of *P. falciparum*, yet *P. reichenowi* exhibits more synonymous than non-synonymous substitution in its *ama1* sequence (Kocken et al., 2000; Escalante et al., 2001; Polley and Conway, 2001). This suggests that the non-synonymous substitutions in the *Pfama1* sequence are under direct selection pressure from the host immune system.

1.8.3.2: AMA1 as the target of protective immune responses

That polymorphic residues in PfAMA1 are the targets of protective immune responses is supported by both *in vitro* and field studies. Healer *et al.* (2004) generated transgenic *P. falciparum* parasite lines expressing heterologous *Pfama1* allelic forms. Using these transgenic lines they demonstrated conclusively the strain specificity of antibody (Ab) mediated invasion-inhibition in *in vitro* culture. In a study of *P. falciparum* patients from an area of endemic malaria in Papua New Guinea, Cortes *et al.* (2003) found an association between certain polymorphic residues on AMA1 and clinical disease in children but not in older individuals. They suggested that some residues are less immunogenic than others, thus requiring longer exposure for the development of an effective immune response. In a recent study, this group demonstrated that the age dependence of the prevalence and titre of anti-PfAMA1 Abs was paralleled by the development of protective immune responses (Cortes et al., 2005). They also observed an increase in prevalence of Abs directed against DII and DIII with age, suggesting a role for Abs

against these more highly conserved regions in immunity. However, the evidence of natural selection on polymorphisms in the AMA1 ectodomain (largely DI) argues strongly for their being a target of protective immune responses.

1.8.3.3: The hyper-variable region of AMA1

Marshall *et al.* (1996) identified a hyper-variable region (HVR) within DI of the PfAMA1 ectodomain. They proposed that the allelic forms of *Pfama1* could be categorised into families based on the restriction fragment length polymorphisms (RFLP) of the HVRs amplified by PCR from the *ama1* sequences of different strains of *P. falciparum*. Eisen *et al.* (1999) identified four *Pfama1* allelic families based on the PCR-RFLP method. This group suggested that in addition to polymorphisms resulting from point mutation, sequence variability also occurred as a result of intragenic recombination, as they identified a gene sequence containing polymorphisms diagnostic of two allelic families.

1.8.3.4: Domain bias of the protective immune response

Most non-synonymous substitutions are primarily found in the sequence encoding DI (Verra and Hughes, 2000; Polley and Conway, 2001; Polley et al., 2003; Chesne-Seck *et al.* in press). These studies found evidence for balancing selection in DI and DIII, but not DII, suggesting that DI and DIII, but not DII, are targets for protective immune responses.

The recently solved crystal structure of DI and DII of the PfAMA1 ectodomain shows all the polymorphic residues in this region to be surface exposed (Bai et al., 2005). This supports the notion that the polymorphic nature of these residues results from positive immune selection pressure. Comparisons between the *P. falciparum* AMA1 sequence and the crystal structure of the full-length ectodomain of PvAMA1, suggests this to be true within DIII as well (Pizarro et al., 2005; Chesne-Seck *et al.* in press). In an extensive analysis of 356 PfAMA1 published sequences, Chesne-Seck *et al.* (in press) identified 32 polymorphic sites in DI, 11 in DII and 9 in DIII, most of which are dimorphic. In the same study, analysis of 232 sequences covering DI of PvAMA1 led to the identification of 17 polymorphic sites, 10 of which are also polymorphic in PfAMA1. In addition, unlike the situation in PvAMA1, all but four of the polymorphic residues in DI and DII appear to be positioned down one face of the ectodomain, suggesting that only this face is exposed on the surface of the parasite (Chesne-Seck *et al.* in press; Bai *et al.* 2005). Thus, the non-polymorphic face either lies close to the merozoite membrane or interacts with some other parasite protein, in both cases being inaccessible to the host immune system. Due to the level of polymorphism observed in accessible regions of the PfAMA1 ectodomain, it has been suggested that multiple allelic forms should be used in a vaccine to maximise the likelihood of generating a protective response.

1.8.4: AMA1 as a vaccine candidate

1.8.4.1: The immunogenic nature of AMA1

The immunogenic nature of AMA1 supports its inclusion in a blood stage vaccine against malaria. Indeed, PkAMA1 (or Pk66) was first identified because a monoclonal antibody (mAb) raised against it blocked merozoite invasion of RBC *in vitro* (Deans et al., 1982). Since then other mAbs, as well as their $F(ab)_2$ and Fab fragments, have been identified that are invasion inhibitory (Thomas et al., 1984; Kocken et al., 1998b; Dutta et al., 2005). Furthermore, immunization of mice and monkeys with native or recombinant forms of AMA1 protects against homologous challenge (Deans et al., 1988; Collins et al., 1994; Crewther et al., 1996b; Anders et al., 1998; Narum et al., 2000; Hodder et al., 2001). Deans *et al.* (1988) immunised rhesus macaque monkeys with PkAMA1 purified from parasites. After immunisation, the level of invasion inhibitory antibodies was high, but these diminished rapidly thereafter. After the first challenge most of the immunised monkeys required drug treatment to clear the parasitaemia. The monkeys were immunised a second time and then re-challenged. This time the pattern of infection was completely different, with all PkAMA1 immunised monkeys showing solid immunity. Control monkeys, that had been drug cured following the primary infection, displayed a similar infection course to their first infection. This suggests that AMA1 is a potent immunogen that can prime the immune system and confer protection against otherwise lethal challenge.

A high prevalence of naturally induced Abs to AMA1 has been found in human populations living in malaria endemic regions (Thomas et al., 1994; Rodrigues et al., 2005). Furthermore, there appears to be a correlation between age and anti-AMA1 seropositivity, although this appears to show some regional variability, possibly related to the level of exposure (Thomas et al., 1994; Dorfman et al., 2005; Rodrigues et al., 2005). Rodrigues *et al.* (2005) found that individuals suffering a primary *P. vivax* infection had a significantly lower frequency of anti-AMA1 immunoglobulin G (IgG) - predominantly IgG1 - than individuals who had suffered previous infections. By comparison, no difference was observed in the frequency of AMA1 specific IgM between these groups. Dorfman *et al.* (2005) demonstrated a deficiency of memory B-cells specific for PfAMA1 in blood samples from individuals living in a malaria endemic region of Kenya. As memory B-cells are believed to be essential for long-term immunity in humans, this may explain the short-lived nature of the Ab response to this malaria antigen. Immunisation of mice with reduced and alkylated recombinant *P. chabaudi* AMA1 (PcAMA1) does not provide protection against subsequent *P. chabaudi* challenge (Crewther et al., 1996; Anders et al., 1998). Furthermore, invasion inhibitory anti-PfAMA1 Abs do not recognise reduced and alkylated forms of PfAMA1 (Kocken et al., 1998a; Dutta et al., 2002). This suggests that protective Abs recognise conformation dependent, reduction sensitive epitopes.

Passively transferred anti-PcAMA1 polyclonal Abs, modulate parasitaemia in challenged mice, protecting them against an otherwise lethal infection (Crewther et al., 1996). However, this

protection is only demonstrated after homologous challenge. Challenge with a heterologous strain of *P. chabaudi* results in a full-blown infection. The *ama1* sequences from these two parasite strains (DS and 556KA) differ by 55 codons, resulting in 36 amino acid substitutions, 21 of which lie in the HVR in DI (Crewther et al., 1996). Whether these particular polymorphisms are responsible for the strain specificity of this protection is unclear. Hodder *et al.* (2001) demonstrated that rabbit Abs raised against PfAMA1 from the clone 3D7 were able to inhibit erythrocyte invasion by this parasite *in vitro* and, to a varying degree, other heterologous *P. falciparum* strains. Invasion by the closely related parasite strain D10 (differs in AMA1 sequence by only 8 amino acids) was more strongly inhibited by these Abs than the homologous 3D7 parasites, while inhibition of the more distantly related strain HB3 (AMA1 sequences differ by 23 amino acids) was less potent. There is clearly some degree of inhibitory Ab cross-reactivity between *P. falciparum* strains, which is not surprising considering that the PfAMA1 sequences share 95% identity. One question that needs to be addressed is whether the potency of Abs against conserved regions of the molecule can be specifically enhanced to improve the "multi-strain' efficacy of a vaccine.

In an extensive study of the immunogenicity of the PfAMA1 ectodomain, Lalitha *et al.* (2004) demonstrated that domains I and II together (DI-II) induce growth/invasion inhibitory Abs in rabbits at a level about one third that induced by the full length ectodomain (DI-III). This study reported no invasion-inhibition with Abs raised against any of the individual domains alone or domains II and III combined (DII-III) or I and III combined (DI+III). This raises the possibility that inhibitory Abs recognise epitopes that overlap more than one domain. Mueller *et al.* (2003) however, identified two peptides from within loop I of DIII that are recognised by certain mAbs that block erythrocyte invasion *in vitro*. These peptides were also recognised by hyper-immune serum from individuals in malaria endemic areas. Polley *et al.* (2004) attempted to identify the domains of PfAMA1 responsible for protection by studying serum samples from individuals living in two areas of endemic malaria. They found that although Abs to DIII were rare, DI-II linked to the prodomain was less strongly associated with protection than DI-III. These findings, taken together, suggest that although DIII overall may not be highly immunogenic, there are certain, possibly cryptic, epitopes found in this region of the PfAMA1 ectodomain that elicit protective Ab responses. A vaccine against malaria would seek to artificially enhance these responses.

1.8.4.2: Attempts to dissect the immune response against AMA1

Burns *et al.* (2004) suggested that immunity induced by vaccination with AMA1 was Ab dependent. However, Ab responses induced by AMA1 based vaccines appear to be short lived (Deans et al., 1988; Pan et al., 2004). This is clearly a problem for any long-term AMA1 based vaccine strategy. Using the *P. chabaudi* system, Xu *et al.* (2000) demonstrated that Ab, induced after immunisation of mice with AMA1, was critical for controlling infection and preventing death. They also showed however, that $CD4^+$ T-cells acted independently of Ab to help control parasitaemia. Attempts have been made to identify immuno-dominant and cryptic T-cell

epitopes within the ectodomain of PfAMA1. Such epitopes may induce more potent, long-term immune responses than the intact molecule, within which they may be masked. In a vaccine, these epitopes could be combined to produce a tightly focussed immune response. Results from these studies have been mixed. Salvatore *et al.* (2002) identified two antigenic peptides from tryptic digestion of PcAMA1 that contain effective epitopes for T-helper cells and B-cells in mice. However, these Abs are not protective in homologous *P. chabaudi* challenge. Lal *et al.* (1996) identified several T-cell determinants in PfAMA1 using the amphipathic scores determined by a computer algorithm. Of these, six were demonstrated to induce proliferation of peripheral blood mononuclear cells from individuals with life-long malaria exposure but not from individuals not previously exposured to malaria. Three of these peptides represent highly conserved regions, which is of interest when considering a vaccine capable of transcending parasite strain differences although the protection conferred by these peptides was not determined. Amante *et al.* (1997) screened overlapping, 20-mer peptides from the entire PcAMA1 sequence for the presence of immunodominant and cryptic T-cell epitopes. Ten peptides were identified as containing cryptic determinants. Two of these peptides (designated P4 and P5) contain a ten residue region of overlap, which contains the cryptic determinant and is conserved in AMA1 from all strains of *P. chabaudi*. These peptides are not recognised by mice immunised with recombinant PcAMA1. However, mice immunised with either of these peptides responded strongly to recombinant PcAMA1. Adoptive transfer of a T-cell line specific for peptide P4, but not P5, was able to aid the production of PcAMA1 specific Abs in athymic (nude) mice following *P. chabaudi* challenge. Furthermore, adoptive transfer of T-cells specific for a pool of eleven peptides, that included P4 and P5, protected 50% of nude mice against lethal *P. chabaudi* infection. This study suggests that peptides containing putative T-cell determinants can be used successfully to prime an anti-AMA1/anti-parasite response.

1.8.4.3: Clinical and pre-clinical vaccination trials involving AMA1

Pre-clinical studies in rabbits assessing the efficacy of a PfAMA1 based vaccine used recombinant PfAMA1 from two strains of parasite (FVO and 3D7) expressed in the yeast *Pichia pastoris* (Kennedy et al., 2002). This study demonstrated Ab titres to both antigens to be high when administered alone or in combination. Effective growth inhibition was observed against the homologous strain *in vitro* but was reduced against the heterologous strain. In rabbits immunised with the antigens combined, the parasite growth-inhibitory properties of the induced Abs were not enhanced over that seen with Abs from sera of single antigen immunised animals tested against heterologous parasites. Phase 1 clinical trials to assess the safety and efficacy of a vaccine based on these two allelic forms of PfAMA1 in formulation with the aluminium based adjuvant Alhydrogel in malaria naive human volunteers, showed it to be well tolerated (Malkin et al., 2005). Both allelic variants were comparably recognised. Furthermore, the Ab titre was found to correlate with the percentage invasion-inhibition *in vitro*, which ranged from 14 to 54%, both strains being inhibited equally. Phase 1 clinical trials have also been carried out using the refolded ectodomain of the 3D7 allelic form of PfAMA1 following expression in *E. coli* (Saul et

al., 2005). Potency and toxicity of the formulation (with adjuvant ISA720) were tested in mice. Unfortunately, the potency of the formulation decreased dramatically during the study and though 6 of the 29 malaria naive human volunteers seroconverted, Ab responses were generally very low and it was impossible to draw any meaningful conclusions from the study.

It is unlikely, considering the polymorphic nature of many malarial antigens, that a vaccine comprising a single subunit antigen will have long-term success. For this reason, many groups are considering AMA1 as a candidate in combination with other malaria blood stage antigens, particularly MSP1. Stowers et al. (2002) combined the FVO allelic form of PfAMA1, expressed in *P. pastoris*, with $PfMSP1_{42}$ from the same strain of parasite, this time expressed in a baculovirus system. This study assessed protection of this combination in *Aotus vociferans* monkeys. The Ab titre to the PfAMA1 component of the vaccine, but not the $PfMSP1_{42}$ component, correlated with protection. The overall efficacy of the vaccine was not significantly better than that for PfAMA1 alone. Burns *et al.* (2004) assessed the efficacy of the response induced by different adjuvant formulations in a PcAMA1/$PcMSP1_{42}$ vaccine. A high level of protection was observed in mice immunised with an adjuvant Quil A formulation, using relatively low doses of antigen. When used alone, PcAMA1 provided slightly more protection than $PcMSP1_{42}$, despite Ab titres being higher to $PcMSP1_{42}$. However, on challenge of immunised mice, the combined formulation resulted in a significantly greater reduction in peak parasitaemia over that seen with either antigen administered alone. In addition, these workers demonstrated that above a critical level, additional Ab was not accompanied by an increase in protection. This suggests that Ab levels alone are not absolutely reliable tools for determining protection against malaria. In an effort to better define the protective responses associated with either antigen, this group immunised immune-deficient mice with the Quil A formulations of these antigens (Burns et al., 2004). They deduced that while protection provided by PcAMA1 was Ab dependent (as previously mentioned) $PcMSP1_{42}$ protection also required both Ab and cell mediated responses. This antigen combination should therefore induce both humoural and cell mediated responses to malaria, a requirement that has been reported previously, at least for clearance of *P. chabaudi* infection.

Pan *et al.* (2004) made a chimeric construct of PfAMA1 DIII and $PfMSP1_{19}$, linked via a hinge region. Immunisation in rabbits with this construct induced high Ab titres to both antigens that inhibited parasite growth *in vitro* by over 95%. Immunisation of rhesus *Macaca mulatta* monkeys resulted in a strong Ab response to both antigens (Pan *et al.* 2004). The ability of serum from these monkeys to inhibit growth of *P. falciparum* parasites when cultured *in vitro*, correlated with the number of immunisations. A decrease in growth inhibition was observed only two months after the last immunisation though the reason for this was not determined. The group also reported proliferation of lymphocytes isolated from the immunised monkeys, in response to stimulation with this antigen. Whether this cellular response can function synergistically with Abs to this chimeric antigen and provide long-term immunity to malaria *in vivo* was not investigated.

1.8.4.4: Alternative delivery systems

1.8.4.4.1: Vaccinia virus: Several groups have investigated the use of alternative delivery systems in the hope of promoting a long-lived immune response. Vaccinia virus induces broad and effective immune responses. The use of this as a delivery system for malarial antigens could help to boost the immune response in the recipient, while overcoming problems associated with storage, transport and delivery of recombinant protein based vaccines. Pye *et al.* (1991) attempted to construct a recombinant vaccinia virus against *P. falciparum* malaria, using the four *P.falciparum* blood stage antigens (Pf) ring associated erythrocyte surface antigen (PfRESA), PfMSP1, PfMSP2 and PfAMA1. *Saimiri sciurus* monkeys were immunised with vaccinia virus constructs expressing these antigens and were challenged with *P. falciparum.* Antibody titres to the four antigens increased to varying degrees post challenge (a good Ab response was observed to PfAMA1). However, no difference was observed in the course of infection between the immunised and control monkeys. This result suggested that the inability of this vaccine to provide protection may result from problems with the vector or with suboptimal expression of the foreign genes. In another study, the highly attenuated NYVAC strain of vaccinia virus was used (Tine et al., 1996). A malaria vaccine based on this strain has previously been shown to confer protection in experimental challenge (Lanar et al., 1996). Seven *P. falciparum* antigens were used in this study; PfCSP, *P. falciparum* sporozoite surface protein 2 (PfSSP2), PfMSP1, serine repeat antigen (SERA), PfAMA1, the 25 kDa sexual stage antigen Pfs25 and LSA1. These were inserted into the NYVAC vector to generate the construct NYVAC-Pf7. Expression of all of these malaria antigens was confirmed by immunoprecipitation from NYVAC-Pf7 infected HeLa cells. Immunisation of mice, rabbits and rhesus macaque monkeys resulted in no detectable adverse effects. Serum from immunised monkeys recognised antigens expressed in the different parasite stages. Identification of Abs directed against PfAMA1, PfLSA1 and SERA was not carried out. However, Abs to PfCSP, PfSSP2, PfMSP1 and Pfs25 were detected in all monkeys. The protective efficacy of this vaccine has yet to be determined.

1.8.4.4.2: DNA vaccines: These are promising tools for the simultaneous delivery of multiple antigens. Rogers *et al.* (1999) investigated the use of DNA vaccine technology for the delivery of four *P. vivax* antigens. This vaccine included two pre-erythrocytic stage antigens CSP (PvCSP) and SSP2 (PvSSP2) and the two erythrocytic stage antigens MSP1 (PvMSP1) and AMA1 (PvAMA1). Transient transfection in mammalian UM449 cells resulted in expression of all four antigens. Serum from mice immunised with the vaccine plasmids recognised sporozoites (PvCSP, PvSSP2 and PvAMA1) or infected erythrocytes (PvAMA1 and PvMSP1) in immunofluorescence assay and in Western blot analysis. Sera from PvCSP immunised mice was unable to inhibit invasion of cultured hepatocytes by *P. vivax* sporozoites in an assay in which a protective anti-PvCSP mAb (NVS3) inhibited invasion by 90%. Nor did they recognise the amino acid motif AGDR, contained within the central repeat sequence of CSP, recognised by this mAb. Sera raised against PvAMA1 did not recognise AMA1 from reduced sporozoite or

infected erythrocyte protein extracts in Western blot. The ability of this conformation dependent antibody response to confer protection was not tested in this animal model. In a further study, Rogers *et al.* (2001) used the same four antigens, this time from *P. knowlesi*, in a prime-boost vaccine strategy. *Macaca mulatta* (rhesus) monkeys were immunised three times with plasmid DNA encoding the antigens. Six months after the final immunisation they were boosted with recombinant canarypox viruses encoding the four antigens. Only one monkey displayed complete protection after challenge with *P. knowlesi* sporozoites. Parasitaemia in the remaining immunised monkeys was significantly lower than that of the control group on days 9 to 12 post challenge. In contrast, the slopes of the parasitaemia curves, from patency to peak parasitaemia, did not differ significantly between the two groups. The group suggested that the limited protection observed in the immunised monkeys was probably directed against the pre-erythrocytic stages resulting in fewer liver stage schizonts completing their development. This would result in a lower initial blood stage infection and an extended pre-patent period. Why this strategy was unable to induce an effective immune response against the blood stage antigens used here is unclear. However it does highlight the fact that an ineffective pre-erythrocytic stage vaccine merely delays the detection of infection, but does not alter its final course. It is also worth noting that as AMA1 is expressed in merozoites as well as sporozoites, the protective response induced in these animals was unlikely to be induced by this antigen, unless AMA1 function in these parasite stages is different.

One possible complication arising from the use of multi-component vaccines is that of antigenic competition. Instead of the components of a vaccine inducing an immune response that is equivalent to the sum of the responses induced to the antigens when used alone, antigenic competition results in the immune response to one antigen down-regulating the response to the other. Ideally, the individual immune responses within a multi-component vaccine should be at least as good as those induced when used alone. A study to investigate the antigenic competition between antigens expressed from DNA vaccine plasmids administered together, considered the three *P. falciparum* erythrocytic stage antigens PfAMA1, PfMSP1 and EBA175 (Jones et al., 2002). No antigenic competition was observed in the combined vaccine. In addition, the collective Ab activities of the trivalent vaccine gave a higher overall Ab titre in IFA than that resulting from immunisation with any of the antigens individually. Rainczuk *et al.* (2004) have investigated the use of a bicistronic DNA delivery system for delivery of a PcAMA1 and PcMSP4/5 based vaccine. This group suggest that a bicistronic vaccine expression system may increase the efficiency of antigen delivery and promote the likelihood of synergistic responses between the antigens. The system utilises an internal ribosome entry site positioned between the two coding sequences, allowing ribosome attachment and translation of the downstream sequence (*Pfmsp1* fused to the monocyte chemotactic protein 3, MCP-3, coding sequence). Translation of the upstream sequence (*Pfama1* fused to a tissue plasminogen activator secretion signal) relies on cap-dependent mechanisms. Intra-muscular delivery of this vaccine enhanced survival of mice after challenge with 10^5 *P. chabaudi* infected erythrocytes.

The stimulation of splenocytes, isolated from immunised animals, with either recombinant antigen resulted in cell proliferation. The presence of MCP-3 fused to AMA1 would recruit dendritic cells to the site of antigen expression and enhance priming of naive T-cells by both antigens. This bicistronic DNA delivery system may prove to be a useful tool for the delivery of a multiple antigen malaria vaccine.

The weight of evidence suggests that while an Ab response to AMA1 is extremely potent against the malaria parasite, it is short lived. Indeed, field studies suggest that Ab responses to blood stage antigens in general are short lived (Cavanagh et al., 1998; Giha et al., 1999). To overcome this problem a vaccine must be designed either to primarily include T-cell determinants from the AMA1 ectodomain or to combine AMA1 with some other parasite antigen that primarily induces a cellular response. In view of the polymorphic nature of many malaria antigens, a combination of these two approaches would probably give the best wide-ranging, long-term results. However, the more components included in a vaccine increase not only the cost but also the difficulty of ensuring minimal batch variability. The target population for a malaria vaccine is largely the developing world; therefore, the expense of a multi-component vaccine could prove prohibitive.

1.8.5: Function of AMA1 in invasion

The function of AMA1 in host cell invasion is unknown. As discussed earlier, proteins residing in the micronemes of apicomplexan parasites are thought to be involved in parasite attachment to host cells and tight junction formation. Its localisation within the micronemes of *Plasmodium* merozoites and sporozoites, as well as *Babesia* merozoites and *Toxoplasma* tachyzoites indicates a role for AMA1 at this stage in the process. Furthermore, the inability to disrupt the gene encoding PfAMA1 indicates that its function is essential for parasite survival.

1.8.5.1: RBC Binding

In apicomplexan parasites, micronemes appear largely to house parasite adhesins involved in host cell binding and tight junction formation (Adams et al., 1990; Kaneko et al., 2000; Mayer et al., 2001; Gilberger et al., 2003b). Each of the cysteine rich domains (M1 and M2) of MAEBL, show sequence identity to DI-II of AMA1 (Hodder et al., 1996; Kappe et al., 1998a). The MAEBL domains M1 and M2 have been demonstrated to bind erythrocytes (Kappe et al., 1998a). Together, these findings have led this, and other, group(s) to suggest that AMA1 is involved in RBC binding. Peptides derived from PfAMA1 bind human erythrocyte and block merozoite invasion (Urquiza et al., 2000; Salazar et al., 2002; Cubillos et al., 2002). Replacement of the *ama1* gene in *P. falciparum* parasites with that of *P. chabaudi*, by reverse genetics, partially complemented the function of PfAMA1, but crucially, enhanced the invasive capability of these parasites for murine erythrocytes (Triglia et al., 2000). Thus, AMA1 must play a direct role in determining host cell specificity. In addition, in the presence of the rat mAb (R31C2) against

PkAMA1 that inhibits *P. knowlesi* invasion of rhesus erythrocytes, there is formation of the initial long-range (12 nm) attachment between the parasite and erythrocyte membranes, however, the intimate interaction (4 nm) resulting from tight junction formation does not form (Mitchell et al., 2004). Expression of *P. yoelii* AMA1 (PyAMA1) DI-II and to a significantly lesser extent the full-length ectodomain, on the surface of COS-7 cells facilitated the binding of rodent but not human erythrocytes to these cells (Fraser et al., 2001). By contrast, Kato *et al.* (2005) demonstrated binding of DIII of PfAMA1, expressed on the surface of CHO cells, to trypsin treated human erythrocytes although DI-II and the full-length ectodomain did not bind. However, in contrast to all these results using recombinant protein, the PfAMA1 shed forms from *P. falciparum* parasites cultured *in vitro* failed to bind human erythrocytes (Howell et al., 2001; E. Knuepfer, personal communication).

1.8.5.2: Re-localisation of AMA1 on the merozoite surface

The cytoplasmic tail of PfAMA1 is highly conserved across all *Plasmodium* species suggesting that it has an essential, conserved function. Howell *et al.* (2001) proposed that the cytoplasmic tail of AMA1 interacts with an actomyosin motor at the merozoite surface in a manner similar to that described for the *T. gondii* tachyzoite microneme protein 2 (MIC2) (Carruthers and Sibley, 1997) and the *Plasmodium* sporozoite protein thrombospondin-related anonymous protein (TRAP) (Kappe et al., 1999; Matuschewski et al., 2002). After secretion from the microneme, both MIC2 and TRAP are capped in a cytochalasin D sensitive manner towards the parasite's posterior end, before being proteolytically cleaved from the surface. The capping of these proteins from the anterior to posterior end of the parasite is thought to be responsible for propulsion of the parasite during gliding motility and invasion (Kappe et al., 1999). Cytochalasin D inhibits actin polymerisation. The sensitivity of MIC2 and TRAP capping to cytochalasin D implicates the actomyosin motor in these processes. In contrast, redistribution of PfAMA1 across the merozoite surface is unaffected by cytochalasin D at levels that block merozoite invasion of erythrocytes (Howell et al., 2003a). This suggests the involvement of an alternative cytoskeletal motor. Alternatively, AMA1 may redistribute across the parasite surface simply by diffusion, which is consistent with its circumferential distribution in free merozoites. If the C-terminus of the molecule is not involved in interaction with the actomyosin motor its conserved nature suggests that it is involved in some alternative, conserved invasion related process.

1.8.5.3: Signal transduction

The degree of homology within the cytoplasmic tail of AMA1 across apicomplexan taxa is not so conserved as between *Plasmodium* species (Hehl et al., 2000, Gaffar *et al.* 2005) and this region in TgAMA1 and BbAMA1 differs considerably from *Plasmodium* AMA1. However, one of two terminal tyrosine residues (positions Y621 and Y622 in PfAMA1), a SFW motif (position 601-603 in PfAMA1) and a threonine residue (position T613 of PfAMA1), all of which are absolutely conserved in AMA1 across *Plasmodium*, are also conserved in TgAMA1. Of these, only the W603 and T613 (in the *P. falciparum* sequence) are conserved in BbAMA1. However,

Y585 and S610 that are conserved in AMA1 from all *Plasmodium* species are also conserved in BbAMA1. Tyrosine, serine and threonine residues are potential candidates for phosphorylation. The abundance of such conserved residues in the cytoplasmic tail could support the putative involvement of AMA1 in signal transduction (Waters et al., 1990). Mass spectrometric analysis of PfAMA1 derived from late stage schizonts (Howell et al., 2001) and immunoprecipitation of [^{35}S] methionine metabolically labelled schizonts, using an anti-phosphotyrosine mAb (Narum and Thomas, 1994b) has indicated that the terminal tyrosine residues do not undergo phosphorylation at this stage of the parasite life cycle. This does not rule out the possibility that these residues participate in signal transduction during merozoite invasion of host erythrocytes and that phosphorylation occurs only after merozoites release from schizonts. Detection of the cytoplasmic tail of PfAMA1 in ring stage parasites indicates that it is taken into the RBC with the merozoite (Narum and Thomas, 1994b; Howell et al., 2005). It is possible that these residues are phosphorylated and function in the early intra-erythrocytic stage of development.

1.9. Aims of this project

The main aim of this project was to attempt to characterise the function of this essential parasite molecule. This relied on the use of recombinant protein expressed in heterologous eukaryotic systems. The conformation of these recombinant forms was assessed using the mAb 4G2dc1 (4G2dc1 expressing hybridoma cells were the kind gift of Alan Thomas, Biomedical Primate Research Centre, The Netherlands) that recognises a conformation dependent, reduction sensitive epitope in the ectodomain of PfAMA1 (Kocken et al., 1998a).

The assertion that AMA1 participates in erythrocyte invasion by mediating host cell recognition and binding was investigated using the system adopted by (Fraser et al., 2001). The ectodomain of PfAMA1 was expressed on the surface of COS-7 cells with its cognate transmembrane and cytoplasmic domains. It was predicted that the presence of the transmembrane and cytoplasmic domains would ensure the presentation of the molecule in the correct orientation on the cell surface. The erythrocyte binding potential of the PfAMA1 ectodomain was further investigated using the soluble, *Pichia pastoris* expressed ectodomain immobilised on a solid support. The requirement for other parasite proteins in AMA1 mediated erythrocyte binding was assessed by immunoprecipitation of PfAMA1 from highly segmented schizonts and merozoites, using the mAb 4G2dc1. Partner proteins should be co-precipitated.

In an attempt to identify the functionally important region(s) of the PfAMA1 ectodomain, the epitope recognised by the rat mAb 4G2dc1, that also inhibits invasion of human erythrocytes by *P. falciparum* merozoites, was characterised (Kocken et al., 1998a). Antibody molecules are large (about 160 kDa), thus, invasion-inhibition may result from non-specific steric hindrance. However, the epitope recognised by 4G2dc1 may be located within a region of AMA1 that is important for its function. To distinguish between these two possibilities, it was necessary to determine the effects

of the 4G2 Fab fragments on invasion, since steric hindrance of AMA1 function should be reduced with this Ab fragment. The epitope recognised by this mAb lies within DI-II of the PfAMA1 ectodomain (Lalitha et al., 2004). In the current study, site directed mutagenesis was performed within this region of the ectodomain in an attempt to specifically disrupt 4G2dc1 recognition, without altering the overall architecture of the molecule. The mutant forms, expressed in COS-7 cells, were assessed for mAb 4G2dc1 recognition.

Microneme (Carruthers et al., 1999a) and rhoptry (Mital et al., 2005) secretion during host cell invasion by apicomplexan parasites requires signal transduction across the parasites plasma membrane. The role of AMA1 in this process was assessed by investigation of the phosphorylation status of the PfAMA1 cytoplasmic tail in segmented schizonts and free merozoites. Parasites lysates were examined in Western blot analysis, using antibodies specific for phospho-serine, -threonine or -tyrosine.

All protein expression in this study relied on the use of a synthetic *Pfama1* gene (*sgPfama1*) designed for use in the methylotrophic yeast *P. pastoris* by Kocken *et al.* (2002). A full description of this gene can be found in section 6.1. Several amino acid substitutions were introduced in designing this gene, and it was therefore desirable to assess the functionality of this gene in *P. falciparum*. Plasmid vectors were designed for single or double homologous recombination into the *P. falciparum* genome, to replace the endogenous *Pfama1* gene with a haemagglutinin (HA) epitope tagged version of *sgPfama1* (*sgPfama1/HA*). Integration was assessed by Southern blot analysis and indirect immunofluorescence analysis of segmented schizonts and merozoites. Furthermore, the effect of the HA epitope tag on protein expression and function was assessed by integration of the tag into the endogenous *Pfama1* gene sequence.

Table 1.1: Summary of several key apical organelle proteins, their location and any features or functions currently identified.

Antigen	Organ.	Suggested Function(s)/Features
RAP1	R	Member of low molecular weight (LMW) complex. Involved in targeting of LMW complex to rhoptries. Non-essential for blood-stage growth (Howard et al., 1998; Baldi et al., 2000)
RAP2	R	Member of a LMW complex. Targeting to rhoptries can be disrupted by knock-out of the *rap1* gene (Baldi et al., 2000).
RAP3	R	Member of a LMW complex.
RhopH1	R	Member of a high molecular weight (HMW) complex.
RhopH2	R	Member of a HMW complex.
RhopH3	R	Member of a HMW complex. Binds RBC components and may be inserted into RBC plasma membrane (Sam-Yellowe et al., 1988; Sam-Yellowe and Perkins, 1991; Ndengele et al., 1995; Doury et al., 1997).
MAEBL	R	Erythrocyte binding protein. Expression can be disrupted without effecting blood-stage growth, but prevents infection of salivary glands by mid-gut sporozoites in the mosquito. (Kappe et al., 1998a; Noe and Adams, 1998; Fu et al., 2005)
AMA1	M	Possible function in RBC binding, reorientation, specificity of host cell recognition. Essential for blood-stage growth (Kappe et al., 1998a; Triglia et al., 2000; Fraser et al., 2001; Mitchell et al., 2004; Triglia *et al.* 2001,).
EBA-175	M	Possible function in tight junction formation. Binds sialic acid on glycophorin A on RBC surface. Non-essential for blood-stage growth (Sim et al., 1990; Adams et al., 1992; Orlandi et al., 1992; Kaneko et al., 2000; Reed et al., 2000).
BAEBL	M	Erythrocyte binding protein. Binds Glycophorin C on RBC surface. (Mayer et al., 2001; Narum et al., 2002)
DBPs	M	Tight junction formation in *P. vivax* and *P. knowlesi*. Binds Duffy blood group antigen on Duffy positive erythrocytes. (Miller et al., 1975; Miller et al., 1976; Haynes et al., 1988; Horuk et al., 1993)
SUB2	M	Subtilisin-like serine protease. MSP1 and AMA1 sheddase. (Hackett et al., 1999; Barale et al., 1999; Howell et al., 2003a)
SUB1	DG	Subtilisin-like serine protease. Minimal recognition sequence VXXD, physiological substrate unknown. (Blackman et al., 1998 ; Sajid et al., 2000 ; Jean et al., 2003)
RESA	DG	Associates with spectrin in erythrocyte cytoskeleton in newly invaded rings. (Foley et al., 1991; Da Silva et al., 1994)

Figure 1.1: Host cell invasion by the *Plasmodium* merozoite

(1) When the Plasmodium merozoite contacts a host erythrocyte, an initial weak interaction occurs between the parasite and the host cell membranes that may be mediated by parasite surface proteins. The parasite then reorientates, by a parasite driven or random process, until its apical end is in contact with the erythrocyte membrane. **(2)** A tight junction forms at the point of contact, irreversibly committing the parasite to RBC invasion. Proteins secreted from the micronemes may be involved in parasite reorientation and tight junction formation. **(3)** The RBC plasma membrane invaginates at the point of tight junction formation and the parasite is internalised in a parasite actinomyosin motor driven process. Parasite penetration of the host cell is coupled with the active redistribution or capping of apical organellar proteins towards the posterior of the parasite. A key feature of apicomplexan invasion is the shedding of parasite surface proteins by a tight junction-associated parasite protease. By comparison, invasion proteins accumulate in the tight junction and extra-cellular surface and are shed from the posterior end of the parasite when invasion in nearly complete. The rhoptry organelles release their contents into the developing parasitophorous vacuole (PV) and may be involved in modification of the PV membrane. As the parasite enters the host cell, the tight junction migrates in an anterior to posterior direction around the parasite surface, maintaining contact with the two membranes. When the parasite is completely internalised, the erythrocyte plasmalemma pinches off behind the parasite, enclosing it within the PV. Dense granule proteins may not be directly involved in the invasion process, but in *P. knowlesi* dense granules have been shown to release their contents by exocytosis into the PV. This event occurs concomitantly with the localised enlargement of the PVM, in which finger like projections protrude from the PVM extending into the erythrocyte cytoplasm. Host cell invasion by other apicomplexan protozoa, shares many of the key features of *Plasmodium* invasion.

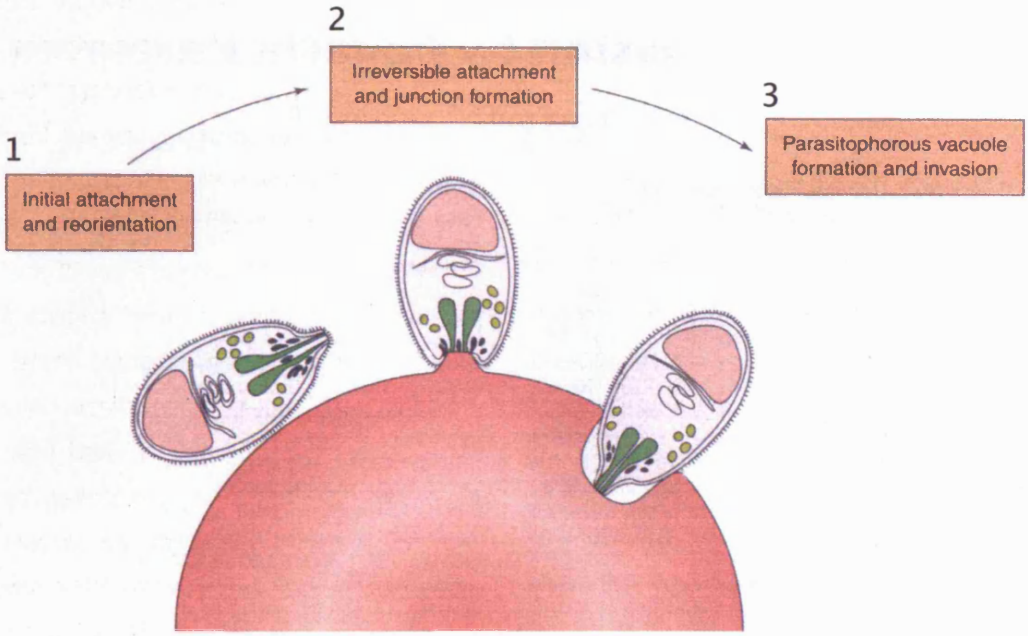

Reproduced from Chitnis and Blackman, 2000

Figure 1.2: The life cycle of *Plasmodium falciparum* parasites

Male (micro-) and female (macro-) gameocytes are taken up by the female *Anopheles* mosquito in a blood meal. The drop in pH and temperature in the mosquito midgut triggers gametogenesis. Microgametocytes undergo a process of maturation known as exflagellation to generate microgametes, while macrogametocytes mature to form macrogametes. **(1)** The male and female gametes fuse to form the diploid zygote, which matures to form the ookinete. This penetrates the midgut wall and develops in the area between the endothelium and the basal lamina, to form the oocyst. **(2)** Within the oocysts, haploid sporoblasts undergo numerous rounds of nuclear divisions, producing thousands of midgut sporozoites (sporogony). The oocysts rupture, releasing the sporozoites which then migrate to the mosquito salivary gland ducts.

The mosquito injects salivary gland sporozoites into the blood stream of the vertebrate host during the next blood meal. From there the sporozoites migrate to the liver, where they invade parenchyma cells, beginning the cycle of exoerythrocytic (pre-erythrocytic) schizogony. **(3)** Here the sporozoites develop into liver trophozoites (feeding stages) and ultimately schizonts, undergoing multiple rounds of nuclear replication and division, producing thousands of merozoites. The liver schizont ruptures, releasing the merozoites into the blood stream, where they invade erythrocytes, and so begins the erythrocytic schizogonic cycle **(4)**. The erythrocytic stage of the parasite life cycle is responsible for the pathology of the disease and for this reason is of greatest clinical significance. This stage of the life cycle is also the focus of this study and for this reason it will be considered in greater detail later (Fig 1.3). During the erythrocytic cycle, some merozoites invading erythrocytes deviate from this pathway and differentiate into micro- or macrogametocytes that move to the peripheral circulation from where they can infect feeding mosquitoes.

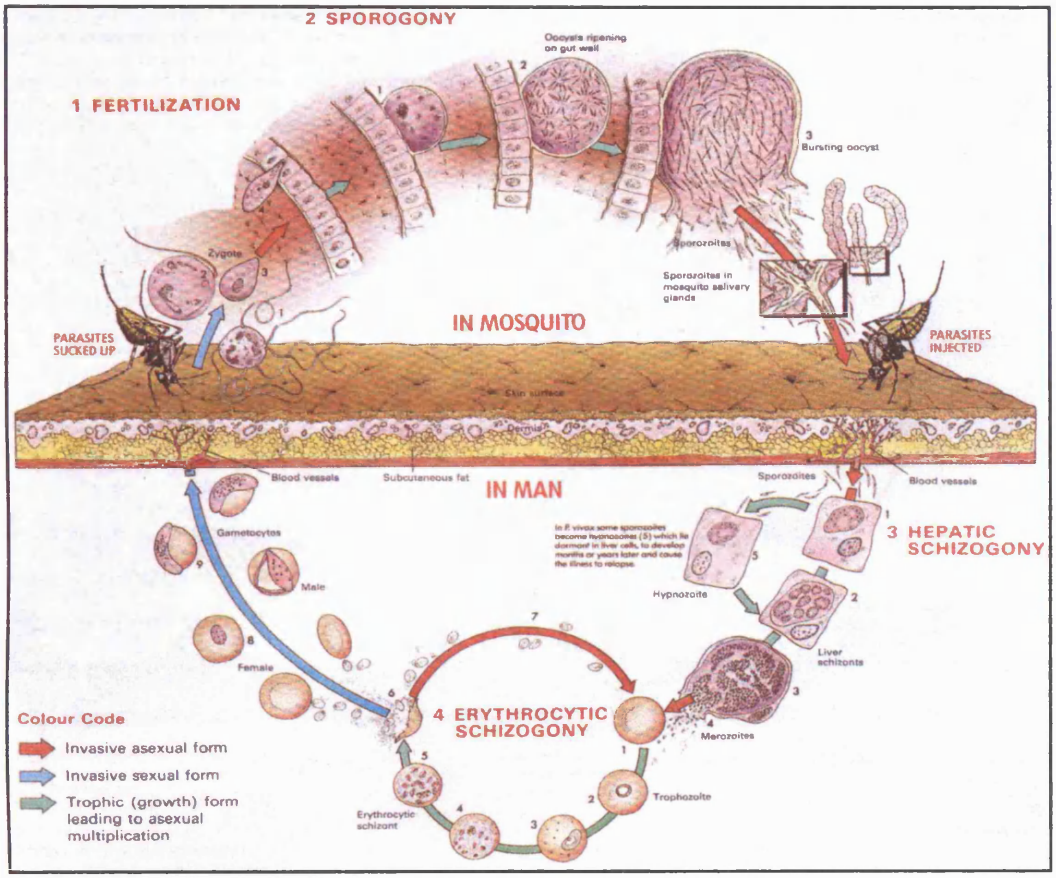

Reproduced from Knell, 1991

Figure 1.3: The erythrocytic cycle

(A) Within the erythrocyte, the parasite develops through ring **(1)**, trophozoite **(2)** and schizont stages **(3a and b)**, undergoing several rounds of nuclear replication and division, to produce 8 - 24 merozoites **(3b)** per schizont, depending on the parasite species. Nuclear division appears to be fairly relaxed, and deviations from these figures are not unusual. The erythrocytic schizont ruptures **(4)** releasing the merozoites into the blood stream where they invade fresh erythrocytes **(5)** and the cycle repeats. Merozoites are free in the circulation for a brief period between schizont rupture and reinvasion and during this period they are vulnerable to chemotherapeutic intervention and immune attack. Thus, the merozoite is of particular interest as a drug target and in vaccine design.

(B) The *P. falciparum* blood stage merozoite is about 1.6 μm long and 1.0 μm wide. This parasite stage exhibits a clearly polarised morphology. Three classes of secretory organelles are found apically located, the rhoptries, micronemes and dense granules. The two pear shaped rhoptries are about 650 nm long and 300 nm wide at their widest part. The micronemes are more numerous (about 40 per merozoite) but these elongated organelles are only about 120 nm by 40 nm and cluster around the rhoptry neck. The dense granules are located in the apical cytoplasm and are about 80 nm in diameter. Secretion from all of these organelles is tightly regulated during the invasion process. The nucleus adopts a basal location. The plasma membrane is connected via filamentous cross-bridges to two additional membranes, together forming the pellicle. Running down the length of the parasite are two (sometimes three) sub-pellicular microtubules that play an essential role in the invasion process. Three polar rings are positioned at the apical tip of the parasite, the third of which anchors the microtubules at their apical end. Towards the apical end of the parasite are a plastid (apicoplast) and a single mitochondrion that lie beneath the band of microtubules, the plastid being attached to them. In addition, numerous free ribosomes are also located towards the apical end, ready for the required burst of protein synthesis by the parasite immediately after invasion.

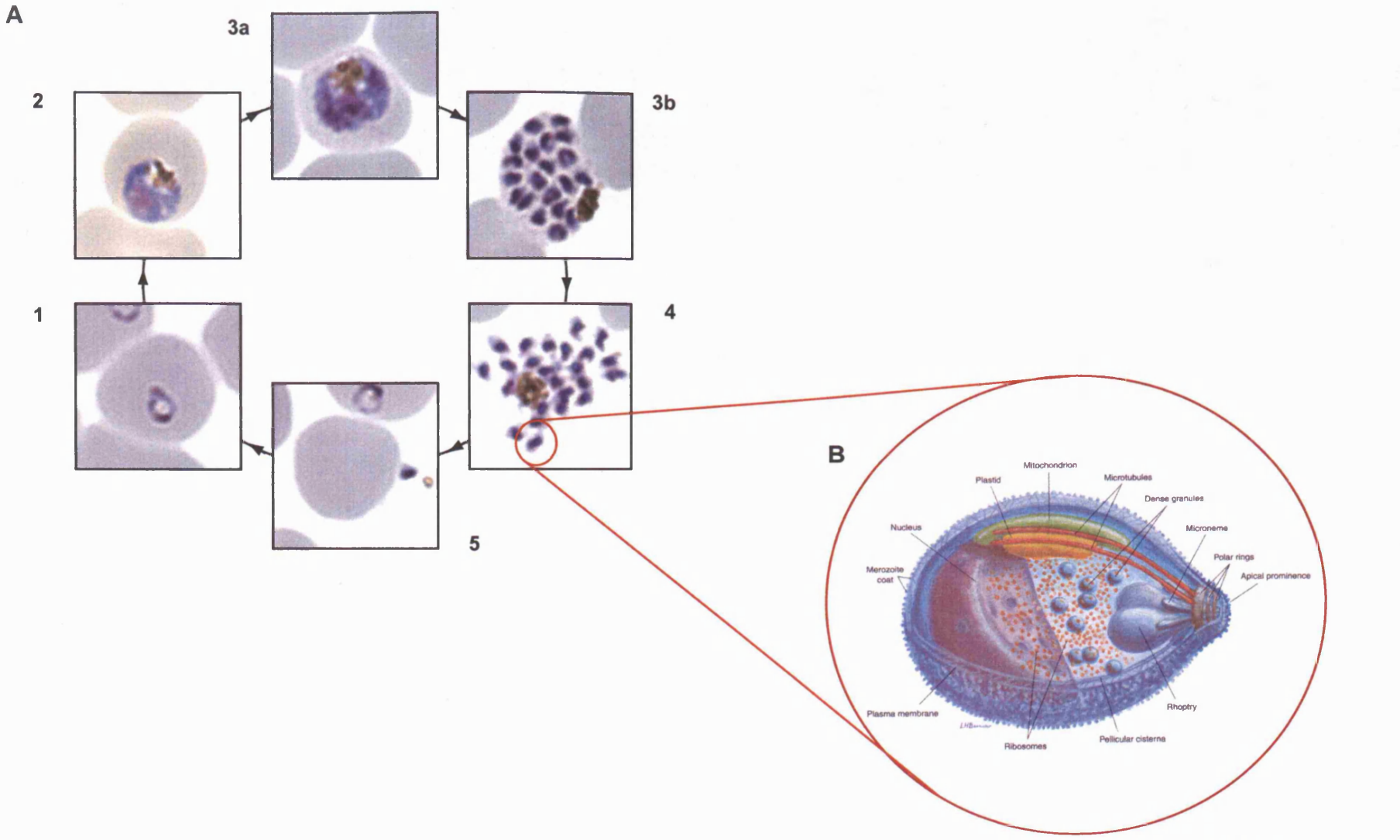

Bannister,L.H. (2000) Parasitology Today

Figure 1.4: Schematic representation of the PfAMA1 domain structure and disulphide bond pattern

PfAMA1 is comprised of an N-terminal signal peptide (SP) that is responsible for targeting AMA1 to the secretory pathway. In *P. falciparum* this is followed by a prodomain (PD), though this is absent in other species of *Plasmodium* with the exception of *P. reichenowi*. The ectodomain is subdivided into three domains (DI, DII, DIII) based on the disulphide bond pattern that has been identified. This type I integral membrane protein has a 21 amino acid transmembrane domain (TD), followed by a 55 amino acid C-terminal cytoplasmic tail (CT).

Sixteen cysteine residues are found in the ectodomain of *Plasmodium* AMA1, all of which are involved in disulphide bond formation. Three disulphide bonds are found in DI, two in DII and three in DIII. These are linked:

DI:

1) C149-C302 (C1-C6)

2) C217-C247 (C2-C3)

3) C263-C275 (C4-C5)

DII:

4) C320-C418 (C7-C10)

5) C337-C409 (C8-C9)

DIII:

6) C443-C502 (C11-C14)

7) C490-C507 (C12-C15)

8) C492-C509 (C13-C16)

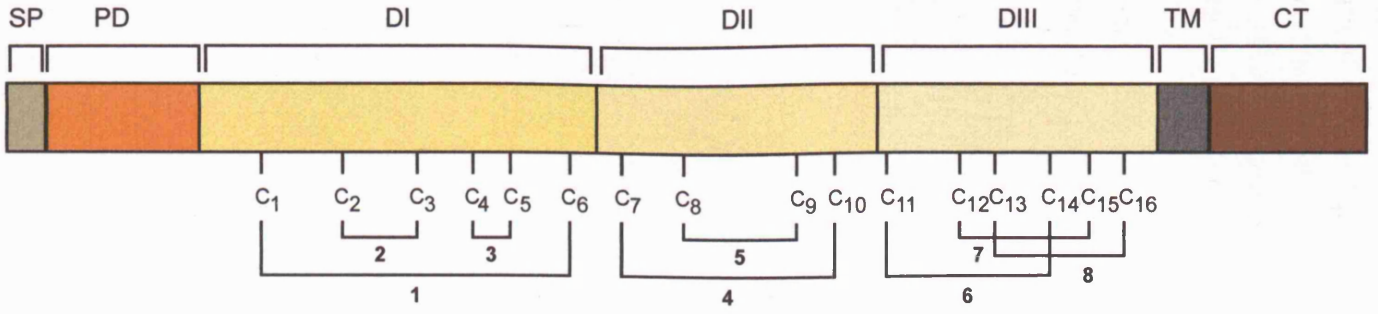

Key:

SP - signal peptide
PD - pro-domain
DI - domain I
DII - domain II
DIII - domain III
TM - transmembrane domain
CT - cytoplasmic tail

Figure 1.5: Schematic representation of PfAMA1 proteolytic processing

PfAMA1 localises to the micronemes of developing merozoites. Before release from the micronemes it is proteolytically processed to remove the N-terminal prodomain after Ser96 **(1)** and subsequently relocalises onto the parasite surface **(2)**. One third of PfAMA1 molecules undergo an additional processing event within DIII after Asn464 **(3)** to produce two fragments that are held together by a disulphide bond (Cys443-Cys502) in DIII. Finally, during the invasion process the molecule is proteolytically shed from the surface by a parasite protease (SUB2) which cleaves after Thr517.

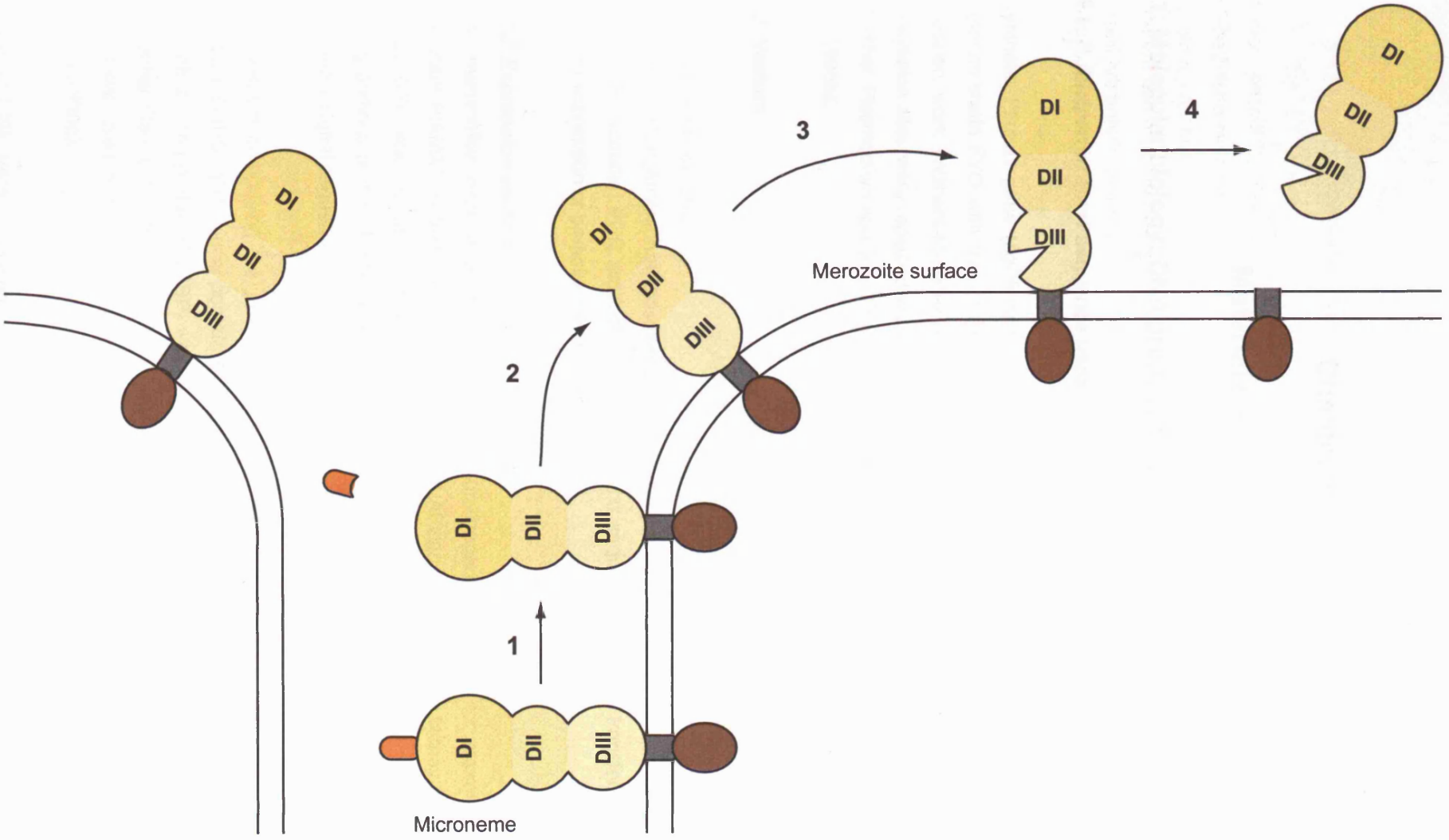
DI
DII
DIII
1
2
3
4
Merozoite surface
Microneme

Chapter 2

Materials and methods

2.1: Molecular biology: DNA production and amplification

2.1.1: *P. falciparum ama1* sequence used

A synthetic *Pfama1* gene (*sgPfama1*), designed to replace the A+T-rich codon usage of *P. falciparum* strain FVO with that of the methylotrophic yeast *Pichia pastoris*, was used for all expression work (Withers-Martinez et al., 1999). The sequence encoding six potential N-glycosylation sites were replaced with sequences encoding amino acid residues found in AMA1 from other *Plasmodium* species. These residues are not glycosylated in *P. falciparum* (Kocken et al., 1998b).

2.1.2: Vectors

2.1.2.1: Cloning vectors:

Vector pMOS*Blue* (Amersham Bioscience) was used as an intermediate vector to clone and amplify PCR products. PCR products were cloned and sequenced prior to transfer to other vectors for expression or parasite transfection.

2.1.2.2: Expression vectors:

(i) The mammalian expression vector pSecTag2a (Invitrogen) was used for expression of recombinant PfAMA1 (rPfAMA1) in SV40 transformed African green monkey kidney fibroblast cells (COS-7) cells. In all constructs, the full-length *sgPfama1* sequence, or regions of it encoding portions of the PfAMA1 ectodomain, was placed downstream of the vector-encoded Igκ secretory signal sequence.

(ii) A construct comprising the pRE4 plasmid containing the herpes symplex virus type I glycoprotein D (HSVgD1) signal peptide and transmembrane domain fused to region II of the *P. vivax* Duffy binding protein (PvDBP) was a kind gift of C. E. Chitnis (Malaria Research Group, International Centre for Genetic Engineering and Biotechnology, New Delhi India). This construct was used to transfect COS-7 cells, acting as a positive control for erythrocyte binding assays (resetting).

(iii) The pPIC9k vector (Invitrogen) was used for expression of the following PfAMA1 ectodomains: domain I (referred to as DI hereafter), domains I and II (referred to hereafter as DI-II) and domains I, II and III (referred to as DI-III hereafter), in *Pichia pastoris* strain KM71H

(Mut^S phenotype) (Fig 2.1) All were derived from *sgPfama1*, and were supplied by Chrislaine Withers-Martinez (Division of Parasitology, NIMR). The appropriate ectodomain sequence was inserted downstream of the vector-encoded α–factor secretory signal to allow secretion of the recombinant protein into the culture supernatant.

2.1.2.3: Parasite transfection plasmids:

(i) The pHAM-ACPGFP vector (kindly donated by Julie Healer, the Walter and Eliza Hall Institute, Melbourne, Australia) contains acyl carrier protein-green fluorescent protein (ACPGFP) under the control of the *Pfama1* promoter and *P.bergei* DT 3' UTR. The ACPGFP coding sequence was replaced with that of *sgPfama1*, for construction of a *sgPfama1* expression cassette. This expression cassette was used for analysis of sgPfama1 function in *P. falciparum* parasites.

(ii) The pHH1 transfection plasmid (Reed et al., 2000) was used for construction of a plasmid for episomal expression of *sgPfama1* and for single cross over integration plasmids designed to regenerate the endogenous *Pfama1* gene or to replace it with *sgPfama1*. This plasmid contains the human dihydrofolate reductase (*hdhfr*) selection cassette. This confers resistance on transfected parasites to the antifolate drug WR99210 (Jacobus Pharmaceuticals).

(iii) The pHH-TK plasmid was used to construct a transfection plasmid to replace the endogenous *Pfama1* gene with the *sgPfama1* expression cassette by double cross-over events. This plasmid contains the positive selection cassette *hdhfr* and the thymidine kinase (*tk*) negative selection cassette. Thymidine kinase (TK) confers parasites susceptible to the drug ganciclovir. In the presence of WR99210 and gancyclovir, only parasites that have undergone a double cross-over event and lost the *tk* gene while retaining the *hdhfr* gene will survive.

2.1.3: DNA modification and manipulation:

2.1.3.1: Restriction enzymes and buffers:

Restriction enzymes and buffers (Roche or NEB) were used according to the manufacturer's instructions. All restriction digestion products were purified using either a QIAquick® PCR purification kit, if there was only a single recoverable fragment, or a QIAquick® gel purification kit, when there were multiple fragments of recoverable size (both kits were supplied by Qiagen).

2.1.3.2: Formation of blunt end linear DNA:

Blunt end formation from complementary DNA ends was achieved using either the Klenow fragment of DNA polymerase (Roche), that has 3' to 5' exonuclease activity, or mung bean exonuclease (Promega), for 5' to 3' exonuclease activity. Both enzymes were used according to the manufacturer's instructions. To remove 3' overhangs and fill in 5' overhangs for blunt end

formation, T4 DNA polymerase (New England Biolabs, NEB) was also used according to the manufacturer's instructions.

2.1.3.3: Ligation:

Prior to ligation all vectors were alkaline phosphatase (Roche) treated to prevent religation, according to the manufacture's instructions and purified using a QIAquick® PCR purification kit (Qiagen). Ligations involving restriction enzyme modified DNA or Klenow blunt ended DNA, were carried out using a Rapid DNA ligation kit according to the manufacturer's instructions (Roche).

2.1.3.4.: Polymerase Chain Reaction (PCR)

Oligonucleotide primers were obtained from Eurogentec Oswel. PCR for the amplification of *sgPfama1* was carried out using AmpliTaq® DNA polymerase (Roche), or cloned *Pfu* polymerase (Stratagene) according to the respective manufacturer's instructions. PCR for the amplification of *P. falciparum* genomic DNA was performed using PLATINUM® *Taq* High Fidelity DNA polymerase (Invitrogen) or *Pfu* Turbo® DNA polymerase (Stratagene) according to the manufacturer's instructions. These enzymes have higher stringency proof reading facilities and therefore amplify this A+T rich DNA more reliably. PCR reactions were carried out in a ThermoHybaid Omn-E PCR machine.

Cloning involving unmodified PCR products was carried out using the pMOS*Blue* blunt ended cloning kit, according to the manufacturer's instructions (Amersham Bioscience).

All PCR products were purified using a QIAquick® PCR purification kit (Qiagen) according to the manufacturer's instructions.

2.1.3.5: Automated sequencing:

Cloned DNA was sequenced using the BigDye™ Terminator v1.1 cycle sequencing kit according to the manufacturer's instructions (Applied Biosystems). The amplification step was carried out in a ThermoHybaid Omn-E PCR machine using a program of 25 cycles of: 96°C for 45 s, 50°C for 30 s and 60°C for 2 min. Samples (20 µl) were ethanol precipitated by incubating for 1 hour in 50 µl 95% ethanol and 2 µl 3 M sodium acetate followed by centrifugation at 13,000 rpm in a micro-centrifuge (Biofuge pico Heraeus) for 20 min. The supernatant was discarded and the DNA washed in 500 µl 70% ethanol and centrifuged at 13,000 rpm for a further 5 min. The DNA pellet was dried by heating at 90°C for 3 min before resuspension in 10 µl MegaBACE™ loading solution (Amersham Bioscience). The sample was loaded onto a MegaBACE™ sequencing machine (Amersham Bioscience) using an injection voltage of 3 kV and injection run time of 40 s. The sample run was carried out at 9kV for 200 min.

2.1.3.6: Site directed mutagenesis (SDM)

SDM was carried out using the QuikChange® Site-Directed Mutagenesis Kit (Stratagene). For cloning purposes this technique was used to introduce restriction sites into, or remove restriction sites from the *Pfama1* coding sequence. The coding sequence was modified in such a way that the primary amino acid sequence was either unaltered or resulted in conservative amino acid substitutions.

SDM was used to alter the primary amino acid sequence and secondary structure of PfAMA1 to specifically disrupt recognition of the protein by the mAb 4G2dc1 (see section 2.4.1).

In order to systematically disrupt the disulphide bonds (DBs) in DI-II in the pSec/sg'Pfama1 plasmid (2.4.1.1), the codon for the first cysteine of each bond was replaced with the codon for alanine (TGC → GCC or TGT → GCT) using SDM. This gave rise to the plasmids pSec/sg'Pfa1ΔsDB1 - pSec/sg'Pfa1ΔsDB5. However, any expressed protein encoded by such a sequence would contain a free, reactive sulphydryl group (S-H), which may interfere with the folding of the protein. The second cysteine in each of the disulphide bonds in DI-II was subsequently replaced with alanine to stabilise the molecule, giving rise to the plasmids pSec/sg'Pfa1ΔdDB1 - pSec/sg'Pfa1ΔdDB5.

Analysis of the PfAMA1 DI-II primary sequence using JNet (Cuff and Barton, 2000) and Emini (Emini *et al.* 1985) algorithms, identified a large number of amino acid side chains predicted to be solvent accessible. Residues with the highest predicted solvent accessibility were analysed by SDM. Contiguous groups of residues were mutated primarily to alanine (e.g. XXX/AAA). Where an effect was observed on the subsequent reactivity with 4G2dc1, individual residues in the group were mutated either to alanine, or to a residue found in the analogous position of AMA1 sequence from another species of *Plasmodium*.

2.1.3.7: Bacterial strains (E. coli)

Sub-cloning efficiency DH5α™ competent cells (Invitrogen) were used for general cloning purposes with constructs intended for COS-7 cell expression. These cells were also used for amplification of parasite transfection plasmids. For increased cloning efficiency in the generation of random mutant libraries, "library efficiency" DH5α™ competent cells (Invitrogen) were used.

MOS*Blue* competent cells were used for cloning and amplification of PCR products, ligated into the pMOS*Blue* vector (competent cells and vector from Amersham Bioscience).

A+T rich *P. falciparum* sequences are often found to be unstable in *E. coli*. This instability can usually be overcome by the use of PMC-103 competent cells (kindly provided by Rebecca O'Donnell) for the initial cloning steps. However, in this study DH5α™ competent cells were

found to give more reliable results, with higher DNA yields and therefore this was the preferred bacterial strain for cloning.

2.1.3.8: Transformation of E. coli

Transformation of plasmid DNA into DH5α^{TM} and MOS*Blue* competent cells was carried out according to the manufacturer's instructions. PMC-103 competent cells were transformed by adding DNA to 100 µl of competent cells and incubating them on ice for 1 hour. The cells were then heat-shock treated at 42°C for 45 sec before being returned to ice for 2 minutes. 50 µl Luria broth was added to the cells and the mixture was incubated in a shaking incubator (New Brunswick Scientific, Innova 4000) for 1 hour at 37°C. The cells were then plated on Luria agar plates containing 50 µg ml^{-1}Ampicillin (Sigma).

2.1.3.9: Plasmid DNA preparation

Bacteria were grown overnight in Terrific broth for maximal bacterial yields. Plasmid DNA was then harvested using S.N.A.P. miniprep kits (Invitrogen) according to the manufacturer's instructions. DNA produced by this method was used for cloning, sequencing and for transfection of COS-7 cells. DNA for transfection into *P. falciparum* parasites was harvested using HiSpeed® plasmid Maxi kits, according to the manufacturers' instructions (Qiagen). DNA yield and purity were determined using a spectrophotometer (UNICAM - UV1). DNA was then ethanol precipitated and resuspended in Tris-EDTA buffer (TE), pH 8.0, to a final concentration of 2.3 - 3.3 µg ml^{-1}.

2.1.3.10: Genomic DNA extraction and plasmid recovery from P. falciparum *parasites*

DNA was extracted from 500 µl of parasitized erythrocytes containing 5% trophozoite/schizont stage parasites. To lyse the red blood cells (RBC), erythrocyte pellets (approximately 400 µl parasitised blood) were resuspended in 800 µl of 0.15% Saponin (BDH). Parasites were recovered by centrifugation at 13,000 rpm in a micro-centrifuge (MSE – Micro Centaur). Parasite pellets were resuspended in 4 × volume of Buffer A (see Appendix) and 1 × volume of 18% SDS was added to solubilise the parasites. This mixture was incubated at room temperature for 2 min. DNA was extracted by adding an equal volume of phenol chloroform (Sigma), vortexing to mix and centrifuging at 13,000 rpm in an micro-centrifuge (Heraeus – Biofuge pico) for 2 min. The aqueous phase was removed to a clean tube and the extraction repeated. DNA was then ethanol precipitated by adding 3 × volumes of absolute ethanol and 1/10th volume of 3 M sodium acetate. The sample was vortexed to mix and incubated at –70°C for 20 min. The sample was centrifuged for 20 min, the supernatant removed and the pellet washed in 250 µl 70% ethanol. This was centrifuged for a further 5 min, the supernatant removed and the pellet air dried, before being resuspended in 200 µl TE, pH 8.0 (see Appendix).

Plasmid DNA recovered from transfection line parasites by this method was cloned back into *E. coli* DH5α™ competent cells and tested by restriction digestion for rearrangements.

2.1.4: Plasmid construction

Oligonucleotide primers for all constructs are shown in Table 2.1.

2.1.4.1: Construction of pSec/sg'Pfama1 for surface expression in COS-7 cells

The *sgPfama1* gene was previously cloned into the *Eco*RI site in the cloning vector pMOS*Blue* (called FIM252, kindly provided by Fiona Hackett, NIMR). This construct contains the full synthetic gene sequence of *Pfama1* encoding the N-terminal signal sequence and prodomain through to the C-terminal cytoplasmic tail. In *P. falciparum*, the signal sequence and prodomain are proteolytically removed from the rest of the protein before it is released onto the parasite surface. Thus, to simulate this situation with COS-7 cell surface expression, we only required the coding sequence downstream of the prodomain i.e. from the beginning of domain I (DI, amino acid sequence 97IEIVE...) through to the cytoplasmic tail (amino acid sequence ...MEKPYY622).

2.1.4.1.1: Removal of the Pfama1 signal peptide and prodomain. The 5' region of *sgPfama1* was removed from FIM252 by restriction digestion with *Xba*I (this enzyme cleaves within the vector, upstream of the *sgPfama1* start site) and *Afl*II (which cleaves within domain I). The 5' region of DI was amplified by PCR, using oligonucleotides AMAfor1 and synthetic gene oligonucleotide 78 (see table 2.1. below). AMAfor1 was designed to introduce a *Xba*I site (shown in bold in table 2.1) for sub-cloning into *Xba*I/*Afl*II digested FIM252, followed by a *Sma*I site (highlighted in bold and underlined respectively in table 2.1) at the 5' end of DI. Oligonucleotide 78 is downstream of the *Afl*II site in DI. The PCR product was digested with *Xba*I and *Afl*II before cloning back into pre-digested FIM252 to give the intermediate plasmid pMOS/sg'Pfama1.

2.1.4.1.2: Cloning of sg'Pfama1 *into pSecTag2A.* The expression vector pSecTag2A was digested with *Sfi*I and blunt ended. This linearised vector was further digested with *Eco*RI. The *sg'Pfama1* coding sequence was excised from the plasmid pMOS/sg'Pfama1 by restriction digestion with *Sma*I (blunt ended digestion) and *Eco*RI. Gel purification of *sg'Pfama1* and ligation into pre-digested pSecTag2a gave the plasmid pSec/sg'Pfama1 (Fig 2.1.).

2.1.4.2: Construction of pSec/sg'DI

This construct was designed for the expression of PfAMA1 DI in COS-7 cells. The 3' half of DI was amplified by PCR from the plasmid pSec/sg'Pfama1, using the synthetic gene oligonucleotide 17 and DomIrev. Oligonucleotide 17 is upstream of the unique *Sac*II site in the plasmid. The reverse primer was designed to introduce an *Eco*RI site (in bold) for cloning

purposes, preceded by a stop codon (underlined) to be incorporated at the 3' end of DI. The plasmid pSec/sg'Pfama1 was digested with restriction enzymes *Sac*II and *Eco*RI, thus excising the *sgPfama1* coding sequence from the downstream 3' half of DI. The PCR product was also digested with *Sac*II and *Eco*RI and ligated into pre-digested pSec/sg'Pfama1. This resulted in the formation of the construct pSec/sg'DI (Fig 2.2.).

2.1.4.3: Construction of pSec/sgPfaΔDI

This construct was designed for expression of sg'PfAMA1 lacking DI. The starting plasmid was pSecΔ*Pst*I/sg'Pfa (generated for making the random mutant library, Section 2.1.4.7.) because the process of excising the *Pst* I site from the vector also resulted in the loss of both *Eco*RI and *Eco*RV sites. SDM was used in two steps to introduce *Eco*RV sites (in bold) at the 5' and 3' ends of sequence encoding PfAMA1 DI in the plasmid pSecΔPstI/sg'Pfa, using primers DI5'*Eco*RVf, DI5'*Eco*RVr, DI3'*Eco*RVf and DI3'*Eco*RVr. The resulting plasmid, sg'Pfa/*Eco*RV3'-5'DI, was digested with *Eco*RV to excise DI and the vector backbone re-ligated to give the plasmid pSec/sgPfaΔDI (Fig 2.3. A).

2.1.4.4: Construction of pSec/sg'PfaΔDII

This construct was designed for the expression of PfAMA1 lacking DII. For this purpose *Kpn*I sites were introduced by SDM at the 5' and 3' ends of the *sg'Pfama1* sequence encoding DII in the plasmid pSecΔ*PstI/sg'Pfa,* using the primers DII5'*Kpn*Ifor, DII5'*Kpn*Irev, DII3'*Kpn*Ifor and DII3'*Kpn*Irev. DI was then excised from the resulting plasmid, sg'Pfa/KpnI5'-3'DII, using these *Kpn*I sites and the vector re-ligated to give the plasmid pSec/sg'PfaΔDII (Fig 2.3. B).

2.1.4.5: Construction of pSec/sgPfaΔDI-II

This construct was designed for expression of PfAMA1 DIII with its transmembrane domain and cytoplasmic tail. A *Kpn*I site (highlighted in bold) was introduced by SDM at the 5' end of the sequence encoding DI using the primers DI5'*Kpn*If and DI5'*Kpn*Ir. The intermediate plasmid from section 2.1.4.4 with a *Kpn*I site at the 3' end of the DII coding sequence was used as the template, giving the plasmid sg'Pfa/KpnI5'DI-3'DII, with *Kpn*I sites flanking the coding sequence for DI-II. The plasmid was digested with *Kpn*I, thus removing the sequence encoding DI-II and the plasmid religated to give pSec/sgPfaΔDI-II (Fig 2.3. C).

2.1.4.6: Construction of pSec/tr1-sgPfama1 and pSec/tr2-sgPfama1

Two constructs were designed in which the 3' region of *sg'Pfama1* was truncated up to the sequence prior to that encoding the first cysteine residue in DI. The first truncation (T1) left the sequence encoding three native amino acid residues upstream of the first cysteine (SGK**C**$_1$...), while the second truncation (T2) left the sequence encoding eleven such amino acid residues (AGTQYRLPSGK**C**$_1$...). An *Eco*RV site (in bold) was introduced at the 5' end of the sequence encoding DI in the plasmid pSecΔPstI/sg'Pfa, using the primers *Eco*RVDIfor and *Eco*RVDIrev. In both cases a further *Eco*RV site (in bold) was introduced into the appropriate position, using

the primers Tr1EcoRVf and Tr1EcoRVr or Tr2EcoRVf and Tr2EcoRVr. The 5' region of the gene was then excised via these *Eco*RV sites and the resulting plasmid backbones re-ligated back together, giving the plasmids pSec/tr1-sgPfama1 and pSec/tr2-sgPfama1 (Fig 2.4 a and b).

2.1.4.7: Construction of a pSecΔPstI/sg'Pfa random mutant library

2.1.4.7.1: Removal of the Pst*I site from the pSecTag2a vector backbone.* The plasmid pSec/sg'Pfama1 was digested with *Eco*RI and *Eco*RV. Both restriction enzymes cleave within the vector just downstream of *sg'Pfama1*, flanking a *Pst*I site, thus digestion with these enzymes excises this site from the vector backbone. The plasmid was blunt ended with the Klenow fragment of DNA polymerase and re-ligated. This resulted in the plasmid pSecΔPstI/sg'Pfa. There is a unique *Pst*I site at the 3' end of *sgPfama1* sequence encoding domain II (DII) of PfAMA1. Removal of the *Pst*I site from the vector backbone allows the use of this site for subcloning purposes.

2.1.4.7.2: Cloning of sequence encoding DI-II random mutants. The plasmid pSecΔPstI/sg'Pfa was digested with *Xcm*I and *Pst*I, thus excising the sequence of *sgPfama1* encoding DI-II. The synthetic gene oligonucleotides 8 and 58 (see table 2.1), were used to amplify DI-II of *sgPfama1* under random mutagenic conditions. PCR conditions were selected to produce an average of 5 point mutations every 1 kb. Reaction conditions were: 10 mM Tris.Cl, 50 mM KCl, 7 or 9 mM $MgCl_2$, 1 mM dCTP, 1mM dTTP, 0.2 mM dATP, 0.2 mM dGTP, 2 μM 5' primer, 2 μM 3' primer, 20 pg μl^{-1} template DNA, 0.5 mM $MnCl_2$ and 0.05 U μl^{-1} Taq DNA polymerase. The PCR conditions were as follows: 94°C for 3 min followed by 58°C for 45 s, 72°C for 2 min and 94°C for 45 s repeated for 29 cycles with a 10 minute extension time at 72°C. PCR products were digested with *Xcm*I and *Pst*I. The digestion products were gel-purified and ligated into *Xcm*I/*Pst*I digested pSec/sg'Pfama1. In order to generate a library of random mutant forms of pSec/sg'Pfama1, *E. coli* transformed with the ligation mixture were grown directly in liquid culture. The library of *sg'Pfama1* random mutants obtained after plasmid recovery from *E. coli* was called sg'Pfa1RML (Fig 2.5.).

2.1.4.8: Construction of pHH1-3'Pfama1

This construct was designed for integration into the 3' region of *Pfama1* coding sequence of *P. falciparum* parasite strain 3D7, thus regenerating the *Pfama1* gene.

The 3' coding region of *Pfama1* was amplified from *P. falciparum* strain T9/96 genomic DNA (kindly provided by Fiona Hackett) using primers 3D7-3'-900f and 3D7-3'-900r. These were designed to introduce 5' *Bgl*II and 3' *Xho*I sites respectively (highlighted in bold). The *Xho*I site in the reverse primer is immediately downstream of the TAA stop codon. The PCR product was cloned into pMOS*Blue* (called pMOS/3'Pfama1) and subsequently digested with *Bgl*II and *Xho*I and gel purified. The SERA4 gene was excised from the plasmid pHH1-ρSERA4 (Miller et al., 2000) using *Bgl*II and *Xho*I and the vector backbone was gel purified. The *Bgl*II/*Xho*I digested 3'

region of *Pfama1* was then ligated into the pHH1 vector backbone to produce plasmid pHH1-3'Pfama1 (Fig 2.6.).

2.1.4.9: Construction of pHH1-Pfa/HA

This construct was designed for integration into the *Pfama1* coding sequence in order to introduce a single haemagglutinin (HA) epitope tag (YPYDVPDYA) into the region of the gene just upstream of the transmembrane coding region. The gene sequence from 46bp downstream of the start codon was amplified to increase the likelihood of integration occurring upstream of the HA tag.

2.1.4.9.1: Amplifying the Pfama1 coding sequence. The *Pfama1* gene was amplified by PCR from T9/96 *P. falciparum* genomic DNA using the primers 3D7-5'-for and 3D7-3'-900r (see above). The forward primer allows amplification from 46bp downstream of the *Pfama1* start codon and was designed to insert a *Bgl*II site (highlighted in bold) at the 5' end of the amplified product for cloning purposes. The resulting PCR product was cloned into pMOS*Blue* (called pMOS/T9/96Pfama1).

2.1.4.9.2: Introducing the HA epitope tag into the Pfama1 *gene.* The HA epitope tag was introduced into the *Pfama1* coding sequence by SDM in a two-step process. The second half of the tag was introduced first using the primers 3D7HA2ndf and 3D7HA2ndr. Once this was successfully achieved, the first half of the HA tag was introduced using the primers 3D7HAflfor and 3D7HAflrev. This gave rise to the plasmid pMOS/Pfa/HA. The plasmid was digested with *Bgl*II and *Xho*I and the insert purified by gel extraction. This was ligated into *Bgl*II/*Xho*I digested pHH1-pSERA4 vector backbone, previously digested for the construction of pHH1-3'Pfama1 and resulted in the plasmid pHH1-Pfa/HA (Fig 2.7.).

2.1.4.10: Construction of pHAM-sgPfa/HA

This construct was designed for episomal expression of HA-tagged *sgPfama1*, under the control of the *Pfama1* promoter and the 3' termination sequence of the *P. berghei* DHFR-thymidylate synthase (DHFR-TS) gene (PbDT3'). Utilising the *Pfama1* promoter should ensure expression at the correct point in the parasite life cycle.

2.1.4.10.1: Removal of the Xho *I site in* sgPfama1. The *Xho*I site in the region of *sgPfama1* encoding DI of PfAMA1 was removed by SDM of pSec/sg'Pfama1, without altering the amino acid sequence encoded by the gene (the DNA sequences CTCGAG and CTGGAA both encode amino acid residues LE). SDM was carried out using the primers Δ*Xho*Ifor and Δ*Xho*Irev giving the plasmid pSec/sg'PfaΔ*X*.

2.1.4.10.2: Insertion of the HA epitope tag into the stub region of sgPfama1. The HA epitope tag was introduced into *sg'Pfama1* in the plasmid pSec/sg'PfaΔ*X* in two steps as for the

endogenous gene. The second half of the tag was introduced first using the primers sgPfA2ndHAf and sgPfA2ndHAr. The primers sgPfAflHAf and sgPfAflHAr were then used to introduce the first half of the HA epitope tag giving the plasmid pSec/sg'PfaΔX/HA. The region of *sg'Pfama1* from which the *Xho*I site had been removed, and into which the HA epitope tag had been introduced, was subcloned into FIM252 via *Ksp*I and *Stu*I restriction sites giving rise to the plasmid pMOS/sgPfaΔ*X*/HA.

2.1.4.10.3: Cloning of sgPfama1 *into pHAM-ACPGFP.* The modified *sgPfama1* was amplified from pMOS/sgPfaΔX/HA by PCR using the primers 5'sgPfama1f and 3'sgPfama1r. These primers were designed to introduce *Xho*I sites (highlighted in bold) at either end of the synthetic gene for cloning purposes. The PCR product was digested with *Xho*I and purified. The vector pHAM-ACPGFP was digested with *Xho*I to excise the ACPGFP fragment and the vector backbone (pHAMΔACPGFP) alkaline phosphatase treated and PCR purified. The modified *sgPfama1* PCR product was ligated into pHAMΔACPGFP, generating the plasmid pHAM-sgPfa/HA (Fig 2.8.).

2.1.4.11: Construction of pHH1-5'-sgPfa/HA

This construct was designed to integrate into the 5' coding sequence of *Pfama1*, thus disrupting the endogenous *ama1* gene and replacing it with the HA tagged synthetic gene sequence.

2.1.4.11.1: Amplification and cloning of the Pfama1 *5' coding sequence.* The *Pfama1* 5' coding sequence was amplified by PCR from T9/96 *P. falciparum* genomic DNA, using the primers 3D7-5'-for (used for construction of pHH1-Pfama1/HA) and 3D7-5'-rev. The resulting PCR product was cloned into the pMOS*Blue* vector giving pMOS/5'Pfama1. This plasmid was digested with *Bgl*II and *Xho*I to remove the 5' *Pfama1* coding sequence and this fragment gel extracted and ligated into *Bgl*II/*Xho*I digested pHH1-pSera4 (prepared for construction of pHH1-3'Pfama1). This gives the plasmid pHH1-5'Pfama1. This plasmid was digested with *Xho*I to linearise it and was subsequently blunt ended using T4 DNA Polymerase and alkaline phosphatase treated. The plasmid was PCR purified between steps and after the alkaline phosphatase treatment.

2.1.4.11.2: Cloning the sgPfama1 *expression cassette into pHH1-5'Pfama.* The *sgPfama1* expression cassette, consisting of the *sgPfama1*, flanked 5' and 3' by *Pfama1* 5' UTR and PbDT3' UTR respectively, was excised from the plasmid pHAM-sgPfa/HA by digestion with *Hind*III and *Not*I. The expression cassette was blunt ended with T4 DNA Polymerase and ligated into pHH1-5'Pfama1 (previously blunt ended), downstream of the 5' *Pfama1* coding sequence, thus producing the plasmid pHH1-5'-sgPfa/HA (Fig 2.9.).

2.1.4.12: Construction of pHTK-sgPfa/HA

This construct was designed for double cross-over integration into the parasite genome on either side of the *Pfama1* coding sequence, thus excising the endogenous *Pfama*1 gene and replacing it with the *sgPfama1* expression cassette.

2.1.4.12.1: Amplification and Cloning of the Pfama1 *3' UTR.* The *Pfama1* 3' UTR was amplified from T9/96 genomic DNA by PCR using the primers Pfa1-3'UTRf and Pfa1-3'UTRr. The primers were designed to introduce *Nco* I and *Bin* I (*Avr* II) restriction sites at the 5' and 3' ends of the PCR product respectively. The amplified product was cloned into pMOS*Blue* (giving the plasmid pMOS-Pfa3') for amplification and then excised using *Nco* I and *Bin* I. The transfection plasmid pHHT-TK was also digested with *Nco* I and *Bin* I and the 3' UTR fragment ligated into it to give the plasmid pHTK-Pfa3'.

2.1.4.12.2: Cloning the sgPfama1 *expression cassette into pHTK-Pfa3'.* The pHTK-Pfa3' plasmid was digested with the restriction enzymes *Spe* I and blunt ended using T4 DNA Polymerase. The *sgPfama1* expression cassette, prepared for cloning into pHH1-5'Pfama1, was ligated into pHTK-Pfa3' to produce the plasmid pHTK-sgPfa/HA (Fig 2.10.).

2.1.5: Southern blot analysis

2.1.5.1: DNA preparation and transfer

To produce suitable sized DNA fragments for analysis by Southern blot, DNA recovered from transgenic parasite lines was digested with restriction enzymes. Digested DNA was electrophoresed in 0.7% agarose gel (BioRad laboratories) containing 0.5 μg ml^{-1} ethidium bromide (BioRad laboratories) for 2 hours at 50 V. The gel was then exposed to UV on a transilluminator (UVP - BioDoc-It™ System) for 5 min to nick the DNA, thus increasing the efficiency of the transfer. The gel was incubated in denaturing buffer (0.5 M NaOH, 0.75 M NaCl) for 1 hour, rinsed in double-distilled water (ddH_2O) and incubated for a further hour in neutralising solution (0.5 M Tris-HCl, pH 7.4, 0.75 M NaCl). The DNA was transferred to a Hybond N^+ membrane (Amersham Biosciences), overnight by capillary transfer (Sambrook 1989).

2.1.5.2: Labelling and hybridisation

The membrane was pre-hybridised for 20 min in hybridisation solution (6 × SSC [1X SSC is 150mM NaCl, 15 mM Na citrate pH7] 5 × Denhardts [0.1% Bovine serum albumin, 0.1% Ficoll, 0.1% polyvinylpyrrolidone], 0.5% SDS, 0.01 mg ml^{-1} salmon sperm DNA) at 62°C. Meanwhile, the probe was labelled with α-[^{32}P] adenine triphosphate (dATP) (Amersham Biosciences) by random priming (Feinberg and Vogelstein, 1983), using a Prime-It® II Random Prime Labelling kit (Stratagene) according to the manufacturer's instructions. Unincorporated nucleotides were removed using ProbeQuant™ G-50 Micro Columns according to the manufacturer's instructions

(Amersham Biosciences). The labelled probe was then added to the hybridisation buffer in the hybridisation tube and incubated with the membrane overnight at 62°C. The probe was removed and the membrane washed three times in 2 × SSC for 20 min at 62°C. The bound probe was visualised by autoradiography, using Kodak® BioMax™ MR film, following incubation at –70°C.

2.2: Culture and manipulation of parasites

2.2.1: *In vitro* culture of *P. falciparum* parasites

Plasmodium falciparum clone 3D7 parasites (supplied by M. Grainger, NIMR) were cultured and synchronised by modifying the methods described by Trager and Jensen (1976) and Lambros and Vanderberg (1979). Briefly, parasites were cultured in plastic tissue culture flasks (Nunc™) at approximately 10% parasitaemia and 1 - 4% haematocrit. The culture medium was replaced every 2 - 3 days at which time the cultures were also gassed (7% CO_2, 5% O_2, 88% N_2). Parasite thin films were stained for light microscopic examination using 10% (v/v) Giemsa (Gurr) stain (BDH) in phosphate buffer pH 7.2 (43 mM KH_2PO_4, 211 mM N_2HPO_4).

2.2.2: *In vitro* synchronisation of *P. falciparum* parasites

Mature stage *P. falciparum* 3D7 parasites were isolated using a 70% Percoll density gradient as described by Rivadeneira et al., (1983). The immature trophozoites, rings and uninfected red blood cells (RBCs) in the pellet were discarded while the late trophozoites and schizonts floating on the top of the cushion were collected and incubated with fresh RBCs for 2 hours at 37°C in a G24 incubator shaker (New Brunswick Scientific) to allow reinvasion. The cultures were further synchronised using 5% D-sorbitol, as described by (Lambros and Vanderberg, 1979; Trager and Jensen, 1976). This procedure preferentially lyses erythrocytes containing late stage parasites (late trophozoites and schizonts), selecting for young ring stages. The parasites were returned to culture or used as required.

2.2.3: Parasite preparation for immunochemical analysis

2.2.3.1: Purification of late trophozoites and schizonts

Mature stage parasites were isolated from mixed parasite culture on a 70% Percoll cushion, as described by (Trager and Jensen, 1976) washed in RPMI-1640 (Invitrogen) and frozen directly at –70°C. Alternatively the parasite pellet was treated with 1.5 volumes 0.15% (w/v) saponin, centrifuged in a micro-centrifuge and the pellets frozen until required. Merozoite preparations were made by culturing purified mature stage parasites with RPMI-Albumax (Invitrogen) supplemented with 2 mM L- glutamine and 5 mM EGTA, in the absence of fresh RBCs, for 3-5 hours at 37°C to allow schizont rupture and merozoite release. The merozoites were harvested by centrifugation at 2000 rpm (Sorval TT7) and frozen at –70°C.

2.2.3.2: Purification of ring stage parasites

Mature stage parasites were purified from a tightly synchronous culture of 3D7 parasites. The parasites were incubated for 2 hours with a 4-fold excess of RBCs, at 4% haematocrit, in a shaker incubator at 37°C to allow reinvasion. The resulting ring stage parasites were purified twice on a 70% Percoll cushion to remove all intact late stage parasites. The resulting purified ring stage parasites were washed in 50 ml RPMI-Albumax and subsequently used in RBC binding assays. This generated a tightly synchronous culture of parasites at about 85% parasitaemia.

2.2.4: Preparation of drugs used for selection of transfected parasites

WR99210 (Jacobus Pharmaceuticals) was made up as a 20 mM stock solution in dimethly sulphoxide (DMSO, Sigma) and stored in aliquots at –20°C. This stock solution was diluted to 20 μM in RPMI-1640 and stored for use at +4°C. WR99210 was used as previously described (Duraisingh 2002). Ganciclovir (Sigma) was made up as a 2 mM stock solution in ddH_2O and aliquots stored at –20°C for use in culture.

2.2.5: Parasite transfection

P. falciparum 3D7 ring stage parasites at approximately 1% parasitaemia were transfected as previously described (Wu et al., 1995) (Crabb and Cowman, 1996) (Crabb et al., 1997) (Duraisingh et al., 2002). Briefly, 80-100 μg ethanol precipitated DNA was dissolved in 200 μl of incomplete cytomix (120 mM KCl, 0.15 mM $CaCl_2$, 2 mM EDTA, 5 mM $MgCl_2$, 10 mM K_2HPO_4/KH_2PO_4, 25 mM N-[2-hydroxyethyl]piperaxine-N'-[2-ethanesulfonic acid] (HEPES), pH 7.6) and the DNA added to 200 μl parasitised RBCs. The mixture was transferred to a 0.2 cm electroporation cuvette (Bio Rad) and electroporated using a Bio-Rad Gene Pulser Xcell^{TM} Electroporation System under conditions of 310 V and 960 μF (Fidock and Wellems, 1997). The electroporation mixture was transferred to an 80 cm^2 culture flask (Nunc^{TM}) containing 25 ml RPMI-1640 medium supplemented with 25 mM HEPES, 200 μL hypoxanthine, 20 μg ml^{-1} gentamicin, 0.25% (w/v) Albumax II, 0.2% $NaHCO_3$, pH 6.72, 2 mM L-glutamine and 5% AB^+ human serum and fresh RBCs at 0.8% haematocrit.

The culture medium was changed daily for three days after transfection, to remove debris resulting from cell lysis and every other day thereafter. Parasites were cultured for 48 hours post-transfection before the addition of WR99210, at a final concentration of 10 nM. From this point onwards, drug pressure was maintained until parasites were detected. Fourteen days post-transfection (and every 14 days thereafter) parasite cultures were diluted 1 in 2 with medium containing fresh RBC at a 0.8% haematocrit. Following the detection of transfected parasites (generally about 4 weeks after transfection) parasites were cultured for 3 weeks in the absence of drug, followed by drug replacement. Drug pressure was maintained until parasites

were again detected. Repeated cycles in the absence (and then presence) of drug were used to enrich the parasite population for parasites with integrated plasmid forms. Once WR99210 resistant parasites were established, parasite lines requiring negative selection (for double cross over) were fed with media containing 10 nM WR99210 and 180 μM Ganciclovir. The integration of plasmid DNA into the parasite genome by homologous recombination was assessed by Southern blot analysis.

2.2.6: Invasion-inhibition assay:

Mature schizont stage parasites were isolated from a tightly synchronous culture of *P. falciparum* (3D7) as described above. The parasites were added to culture medium containing RBCs at 2% haematocrit to give a 10% parasitaemia.

Purified mAb 4G2dc1 or 4G2dc1 Fab (2.4.5.2.) was dialysed in Phospahate buffered saline (PBS) or desalted using a PD10 desalting column (Amersham Biosciences), eluted in PBS and filter sterilised. Varying concentrations of purified Ab or Fab were placed in 0.5 ml eppendorf tubes. Volumes were made up to 50 μl with sterile PBS to maintain a constant final volume.

The concentrations of Abs used in the invsion inhibition assays are shown in table 2.2. To each of the Ab preparations described, 100 μl of the prepared parasite culture was added. The cultures were incubated at 37°C on a rotating arm for 4 hours. Thin smears were made from the parasite cultures and stained with Giemsa's stain. The number of invasion events per 10^4 RBCs was counted for each treatment condition.

2.2.7: Assay to determine whether 4G2dc1 Fab invasion-inhibition is blocked by rPfAMA1:

Recombinant PfAMA1 DI-III expressed in *P. pastoris* (kindly provided by Mike Blackman) was purified and concentrated in a Vivaspin 500 μl concentrator with a 10 kDa molecular weight (MW) cut-off membrane (Vivascience). Prior to determining the effect of rPfAMA1 DI-II on 4G2dc1 Fab invasion-inhibition, the ability of mAb 4G2dc1 Fab to stabily bind rPfAMA1 DI-II was assessed. Recombinant PfAMA1 DI-II was incubated for 15 minutes on ice, at a 10 fold excess, with mAb 4G2dc1 Fab (50 μg and 2.4 μg, respectively). The mixture was run on a high performance liquid chromatography (HPLC) gel filtration column G300 SWXL (TSK) in 0.1 M phosphate buffer, pH 7.0. Equivalent amounts of rPfAMA1 DI-II and 4G2dc1 Fab were run separately under identical conditions.

P. falciparum mature stage parasites were prepared at 10% parasitaemia, 2% haematocrit as described above. The 4G2dc1 Fab, with or without rPfAMA1 DI-III (concentrations shown in table 2.3) was incubated for 20 min at 4°C in 0.5 ml eppendorf tubes in a total volume of 50 μl

(made up with PBS).To each tube was added 100 µl of culture medium, containing RBCs at 2% haematocrit with 10% mature schizonts. Cultures were incubated and merozoite reinvasion assessed on thin smears as before (2.2.6).

2.3: Expression systems

2.3.1: COS-7 cell culture and transfection

COS-7 cells, adapted for growth in serum-free medium (Invitrogen) were cultured in Dulbecco's Modified Eagle's Medium (DMEM, Invitrogen), supplemented with 10% Ultra low IgG Foetal calf serum (FCS) (Invitrogen), 80 µg ml^{-1} L-glutamine and 50 U ml^{-1} penicillin/streptomycin (Sigma). Cells were cultured in 175 cm^2 tissue culture flasks (Nunc™) and incubated at 37°C in 5% CO_2 and grown until nearly confluent (about 1×10^7 cells per flask) before passage. Cells were harvested for passage using 5 ml 0.25% trypsin/EDTA (Sigma). Trypsin activity was neutralised using a two-fold excess of COS-7 cell culture medium.

Cells were transfected, according to the manufacturer's instructions, using 6 µl Fugene 6 (Roche) and 3 µg plasmid DNA in 6 well plates (Nunc™) ($1.2 - 1.8 \times 10^5$ cells per well). For immunofluorescence assays (IFA), coverslips were placed in the bottom of the wells before adding COS-7 cells. Cells were harvested 48 hours post transfection. For Western blot analysis the cells were harvested by scraping whereas for antibody selection assays the cells were harvested using 200 µl 0.25% trypsin.

2.3.2: *Pichia pastoris* expression system

2.3.2.1: Small-scale expression

A *P. pastoris* clone for expression of rPfAMA1 DI-II (glycerol stock) was used to inoculate 25 ml BMGY (1% yeast extract, 2% peptone, 100 mM potassium phosphate, pH6.0, 1.34% yeast nitrogen base, 4×10^{-5}% biotin, 1% glycerol) in a 250 ml flasks and was incubated at 30°C in an incubator shaker (Innova 4000, New Brunswick Scientific) at 250 - 300 rpm, until the culture reached OD_{600} = 2-6 (16 - 18 hours). Cultures were centrifuged at 3000 rpm for 5 minutes (Centaur 2) the supernatant removed and the pellet resuspended to OD_{600} = 1 in BMMY (as for BMGY, with 0.5% methanol replacing the 1% glycerol). Methanol was added to a final concentration of 0.5% (v/v) every 24 hrs to maintain induction. Samples (1 ml) were taken at 24 h intervals and the cells centrifuged at 3200 rpm for 1 minute (IEC MicroMax). The cell pellet and supernatant were frozen separately at -70°C.

2.3.2.2: Large-scale expression

Two 500 ml flasks, each containing 50 ml BMGY, were inoculated with a *P. pastoris* clone and incubated at 30°C for 24 hours as described for small-scale expression. Cultures were then

expanded to 2 × 200 ml in 2 L flasks, incubated for a further 24 hours, pooled and their OD_{600} measured. Cells were centrifuged at 4000 rpm (Beckman J6B) for 10 minutes and the cell pellet resuspended to OD_{600} = 3 in BMMY with chymostatin (2 μg ml^{-1}) and methanol (1% v/v). The cells were divided between 2 L flasks (200 ml per flask) and grown as for small-scale expression, methanol being added every 8 hours to 1% (v/v).

2.3.3. Culturing of the 4G2 hybridoma cell line

Hybridoma cells were grown in 80 cm^2 tissue culture flasks in 50 ml DMEM supplemented with 10% Ultra low IgG FCS, 80 μg ml^{-1} L-glutamine and 50 U ml^{-1} penicillin/streptomycin. This was used to inoculate a 20 L culture (in the large-scale facility, NIMR) the culture supernatant of which was harvested, concentrated and filtered using a 22 μm filter unit. NaN_3 was added to 0.02% (w/v).

2.4: Immunochemical and biochemical methods

2.4.1: Antibodies

The general properties of the primary Abs used in this study are outlined in Table 2.4.

The monoclonal antibody 4G2 recognises a reduction sensitive, conformational epitope in the ectodomain of PfAMA1. Culture supernatant of the 4G2 hybridoma (2.3.3.) was used in Western blots and indirect Immunofluorescence assays (IFA).

Mouse polyclonal antibodies against "native" (i.e. non-reduced) (N1) and reduced and alkylated (R1) recombinant PfAMA1 (rPfAMA1) were raised by immunization of mice (a kind gift from Sue Fleck, MRCT) and used in Westerns and IFA. The polyclonal serum AdsN1 was generated by adsorbing the polyclonal serum N1 against reduced and alkylated rPfAMA1 and has been shown in Western blot analysis (see Fig 4.19.) to recognise only reduction-sensitive epitopes within rPfAMA1.

Table 2.5 outlines the properties of the secondary Abs used in this study and table 2.6 summaries the tertiary detection reagents used.

All antibodies were diluted in PBS or Tris buffered saline (TBS) with 1% (w/v) bovine serum albumin (BSA). Culture supernatants from hybridoma cells expressing 4G2dc1 and 12CA5 were used neat.

2.4.2: Western blots

2.4.2.1: Basic Western blot analysis

COS-7 or *P. pastoris* cells were solubilised in 400 µl of 2X sodium dodecyl sulphate (SDS) sample buffer (1.51% Tris-base, 20% glycerol, 4.6% SDS, 1×10^{-2}% bromophenol blue) and cell supernatants were added at a ratio of 1:1 with 2X SDS sample buffer. Samples were electrophoresed on 10% or 12.5% SDS polyacrylamide gels (SDS-PAGE) (Laemmli 1970), under non-reducing or reducing conditions and then electrophoretically transferred to nitrocellulose membrane (Hybond-C extra, Amersham Biosciences) using a Trans-Blot™ Cell (Bio-Rad). Membranes were blocked in 5% milk in PBS containing 0.05% (v/v) Tween 20 for 30 min. The antibodies used and the concentrations at which they were used are described in (Table 2.4 and 2.5). Samples from the immunoprecipitation of biotinylated (See section 2.4.4.1) parasite lysates were probed directly with Streptavidin-HRP polymer (Table 2.6). Bound antibody was detected using Enhanced Chemiluminescence solution (ECL) according to the manufacturer's instructions (Perbio).

2.4.2.2: Western blots involving anti-phosphate antibodies

Western Blots to be probed with an anti-phosphate primary antibody were blocked in 5% BSA, rather than in 5% milk as many milk proteins are phosphorylated. Its use as a blocking agent would result in a high degree of non-specific binding by the anti-phosphate antibodies. Similarly, to reduce non-specific Ab binding, washes were performed in Tris buffered saline (TBS) containing 0.05% Tween 20 rather than PBS. All the antibodies used in these assays were diluted in TBS-Tween, 0.1% BSA and 0.02% sodium azide.

2.4.3: Indirect immunofluorescence assay (IFA)

IFAs were carried out on COS-7 cells grown on coverslips and either fixed with 100% acetone or left unfixed. Coverslips with unfixed COS-7 cells were handled with care to avoid dislodging the cells.

Sub-cellular localisation of transgenic proteins during the erythrocytic stages of the *P. falciparum* life cycle was analysed by IFA. *P. falciparum* thin smears were prepared from different life cycle stages and stored in the presence of silica gel dessicant (Sigma) at –70°C for future use. Prior to use, smears were fixed with ice cold 100% acetone or 80% acetone/20% methanol.

After antibody treatment the cells were stained with 4,6-diamidino-2-phenylindole (DAPI), for nuclear staining and Evans Blue, for cytoskeletal staining. Both COS-7 cell and parasite IFA preparations were mounted in Citifluor (Citifluor Ltd.) on slides and under coverslips respectively and the mounts sealed with nail varnish. Fluorescence labelling was detected using a Zeiss

Axioplan 2 imaging system at 1000 × magnification. Images were captured using a Zeiss AxioCam HRc camera and AxioVision version 3.1 software.

2.4.4: Immunoprecipitation of PfAMA1 from parasite lysate

2.4.4.1: Biotin labelling

Merozoite samples were thawed directly into 1 ml PBS, 1mM EDTA and centrifuged at 13000 rpm for 1 min, at 4°C. The merozoite pellet was carefully resuspended in 500 µl 0.2 mg ml^{-1} Sepharose-NHS-Biotin in PBS, 1mM EDTA and incubated at 4°C for 15 min. The reaction was stopped by the addition of 500 µl PBS, 1mM EDTA, 100 mM glycine. The merozoites were centrifuged as above, the supernatant removed and the pellet washed three times in 500 µl glycine buffer. The parasites were aliquoted and solubilised in one of three different detergents for immunoprecipitation (section 2.4.4.4).

2.4.4.2: [^{35}S] metabolic labelling

Mature stage parasites were purified as described above (section 2.2.3.1.) and washed in 2 × 50 ml cysteine and methionine free medium (Invitrogen). Parasites were cultured for a further 30 min in 30 ml cysteine and methione free medium supplemented with 10% AB+ filter sterilised human serum and 4 mM L-glutamine. Promix (Amersham Biosciences) containing L-[^{35}S] – methionine and cysteine, was added to the culture at a specific activity of 100 µCi ml^{-1} and incubated for one hour at 37°C. The parasites were centrifuged at 2000 rpm for 3 minutes (Sorvall RT7, Du Pont), the cell pellet washed twice with 50 ml RPMI-Albumax and frozen directly for schizont samples. Merozoite samples were prepared as described above (section 2.2.3.1.).

2.4.4.3: Surface cross-linking of merozoites

Merozoite samples labelled with [^{35}S]-methionine and cysteine (2.4.4.2.) were thawed into 200 µl PBS. To thawed samples, 3,3'–dithiobis [sulfosuccinimidyl] propionate (DTSSP) (prepared as a 2 mM stock in PBS) was added to final concentrations of 100 µM, 200 µM and 300 µM and the samples incubated at room temperature for 15 min. The reaction was stopped by the addition of 1 M Tris-HCl, pH 7.4 in PBS, to a final concentration of 50 mM. The parasites were micro-centrifuged at 13000 rpm (Biofuge pico Heraeus) and washed twice in 1 ml of 50 mM Tris-HCl pH 7.4 in PBS. Merozoite pellets were frozen at –70°C until required.

2.4.4.4: Immunoprecipitation

Parasite pellets were thawed directly into 200 µl 50 mM Tris-HCl, pH 8.2 with 1 mM EDTA, 1 mM phenylmethyl sulphonyl fluoride (PMSF), 1 µg ml^{-1} pepstatin A (Sigma) and 10 µM E64 (Sigma), as well as one of the following detergents: 1% (v/v) Nonidet® P40 (NP40, Boehringer Mannheim), 1% (w/v) CHAPS (3-[(3cholamidopropyl)-dimethylammonio] propanesulfonate -

Sigma), 1% (w/v) sodium deoxycholate (Sigma). The parasite lysates were incubated on ice for 30 min, before being clarified by centrifugation at 13000 rpm at 4°C for 20 min. The parasite lysate was then added to 100 µl prewashed, dried Sepharose® 4B (Pharmacia) or Protein-G Sepharose™ (Amersham Biosciences) and incubated at 4°C for 15 min. It was anticipated that this extra clarification step should eliminate or minimise non-specifiic interaction of protein with the beads. The Sepharose® 4B beads were removed using a Spin-X® filter (Corning) and 20 µl of the clarified lysate frozen for comparison. The remaining lysate was added to 100 µl prewashed, dried 4G2dc1-bound Sepharose beads (kindly provided by Mike Blackman) and incubated on a rotating wheel at 4°C for 2 hours. The beads were washed 4 times in 1 ml of the appropriate detergent solution (described above), dried and solubilised directly into 200 µl 2X SDS sample buffer (with or without 1 mM α-dithiothreitol, [DTT]) for Western Blot analysis. Samples from [^{35}S] labelled parasites were electrophoresed on 10% SDS-PAGE and the gels dried (SCIE-PLAS gel dryer). Labelled bands were visualised using BioMax™ MR film (Kodak®).

2.4.5: Antibody selection assay

This assay was designed to identify mutant forms of rPfAMA1 produced by random or SDM and that were altered only by virtue of the fact that they were no longer recognised by the mAb 4G2dc1 (hereafter referred to as 4G2dc1$^-$ forms).

COS-7 cells were transfected with sg'Pfama1RML as described (2.1.4.7.). The cells were harvested with 0.25% trypsin/EDTA as described. Trypsin activity was neutralised by washing the cells twice in 15 ml COS-7 cell culture medium and the cells resuspended in wash buffer (PBS, 0.1% BSA), containing the trypsin inhibitors 1 mg ml^{-1} soyabean trypsin inhibitor and 200 µM tosyl-lysine chloromethyl ketone (TLCK). Transfected COS-7 cells were subjected to a double selection process, as follows (Fig 2.11.).

2.4.5.1: Negative selection

Firstly, the cells were selected for the absence of the mAb 4G2 epitope. For this, transfected cells were resuspended in 200 µl culture supernatant from mAb 4G2 hybridoma cells and incubated for 20 min at 4°C. The cells were washed 2 times in 1ml wash buffer (described above - 2.4.6) and incubated with Dynabeads coupled to anti-mouse IgG (Dynal Biotech.) for a further 20 min. Selection was carried out according to the manufacturer's instructions using 20 µl of resuspended Dynabeads per reaction. The Dynabead-bound and unbound fractions were separated using a Dynal magnet. The unbound 4G2$^-$ cells were recovered and washed in 3 × 1 ml wash buffer.

2.4.5.2: Positive selection

For the selection of mutants with native conformation (native$^+$), the 4G2$^-$ cells were resuspended in 200 µl wash buffer containing the polyclonal Ab N1 (1 in 100 dilution) and incubated at 4°C for 20 min. COS-7 cells bound to N1 were recovered by incubation with anti-mouse IgG-linked Dynabeads for 20 min at 4°C. The DNA from 4G2$^-$/native$^+$ cells was then recovered (using a SNAP kit [Invitrogen]), cloned and sequenced, to identify mutations that resulted in loss of the 4G2 epitope

2.4.6: Protein purification

2.4.6.1: Purification of recombinant PfAMA1 DI-II

After 24 hours of induction of DI-II expression in *P. pastoris*, the cultures were pooled and the pH increased to 8.2 with NaOH. PMSF was added to a final concentration of 0.1 mM. The cells were centrifuged (as for 2.3.2.2.), and the supernatant passed through a 0.22 µm filter unit, to remove any remaining cell debris. PfAMA1 DI-II was then purified using nickel nitrilotriacetic (Ni-NTA) resin agarose beads (QIAGEN) as follows. The culture supernatant (2 L) was incubated with Ni-NTA beads for 2 hours at 4°C. The beads were washed 5 times with 100 ml ice-cold 10 mM imidazole in 1 × Ni-NTA buffer pH 8.2 (20 mM Tris-HCl, 300 mM NaCl, 30 mM imidazole) prior to elution of PfAMA1 DI-II, by washing the beads three times in 33 ml ice-cold 200 mM imidazole in 20 mM Tris-HCl, 300 mM NaCl. PMSF (0.1 mM) and chymostatin (2 µg ml^{-1}) were added to the pooled eluates before further purification by gel filtration on a Superdex 200 HR gel filtration column, pre-equilibrated in Superdex running buffer (20 mM Tris-HCl, 150 mM NaCl, pH 8.2 - SRB). The column was run at 1 ml min^{-1} and 5 ml fractions were collected.

2.4.6.2: 4G2 F(ab)$_2$ and Fab (antigen binding) fragment production and purification

2.4.5.2.1: Ab purification. Concentrated hybridoma supernatant was passed over a Protein G Sepharose^{TM} column (Pharmacia Biotech) overnight and the column was washed in PBS. Bound antibody was eluted in 0.2 M glycine-HCl, 0.15 M NaCl, pH 2.7 with 0.02% NaN_3, directly into 1 M Tris-HCl pH 8.2, to neutralise the eluate. The purified Ab was concentrated in a stirred concentrator fitted with a 50 kDa MW cut off ultrafiltration membrane (Amicon).

2.4.6.2.2: Pepsin digest to generate F(ab)$_2$. Purified mAb 4G2 (2.4.5.2.1.) was added to 1 M NaOH/citrate buffer, pH 3.5, to give a 0.1 M NaOH/Citrate solution and the mixture pre-warmed to 37°C. Pepsin (in 0.1 M NaOH/Citrate buffer, pH 3.5) was added to a final concentration of 0.1 mg ml^{-1} and the mixture incubated at 37°C for 2 hours. The reaction was terminated by the addition of an equal volume of 1 M Tris-HCl, pH 8.2. The F(ab)$_2$ was then purified by gel filtration as described in 2.4.5.1.

2.4.6.2.3: Reduction and alkylation to generate Fab. F(ab)$_2$ was concentrated as described for the intact antibody, using a 10 kDa MW cut off ultrafiltration membrane (Amicon) and L-cysteine

added to a final concentration of 10 mM from a 1 M stock in degassed gel filtration buffer (20 mM Tris-HCl, 0.15 M NaCl, pH 8.2). The mixture was gassed with nitrogen and incubated at 37°C for 2 hours, with stirring. The reaction was terminated by the addition of a freshly prepared solution of 1 M iodoacetamide, in 0.1 M Tris-HCl, pH 8.2, to a final concentration of 130 mM and the mixture incubated at room temperature for 2 hours. The resulting Fab fragment was purified by gel filtration, as described in 2.4.5.1.

The purified antibody and antibody fragments were electrophoresed on 15% SDS PAGE and visualised by staining with Coomassie blue.

2.4.6.3: 4G2 mAb F(ab)$_2$ complexed to DI-II

Purified PfAMA1 DI-II (2.3.2.3), was added to 4G2 F(ab)$_2$ (2.4.3.2) and incubated at 4°C for 24 hours. The resulting complex was purified by gel filtration as described in 2.4.5.1.

2.4.7: Proteolytic digestion of rPfAMA1

Digestion reactions were carried out using reagents prewarmed to 37°C. The reactions were incubated at 37°C and at time t = 0, 10, 30, and 60 minutes post initiation, 10 µl samples were taken and added directly to protease inhibitors (described below) to stop the reaction. Samples were boiled for 5 minutes, following the immediate addition of 20 µl 2 X SDS sample buffer.

2.4.7.1: Trypsin/Chymotrypsin

Trypsin and chymotrypsin (Sigma) at 50 µg ml^{-1} in SRB were added to rPfAMA1 (in 10 mM $CaCl_2$) at an enzyme:substrate ratio of 1:10 or 1:100. The reactions were stopped by the addition of an equal volume of 4 mM Pefabloc (Sigma). Digests were also carried out in the presence of 1 M urea, or 0.01% (w/v) SDS.

2.4.7.2: Subtilisin

Subtilisin (Sigma) at 50 µg ml^{-1} in SRB were used to digest rPfAMA1 at enzyme:substrate ratios of 1:10 and 1:100. The reaction and reaction termination conditions used were the same as in 2.4.6.1.

2.4.7.3: Papain

Papain, (Boehringer Mannheim GmbH) at 1 mg ml^{-1} in SRB with 20 mM EDTA, was added to rPfAMA1 with 10 mM cysteine, at an enzyme:substrate ration 1:10. The protease was neutralised by adding 0.1 M iodoacetamide (50 mM final concentration).

2.4.7.4: Pepsin

Pepsin at 1 mg ml^{-1} in 0.1 M citrate/NaOH buffer, pH 3.5 was added to the rPfAMA1, in 0.1 M citrate/NaOH buffer (pH 3.5) to give an enzyme:substrate ratio of 1:10, or 1:100. The reaction was stopped by the addition of 1 M Tris-HCl, pH 8.0 (0.5 M final concentration).

Pepsin digestion of PfAMA1 DI-II complexed with mAb 4G2 was carried out in 0.1 M citrate/NaOH buffer, pH 5.2. The pH of the buffer was chosen to ensure pepsin activity was maintained, without disrupting the Ab-protein interaction. Pepsin was used at an enzyme:substrate ratio of 1:10 or 1:100.

All digestion products were electrophoretically separated on 10% SDS-PAGE gels, which were stained with Coomassie blue or transferred to nitrocellulose for analysis by Western blot.

2.5: RBC binding assay

COS-7 cells were transfected on day 0 and the transfected cells used in erythrocyte binding assays on day 2 post-transfection. In all cases, the adherence of human erythrocytes to transfected COS-7 cells (rosette formation) was analysed using an inverted light microscope (Zeiss). Binding was assessed under a number of different conditions, as follows:

2.5.1: Normal conditions

The RBC binding assay was carried out essentially as described by Chitnis and Miller (1994). Briefly, COS-7 cells were transfected in 6 well plates as described above (section 2.3.1.). Medium was aspirated from the wells and 2 ml of a suspension of human RBCs (hRBCs) (0.1% haematocrit in RPMI-1640) were added. Plates were incubated at 37°C in a 5% CO_2 incubator for 2 hours. COS-7 cells were then washed 3 times in complete medium and the COS-7 cell monolayer observed.

2.5.2: Static conditions

Transfected COS-7 cells were grown in 25 cm^2 tissue culture flasks (Corning/Costar) and then the flask completely filled with a suspension of hRBCs in CO_2 gassed medium. After 2 hours incubation, as described above, flasks were gently inverted, allowing unbound erythrocytes to detach.

2.5.3: Sheer stress conditions

Cells were treated as described for normal conditions, but were incubated with a hRBC suspension in CO_2 gassed medium, on a A600 rocker (Denley) at 37°C to simulate sheer stress conditions.

2.5.4: Binding using ring stage parasites

Transfected COS-7 cells were incubated for 2 hours with purified ring stage parasites at about 85% parasitaemia (2.2.2.2.), in suspension at 4% haematocrit with RPMI-1640, at 37°C under sheer stress conditions.

2.5.5: Recombinant PfAMA1 bound to a solid support

Recombinant PfAMA1 DI-III from 1 mg ml^{-1} stock was bound either to nitrocellulose (10 μg of protein loaded) or to polystyrene plates (Nunclon) using a two fold serial dilution (with a starting loading of 20 μg). The solid supports were then blocked in 5% BSA for 2 hours. These were incubated with hRBC suspensions (as described above) in CO_2 gassed medium, under sheer stress conditions. Erythrocyte binding to nitrocellulose was assessed visually by placing the membrane on a light box. Erythrocyte binding to the polystyrene plates was assessed microscopically.

Table 2.1: Oligonucleotide sequences used for plasmid construction.

Oligo. Name	Sequence (5' 'to 3')
AMAfor1	GGGT**TCTAGA**CCCGGGCAATCGAAATCGTGGAAAGATCC
sgOligo 78	TATTCGTTGTTCTTGTAGAAGTCACGCATACCGTTCAAAG
sgOligo 17	TGACTTTGTGTAGTAGACACGCTGGAAACATGAACCCTGA
DomIrev	TTCACAGTT**GAATTC**GACCTACAGACCGAA
DI5'EcoRVf	GACGCGGCCCG**GATATC**CGAAATCGTGGAA
DI5'EcoRVr	TTCCACGATTTCG**GATATC**CGGGCCGCGTC
DI3'EcoRVf	AACCTCGAGAA**GATATC**GTTCGGTCTGTGG
DI3'EcoRVr	CCACAGACCGAAC**GATATC**TTCTCGAGGTT
DII5'KpnIfor	GTCGAT**GGTACC**TGTGAAGAC
DII5'KpnIrev	GTCTTCACA**GGTACC**ATCGAC
DII3'*Kpn*Ifor	GCGACTACT**GGTACC**TCTCATCCA
DII3'*Kpn*Irev	TGGATGAGA**GGTACC**AGTAGTCGC
DI5'*Kpn*If	GCGGCCCGGGCAATC**GGTACC**GTGGAAAGATCC
DI5'*Kpn*Ir	GGATCTTTCCAC**GGTACC**GATTGCCCGGGCCGC
*Eco*RVDIfor	GCGGCCCGG**GATATC**GAAATCGTG
*Eco*RVDIrev	CACGATTTC**GATATC**CCGGGCCGC
Tr1*Eco*RVf	GCTGGTACTCAGTACAGA**GATATC**TCTGGTAAGTGCCCTGTT
Tr1*Eco*RVr	AACAGGGCACCTACCAGA**GATATC**TCTGTACTGAGTACCAGC
Tr2*Eco*RVf	CTGGGTGAAGATGCC**GATATC**GCTGGTACTCAGTAC
Tr2*Eco*RVr	GTACTGAGTACCAGC**GATATC**GGCATCTTCACCCAG
*Eco*RVD Ifor	GCGGCCCGG**GATATC**GAAATCGTG
*Eco*RVDIrev	CACGATTTC**GATATC**CCGGGCCGC
sgOligo 8	TCTCTTCCATCGAAATCGTGGAAAGATCCAACTACATGGG
sgOligo 58	TCTTCTTGTTACCTTCGTCGTCGTTATCGTTCAACTTGAT
3D7-3'-900f	GGGTCGATGGAAATTGTGA**AGATCT**ACCACATG
3D7-3'-900r	GTT**CTCGAG**TTAATAGTATGGTTTTTCC
3D7-5'-for	CATATATGA**AGATCT**TTGGAAGAGGACAG
3D7HA2ndf	CCTGAACATGTGCCAGATTATGCTAAAATGAAA
3D7HA2ndr	TTTCATTTTAGCATAATCTGGCACATGTTCAGG
3D7HAflfor	ATATGCAGATTATCCTTACGATGTGCCAGATTATGCTAAAATGAAA
3D7HAflrev	TTTCATTTTAGCATAATCTGGCACATCGTAAGGATAATCTGCATAT
Δ*Xho*Ifor	CCAAGAAAGAACCTGGAAAACGCAAAGTTCGGTCTGTGG
Δ*Xho*Irev	CCACAGACCGAACTTTGCGTTTTCCAGGTTCTTTCTTGG
sgPfA2HAf	GAGCATAAGCCTGACTATGCTAACATGAAG
sgPfA2HAr	CTTCATGTTAGCATAGTCAGGCTTATGCTC
sgPfAflHAf	GCAGATTATCCATACGATGTGCCTGACTATGCTAACATGAAG
sgPfAflHAr	CTTCATGTTAGCATAGTCAGGCACATCGTATGGATAATCAGCGTATTC
5'sgPfama1f	ACCGAG**CTCGAG**TTCATGAGGAAG
3'sgPfama1r	GCCAGT**CTCGAG**TTAGTAGTAAGGC
3D7-5'-rev	CTCGAGGTATATCTTCTCAATTTCCATCGACCC
Pfa1-3'UTRf	CAACGTCTG**CCATGG**TCAGCTTCTCTTTTATGC
Pfa1-3'UTRr	CCTTTTTAATTATATAT**CCTAGG**TCA CATACGTC

Table 2.2: Antibody concentrations (mM) in invasion-inhibition assays

(a) 4G2dc1 and 4G2dc1 Fab

Sample	1	2	3	4	5
mg ml^{-1}	0	0.4	0.7	1.6	2.7

(b) 4G2dc1 Fab

Sample	1	2	3	4	5	6
mg ml^{-1}	0	0.07	0.05	0.11	0.27	0.43

Table 2.3: Concentrations of 4G2dc1 Fab and rPfAMA1 used in invasion -inhibition blocking assay

	1	2	3	4
4G2dc1 Fab	0	0.98 mM	0.98 mM	0
rPfAMA1 DI-III	0	0	1 mM	1 mM

Table 2.4: Primary antibodies used in immunofluorescence assays (IFA) and Western blot analysis

Antibody	Polyclonal/ Monoclonal	Species of Origin	Concentration		Specificity
			IFA	Western	
4G2*	Monoclonal	Rat	Culture supernatant		NR only
N1*	Polyclonal	Mouse	1/100	1/1000	NR/R
AdsN1*	Polyclonal	Mouse	1/100	1/1000	NR only
R1*	Polyclonal	Mouse	1/100	1/1000	R/NR
3F10**	Monoclonal	Rat	1/500	1/8000	HA tag
12CA5***	Polyclonal	Mouse	-	Cult. Sup.	HA tag
α-p-Thr****	Polyclonal	Mouse	-	1/100	p-Thr
α-p-Ser***	Polyclonal	Mouse	-	1/100	p-Ser
4G10	Monoclonal	Mouse	-	1/1000	p-Tyr

Notes:

* Antibodies recognising epitopes within the PfAMA1 ectodomain.

** 3F10 (Roche) is a high affinity monoclonal antibody for detection of the HA epitope tag.

*** 12CA5 culture supernatant was the kind gift of Pippa Harris. This Ab gives a non-specific band in Western blot analysis of COS-7 cell lysate.

**** Anti-phospho-serine or threonine antibodies (Qiagen) recognise phosphorylated serine and threonine amino acid residues respectively.

Table 2.5: Secondary antibodies used in IFA and Western blot analysis

Antibody specificity	Species of Origin	Source	Concentration		Conjugate
			IFA	Western	
α-mouse IgG	Goat	Pierce	-----	1/10000	HRP
α-mouse IgG	Goat	Sigma	1/100	-----	FITC
α-rat	Goat	Chemicon	1/500	1/8000	Biotin

Table 2.6: Summary of tertiary reagents used in IFA and Western blot analysis

Streptavidin*	------	Sigma	-----	1/1000	HRP
Streptavidin*	------	Vector	1/500	-----	FITC

Note:

*A three step labelling procedure, which relies on the high affinity binding of streptavidin and biotin, was used with both rat monoclonal primary antibodies to enhance the observed signal.

Figure 2.1: Construction of the plasmid pSec/sg'Pfama1 for expression of the *Pfama1* synthetic gene in COS-7 cells

(1) The 5' region of DI was PCR amplified from the full length synthetic gene in Fim252, introducing *Xba*I and *Sma*I sites just 5' of the IEIVE processing site in DI. The region amplified extended beyond the *Afl*II site in DI. **(2)** The PCR product was digested with *Xba*I and *Afl*II. **(3)** Fim 252 was digested with *Xba*I and *Afl*II to remove the sequence coding for the signal peptide and prodomain. **(4)** The two digestion products were then ligated together to give the plasmid pMOS/sg'Pfama1, containing the PfAMA1 synthetic gene minus the sequence encoding the signal peptide and prodomain (*sg'Pfama1*). **(5)** This gene was excised from the plasmid using the restriction enzymes *Sma*I and *Eco*RI (at the 3' end of the gene). **(6)** The expression plasmid pSecTag2A was digested with SfiI (3' of the Igκ secretory signal in the plasmid) and blunt ended. **(7)** This was followed by EcoRI digestion of the plasmid. **(8)** The gene sg'Pfama1 was ligated into the plasmid pSecTag2A, to give the construct pSec/sg'Pfama1.

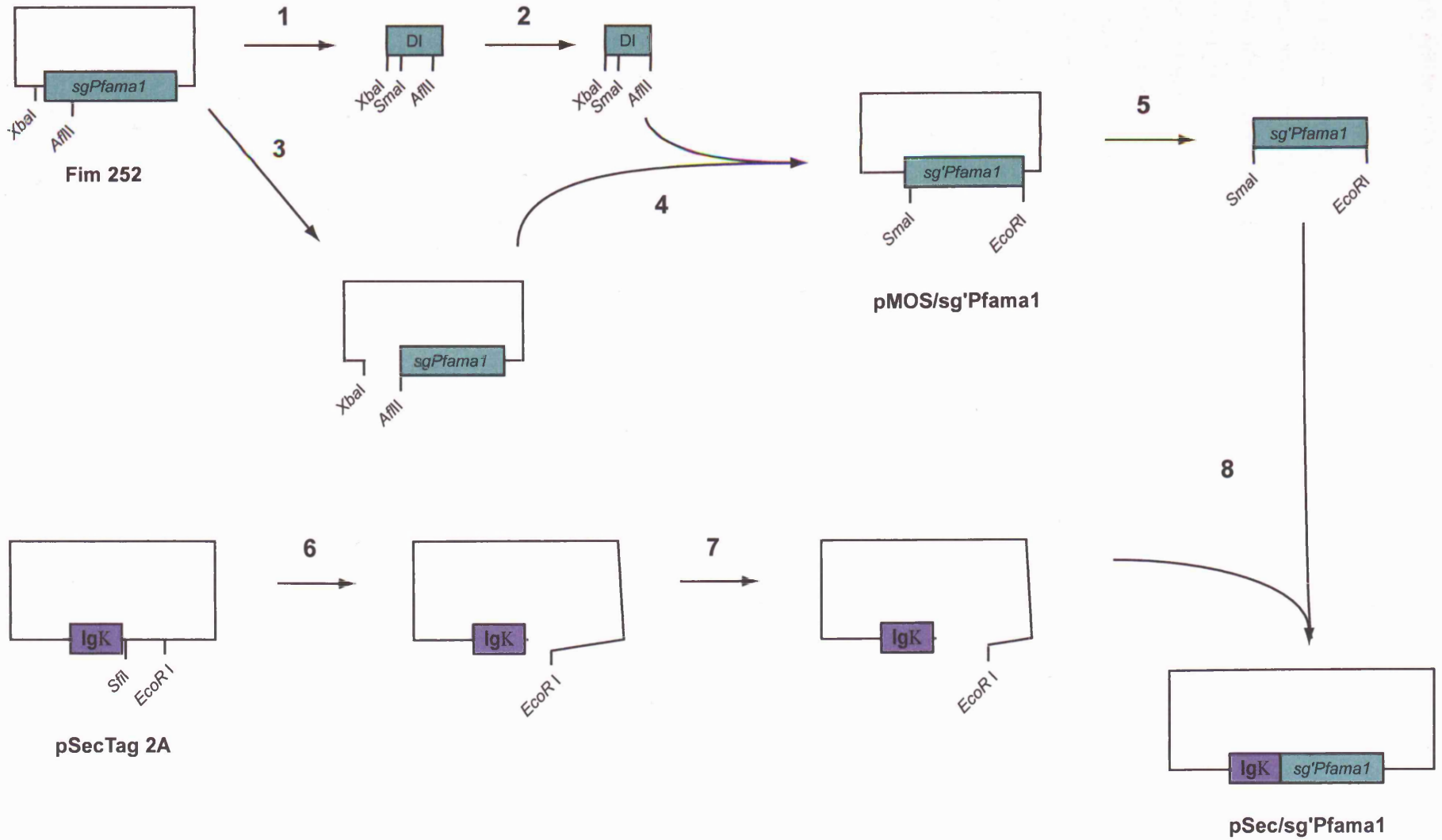
sgPfama1
XbaI
AflII
Fim 252
1
DI
XbaI
SmaI
AflII
2
DI
XbaI
SmaI
AflII
3
sgPfama1
XbaI
AflII
4
sg'Pfama1
SmaI
EcoRI
pMOS/sg'Pfama1
5
sg'Pfama1
SmaI
EcoRI
8
IgK
SfiI
EcoR I
pSecTag 2A
6
IgK
EcoR I
7
IgK
EcoR I
IgK
sg'Pfama1
pSec/sg'Pfama1

72

Fig 2.2: Design of the plasmid pSec/sg'DI, for secreted expression of sg'DI in COS-7 cells

(1) DI was PCR amplified from just 5' of the *Sac*II site in DI, to just downstream of the 3' end of DI. The reverse primer was designed to introduce an *Eco*RI site downstream of DI. **(2)** The PCR product was digested with *Sac*II and *Eco*RI. **(3)** To remove DII and DIII, the plasmid pSec/sg'Pfama1 was digested with *Sac*II and *Eco*RI. **(4)** The plasmid backbone and digestion PCR product were then ligated together, giving the construct pSec/sg'DI.

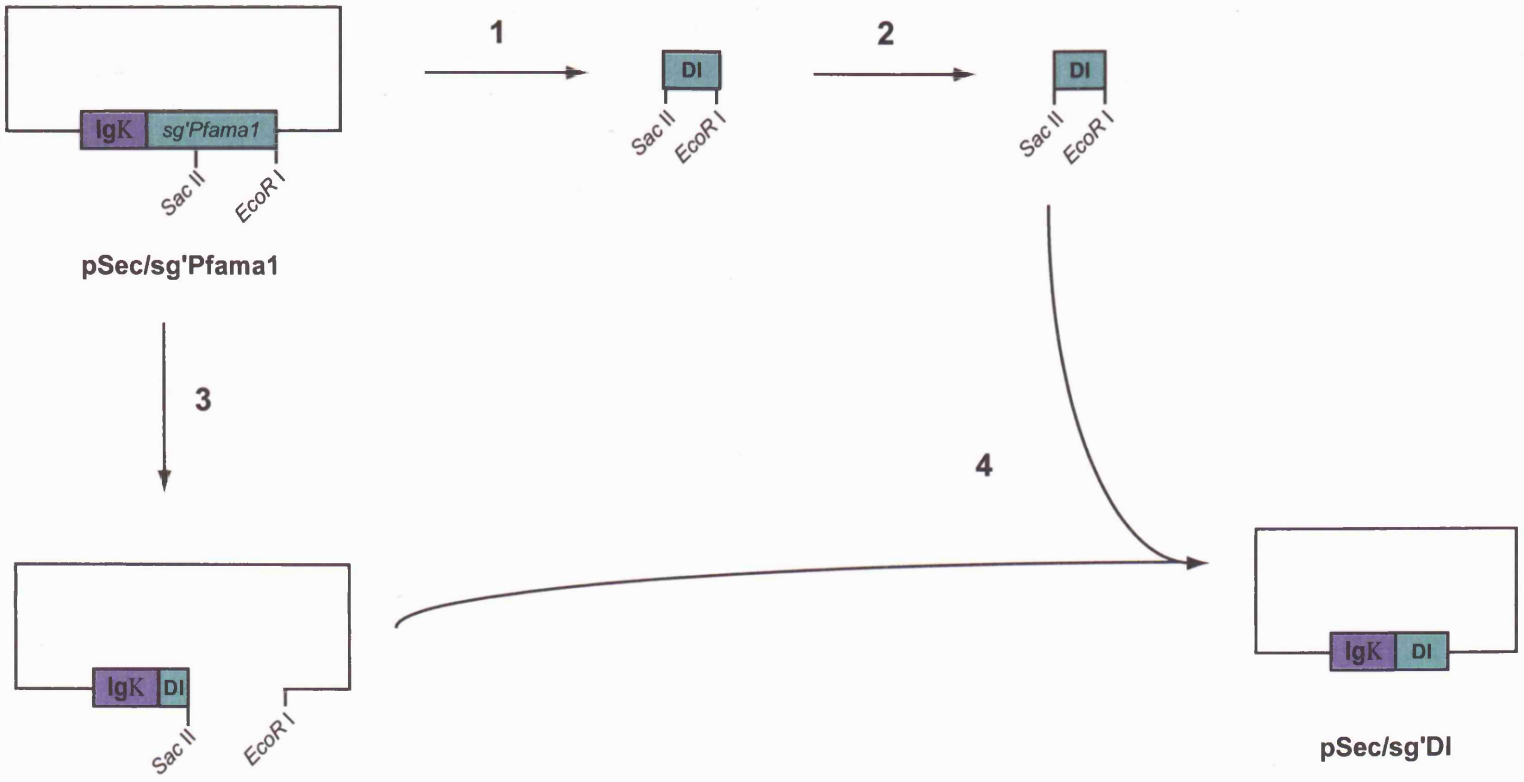
IgK
sg'Pfama1
Sac II
EcoR I
pSec/sg'Pfama1
1
DI
Sac II
EcoR I
2
DI
Sac II
EcoR I
3
IgK
DI
Sac II
EcoR I
4
IgK
DI
pSec/sg'DI

Figure 2.3: Construction of plasmids for the expression of different combinations of the PfAMA1 subdomains in COS-7 cells.

A To generate a construct for expression of DII and DIII in COS-7 cells **(1)** two rounds of SDM were carried out to introduce an *Eco*RV site at the 5' and 3' ends of DI. **(2)** The plasmid was digested with *Eco*RV to excise DI and then **(3)** re-ligated to give the plasmid sgPfaΔDI.

B A construct for expression of DI and DIII together in COS-7 cells was created by **(1)** introducing *Kpn*I sites at the 5' and 3' ends of DII in two rounds of SDM. **(2)** The resulting plasmid was digested with *Kpn*I to excise DII and then **(3)** the plasmid backbone re-ligated to generate the plasmid sg'PfaΔDII.

C A plasmid was designed for expression of DIII on its own on the surface of COS-7 cells. **(1)** In two rounds of SDM, *Kpn*I sites were introduced at the 5' end of DI and at the 3' end of DII. **(2)** The resulting plasmid was digested with *Kpn*I to excise both DI and DII and then the plasmid backbone was re-ligated to give the construct sgPfaΔDI-II.

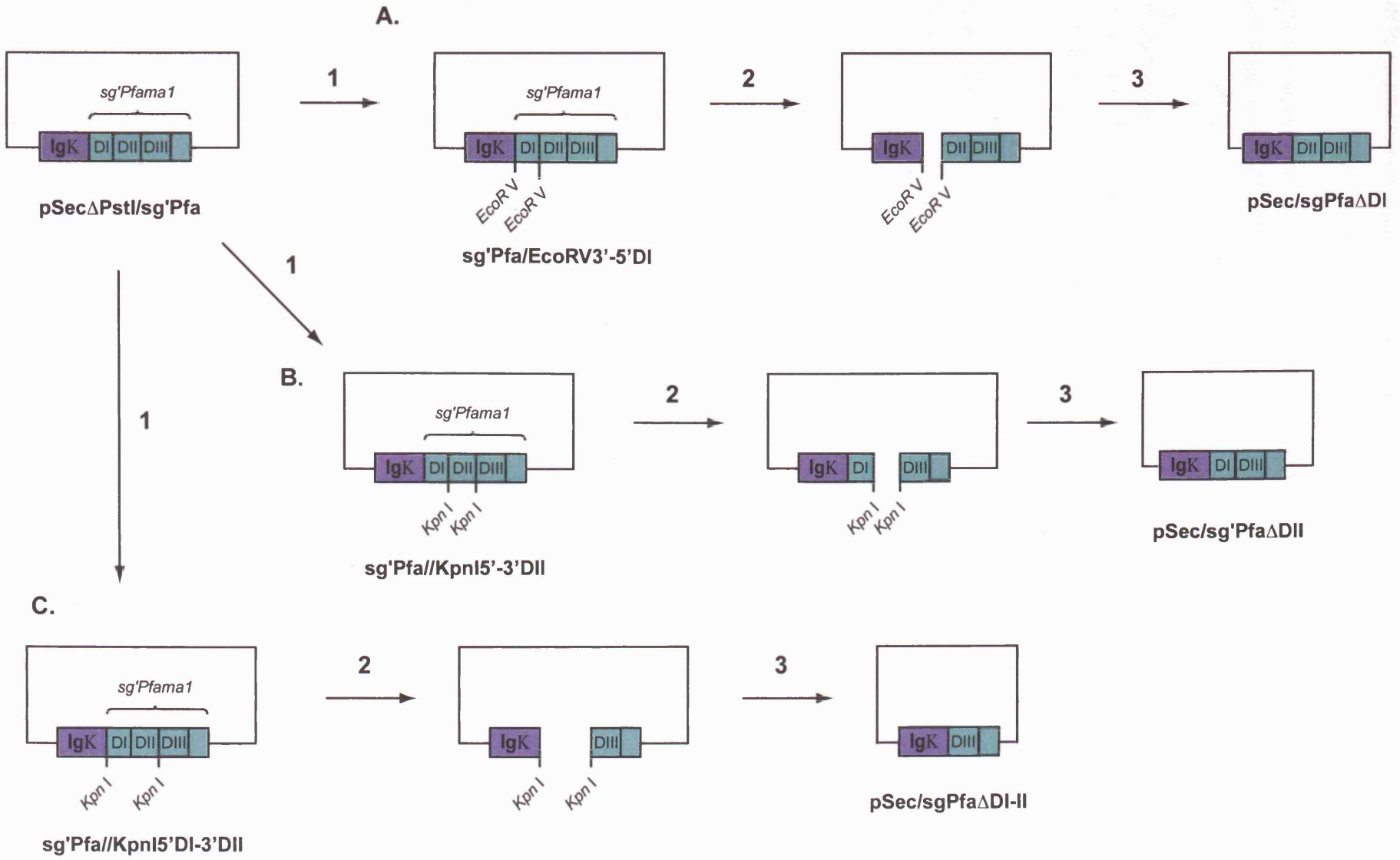
A.
sg'Pfama1
IgK
DI
DII
DIII
1
2
3
pSecΔPstI/sg'Pfa
EcoR V
EcoR V
sg'Pfa/EcoRV3'-5'DI
pSec/sgPfaΔDI
1
B.
Kpn I
Kpn I
sg'Pfa//KpnI5'-3'DII
pSec/sg'PfaΔDII
1
C.
sg'Pfa//KpnI5'DI-3'DII
pSec/sgPfaΔDI-II

Figure 2.4: Plasmid design for the expression of a truncated form of sg'PfAMA1 in COS-7 cells

(1) SDM was used to introduce an *Eco*RV site at the 5' end of the *sgPfama1* coding sequence in the plasmid pSec/sg'Pfama1. SDM was used to introduce a further *Eco*RV site at the 5' side of the first cysteine residue in DI (C149), to leave the sequence encoding either **(2)** 146SGKC$_1$... or **(3)** 138AGTQYRLPSGKC$_1$... at the 5' end of the gene. **(4)** The two plasmids were then digested to excise the 5' end of the sequence encoding DI and **(5)** the plasmid backbones re-ligated to give constructs (a) pSec/tr1-sgPfama1 and (b) pSec/tr2-sgPfama1 respectively.

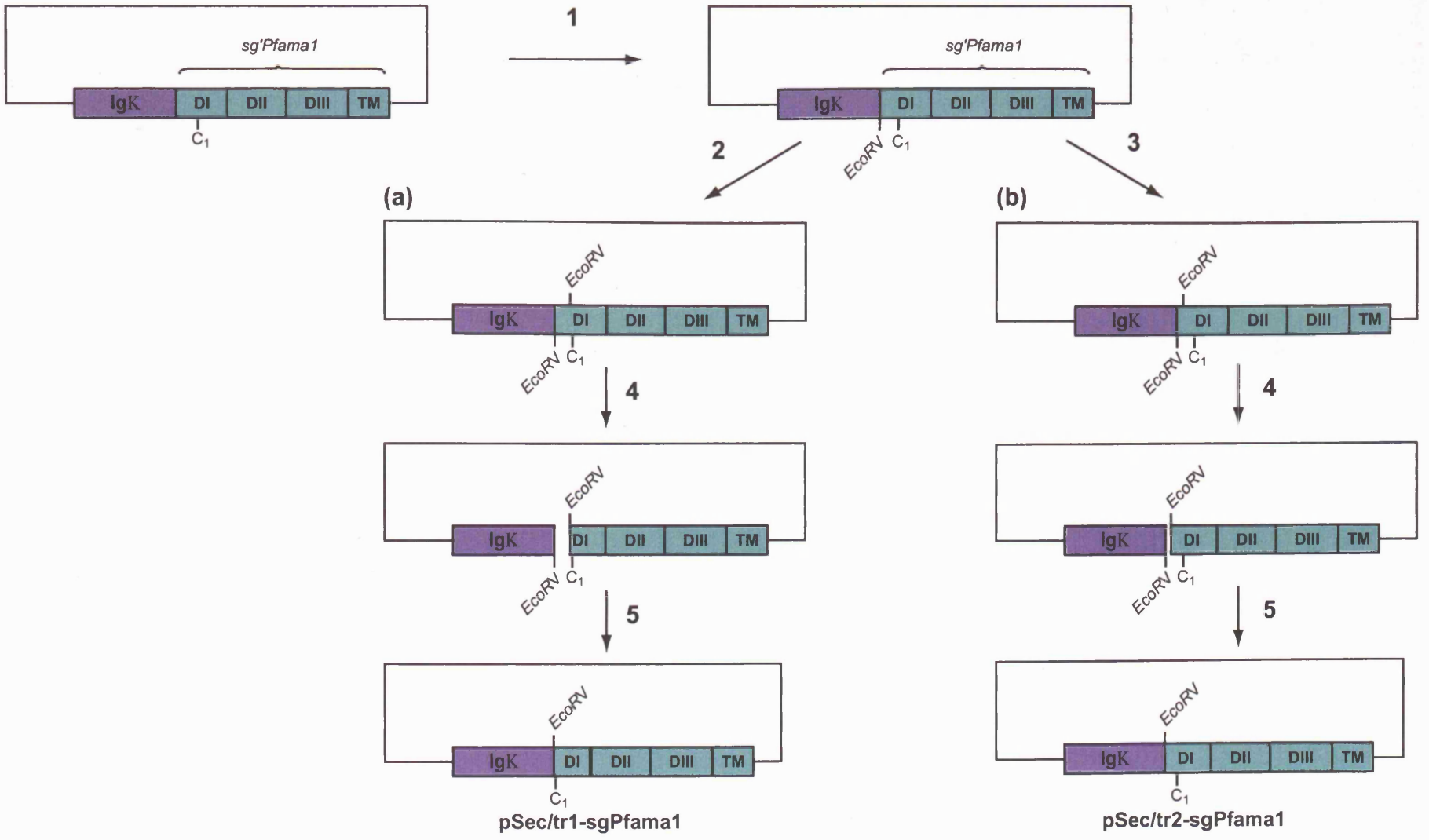
sg'Pfama1
IgK
DI
DII
DIII
TM
C1
1
EcoRV
2
3
(a)
(b)
4
5
pSec/tr1-sgPfama1
pSec/tr2-sgPfama1

Figure 2.5: Schematic representation of the approach used to generate a random mutant library of sg'Pfama1 (sg'Pfama1RMLib)

(1) The *Pst*I site in the plasmid backbone was excised by digestion with *Eco*RI and *Eco*RV, so that the *Pst*I site at the 3' end of the sequence encoding DII of *sg'Pfama1* was unique. **(2)** The vector backbone was religated to give the construct pSecΔPstI/sg'Pfa. **(3)** SDM was used to introduce a *Cla*I site at the 5' end of the sequence coding for DI, giving the plasmid pSecΔP/sg'Pfa/ClaI. **(4)** This plasmid was digested with *Cla*I and *Pst*I to excise the sequence encoding DI-II. **(5)** Under random mutagenic PCR conditions, the sequence encoding DI-II, incorporating *Cla*I and *Pst*I sites, was amplified from pSecΔP/sg'Pfa/ClaI and then **(6)** digested with *Cla*I and *Pst*I. The *Cla*I/*Pst*I digested PCR product was ligated into the linearised plasmid, giving the random mutant library sg'Pfama1RMLib.

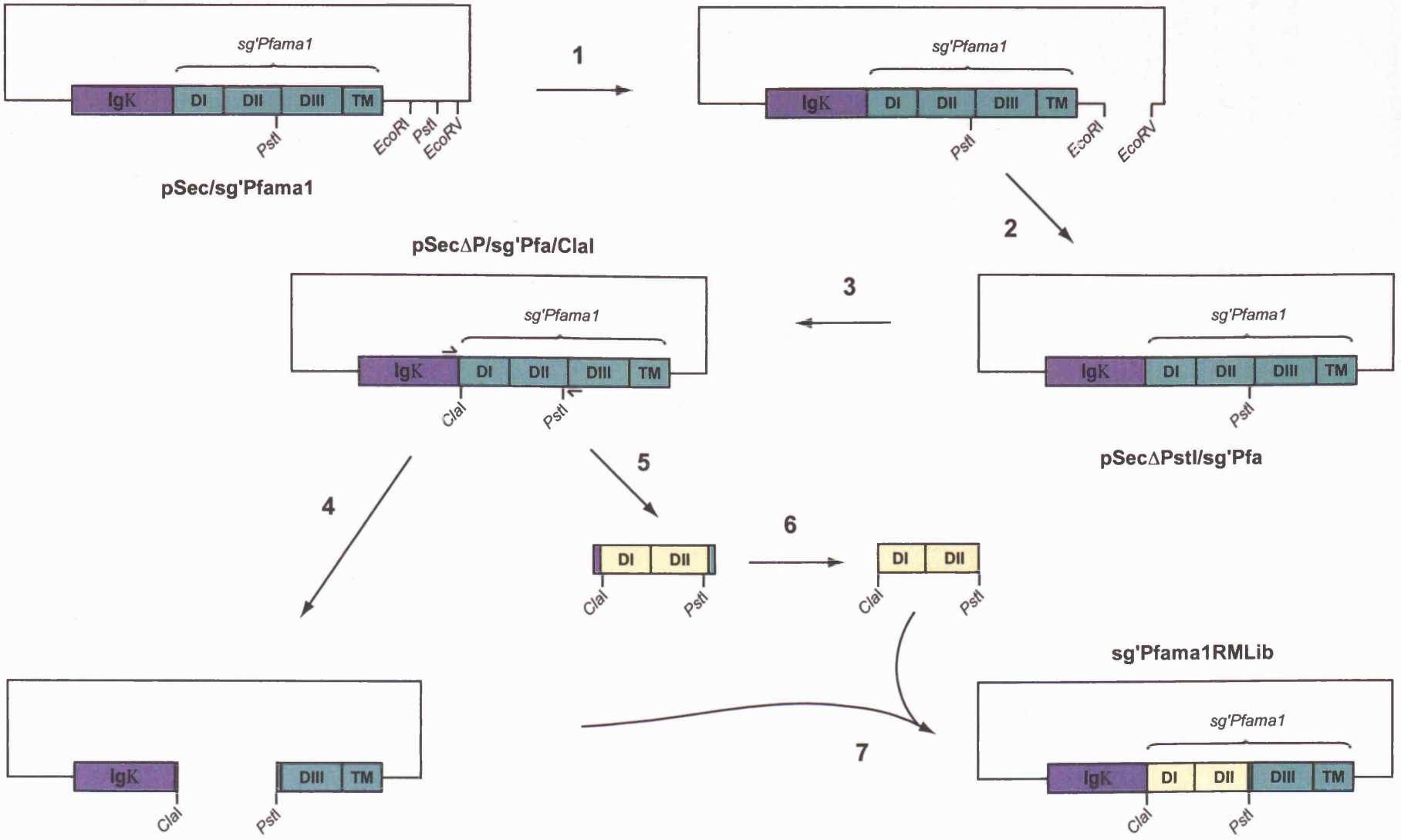
sg'Pfama1
IgK
DI
DII
DIII
TM
PstI
EcoRI
EcoRV
pSec/sg'Pfama1
1
2
pSecΔP/sg'Pfa/ClaI
3
ClaI
pSecΔPstI/sg'Pfa
4
5
6
sg'Pfama1RMLib
7

Figure 2.6: Construction of the plasmid pHH1-3'Pfa for 3' replacement in *P. falciparum*

(1) The 900bp 3' region of the *Pfama1* endogenous gene sequence was amplified by PCR from *P. falciparum* strain T9/96 genomic DNA. The PCR primers were designed to incorporate a *Bgl*II site at the 5' end of the coding sequence and an *Xho*I site at the 3' end for cloning purposes. **(2)** The PCR product was cloned into pMOSblue, giving rise to the plasmid pMOS/3'Pfama1. **(3)** The 3' coding region was excised from this plasmid by restriction digestion with BglII and XhoI. **(4)** The plasmid pHH1-ρSERA4 was digested with *Bgl*II and *Xho*I to remove the *sera4* gene and **(5)** the *Bgl*II/*Xho*I digested 3' coding region of *Pfama1* was ligated into the plasmid backbone, giving rise to the plasmid pHH1-3'Pfa.

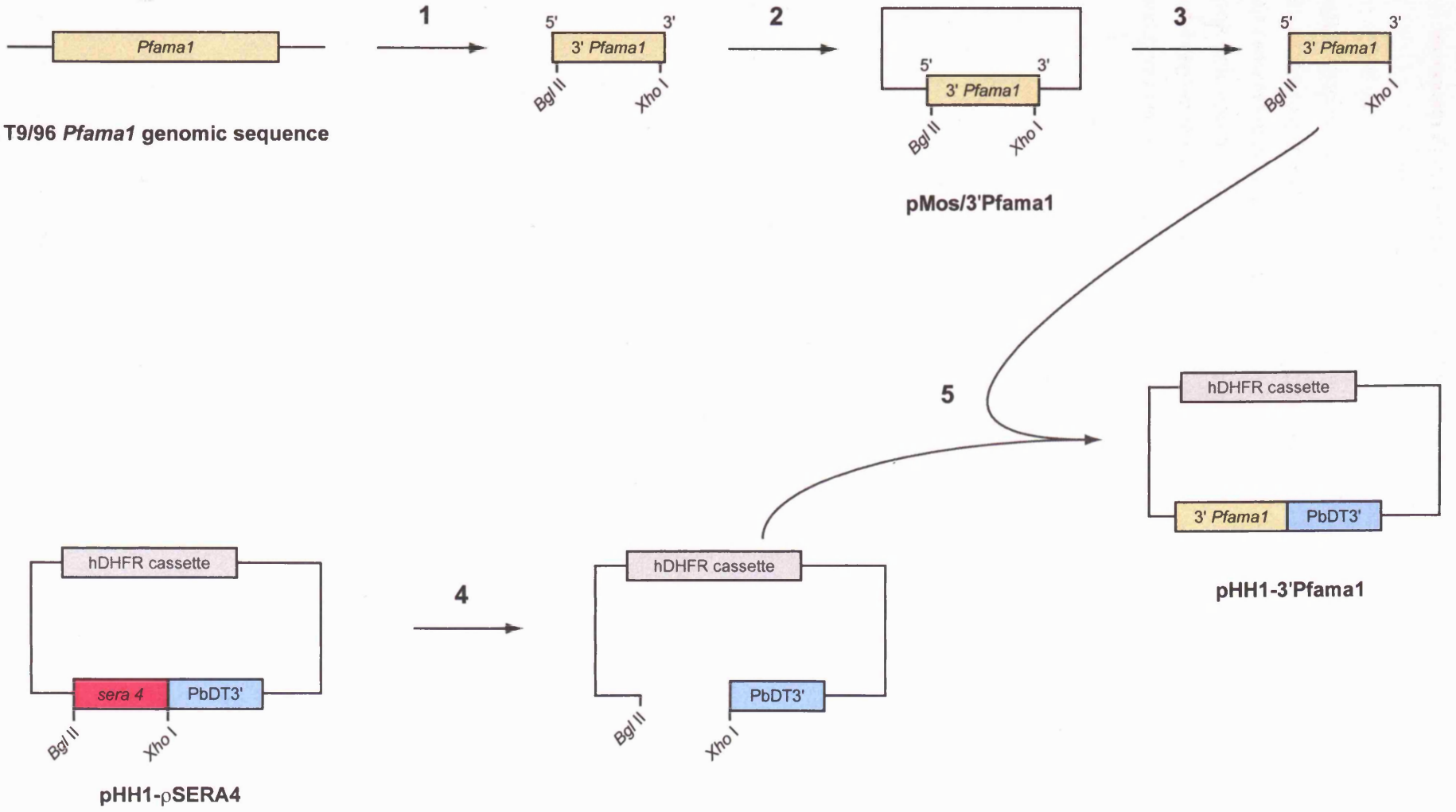
Pfama1
1
5'
3'
3' Pfama1
Bgl II
Xho I
2
5'
3'
3' Pfama1
Bgl II
Xho I
3
5'
3'
3' Pfama1
Bgl II
Xho I
T9/96 Pfama1 genomic sequence
pMos/3'Pfama1
5
hDHFR cassette
3' Pfama1
PbDT3'
pHH1-3'Pfama1
hDHFR cassette
sera 4
PbDT3'
Bgl II
Xho I
pHH1-ρSERA4
4
hDHFR cassette
PbDT3'
Bgl II
Xho I

Figure 2.7: Construction of the plasmid pHH1-Pfa/HA designed to introduce an HA epitope tag into the 3' region of the Pfama1 endogenous gene sequence

(1) The *Pfama1* gene sequence (minus the first 46 bp) was amplified by PCR from the T9/96 genomic sequence. The PCR primers were designed to introduce a *Bgl*II site and a *Xho*I site at the 5' end and 3' end of the gene sequence respectively. **(2)** The PCR product was cloned into pMOSblue and **(3)** the HA epitope tag introduced into the sequence encoding the stub region of PfAMA1 by two rounds of SDM. **(4)** The modified *ama1* gene was excised by restriction digestion using the enzymes *Bgl*II and *Xho*I. **(5)** This digestion product was cloned into BglII/XhoI digested pHH1, from construction of pHH1-3'Pfa (see figure 2.6, step **4**), giving rise to the plasmid pHH1-Pfa/HA.

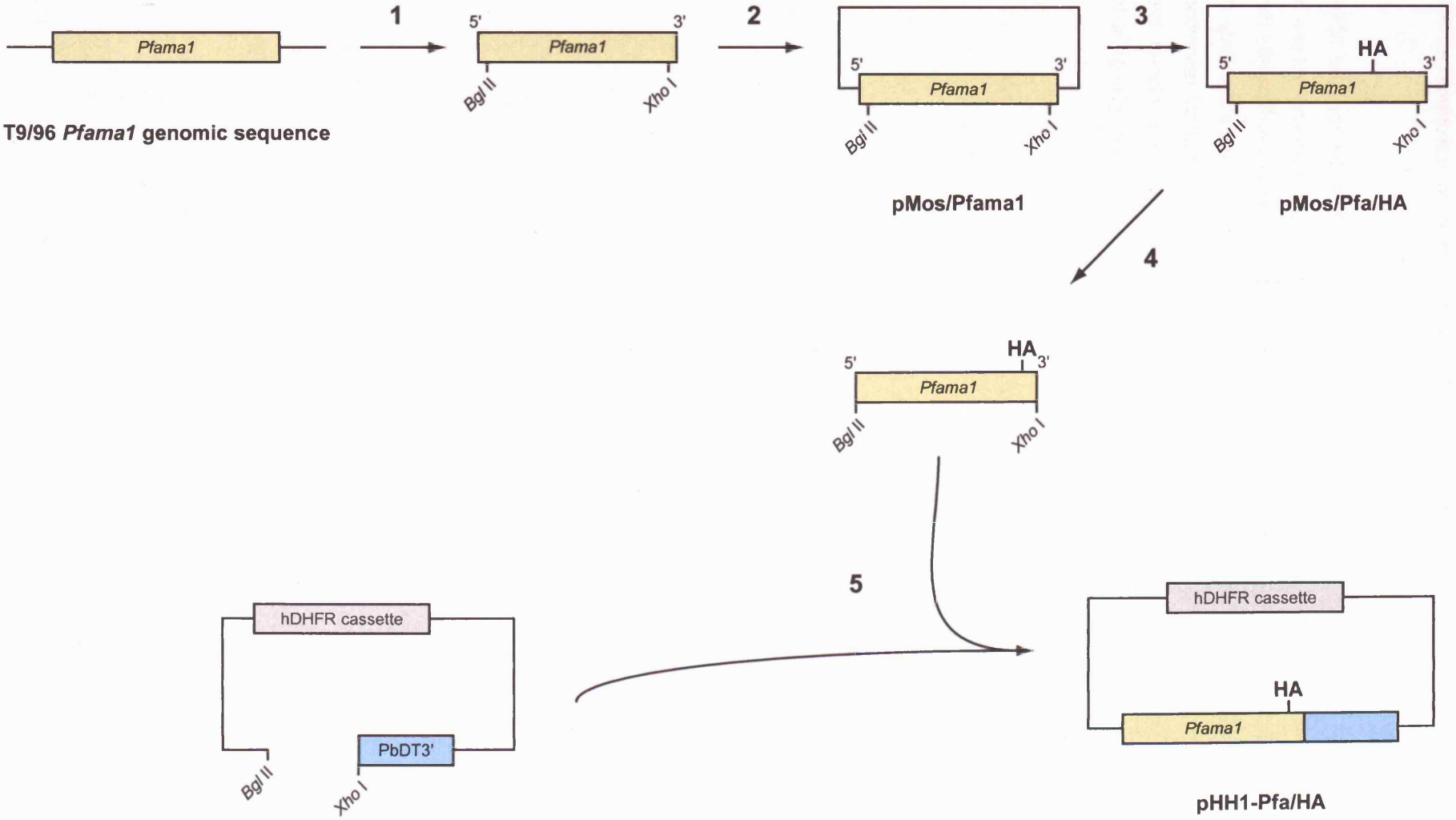
Pfama1
1
5'
3'
Pfama1
Bgl II
Xho I
2
5'
3'
Pfama1
Bgl II
Xho I
3
HA
5'
3'
Pfama1
Bgl II
Xho I
T9/96 Pfama1 genomic sequence
pMos/Pfama1
pMos/Pfa/HA
4
HA
5'
3'
Pfama1
Bgl II
Xho I
5
hDHFR cassette
PbDT3'
Bgl II
Xho I
hDHFR cassette
HA
Pfama1
pHH1-Pfa/HA

Figure 2.8: Construction of the plasmid pHAM-sgPfa/HA for episomal expression of an HA epitope tagged version of sg'PfAMA1 in *P. falciparum*

(1) The *Xho*I site found in the sequence encoding DI in *sg'Pfama1* was removed by SDM of the plasmid pSec/sg'Pfama1. In addition, two rounds of SDM-PCR were performed to introduce a copy of the HA epitope tag into the sequence encoding the stub region of sg'PfAMA1. **(2)** The region encoding the incorporated HA tag and the mutated XhoI site (Δ*Xho*I + HA) was excised by restriction digestion using the enzymes *Ksp*I and *Stu*I. **(3)** The construct Fim252, comprising sgPfama1 in pMOSblue was digested using the restriction enzymes *Ksp*I and *Stu*I to remove the corresponding region of the *sgPfama1* gene. **(4)** The excised fragment, ΔXhoI + HA, was ligated into the linearised Fim252 backbone. **(5)** The entire sgPfama1 gene, including Δ*Xho*I + HA, was PCR amplified to introduce *Xho*I sites at both 5' and 3' ends and then **(6)** the PCR product was digested with *Xho*I. **(7)** The plasmid pHAM-ACPGFP was digested with *Xho*I to remove the sequence encoding ACPGPF. **(8)** The *sgPfama1* gene sequence containing the sequence encoding the HA tagged was cloned into the linearised pHAM vector backbone, giving rise to the plasmid pHAM-sgPfa/HA.

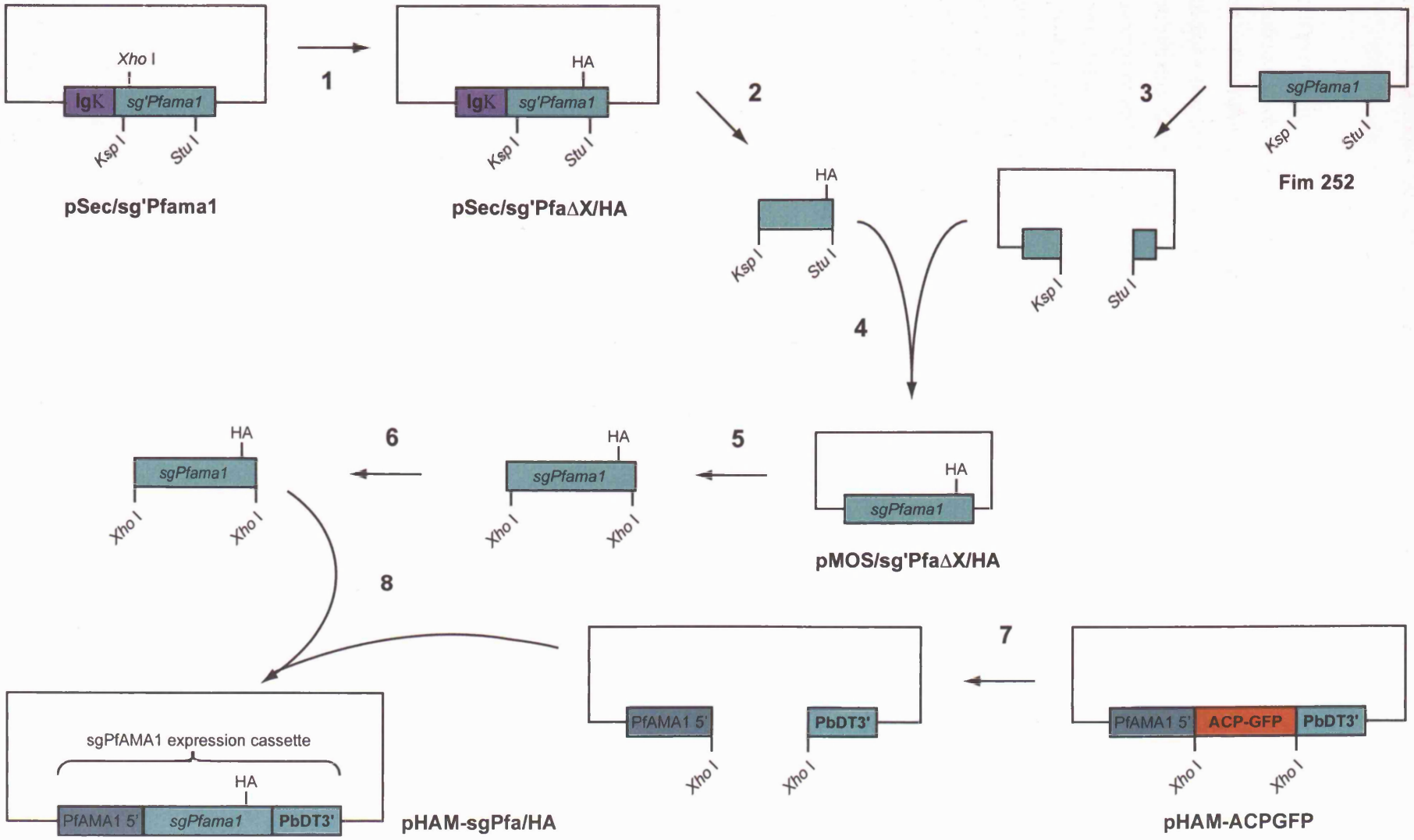
Xho I
IgK
sg'Pfama1
Ksp I
Stu I
pSec/sg'Pfama1
1
HA
pSec/sg'PfaΔX/HA
2
3
sgPfama1
Fim 252
4
pMOS/sg'PfaΔX/HA
5
6
8
7
sgPfAMA1 expression cassette
PfAMA1 5'
PbDT3'
pHAM-sgPfa/HA
ACP-GFP
pHAM-ACPGFP

Figure 2.9: Construction of the plasmid pHH1-5'-sgPfa/HA designed to replace the endogenous *Pfama1* gene sequence with that of *sgPfama1*, by single cross-over homologous recombination

(1) The 5' region of the PfAMA1 coding sequence was amplified by PCR, to introduce a 5' *Bgl*II site and a 3' *Xho*I site. **(2)** The PCR product was cloned into pMOSblue, giving rise to the plasmid pMOS/5'Pfama1 and **(3)** then excised by restriction digestion using the enzymes BglII and XhoI and **(4)** ligated into the BglII/XhoI digested pHH1 plasmid prepared for generation of the plasmid pHH1-3'Pfa earlier (see figure 2.6 step **4**), giving rise to the plasmid pHH1-5'Pfama1. **(5)** This plasmid was digested with XhoI and blunt ended. **(6)** The sgPfama1 expression cassette was excised from the plasmid pHAM-sgPfa/HA (see figure 2.8 step **8**) by restriction digestion using the enzymes *Hind*III and *Not*I and blunt ended. **(7)** The synthetic gene expression cassette was then ligated into the linearised pHH1-5'Pfama1 downstream of the 5'Pfama1 sequence, giving rise to the plasmid pHH1-5'-sgPfa/HA.

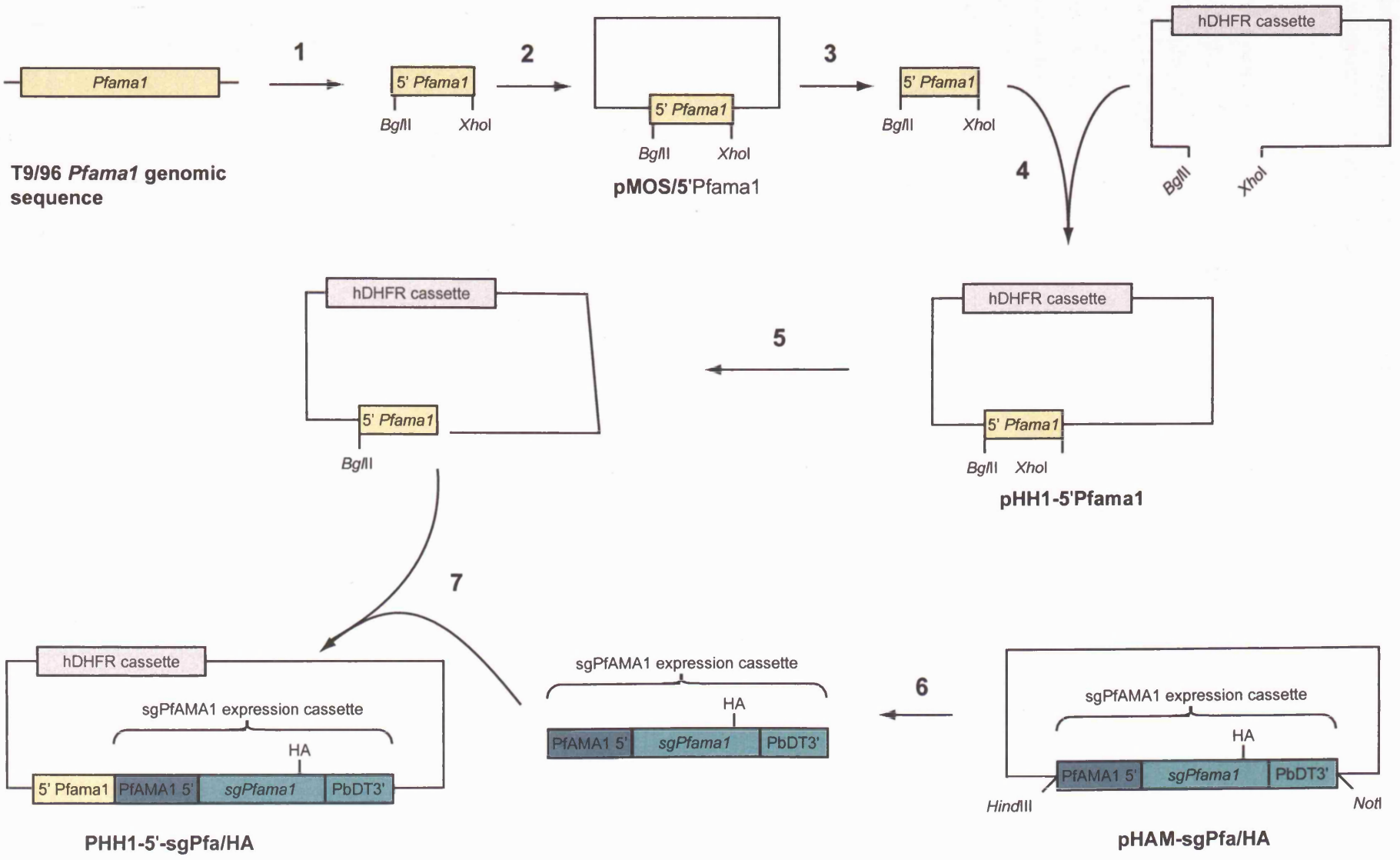
Pfama1
1
5' Pfama1
BglII
XhoI
2
5' Pfama1
BglII
XhoI
3
5' Pfama1
BglII
XhoI
hDHFR cassette
BglII
XhoI
4
T9/96 Pfama1 genomic sequence
pMOS/5'Pfama1
hDHFR cassette
5' Pfama1
BglII XhoI
pHH1-5'Pfama1
5
hDHFR cassette
5' Pfama1
BglII
7
hDHFR cassette
sgPfAMA1 expression cassette
HA
5' Pfama1
PfAMA1 5'
sgPfama1
PbDT3'
PHH1-5'-sgPfa/HA
sgPfAMA1 expression cassette
HA
PfAMA1 5'
sgPfama1
PbDT3'
6
sgPfAMA1 expression cassette
HA
PfAMA1 5'
sgPfama1
PbDT3'
HindIII
NotI
pHAM-sgPfa/HA

Figure 2.10: Construction of the plasmid pHTK-sgPfa/HA designed to replace the endogenous *Pfama1* gene sequence in *P. falciparum* by double integration homologous recombination

(1) A 900 bp stretch of the Pfama1 3' UTR was amplified by PCR from the T9/96 genomic sequence. The primers used were designed to introduce a 5' *Nco*I site and a 3' *Bin*I site. **(2)** The PCR product was cloned into pMOSblue to generate the plasmid pMOS-Pfa3'. **(3)** The plasmid was restriction digested with *Nco*I and *Bin*I, to excise the Pfama1 3' UTR sequence. **(4)** the plasmid pHHT-TK was digested with *Nco*I and *Bin*I and **(5)** the Pfama1 3' UTR ligated into it to generate the plasmid pHTK- Pfa3'. **(6)** This plasmid was digested with *Spe*I and blunt ended and **(7)** the sgPfAMA1 expression cassette, generated during the cloning of pHH1-5'-sgPfa/HA (see Fig 2.9. step **5**), ligated into it.

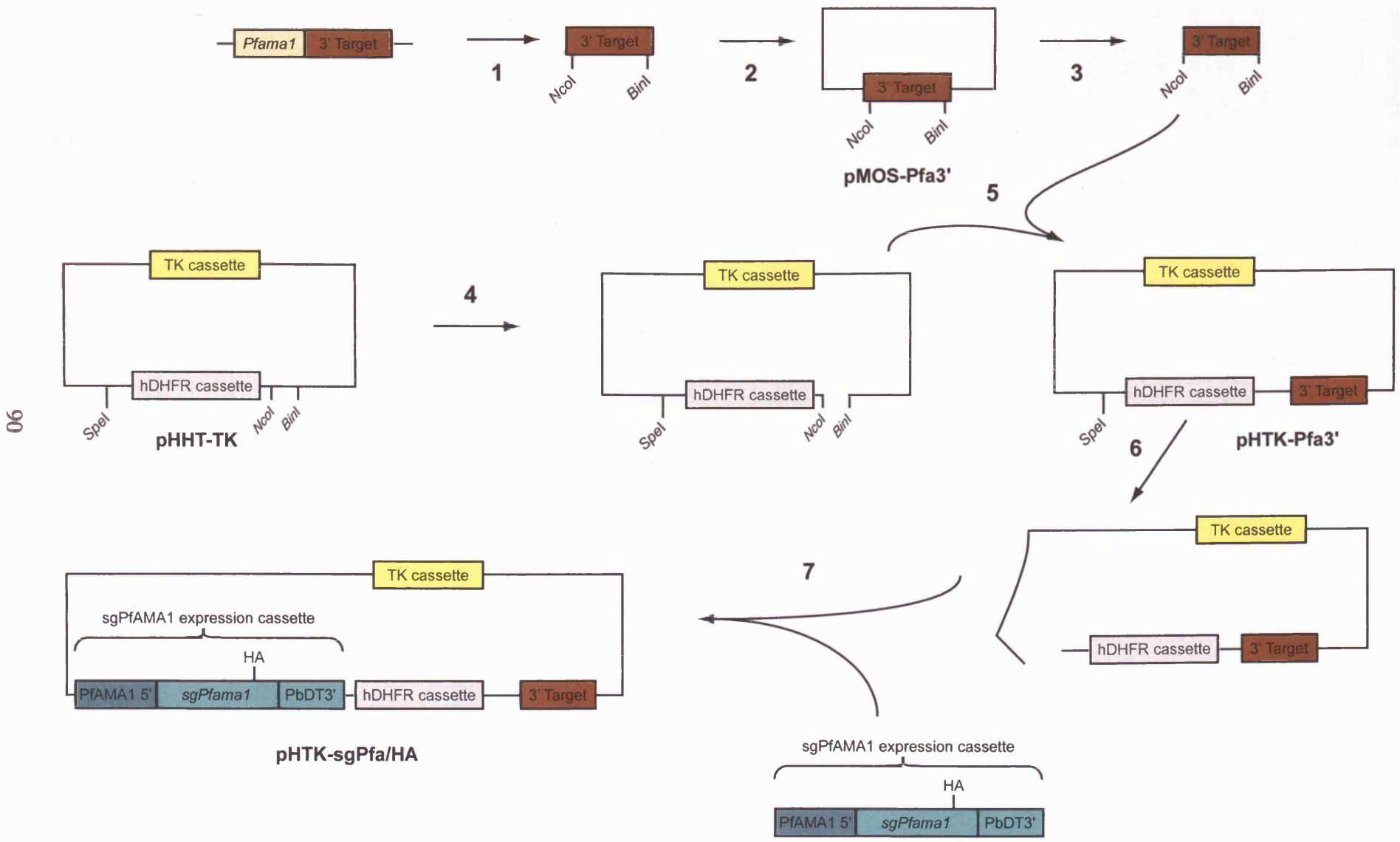
Pfama1
3' Target
1
NcoI
BinI
2
pMOS-Pfa3'
3
5
TK cassette
hDHFR cassette
SpeI
NcoI
BinI
pHHT-TK
4
6
pHTK-Pfa3'
7
sgPfAMA1 expression cassette
HA
PfAMA1 5'
sgPfama1
PbDT3'
pHTK-sgPfa/HA

Figure 2.11: Schematic representation of the selection procedure for isolating random mutants that are correctly folded (native$^+$) but lack the 4G2dc1 epitope (4G2dc1$^-$)

(1) COS-7 cells transfected with the random mutant library (sg'Pfama1RMLib) were harvested by trypsinisation to generate a single cell suspension. After trypsin neutralisation, these cells were incubated with 4G2dc1 **(2)**, followed by incubation with anti-mouse IgG coupled to Dynabeads **(3)**. Cells expressing a form of sg'PfAMA1 on their surface in which the 4G2dc1 epitope was intact (4G2dc1$^+$) bound indirectly to the Dynabeads and were extracted from the sample by application of a Dynal magnet **(4)**. The unbound cell culture (containing 4G2dc1$^-$ cells) was isolated **(5)** and incubated with the polyclonal serum N1 **(6)**, followed by incubation with fresh anti-mouse IgG coupled to Dynabeads **(7)**. The bound cells (4G2dc1$^-$/native$^+$) were again isolated by application of a Dynal magnet **(8)** and the unbound cells discarded **(9)**. Plasmid was rescued from the IgG-Dynabead bound cells **(10)**, amplified in *E. coli* and transfected back into COS-7 cells **(11)** to repeat the selection process.

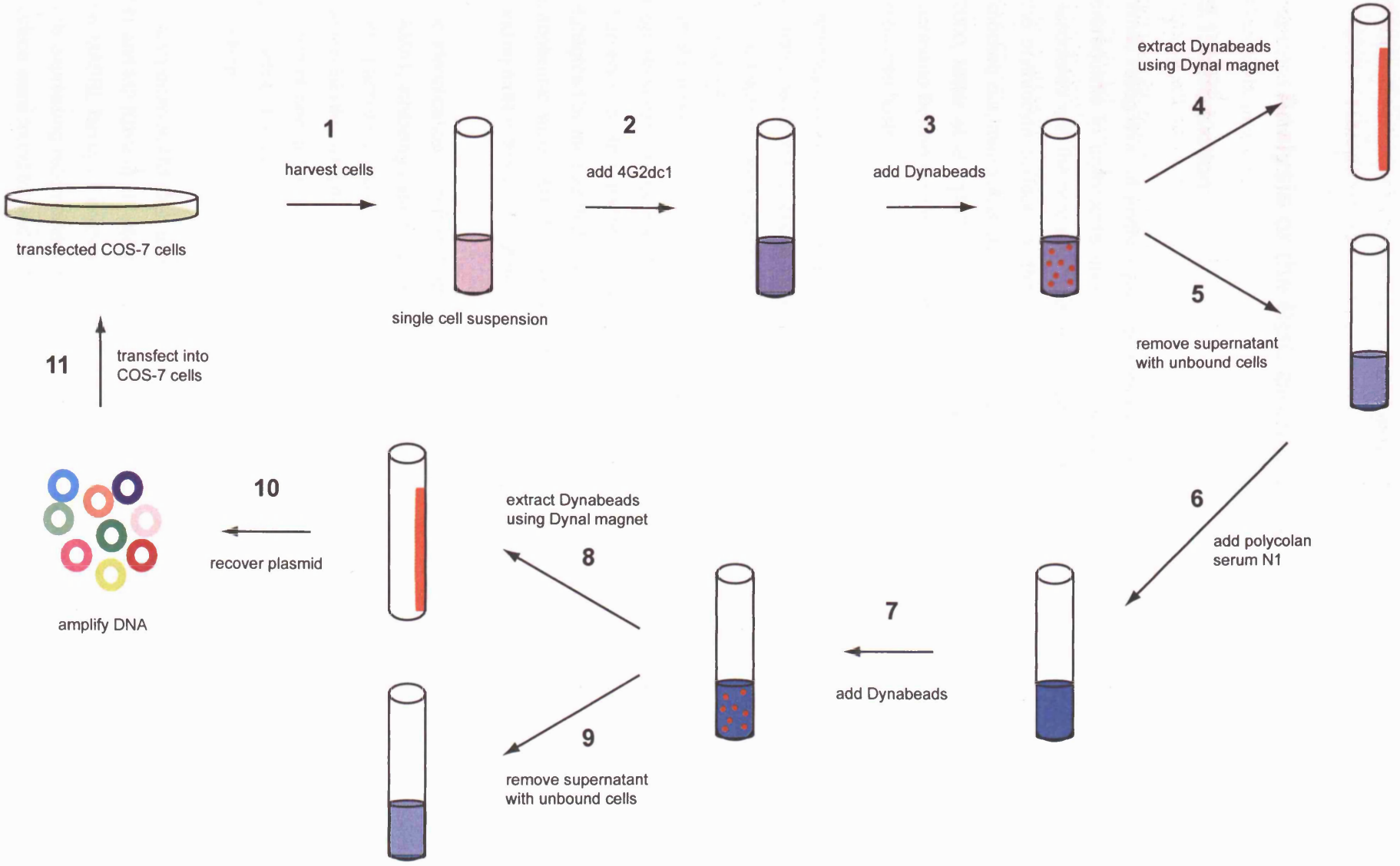
transfected COS-7 cells
1
harvest cells
single cell suspension
2
add 4G2dc1
3
add Dynabeads
extract Dynabeads
using Dynal magnet
4
5
remove supernatant
with unbound cells
6
add polycolan
serum N1
7
add Dynabeads
extract Dynabeads
using Dynal magnet
8
9
remove supernatant
with unbound cells
10
recover plasmid
amplify DNA
11
transfect into
COS-7 cells

Chapter 3

Analysis of the RBC binding properties of PfAMA1

3.1: Introduction

While recognition of erythrocyte receptors by *Plasmodium* merozoite ligands is an essential prerequisite to erythrocyte invasion, there appears to be a degree of "built-in" redundancy associated with the process. Thus, if a particular RBC receptor is enzymatically removed from the erythrocyte surface, or the gene for a particular parasite invasion-associated ligand is knocked out, merozoites may still invade, albeit possibly with reduced efficiency (Reed et al., 2000; Miller et al., 1977; Haynes et al., 1988). This redundancy possibly contributes to an increased likelihood of invasion of RBCs of different phenotypes and to survival of the parasite in diverse hosts.

Erythrocyte binding peptides have been identified from the sequence of PfAMA1 from a library of non-overlapping peptides covering the entire length of the protein (Urquiza et al., 2000). These peptides were found to inhibit erythrocyte invasion and development by *P. falciparum*. Interestingly, one of these peptides (MIKSAFLPTGAFKADRYKSH) overlaps with the second half of the domain II loop indicating a potential erythrocyte binding function for this region of the loop. However, caution should be exercised in drawing too many conclusions about the function of an entire protein, based on the properties of small peptides within the molecule. This point is highlighted by the fact that one of the peptides demonstrating high binding activity lies within the cytoplasmic tail of PfAMA1. It is difficult to envisage the functional significance of an erythrocyte binding motif in this region of this type I integral membrane protein.

The identification of phage-display peptides from a random phage display library that bind to PfAMA1, inhibiting merozoite invasion of RBCs has been used as evidence of the erythrocyte binding activity of AMA1 (Li et al., 2002; Keizer et al., 2003). However, it is equally possible that peptide binding inhibits the interaction of AMA1 with some other parasite protein. Interestingly, binding of one of these phage display peptides to PfAMA1 was inhibited by the mAb 4G2dc1, suggesting that they have similar binding sites and possibly similar mechanisms of invasion-inhibition.

P. falciparum AMA1 DI-II share 12% similarity with the PfMAEBL erythrocyte binding domains M1 and M2 (Ghai et al., 2002). Thus, the suggestion has been made that AMA1 is a member of the MAEBL family of erythrocyte binding proteins (Kappe et al., 1998a). Furthermore, COS-7 cells expressing recombinant AMA1 DI-II, from the rodent malaria *P. yoelii* (PyAMA1), on their surface were found to bind rodent RBCs (Fraser et al., 2001). In the current study, to determine

whether the *P. falciparum* protein shares this capacity, PfAMA1 was expressed on the surface of COS-7 cells and a number of experiments performed to assess RBC binding.

3.2: Surface expression of PfAMA1 in COS-7 cells

The COS-7 cell expression system has been used successfully in numerous studies assessing the erythrocyte binding capabilities of putative *Plasmodium* erythrocyte binding antigens (Sim et al., 1994a; Ranjan and Chitnis, 1999; Fraser et al., 2001; Prasad et al., 2003). This adherent cell line forms monolayers on the bottom of plastic tissue culture dishes and flasks in which they are cultured. The erythrocyte binding activity of *Plasmodium* antigens expressed in this system can easily be determined by incubating the transfected cells with dilute solutions containing the appropriate erythrocytes. Unbound erythrocytes are then washed off, leaving the COS-7 cells and any bound erythrocytes intact on the bottom of the culture dish. Rosettes formed by erythrocytes bound specifically to transfected COS-7 cells are readily detected by light microscopy at 200 X magnification. Most of these studies have relied on conjugation of the malaria antigen, or subdomains thereof, to the transmembrane domain and cytoplasmic tail of the type I integral membrane protein HSVgD1 to ensure membrane association. The HSVgD1 signal peptide was used in these studies to target the chimera to the secretory pathway and from there to the cell surface. In the current study, the COS-7 cell system was used to assess the erythrocyte binding capabilities of PfAMA1. However, and for the first time reported here, PfAMA1 was expressed in a heterologous system with its cognate transmembrane domain and cytoplasmic tail. It was hoped that this would increase the likelihood of the molecule being presented on the surface in a form comparable to that seen on the merozoite surface.

In *P. falciparum* merozoites, the signal peptide is cleaved from translated PfAMA1 on entry to the endoplasmic reticulum. The $PfAMA1_{83}$ kDa form is targeted to the micronemes and in these organelles is proteolytically processed, by removal of the prodomain, to the $PfAMA_{48}$ kDa form that is redistributed to the merozoite surface. The exact function of the prodomain is unclear as it is only found in AMA1 from *P. falciparum* and *P. reichenowi*. However, Healer *et al.* (2005) demonstrated that the inability of the parasite to proteolytically remove the prodomain from a chimeric version of AMA1, comprising the PfAMA1 prodomain, DI and DII and PcAMA1 DIII, resulted in the inhibition of surface relocalisation of the molecule. The proteases required for this processing event may not be present in the COS-7 cell system and therefore the unprocessed molecule may be presented on the COS-7 cell surface. Furthermore, the ability of AMA1 from most other parasite species to function without the presence of a prodomain, together with the fact that in *P. falciparum* the prodomain is cleaved prior to relocalisation onto the surface, suggests that this domain is not essential for the erythrocyte binding activity of the molecule. For this reason the sequence encoding the prodomain and signal peptide of PfAMA1 were not included in the construct for expression in COS-7 cells, in this study.

In the current study, COS-7 cells were transfected with pSec/sg'Pfama1. This construct was designed for expression of the entire *sgPfama1* gene minus the authentic signal peptide and prodomain (*sg'Pfama1*) and directed for secretion using the murine Igκ signal sequence (2.1.4.1). Correct expression of the gene product was assessed by mAb 4G2dc1 studies. Expression of PfAMA1 on the surface of the transfected COS-7 cells was confirmed by IFA of live, unfixed cells (Fig. 3.1 A). By comparison, no surface fluorescence is exhibited by untransfected COS cells when examined under the same conditions (Fig. 3.1 B). The synthetic gene product expressed in these cells ran at just below 67 kDa when the cell lysate was electrophoresed under non-reducing conditions in SDS-PAGE, as shown by Western blot analysis (data not shown).

3.3: Analysis of the human RBC binding activity of sg'PfAMA1

3.3.1: Does sg'PfAMA1 expressed on the surface of COS-7 cells facilitate RBC binding

The binding activity of sg'PfAMA1 expressed on the surface of COS-7 cells for human erythrocytes was assessed using the conditions described by Chitnis and Miller (1994). Briefly, COS-7 cells expressing sg'PfAMA1 (referred to hereafter as COS-7-sg'PfAMA1 cells) on their surface were incubated with human erythrocytes in RPMI-1640 for two hours at 37°C. The cells were then washed in prewarmed RPMI-1640 to remove unbound RBCs and visualised using an inverted light microscopy at 200 X magnification. No difference in RBC binding activity was observed between the transfected and untransfected cells. However, this does not rule out the possibility that this protein binds human erythrocytes under different reaction conditions.

3.3.2: The use of static conditions to prevent disruption of PfAMA1-erythrocyte interactions

It is possible that the affinity of PfAMA1 for its receptor on the human erythrocyte is very low and that this affinity is enhance by increasing the number of AMA1-receptor interactions. If the concentration of sgPfAMA1 on the COS-7 cell surface in the previous assay was too low to facilitate the stable attachment of RBCs to the transfected COS-7 cells, any lightly interacting RBCs would have been lost during the vigorous washing steps. To test this hypothesis, flasks containing transfected COS-7 cells were filled completely with RBCs in pre-gassed RPMI-1640 and incubated for 2 hours at 37°C as before. The flasks were then very gently inverted to allow detachment of unbound RBCs. Binding was then assessed by microscopic examination of the COS-7 cell monolayer. Once again, there was no detectable difference between the RBC binding to the transfected and untransfected cells.

3.3.3: sg'PfAMA1 binding activity under shear stress conditions

Shear stress is used to define the hydrodynamic forces acting upon objects in conditions of fluid flow, typically in the blood stream. In certain cell binding systems, shear stress above a critical threshold is required for the initiation and maintenance of the intermolecular interactions mediating binding (Finger et al., 1996; Alon et al., 1997; Lawrence et al., 1997). Under normal physiological conditions in the blood stream, the parasite surface antigens interacting with receptors on the erythrocyte surface must be subjected to a considerable amount of flow induced shear stress. It is possible that this stress is required to generate and maintain a stable interaction between PfAMA1 and its erythrocyte receptor. To assess the requirement for shear stress to facilitate PfAMA1-erythrocyte binding, RBCs in RPMI-1640 were incubated with sg'PfAMA1 transfected and untransfected COS-7 cells for 2 hours at 37°C on a rocker. The movement of the rocker washed the RBCs back and forth across the surface of the COS-7 cells, simulating a low level of shear stress. The RBCs were then washed off as before and the cells examined for rosette formation. As with the static conditions used above, no difference in RBC binding was observed between the transfected and untransfected COS-7 cells. Under physiological conditions, the shear flow experienced by parasites would be considerably greater than that induced in these experiments. This may account for the lack of binding observed in this study.

3.3.4: Does DIII of sgPfAMA1 bind human erythrocytes?

Kato *et al.* (2005) have suggested that DIII of PfAMA1 when expressed on the surface of CHO cells facilitates erythrocyte binding to the transfected cells. In the current study, a construct (pSec/sg'Pfama1DI-II) was designed for expression of sgPfAMA1 DIII, in conjunction with its transmembrane domain and cytoplasmic tail, on the surface of COS-7 cells. To investigate the possibility that DIII of PfAMA1 possesses RBC binding properties, the transfected COS-7 cells were analysed for their ability to mediate the binding of human erythrocytes. The erythrocyte binding activity of this truncated form of AMA1 was assessed under normal conditions as well as shear stress conditions, as described above (sections 3.3.1. and 3.3.3. respectively). No difference was observed between the RBC binding activity of the transfected and untransfected COS-7 cells, under either of the conditions used. This suggests that PfAMA1 DIII may not mediate RBC binding as has been asserted.

3.3.5: Binding of sg'PfAMA1 to the modified erythrocyte surface of ring stage parasites

It has been suggested that the malaria parasite modifies the RBC surface during invasion (Dluzewski et al., 1986). These modifications may be required for the interactions necessary for successful binding, reorientation and tight junction formation. If AMA1 is required at any of these stages in the invasion pathway, it is possible that the interaction between recombinant AMA1

and its host cell receptor would not be observed in the absence of such modifications. To investigate this hypothesis, ring stage parasites (at about 85% parasitaemia) were prepared by double synchronisation on a 70% percoll cushion within two hours of reinvasion. These parasites were mixed at 0.1% haematocrit with RPMI-1640 and incubated for 2 hours with COS-7-sg'PfAMA1 cells, at 37°C, under shear stress conditions. The cells were washed in RPMI-1640 and then once again inspected microscopically as described above for the presence of bound erythrocytes. No RBC binding was observed under these conditions.

3.3.6: Analysis of the binding of sg'PfAMA1to enzyme treated erythrocytes

To further assess the requirement for erythrocyte modifications for PfAMA1 interaction, human RBCs were enzymatically treated with trypsin, chymotrypsin or neuraminidase. The enzymatically modified RBCs were resuspended at 0.1% haematocrit in RPMI-1640 and incubated at 37°C for 2 hours with COS-7-sg'PfAMA1 cells under the shear stress conditions described above. The cells were analysed microscopically, as described above, to determine the binding activity of sg'PfAMA1. No detectable erythrocyte binding activity was observed under these conditions.

3.4: Analysis of erythrocyte binding activity of rPfAMA1

Surface fluorescence of COS-7-sg'PfAMA1 cells (Fig 3.1 Ai) in IFA analysis using the mAb 4G2dc1 appeared to be greater in intensity than that of free *P. falciparum* merozoites. This suggests that at any point on the COS-7-sg'PfAMA1 cell surface, the local concentration of AMA1 is greater than that at any point on the merozoite surface. COS-7 cells are morphologically diverse, so it is difficult to specify their exact size. However, in comparison with merozoites (1.2 - 1.8 μm long and 0.7 μm wide) COS-7 cells are very large. A crude, conservative estimate of 10 μm for the COS-7 cell diameter (assuming the cell surface to be circular) would put the 2D surface area of the COS-7 cell at 2 orders of magnitude greater than that of the merozoite (assumed to be elliptical). It is possible that the apparent fluorescence intensity with COS-7-sg'PfAMA1 is more a result of visual interpretation because of the large cell size than a reflection of the true local surface fluorescence intensity. Thus, the apparent surface fluorescence may not reflect the true cell surface density in COS-7-sg'PfAMA1 cells. A more quantitative method of comparison would be required to confirm this.

It follows therefore that one possible explanation for the lack of rosette formation in the RBC binding assays using transfected COS-7 cells, was that the sg'PfAMA1 concentration on the cell surface was insufficient to mediate RBC binding. The use of recombinant protein immobilised on a solid support would allow tighter regulation of the protein concentration present. For this reason, solid phase RBC binding assays were carried out, in which purified rPfAMA1 DI-III was bound either to nitrocellulose or polystyrene plates. In the first assay, 10 μg rPfAMA1 DI-III was

electrophoresed on 10% SDS-PAGE and then electrophoretically transferred to nitrocellulose membrane. The membranes were blocked in 5% BSA and then incubated with RBCs at 0.1% haematocrit in RPMI-1640. The membrane was washed and observed by light microscopy. Alternatively, drops of rPfAMA1 were placed onto polystyrene tissue culture plates using 2-fold serial dilution, from a starting sample of 20 μg. The plates were incubated overnight at 4°C and then incubated for 2 hours at 37°C with a human RBC suspension as described earlier, under shear stress conditions. The plates were visualised by light microscopy to assess RBC binding to the immobilised rPfAMA1. However, no RBC binding was observed to either the nitrocellulose or the polystyrene plates.

3.5: Analysis of PfAMA1-protein interactions

A possible explanation for the lack of RBC binding observed in this study is that PfAMA1 forms a complex with another parasite surface protein and complex formation is a prerequisite to RBC interaction. To assess this possibility, AMA1 was immunoprecipitated from late schizont stage parasites and free merozoites under different detergent conditions and analysed for the presence of associated molecules. The technique has been used extensively in many systems to identify protein-protein interactions. One such example is the identification of the $MSP1_{42}$-MSP9 (or acidic basic repeat antigen, ABRA) complex (Li et al., 2004a) in *P. falciparum* merozoites by immunoprecipitation with polyclonal Abs raised against a region of MSP9 that has previously been shown to bind band 3 on the erythrocyte surface. Immunoprecipitation was carried out in the presence of a detergent to ensure the extraction of PfAMA1 from the lipid bilayer. If the interactions holding AMA1 and its putative partner protein together are weak, the use of detergent may result in the disruption of the complex. For this reason, three different detergents were used in an attempt to identify one that supported this potential interaction.

3.5.1: Detection of a putative PfAMA1 partner protein of 55 - 60 kDa

Naturally-released free merozoites were surface-labelled with biotin then solubilised into buffers containing NP40, CHAPS or sodium deoxycholate (DOC) and supplemented with protease inhibitors PMSF, Pepstatin A and E64. Immunoprecipitation was carried out on the detergent soluble fraction using mAb 4G2dc1 immobilised on Sepharose beads (4G2 Sepharose) and immunoprecipitated proteins analysed by Western blot with HRP-conjugated streptavidin or with the polyclonal serum R1.

Immunoprecipitation from the NP40 and CHAPS soluble fractions resulted in the isolation of a large number of faint bands when blots were probed with HRP-streptavidin, probably due to non-specific binding of biotin-labelled proteins to the 4G2 Sepharose (Fig 3.2 A, lanes N and C respectively). However, clear, strong bands indicated the presence of the 83 kDa and 66 kDa forms of PfAMA1. An additional strong band could be seen at about 55 kDa and a doublet at

about 34 kDa. When analysed further, all these bands were reactive with the polyclonal Ab R1 (Fig 3.2 B, lanes N and C respectively), identifying them as break down products of PfAMA1. By contrast, little immunoprecipitation was observed from the DOC solubilised fraction (Fig 3.2 A, lane S). In this sample, the 83 kDa and 66 kDa 4G2dc1 bands were very weak but the 34 kDa doublet still gave a strong signal (Fig 3.2 A and B, lane S). This doublet may represent fragments that were membrane associated and therefore preferentially partitioned into the DOC fraction over the membrane bound forms. A 55 - 60 kDa band was recognised by the secondary Ab in all samples (Fig 3.2 C). A band of this size was present in all the samples probed with streptavidin, though only very weakly in the DOC sample compared with very strongly in the NP40 and CHAPS samples. However, when probed in Western with either the polyclonal serum R1 or the secondary Ab on its own, this band was of equal intensity in all samples. This suggests that in the NP40 and CHAPS extracted samples two proteins co-migrated at 55 - 60 kDa. One of these proteins was of low intensity and was detected by the secondary Ab, possibly representing the mAb 4G2dc1 light chain from the immunoprecipitation. The other protein, highly abundant in the NP40 and CHAPS extracted samples when probed with streptavidin, was distinct from PfAMA1 as it was not recognised by the polyclonal serum R1 and may have been a parasite protein that co-precipitated with PfAMA1. This raises the possibility that the strong intensity band detected with streptavidin in the NP40 and CHAPS fractions was a potential PfAMA1 partner protein.

3.5.2: Immunoprecipitation of PfAMA1 from metabolically radiolabelled *P. falciparum*

Biotin labelling of schizont stage parasites will also result in the labelling of RBC structures. It is therefore possible that immunoprecipitation of PfAMA1 from this mixture would result in the non-specific co-precipitation of a RBC protein. Such proteins would be indistinguishable from parasite proteins in this assay and might complicate interpretation of the result. In addition, the interactions between PfAMA1 and other parasite proteins may only occur once PfAMA1 is transported onto the merozoite surface. In schizonts, most of the protein is present in the micronemes, therefore such interactions might not be readily observed at this stage of the life cycle. To investigate this possibility, immunoprecipitation profiles of schizont and free merozoites were compared. A highly synchronous culture of *P. falciparum* schizonts was metabolically labelled with L- [^{35}S] -methionine and cysteine to specifically label only parasite proteins. Schizonts were either returned to culture in the absence of labelled amino acids to allow merozoite development and release or harvested directly. PfAMA1 was immunoprecipitated with mAb 4G2dc1 or with the polyclonal serum N1 from CHAPS solubilised fractions as NP40 and CHAPS gave similar results previously (3.5.1.).

3.5.2.1: Identification of a 46 kDa putative PfAMA1 merozoite partner protein by immunoprecipitation with mAb 4G2dc1

Fluorometric analysis of mAb 4G2dc1 immunoprecipitated samples (Fig 3.3 A) revealed major bands corresponding to the PfAMA1 83 and 66 kDa processed forms, as well as many other bands. However, the 83 kDa form was less obvious in the merozoite fraction (Fig 3.3 A, lane m) indicating that processing of PfAMA1 to the 66 kDa form had almost gone to completion in free merozoites. There was a doublet in the merozoite fraction at about 46 kDa (Fig 3.3 A, lane m) only the upper band of which was present in the schizont fraction (Fig 3.3 A, lane s). The lower band in the merozoite fraction was detectable by Western blot analysis with the polyclonal serum R1 (Fig 3.3 B, lane m) indicating that it was of PfAMA1 origin. This band was also present in the CHAPS immunoprecipitated fraction of biotinylated merozoites (3.5.1) after longer exposure (data not shown). This raises the possibility that the upper band of the 46 kDa doublet was a putative PfAMA1 partner protein. A 55 - 60 kDa band detected by the HRP-conjugated secondary antibody was present in Western blot analysis (Fig 3.3 C, lanes s and m) but not the [^{35}S] autoradiograph indicating that it represented a mAb 4G2dc1 fragment. This probably corresponds to the low intensity 55 - 60 kDa band observed in the previous assay. The high intensity band detected previously in NP40 and CHAPS extracted samples were not present in the [S^{35}] labelled samples. It is possible that this molecule was of RBC origin, labelled with biotin, and co-precipitated non-specifically in the previous assay.

3.5.2.2: Attempts to identify the putative PfAMA1 partner protein by immunoprecipitation from [^{35}S] metabolically labelled parasites using the polyclonal serum N1

The mAb 4G2dc1 is invasion inhibitory and may function by blocking the interaction between PfAMA1 and its partner protein on the merozoite surface. If so, it might be impossible to immunoprecipitate the putative AMA1-partner protein complex using this mAb. For this reason, immunoprecipitations using metabolically labelled parasites from both developmental stages were repeated using the polyclonal serum N1. When this was done, the upper band of the doublet previously observed at 46 kDa was no longer present (Fig 3.4 A, lanes s and m). However, the lower band was again present in the merozoite fraction only (Fig 3.4 A, lane m). This band was also detected in the merozoite fraction by Western blot analysis using the polyclonal serum R1 (Fig 3.4 B, lane m) and this time a faint band was detected at this position in the schizont fraction (Fig 3.4 B, lane s). This suggests that in the mAb 4G2dc1 immunoprecipitation the larger of the 46 kDa double bands immunoprecipitated non-specifically. Alternatively, immunoprecipitation with the polyclonal serum N1 may have resulted in disruption of the interaction between PfAMA1 and this protein. When probed with the secondary Ab alone (Fig 3.4 C), the 55 kDa band previously detected was again visible for both samples.

No additional proteins co-precipitated with PfAMA1 from the merozoite fraction than the schizont fraction. This suggests that during these developmental stages PfAMA1 does not interact with any other parasite proteins.

3.5.3. Attempts to cross-link PfAMA1 and its putative partner protein prior to immunoprecipitation

It was hypothesised that one reason for the lack of co-precipitation observed so far with PfAMA1 may be that the interaction between PfAMA1 and its partner protein is transient and weak. If this was the case, the detergent conditions used might disrupt this interaction. To overcome this potential problem, merozoite and schizont samples metabolically labelled with [^{35}S], were covalently cross-linked using DTSSP prior to immunoprecipitation with mAb 4G2dc1.

Under these conditions nothing appeared to co-precipitate with PfAMA1 and the PfAMA1 83 and 66 kDa bands themselves were very weak (Data not shown).

3.6: Discussion

Invasion of erythrocytes by the malaria parasite is a complex process, involving multiple parasite-host interactions at each stage. The initial interaction occurs between any point on the merozoite surface and the RBC membrane. Reorientation of the parasite to bring its apical prominence into direct contact with the host cell is rapidly followed by tight junction formation between the parasite and host cell membranes (Dvorak et al., 1975). The merozoite enters the RBC and the membrane pinches off behind it, enclosing it in the PV. The whole process takes about 30 seconds.

3.6.1: Does AMA1 mediate the initial attachment of the merozoite to the RBC?

Molecules involved in the initial interaction must either already be on the surface of the parasite at the time of schizont rupture or be released onto the surface immediately following it. As this interaction may occur at any point on the parasite surface, this receptor/ligand is likely to be present across the entire surface. The parasite determinants responsible for reorientation, if this is a controlled rather than random process, must show some directionality so that the movement is exclusively towards the apical end. This may be achieved by protein release from an organelle within the apical complex and redistribution across the parasite resulting in the formation of a concentration gradient. Proteins involved in tight junction formation need only be released from the apical organelles as the apical prominence comes into contact with the RBC membrane. Furthermore, it may be deleterious to the parasite if these proteins are released before the parasite has reorientated. These proteins can therefore be retained until some signal to the parasite indicates the need for their release. This signal could occur as a result of initiation of either of the preceding steps.

Other than the major merozoite surface proteins, such as MSP1, two other potential candidates for a role in initial attachment are the DBL-EBP MAEBL and AMA1. Both these proteins have an

apical localisation in developing merozoites but are released onto the surface around the time of schizont rupture and can be shown to have a circumferential localisation in free merozoites (Kappe et al., 1998a). Thus, unlike other DBL-EBPs, MAEBL (and AMA1) are in the correct location at the appropriate time to facilitate initial binding of invasive merozoites to host erythrocytes.

3.6.2: Does AMA1 interact directly with the host erythrocyte?

That AMA1 plays a role in erythrocyte invasion has been demonstrated. Triglia *et al.* (2000) demonstrated that *P. chabaudi* AMA1 (PcAMA1) was unable to completely complement the function of PfAMA1. However, transgenic expression of PcAMA1 under the control of the *Pfama1* promotor, in addition to endogenous PfAMA1, enabled *P. falciparum* parasites to invade human erythrocytes in the presence of anti-PfAMA1 antibodies at 35% the efficiency of wild type D10 parasites in the absence of antibodies (Triglia et al., 2000; Healer et al., 2005). In the presence of anti-PfAMA1 Abs invasion by wild type D10 parasites was almost completely inhibited. This indicates that PcAMA1 can partially complement the function of PfAMA1. In addition, invasion of murine erythrocytes by this transgenic line was enhanced (Triglia et al., 2000). Thus, AMA1 plays a critical role in host cell invasion and in addition contributes to host species specificity, suggesting that it interacts directly with the host erythrocyte.

3.6.3: Could AMA1 play a role in erythrocyte invasion down-stream of the initial attachment event?

Due to the initial localisation in the micronemes and the subsequent redistribution to the surface via the apical prominence, AMA1 could participate in parasite reorientation once the initial attachment has been achieved. In support of this, in the presence of an invasion inhibitory rat mAb against PkAMA1, the initial interaction between *P. knowlesi* merozoites and erythrocytes occurs, however reorientation and tight junction formation do not (Mitchell et al., 2004). This suggests that the initial interaction occurs independently of AMA1, which must perform a role in erythrocyte invasion downstream of this initial attachment event. The membranous vesicles previously observed during normal invasion (Dvorak et al., 1975) were found to be present in some RBCs, suggesting that some merozoites did contact the erythrocyte via their apical prominence, releasing some of the contents of their apical organelles, but were unable to complete the invasion process (Mitchell et al., 2004). It is possible that merozoite reorientation following initial binding is a random process facilitated by the deformations of the RBC following the initial binding step (Dvorak et al., 1975). During this process the RBC membrane is observed to wrap itself around the parasite (Mitchell et al., 2004). This parasite-induced activity brings the RBC membrane into contact with different regions of the merozoite membrane and thus may randomly promote interaction with the apical end of the parasite.

3.6.4: AMA1, a component of the tight junction?

In *P. knowlesi* and *P. vivax*, the DBPs have been implicated in tight junction formation(Miller et al., 1979a). This role may be filled in other parasite species, not dependent on the Duffy antigen for invasion, by other EBPs. As antibodies against AMA1 block invasion in several species of *Plasmodium* (Deans et al., 1982; Thomas et al., 1984; Kocken et al., 2000) and it is highly conserved across the genus at the amino acid level (Waters *et al.* 1990), it is likely that AMA1 function is also conserved. The requirement for the DBPs in *P. vivax* and *P. knowlesi* for tight junction formation and the essential, conserved nature of AMA1 across *Plasmodium* spp suggests that if AMA1 participates in tight junction formation it is unlikely to do so in isolation. One possible scenario is that AMA1 is involved in tight junction formation in the context of a multi-component complex comprising other parasite proteins, such as the DBPs. However, the time of relocalisation of AMA1 across the parasite surface argues against a role in tight junction formation. If AMA1 is a member of the complex that forms a tight junction between the apical end of the merozoite and the RBC it must then be translocated across the parasite surface as the merozoite invades. If this occurs, what is its function on the surface of the merozoite so early after and in some cases before (Waters et al., 1990) schizont rupture? One possible explanation is that the surface distributed AMA1 is drawn into the tight junction as it necessarily expands to move around the parasite surface. The observation in IFA that the MESH SUB2 is translocated around the surface of free merozoites from anterior to posterior in a manner mirroring tight junction movement (Harris *et al.* submitted) suggests that during invasion it is a component of the tight junction. This suggests a sheddase role for SUB2 at the orifice of entry, allowing internalisation of the parasite and invagination of the RBC membrane. The identification of SUB2 as the protease that cleaves AMA1 from the merozoite surface (Harris *et al.* submitted) and its putative presence in the tight junction would support the hypothesis that AMA1 is a tight junction component. The surface localisation of AMA1 would allow the replenishment of parasite molecules within the junction that are shed during this internalisation process. Miller *et al.* (1979) demonstrated that cytochalasin B treated *P. knowlesi* merozoites attach to and reorientate normally with Duffy-positive and negative erythrocytes. However, in the absence of the Duffy antigen on the RBC surface tight junction formation does not occur. By comparison, Mitchell *et al.* (2004) demonstrated that anti-AMA1 antibodies allow the initial interaction between the merozoite and RBC membranes, but inhibit reorientation and subsequent tight junction formation. In contrast with the arguments for AMA1 involvement in tight junction formation, these findings suggest a role for AMA1 in the interim between initial attachment of the parasite to the host cell and junction formation. Whether this is the role of SUB2 in the tight junction, or if this is indeed where it is located during erythrocyte invasion, is unclear.

3.6.5: sgPfAMA1 may not mediate erythrocyte binding

To investigate the role of PfAMA1 in invasion of human erythrocytes in the current study, the full-length synthetic gene product (sgPfAMA1) was expressed in COS-7 cells with its cognate transmembrane and cytoplasmic domains. Recognition of the expressed protein by mAb 4G2dc1, on unfixed, unpermeabilised cells confirmed that the protein was expressed in the correct topological orientation on the cells (Fig 3.1). Despite numerous attempts in a variety of assays, it was not possible to demonstrate binding of human RBC to these transfected cells. Further assays using recombinant protein immobilised at high density on polystyrene or nitrocellulose similarly failed to demonstrate any capacity for the protein to bind RBCs even though solid phase binding assays have been used previously to demonstrate binding of parasite antigens to host cells (Buffet et al., 1999). This group demonstrated that parasitised erythrocytes (trophozoite stage) bound to the erythrocyte receptors CD36 and chondriotin sulphate A that had been bound to plastic Petri dishes. In a "cell blot" assay involving the *T. gondii* antigen MIC3, Garcia-Reguet *et al.* (2000) demonstrated binding of Vero cells to purified TgMIC3 and mouse intestinal epithelial cells (MODE-K cells) to MIC3 from parasite lysates, electrophoresed in SDS-PAGE and electrophoretically transferred to nitrocellulose membrane as in the current study. In the current study there was no positive control for erythrocyte binding to immobilised antigen with either of the methods used. It is possible that a cell lysate from the COS-7 cells transfected with PvDBL region II could have been electrophoresed in SDS-PAGE and transferred to nitrocellulose as a positive control in this assay. However, the identity of the protein supporting erythrocytes binding could not have been confirmed, as no anti-PvDBL region II Abs were available. The method of detection used to determine RBC binding to nitrocellulose-bound rPfAMA1 in the current study would not have allowed the detection of low-level erythrocyte binding. More reliable detection might have been achieved by fixing bound erythrocytes to the nitrocellulose and then carrying out a Western blot using an anti-RBC Ab, such as an anti-Band 3 Ab. An alternative approach would have been to generate RBC ghosts and solubilise these in SDS-sample buffer before electrophoresis in SDS-PAGE. An overlay assay could then have been carried out using a solution of rPfAMA1 and binding of this recombinant protein to its erythrocyte receptor molecule determined by Western blot analysis using an anti-PfAMA1 Ab. This approach was used by Maier *et al.* (2003) to demonstrate binding of the DBL-EBP BAEBL to erythrocyte ghosts. One problem with the use of this approach in the current study is that it relies on the one-to-one binding affinities of PfAMA1 and its receptor being strong enough to maintain the interaction. It has already been noted that Howell *et al.* (2001) were unable to demonstrate that the ectodomain of PfAMA1 shed from merozoites possessed RBC binding activity. This suggests that the binding affinity of monomeric PfAMA1 is not great enough to maintain such interactions and allow detection. It is possible that after release from the merozoite surface PfAMA1 undergoes conformational changes that might disable its RBC binding activity, however, evidence from the current study suggests that even when membrane bound, PfAMA1 does not exhibit such activities.

3.6.6: Shear stress is unlikely to be required for AMA1-erythrocyte interactions

It has been demonstrated that leukocyte adhesion to endothelial venules mediated by the selectins (L-, P- and S-selectin) is enhanced by fluid shear stress (Finger et al., 1996; Lawrence et al., 1997; Alon et al., 1997). The physiological conditions under which merozoites adhere to and invade RBCs in the blood stream are the same as those encountered by leukocytes near a site of infection or tissue damage, except that both merozoites and erythrocytes are moving. To investigate the possibility that shear stress forces, operating on interacting merozoites and RBCs *in vivo*, might enable RBC binding to COS-7 cells expressing sgPfAMA1 *in vitro*, transfected cells expressing sgPfAMA1 were incubated with human erythrocytes under conditions designed to simulate such forces. A possible explanation for the inability to observe erythrocyte binding in these assays is that the conditions did not accurately resemble those experienced by the merozoite in the blood stream. In leukocyte binding studies, parallel wall-flow chambers are used in which the flow rate can be determined and varied (Alon et al., 1997; Chen and Springer, 2001). This allows direct and quantifiable analysis of the effects of shear flow/stress on ligand interaction and the determination of the critical flow rate to maintain such interactions. Clearly the use of a flow chamber in the current study would have provided clearer evidence of whether such flow is required for PfAMA1-erythrocyte interactions in this system.

Chitnis and Miller (1994) have shown by transfection in COS-7 cells that region II of the *P. vivax* DBP is responsible for RBC binding. By using region II of *P. vivax* DBP (PvDBP) in the current binding assays it was shown that the conditions used in the current study were conducive to binding at least for this molecule. It might be imagined that the effects of shear stress acting against two free moving cells is greatest before they bind to each other. The involvement of DBPs in tight junction formation, when the stress acting on the cells to pull them apart is possible reduced as they are already interacting, is unlikely to be dependent on shear stress. This may explain why erythrocyte binding by region II of PvDBP occurs in this study irrespective of the flow conditions used. If the initial interaction between merozoite and erythrocyte is mediated by a resident surface parasite molecule, as has already been suggested, and PfAMA1 functions down stream of this event (Mitchell et al., 2004) it is probable that shear stress is not critical for PfAMA1 based RBC binding. This would suggest that if PfAMA1 is an erythrocyte binding molecule some other factor, lacking in the current study, is required for this interaction to be observed.

3.6.7: Is the PfAMA1 synthetic gene product functional?

The failure of this study to attribute erythrocyte-binding activity to PfAMA1 may in part be due to differences between the synthetic gene product and the endogenous gene sequence. The FVO AMA1 sequence contains 6 potential N-glycosylation sites. Despite early reports that *P. falciparum* lacked the machinery for N-glycosylation (Dieckmann-Schuppert et al., 1992) recent

studies have shown this parasite to have a low N-glycosylation capability (Gowda et al., 1997; Gowda and Davidson, 1999). However, identification of five of the six potential N-glycosylation sites by MALDI-TOF analysis of proteolytically digested $PfAMA1_{83}$ and $PfAMA1_{48/44}$ failed to show any glycosylation (Howell et al., 2001). For this reason all six sites were replaced in the *Pfama1* synthetic gene sequence with amino acids found at the corresponding position in AMA1 from other species of *Plasmodium*. These alterations in the primary sequence of PfAMA1 may have had a deleterious effect on function. It is possible that the sixth N-glycosylation site that was not identified in the study of Howell et al. (2001), is in fact glycosylated and that glycosylation at this position is essential for the adhesive properties of the protein. Alternatively the alteration in amino acid sequence itself could deleteriously alter the charge interactions between receptor and ligand. The functionality of the *Pfama1* synthetic gene sequence is considered in chapter 6.

3.6.8: Potential erythrocyte binding domains in the PfAMA1 ectodomain

The similarity identified between AMA1 DI-II with domains M1 and M2 of the EBP MAEBL (Ghai et al., 2002) add weight to the suggestion that AMA1 is an erythroycte binding protein. Thus, the implication is that DI-II of AMA1 facilitate invasion of erythrocytes by *Plasmodium* species by binding to a ligand on the RBC surface. The work of Fraser et al. (2001) added support to this idea. This group expressed the ectodomains of PyAMA1 on the surface of COS-7 cells as a chimera with the transmembrane region and cytoplasmic domain of HSVgD1. Significantly less erythrocyte binding activity was then observed with a chimera of DI-III (full length ectodomain) than with DI-II, even though the molecule was properly folded and expressed on the cell surface (shown by IFA using mAb 45B1, which recognises a conformation dependent epitope in the PyAMA1 ectodomain). Indeed, DI-III demonstrated less erythrocyte binding than DI and DII together or alone, or DII and III together. The possibility that PfAMA1 DI-II mediates erythrocyte binding was not investigated in the current study. However, if RBC binding was a genuine property of AMA1, it could be argued that the full-length protein would also be expected to demonstrate this property. Therefore, it is possible that erythrocyte binding is not a function of AMA1. The RBC binding property of DI-II may be a non-specific property of these two domains expressed on their own, exposing a normally buried region of the molecule.

In a recent study (Kato et al., 2005) varying regions of the PfAMA1 ectodomain (FVO clone) were expressed in GPI anchored form on the surface of CHO-K1 cell. When expressed alone, DIII was found to bind trypsin treated erythrocytes but not intact erythrocytes. Neither DI-III nor DI-II was able to facilitate binding of normal or trypsinised RBC. The authors suggest that proteolytic processing of AMA1 may explain the binding of DIII in preference to DI and DII. It is unclear how this can occur when none of the processing of AMA1 thus far described (Howell et al., 2001; Howell et al., 2003b; Howell et al., 2005) identifies DIII on the erythrocyte surface in the absence of the rest of the ectodomain. Furthermore, this finding was not corroborated by the

current study. Expression of DIII on the surface of COS-7 cells did not induce RBC binding to the transfected cells.

The possibility cannot be ruled out that a parasite induced conformational change occurs in the PfAMA1 ectodomain at the time of invasion, which results in the exposure of otherwise hidden domains, that are artificially exposed in these studies in heterologous systems. However, this does not explain the inconsistency between the results of Kato *et al.* (2005) and the current study.

3.6.9: AMA1 DI-II comprises characterised adhesion modules

The crystal structure of PvAMA1 has identified two PAN modules, one in each of DI and DII (Pizarro *et al.* 2005). In other systems PAN modules are functionally diverse (Baglia and Walsh, 1996; Ho et al., 1998; Tordai et al., 1999). However, they share the common feature of mediating protein-protein or protein-carbohydrate interaction (Ho *et al.* 1998). Owing to the functional diversity of these proteins it is impossible to suggest a precise role for AMA1, other than that it probably has some adhesion function (Tordai *et al.* 1999). This lends support to the idea outlined above that DI-II possess erythrocyte binding properties.

Pizarro *et al.* (2005) compared the PAN module of PvAMA1 DII with the heparin-docking site of the hepatocyte growth factor, NK1. The putative receptor-binding site of DII could be composed of strand β14 and helix α7, equivalent to β2 and the PAN domain helix of NK1 respectively. The loop connecting the helix and sheet β15 is not in a position to interact with the substrate as the equivalent loop is in NK1. However, it is feasible that upon substrate docking the flexible DII loop closes over it to lock it in place (Fig 3.5). Clearly heparin need not be the ligand for AMA1 and the charge distribution at this site on AMA1 is unlikely to support interactions with such a ligand. However, this identifies at least one potential, sterically favourable binding site on AMA1. It is possible that AMA1 may directly, or in conjunction with a parasite encoded partner protein, interact with an erythrocyte ligand via this site. PAN modules have been identified in micronemal proteins from the apicomplexan parasites *T. gondii* and *Eimeria tenella* (Brown et al., 2001) (Brecht et al., 2001). As micronemal proteins have been implicated in host cell recognition and attachment, it is possible that these parasites use conserved structures to overcome this problem despite the fact that they invade very different cell types.

Determination of the crystal structure of PfAMA1 has enabled (Bai et al., 2005) to identify a hydrophobic trough in DI of the PfAMA1 ectodomain, two residues of which are contributed by the DII loop. The work from this group suggests that the trough acts as a binding pocket for the PfAMA1 ligand. The group have obtained several crystal structures for PfAMA1 DI-II. In two of these structures the DII loop occupied different orientations and in the third this loop lacked electron density and its structure could not be solved (Adrian Batchelor, personal

communication). This suggests that, as was indicated from the PvAMA1 structure Pizarro et al. 2005) the loop is flexible and can adopt multiple conformations. One possibility is that two binding sites exist in the PfAMA1 ectodomain, one in DI and the other in DII. Ligand interaction with the heparin-like binding site in DII requires the DII loop to close over it, thus holding it in place. In contrast, ligand interaction with the hydrophobic trough of DI requires that the DII loop be in a suitable orientation to provide two residues that lie at the base of the trough. In the event that both sites could be occupied simultaneously, the DII site could bind the AMA1 partner molecule on the parasite surface, while the DI site binds the ligand on the erythrocyte surface. Alternatively occupation of one site may preclude binding to the other. For instance, homo-multimerisation of AMA1 may occur when AMA1 is at a high local concentration. When AMA1 is released onto the parasite surface and the local concentration decreases, this could result in dissociation of the homo-multimer, thus allowing the DII loop to complete formation of the hydrophobic trough in DI, allowing binding of the erythrocyte ligand. A mechanism of this type may prevent the premature interaction of AMA1 with its erythrocyte ligand, for instance on the cell from which the merozoite is egressing. However, this is not consistent with the inability to detect AMA1 complex formation in schizonts or free merozoites in the current study.

3.6.10: AMA1 as a component of a parasite protein complex involved in erythrocyte attachment

PfAMA1 may interact indirectly with a RBC surface receptor(s) via a complex, containing proteins expressed at or released onto the merozoite surface during invasion. Alternatively, a homo-multimer mediated by the PfAMA1 transmembrane domain, may form at the merozoite surface. Whilst COS-7 cell expression of full-length sgPfAMA1 could also support such multimerisation, the possibility cannot be ruled out that multimerisation requires some form of protein modification to occur. PfAMA1 is shed from the merozoite membrane in two forms, two thirds as $PfAMA1_{48}$, being cleaved downstream of DIII and one third as $PfAMA1_{44}$, cleaved within as well as downstream of DIII (see Fig 1.5) (Howell et al., 2003a). The same proportion of secondary processing is also seen in AMA1 derived from other *Plasmodium* species (Blackman, unpublished data). This might suggest some functional significance for the internal DIII cleavage. While Howell *et al.* (2003) have shown conclusively that PfAMA1 is shed as a monomer, multimerisation may be dependent upon membrane association. Thus, the cleavage ratio of 48 to 44 kDa forms (2:1) may be explained by the presence of PfAMA1 as a homo-trimer, consisting of two intact molecules interacting via their transmembrane domains and a third molecule cleaved within and possibly also downstream of DIII.

To investigate the possibility that PfAMA1 forms a complex at the parasite surface with other parasite proteins, co-precipitation studies were carried out from purified schizont and merozoite samples. Multiple bands immunoprecipitated with mAb 4G2dc1 and the polyclonal serum N1 in the absence of cross-linking agents, however, most of these were of PfAMA1 origin. Co-

precipitated of proteins that were not of AMA1 origin were not reproducible, suggesting that co-precipitation of these proteins was non-specific.

In the event that interactions between AMA1 and its putative partner protein(s) were too weak to be detected under the detergent conditions used, merozoite and schizont samples were cross-linked in order to stabilise the interaction(s) prior to immunoprecipitation. The results from this attempt were inconclusive as nothing co-precipitated although the actual AMA1 bands were very faint suggesting the immunoprecipitation itself was relatively inefficient. To be able to draw any conclusions from this, it will be necessary to repeat these experiments.

Camus and Hadley (1985) demonstrated that EBA-175 bound to *P. falciparum* merozoites as well as human erythrocytes. Schizonts from which these merozoites were purified had been pre-treated with trypsin, which abrogates EBA-175 recognition, suggesting that EBA-175 bound specifically to the merozoites and not to erythrocyte membrane contamination resulting from the parasite preparation. If this result is valid, EBA-175 may form a bridge between a membrane bound receptor at the merozoite surface (e.g. AMA1) and a ligand on the erythrocyte surface. The formation of a bridge between a parasite and host cell is not without president. The *T. gondii* microneme protein MIC3 (TgMIC3) is secreted from the micronemes during invasion and detected on the surface of invading tachyzoites (Garcia-Reguet et al., 2000). This protein has no transmembrane domain and the finding that TgMIC3 binds both host cells and tachyzoites has led this group to deduce that TgMIC3 forms a bridge between the parasite and host cell membranes during invasion. In *Plasmodium*, a complex involving soluble and membrane bound parasite antigens may assemble in the micronemes of developing merozoites or at the parasite surface upon schizont rupture. EBA-175 is believed to form homo-dimers on contact with its erythrocyte receptor, glycophorin A, on the RBC surface (Tolia et al., 2005). From the crystal structure of EBA-175, with and without glycophorin A, this group have identified six glycan binding sites within the dimer, all six of which are important for glycophorin A binding. In addition, as these binding sites all contact both monomers, this suggests that dimerisation is important for receptor binding. Dimerisation of TgMIC3 is also required for host cell receptor binding although this is believed to be mediated by its C-terminal region while receptor binding is mediated via its N-terminal lectin-like domain (Cerede et al., 2002). Camus and Hadley (1985) demonstrated that human erythrocytes coated with EBA-175 were successfully invaded by the homologous strain of parasite, but were refractory to invasion by heterologous strains. This suggests that EBA-175 from the homologous parasites can act as a bridge between the merozoite and the RBC, thus mediating binding. It further indicates that the cytoplasmic tail of EBA-175 may not be essential at the time of invasion. In contradiction to the possibility of EBA-175 being released from the micronemes in soluble form is the observation by Gilberger *et al.* (2003) that its cytoplasmic tail is essential for invasion, though not for microneme targeting. Putting these two findings together, it is possible that EBA-175 requires membrane tethering to prevent premature release from the micronemes, but not for signal transduction during invasion

as was suggested by Gilberger *et al.* (2003). EBA-175 could be proteolytically released from the micronemes by a resident microneme rhomboid, such as ROM1 (O'Donnell unpublished data). In *T. gondii*, soluble microneme proteins such as MIC3 are present in complex with integral membrane proteins. Among other functions, this membrane association may prevent premature release of soluble proteins from the micronemes. In *Plasmodium,* microneme proteins appear largely to be integral membrane proteins and it is possible that these parasites utilise different mechanism for the regulation of microneme secretion. In the case of AMA1 interacting with a soluble partner protein involved in tight junction formation, it would be anticipated that the complex would form at the apical tip of the parasite immediately prior to junction formation. This may explain why the current study failed to identify any specific PfAMA1-partner protein interaction in schizonts and free merozoites. If invasion could be halted, for instance using cytochalasin D, this possibility could be analysed further.

In conclusion, the results from erythrocyte binding studies involving AMA1 as discussed above, are varied and not easy to interpret. While on the one hand there is evidence to suggest that AMA1 is an erythrocyte binding protein (Mitchell et al. 2004; Triglia et al., 2000), the studies purporting to provide direct evidence of such activity are not conclusive (Fraser et al. 2001; Kato et al. 2005). This latter conclusion is supported in the current study. If the function of AMA1 in erythrocyte invasion is one of erythrocyte binding, more work is required to understand the conditions under which such interactions are able to occur.

Figure 3.1: IFA revealing surface localisation of sg'PfAMA1 in transfected COS-7 cells

COS-7 cells were analysed unfixed and unpermeabilised to detect surface localised protein only. COS-7 cells transfected with the plasmid pSec/sg'Pfama1 **(A)** or untransfected **(B)** as a negative control, were incubated with **(i)** culture supernatant from 4G2dc1 expressing hybridoma cells (undiluted) or **(ii)** the polyclonal serum N1 (at 1 in 100 dilution). The image is a composite of DAPI (blue), Evans blue (red) and FITC conjugate (green) images from fluorescence microscopy as described in materials and methods (section 2.4.3).

A

(i)

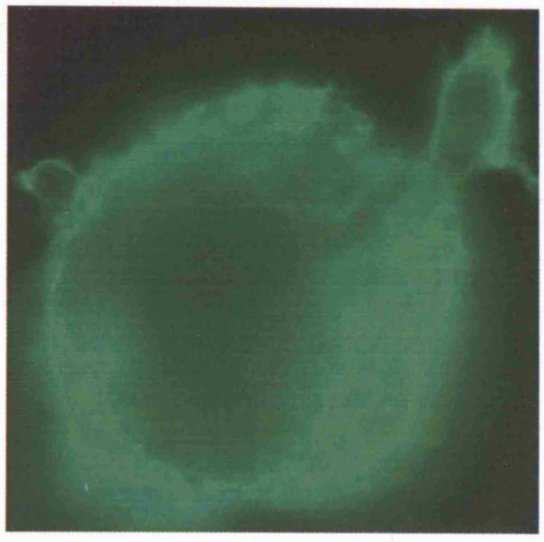

(ii)

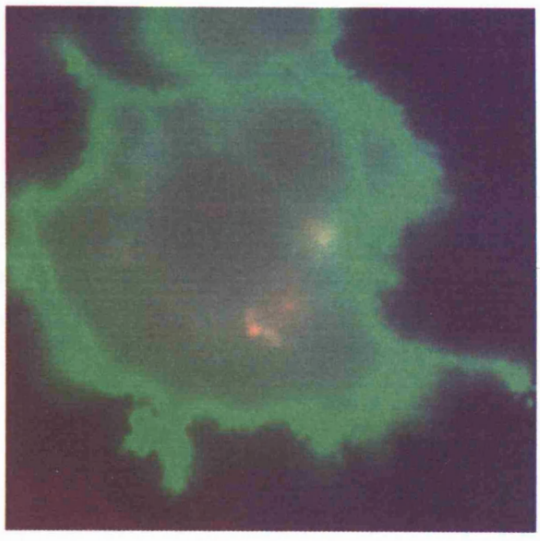

B

(i)

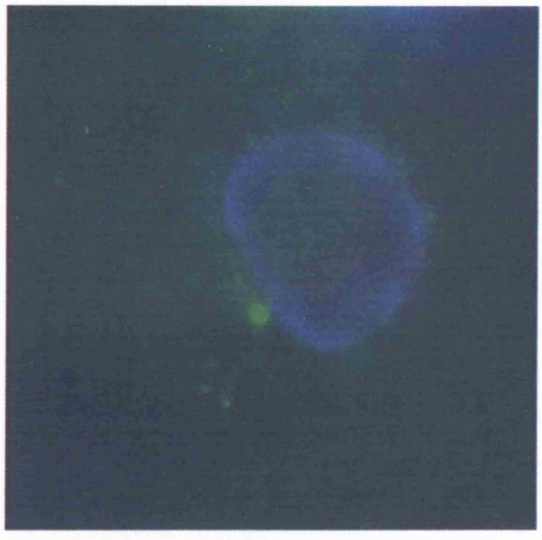

(ii)

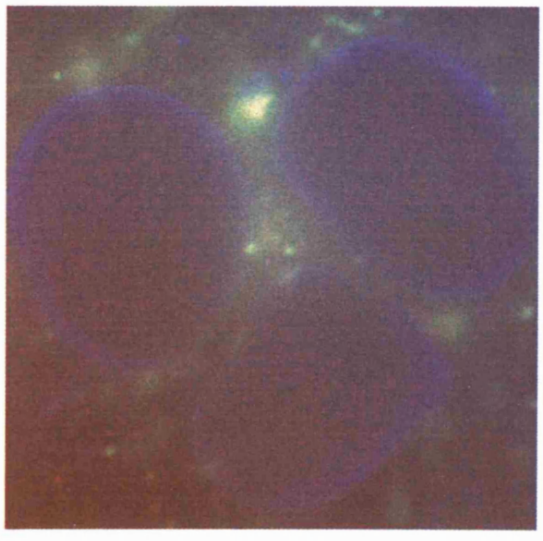

Figure 3.2: Immunoprecipitation of PfAMA1 from biotin surface labelled *P. falciparum* schizonts using mAb 4G2dc1

Biotin labelled schizont samples were solubilised in buffers containing either NP40 **(N)**, CHAPS **(C)** or sodium deoxycholate **(S)** and processed for immunoprecipitation using Sepharose bound 4G2dc1. The immunoprecipitated protein samples were separated by SDS-PAGE on 12.5% gels. The samples were transferred to nitrocellulose and probed with; **(A)** HRP-conjugated streptavidin, **(B)** polyclonal serum R1 followed by HRP-conjugated anti-mouse IgG or **(C)** HRP-conjugated anti-mouse IgG) alone. Major bands detected are highlighted (black arrows) and their calculated masses indicated in kDa.

A

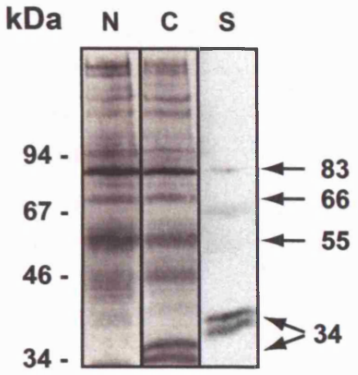
kDa
N
C
S
94 -
67 -
46 -
34 -
83
66
55
34

B

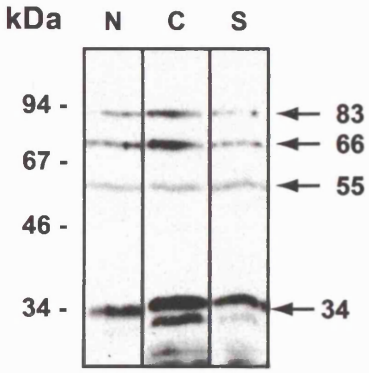
kDa
N
C
S
94 -
67 -
46 -
34 -
83
66
55
34

C

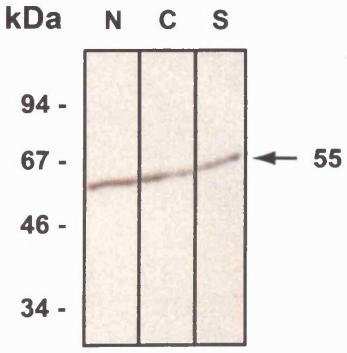
kDa
N
C
S
94 -
67 -
46 -
34 -
55

Figure 3.3: Immunoprecipitation of PfAMA1 from [^{35}S] cysteine/methionine metabolically labelled *P. falciparum* (3D7) schizonts and merozoites, using mAb 4G2dc1

PfAMA1 was immunoprecipitated from CHAPS extracts of metabolically radiolabelled merozoite **(m)** and schizont **(s)** fractions. Immunoprecipitates were electrophoresed on 12.5% SDS-PAGE gels and transferred to nitrocellulose for either; **(A)** direct detection of radiolabelled proteins by fluorography or Western blot analysis, using; **(B)** polyclonal serum R1 followed by HRP-conjugated anti-mouse IgG or **(C)** secondary Ab only. The major bands detected are indicated (black arrows) and their calculated masses indicated in kDa.

A

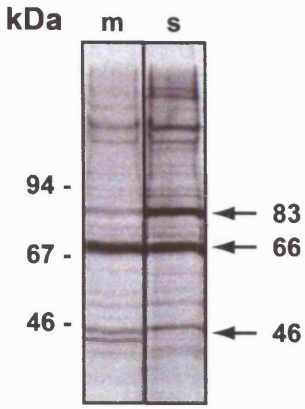
kDa
m
s
94 -
67 -
46 -
83
66
46

B

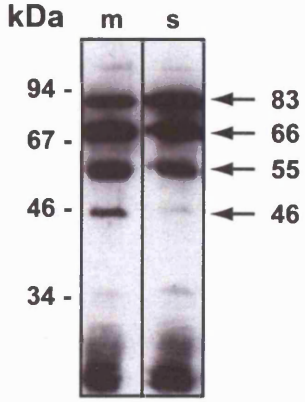
kDa
m
s
94 -
67 -
46 -
34 -
83
66
55
46

C

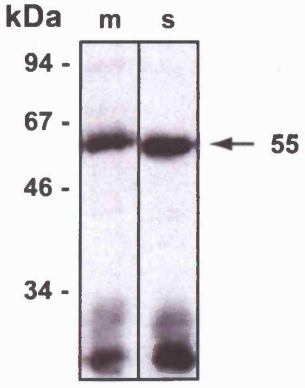
kDa
m
s
94 -
67 -
46 -
34 -
55

Figure 3.4: Immunoprecipitation of PfAMA1 from [^{35}S] cysteine/methionine metabolically labelled *P. falciparum* (3D7) schizonts and merozoites, using polyclonal serum N1

PfAMA1 was immunoprecipitated from CHAPS extracts of metabolically radiolabelled merozoite (m) and schizont (s) fractions. Immunoprecipitates were electrophoresed on 12.5% SDS-PAGE gels and transferred to nitrocellulose for either; **(A)** direct detection of radiolabelled proteins by fluorography or Western blot analysis using; **(B)** polyclonal serum R1 followed by HRP-conjugated anti-mouse IgG or **(C)** secondary Ab only. The major bands detected are indicated (black arrows) and their calculated masses indicated in kDa.

A

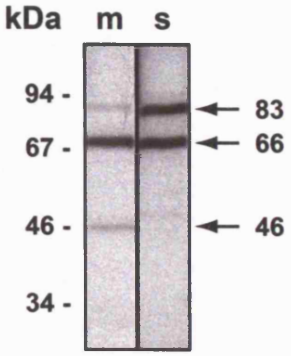
kDa
m
s
94 -
67 -
46 -
34 -
83
66
46

B

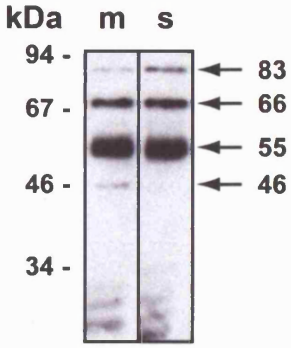
kDa
m
s
94 -
67 -
46 -
34 -
83
66
55
46

C

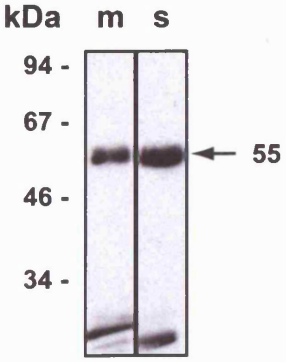
kDa
m
s
94 -
67 -
46 -
34 -
55

Figure 3.5: Surface view of PfAMA1 DI (orange) and DII (blue) demonstrating the potential binding surfaces in this region of the ectodomain.

(A) Surface view of the hydrophobic trough of PfAMA1 (the residues involved in this trough are highlighted in red) as determined by Bai *et al.* (2005). The two residues (Phe367 and Leu357) contributed by the DII loop are indicated (black arrows) as is the remainder of the DII loop (blue arrow). In this conformation, the DII loop can be seen to reach up over the top of the molecule.

(B) Surface view of the putative DII binding site as determined by Pizarro *et al.* (2005). The surfaces contributed by α-helix 7 and β-sheet 14 (indicated by black arrows) are denoted in green.The top of the hydrophobic trough and part of the 4G2dc1 binding site are visible (red and black respectively). From the proximity of the loop to both sites, it is possible that under different conditions it can adopt alternative conformations to interact with one or other of the sites.

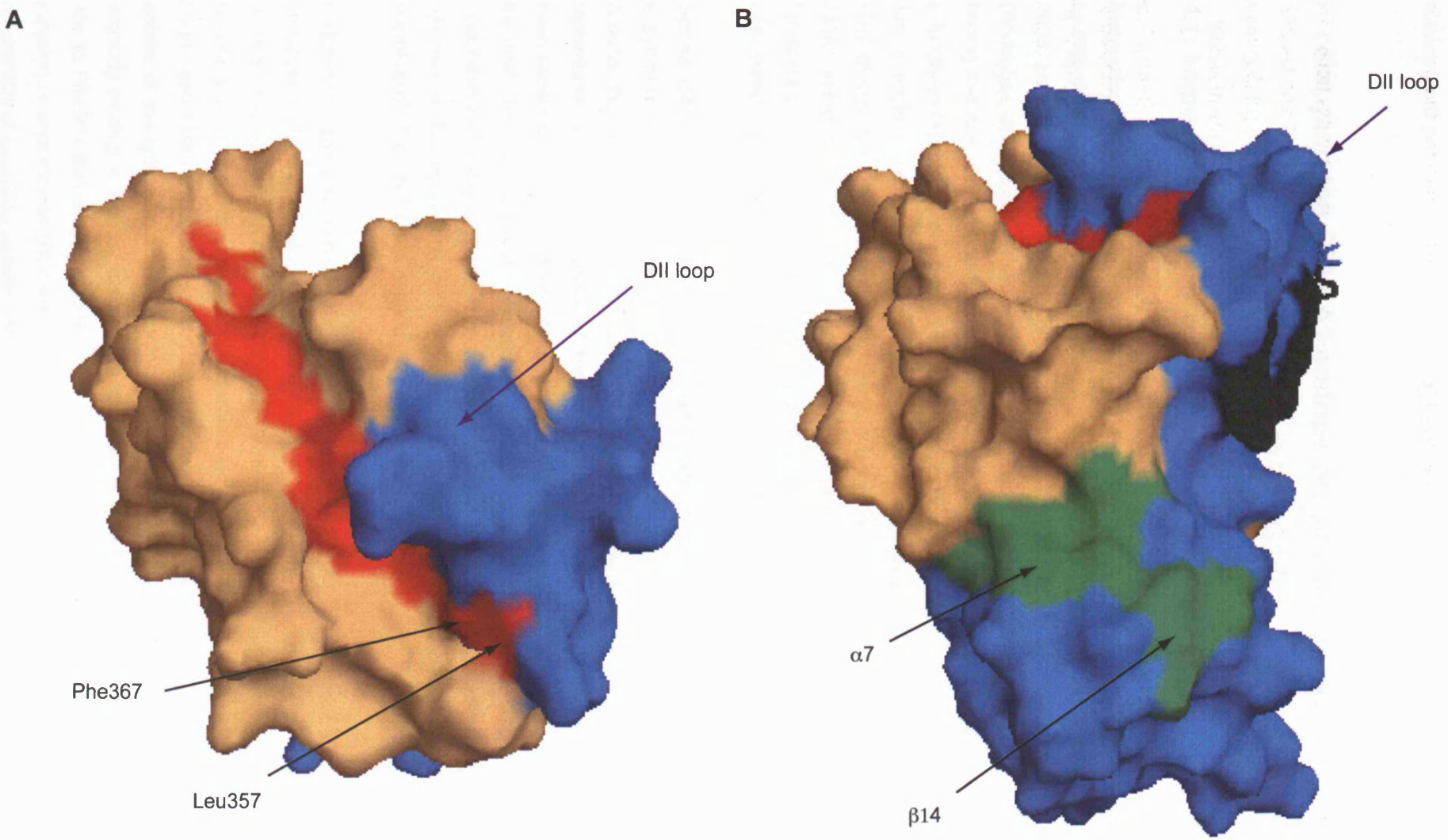
A
DII loop
Phe367
Leu357
B
DII loop
α7
β14

Chapter 4

Mapping the PfAMA1 epitope recognised by the invasion-inhibitory mAb 4G2dc1

4.1: Introduction

Many different Abs reactive against AMA1 have been described that block asexual replication by different species of *Plasmodium in vitro* (Dutta et al., 2005; Casey et al., 2004; Mueller et al., 2003; Hodder et al., 2001; Kocken et al., 2000; Crewther et al., 1996b) as well as *in vivo* (Rodrigues et al., 2005; Polley et al., 2004; Stowers et al., 2002; Anders et al., 1998). The finding that Abs against AMA1 inhibit erythrocyte invasion by *Plasmodium* merozoites indicates a fundamental role for the protein in this process. However, the mechanism of action of such Abs is unclear and may be diverse. The relatively large molecular mass (approximately 160 kDa) of invasion inhibitory anti-AMA1 Abs (IgG) suggests that they may block the function of AMA1 indirectly by steric hindrance. They may bind close to a region of AMA1 that is of functional significance, thus blocking access to some receptor or ligand in the parasite or on the RBC surface. Alternatively they may bind directly to a functional site, thus inhibiting its activity.

Several different mechanisms of Ab-mediated invasion-inhibition have been postulated. AMA1 is synthesised in late schizogony and localises to the micronemes of developing merozoites. Around the time of schizont rupture, the protein undergoes proteolytic maturation and redistributes across the surface of the merozoite. Some invasion-inhibitory antibodies have been shown to cross-link AMA1 at the apical end of the parasite, thus blocking redistribution of the molecule across the merozoite surface (Dutta et al., 2005; Dutta et al., 2003). These authors postulated that, either redistribution of AMA1 is essential for invasion or that cross-linked AMA1, retained at the apical end of the parasite, acts as a plug preventing efficient microneme secretion of other molecules essential for merozoite invasion.

Following translocation onto the merozoite surface, the ectodomain of PfAMA1 is shed from the merozoite surface by a calcium-dependent serine protease or "sheddase" (Howell et al., 2003b) (Howell et al., 2001) with cleavage occuring 29 residues N-terminal to the predicted membrane spanning sequence. An alternative mechanism proposed for the invasion-inhibitory activity of certain anti-AMA1 antibodies is that of blocking this processing event, presumably by preventing access of the protease to the cleavage site (Dutta et al. 2005). Whether this consequence of antibody binding is directly responsible for invasion-inhibition is unclear. The identification of Abs to PfMSP1 that directly preventing its processing and shedding and thus inhibit merozoite invasion of erythrocytes (Blackman, 1994; Nwuba et al., 2002) may lend support to a similar mechanism of operation against AMA1.

Studies in all apicomplexan parasites investigated so far indicate a high conservation of function of AMA1 during host cell invasion. The (IgG2a) mAb 4G2dc1 inhibits *P. falciparum* merozoite invasion of human erythrocytes by 60 - 70% compared with isotype control antibodies (Kocken et al., 1998b). In addition, this mAb has also been shown to inhibit invasion of chimpanzee erythrocytes by the phylogenetically closely related chimpanzee parasite *P. reichenowi* (Kocken et al., 2000). The presence of the epitope recognised by this mAb in both parasite species indicates a similarity of structure in AMA1. In the current study, an attempt was made to map the epitope recognised by the mAb 4G2dc1 in PfAMA1 to identify a functionally significant region of its ectodomain. Subsequent strategic modification of this region of the molecule by site directed mutagenesis might then aid elucidation of the function of AMA1 in these parasites.

4.2: The mAb 4G2dc1 Fab fragment exhibits greater invasion-inhibition than the intact Ab

Characterisation of the anti-parasitic activity of the mAb 4G2dc1 was based on its inhibitory effect on erythrocyte invasion by *P. falciparum* merozoites. The possibility that this inhibitory activity resulted from a steric hindrance effect when 4G2dc1 bound to AMA1 was investigated in the current study by assessing the inhibitory potential of Fab fragments of 4G2dc1 (4G2dc1-Fab) on merozoite invasion.

At varying concentrations of intact 4G2dc1 and 4G2dc1-Fab, invasion-inhibition was calculated as a percentage of that observed in control assays, in the absence of Ab (Table 4.1). The mAb 4G2dc1 is of the IgG isotype, which is bivalent. A comparison between the concentrations of intact 4G2dc1 versus 4G2dc1-Fab is not direct, as it does not reflect the concentration of 4G2dc1 binding domains. Only about two thirds of an intact mAb fragment is composed of Fab fragments, the remainder comprising the Fc (crystallisable) fragment. In order that a direct comparison can be made, the concentration of mAb 4G2dc1 has been adjusted to reflect the concentration of these antigen binding sites (shown in brackets in Table 4.1). All future discussion will refer to the concentration of 4G2dc1 binding sites. As shown in Fig 4.1 (A), the 4G2dc1-Fab was a more potent inhibitor of invasion than the intact Ab. The mAb 4G2dc1 mediated about 74% invasion-inhibition at a concentration of 0.18 mg ml^{-1}, compared with about 99% inhibition produced by the approximately equivalent concentration (0.16 mg ml^{-1}) of 4G2dc1-Fab.

The assay was repeated with lower concentrations of the 4G2dc1-Fab, to investigate the degree to which the Fab preparation could be diluted while retaining its inhibitory properties. In accordance with the previous results, on titration the 4G2dc1-Fab was found to mediate significant invasion-inhibition down to relatively low concentrations, showing 24% inhibition at 0.05 mg ml^{-1} (Fig 4.1 B). This represents a concentration of 4G2dc1-Fab fragment one fifth that found in the intact antibody assay, giving a percentage inhibition of 30%.

4.2.1: Recombinant PfAMA1 DI-III exhibits anti-invasion inhibitory properties

After purification of 4G2dc1-Fab (see section 2.4.5.2.), the Ab fragment was dialysed against PBS to remove the salts present in the gel filtration running buffer (SRB). However, it was possible that the enhanced inhibitory activity of 4G2dc1-Fab over that of the intact mAb resulted from the presence of residual salts in the Fab preparation, rather than a direct effect of the Fab. In an attempt to rule out this possibility, the invasion-inhibition assay was repeated in the presence of rPfAMA1 DI-III.

4.2.1.1: Binding assay confirming the interaction between 4G2dc1-Fab and rPfAMA1 DI-III

To ensure that the 4G2dc1-Fab and the antigen PfAMA1 DI-III were able to interact, binding assays were performed prior to repeating the invasion-inhibition assay. Binding of the Fab and antigen were monitored by HPLC (Fig 4.2.). This resulted in a shift in the position of the peaks, due to complex formation. The peak representing the soluble unbound antigen diminished slightly, while the Fab alone peak was no longer visible. The antigen concentration was far in excess of the Fab, and therefore it was anticipated that only a fraction of the antigen would bind. The Fab and antigen on their own are eluted from the column very close together. When complexed and separated by HPLC, there was a slight broadening of the antigen alone peak. This was probably due to overlap between the two peaks due to their close migration and indicates that some Fab remains unbound, perhaps due to an inablility to bind to the antigen. However, the size of the peak that is generated by complex formation indicates that a considerable amount of Fab has bound. This suggested that the presence of the recombinant ectodomain of PfAMA1 in invasion-inhibition assays with Fab-4G2dc1 could be effective at countering the activity of the Fab-4G2dc1.

4.2.1.2: Merozoite invasion-inhibition in the presence of rPfAMA1 DI-III

The invasion-inhibition assays were repeated in the presence of 1 mg ml^{-1} rPfAMA1 DI-III, with 4G2dc1-Fab at the lower concentrations described earlier. Thus, at the highest Fab concentration, there was over a two fold excess of antigen to 4G2dc1-Fab (Table 4.2.). It was anticipated that during pre-incubation of the 4G2dc1-Fab with the antigen, they would bind to each other, thus reducing or eliminating free 4G2dc1-Fab from the reaction mixture and consequently disrupting the invasion inhibitory effect of the Fab. However, if the invasion inhibitory effect was not a direct consequence of 4G2dc1-Fab in the assay, there would have been no difference in invasion-inhibition in the presence or absence of antigen. Once again, invasion-inhibition was calculated as a percentage of the invasion rate in the absence of 4G2dc1-Fab and antigen. Figure 4.3 shows the invasion-inhibition observed in this assay. There was an overall increase in invasion-inhibition as the concentration of 4G2dc1-Fab increased, in the presence and absence of rPfAMA1 DI-III. Overall, there was slightly greater inhibition of invasion in the absence of rPfAMA1, as was expected. However this anti-invasion inhibitory

effect was not significant. There was an inexplicable drop in invasion-inhibition at a 4G2dc1-Fab concentration of 0.16 mg ml^{-1}. In addition, invasion-inhibition in the presence of antigen at a 4G2dc1-Fab concentration of 0.43 mg ml^{-1} was greater than that observed in its absence. The assay was repeated, this time with a 10 fold excess of rPfAMA1 DI-III over 4G2dc1-Fab (Data not shown). On this occasion, no invasion-inhibition was observed in the presence of 4G2dc1-Fab and in contrast PfAMA1 DI-III had an invasion enhancing effect, both in the presence and absence of 4G2dc1-Fab. These findings were unexpected and need further investigation. In this assay rPfAMA1 DI-III was able to bind nearly all the 4G2dc1-Fab present resulting in a shift in the position of the peak in HPLC. This indicated that in the invasion-inhibition assay these two molecules should interact, thus diminishing the invasion inhibitory effect of the Fab. One explanation for the inability to detect a significant difference in invasion-inhibition in the presence and absence of PfAMA1 DI-III is that the affinity of the interaction between soluble antigen and the monovalent Fab fragment is low. As a result, competition for 4G2dc1-Fab binding is high between the released merozoites and the soluble antigen, thus reducing the anti-invasion-inhibition effect of the antigen.

The 4G2dc1-Fab fragment is approximately one third the size of the intact antibody. The ability of the 4G2dc1-Fab to inhibit erythrocyte invasion by *P. falciparum* merozoites to a greater degree than the intact antibody increases the likelihood that the inhibition mediated by this mAb results from binding to a functionally important region of the PfAMA1 ectodomain. For this reason, the focus of this study was to identify the amino acid residues that contribute to the epitope recognised by this mAb and in this way identify a region of the molecule that contributes significantly to its function.

4.3: Identification of the PfAMA1 subdomains that contribute residues to the epitope recognised by the mAb 4G2dc1

Several different combinations of the subdomains of the rPfAMA1 ectodomain were expressed in heterologous systems (*P. pastoris* or COS-7 cells). The aim behind this approach was to identify the subdomains that contributed amino acid residues to the epitope recognised by the mAb 4G2dc1. This method might narrow the region of the ectodomain known to accommodate this epitope thereby reducing the number of amino acids under consideration.

4.3.1: The epitope recognised by mAb 4G2dc1 is located within DI-II of the rPfAMA1 ectodomain

Cell pellets and culture supernatants from recombinant *P. pastoris* clones expressing regions (DI, DI-II and DI-III) of the rPfAMA1 ectodomain were harvested by centrifugation. The samples were analysed by Western blot with the polyclonal sera N1 and R1 (data not shown) and with

mAb 4G2dc1 (Fig 4.4) to check for expression and the presence of the 4G2dc1 epitope, respectively.

The full-length rPfAMA1 ectodomain (DI-III) was successfully expressed as confirmed by 4G2dc1 binding (Fig 4.4, lane 9). When expressed alone, DI was not detectable in either the *P. pastoris* cell pellet (result not shown) or in the culture supernatant in Western blots probed with either mAb 4G2dc1 (Fig 4.4, lanes 6-8) or the polyclonal sera N1 or R1 (data not shown). However, DI-II was readily detected in culture supernatants by Western blots analysis when probed with mAb 4G2dc1 (Fig 4.4, lanes 2 - 5) showing that this epitope lies within DI-II of the rPfAMA1 ectodomain.

4.3.2: Use of the COS-7 cell expression system to identify the subdomain(s) within which the epitope recognised by mAb 4G2dc1 lies

The PfAMA1 synthetic gene product was expressed successfully in COS-7 cells (section 3.2.). For this reason it was decided to express DI of PfAMA1 ectodomain in this system, as expression of this subdomain was not possible in *P. pastoris*. In addition to DI, several combinations of the subdomains within the PfAMA1 ectodomain were expressed in this system with a view to pinpointing the epitope recognised by mAb 4G2dc1. It was anticipated that this system might be more conducive to expression and adoption of the correct conformation of non-native forms of PfAMA1, as this expression system has frequently been used for expression of regions of *Plasmodium* antigens (Sim et al., 1994b; Ranjan and Chitnis, 1999; Fraser et al., 2001; Prasad et al., 2003). COS-7 cells transfected with constructs designed for the expression of various regions of PfAMA1 were analysed by Western blot using mAb 4G2dc1 and the polyclonal sera AdsN1 and R1. A schematic representation of the different domain combinations used is shown in Figure 4.5 (A).

4.3.2.1: Expression of DI alone

Construct pSec/sg'DI was designed for expression of PfAMA1 DI. In order to target the DI protein to the secretory pathway of the host cell, the sequence was cloned downstream of the Igκ secretory signal. However, Western blot analysis with the polyclonal serum R1 demonstrated expression of DI in the cell pellet but not in the culture supernatant suggesting that the protein was being synthesised but not secreted (Data not shown). Multiple bands were detectable on the Western blot indicating the DI product may have been partially aggregated and/or degraded (Fig 4.5 B). A shift in the migration of the protein product was detected under reducing condition, suggesting that it was reduction sensitive and indicating that a measure of secondary structure (disulphide bond formation) had been achieved (Fig 4.5 B). The finding that the protein was expressed but not secreted in this expression system, together with the absence of recognition by AdsN1 on Western blots, supports the idea that it may only have been partially folded.

4.3.2.2: Expression of ΔDII

An artificial construct was designed for expression of DI linked directly to DIII, the transmembrane region and cytoplasmic tail (ΔDII) using the plasmid pSec/ sg'PfamaIΔDII. Expression was confirmed by R1 in Western blot (Fig 4.5 C, i). However, recognition by AdsN1 was reduced (Fig 4.5 C, ii), and recognition by 4G2dc1 was abolished (Fig 4.5 C, iii) suggesting that this chimeric protein did not fold correctly.

4.3.2.3: Expression of rPfAMA1 lacking DI

A further construct (pSec/sg'Pfama1ΔDI) was designed for expression of rPfAMA1 lacking DI (ΔDI). Expression was confirmed by R1 in Western blot (Fig 4.5 D, i). However recognition by Ads N1 was significantly reduced (Fig 4.5 D, ii) and mAb 4G2dc1 (Fig 4.5 D, iii) showed no recognition of this recombinant protein. The reduced recognition by Ads N1 indicates that the protein was only partially folded.

4.3.2.4: Expression of two truncated forms of PfAMA1, T1 and T2

In *P. falciparum*, the prodomain of AMA1 is cleaved from the molecule when located in the micronemes. The processed form is then relocalised to the merozoite surface. This processing event occurs immediately prior to Ile97, which denotes the beginning of DI.

To determine whether the N-terminal region of DI, preceding to the first cysteine residue (Cys149), contributes to mAb 4G2dc1 recognition of the molecule, two constructs were designed for the expression of truncated forms of PfAMA1 in COS-7 cells (T1 and T2 from the plasmids pSec/tr1-sgPfama1 and pSec/tr2-sgPfama1 respectively). The constructs were designed to leave two varying length sequences upstream Cys149 in DI. The presence of a cysteine at the extreme N-terminus of a molecule may inhibit its ability to participate in disulphide bonding. As all the cysteine residues in the AMA1 ectodomain are involved in disulphide bonding and 4G2dc1 recognition of the molecule is reduction sensitive, it was considered expedient to design two truncated forms. Thus, if T1 (having only three amino acid residues preceding Cys149) failed to be expressed or fold correctly, T2 (with eleven amino acid residues immediately preceding the Cys149) may successfully do so. Expression of both these recombinant forms of PfAMA1 was detected by means of the polyclonal Ab R1 (Fig 4.6 A and B). However, they displayed incorrect folding as indicated by nearly complete loss of recognition by AdsN1 (Fig 4.6 C and D) and loss of recognition by mAb 4G2dc1. It is therefore apparent that the extreme N-terminus of DI is critical for the correct folding of the molecule. Despite this there is some indication of disulphide bond formation with T1, indicated by a slight shift when electrophoresed under reducing conditions compared to non-reducing conditions (Fig 4.6 E).

4.4: Proteolytic digestion of the PfAMA1 ectodomain to generate small fragments containing the intact 4G2dc1 epitope

From the above results it can be concluded that the epitope recognised by mAb 4G2dc1 lies within DI-II. Attempts to express these two domains in isolation from each other have failed suggesting that their tertiary structure is interconnected and therefore folding of these two domains are interdependent. These findings indicate that the epitope recognised by 4G2dc1 may overlap the two domains; alternatively it may be contained solely within either one of them. The inability to express either of these domains in isolation in a correctly folded form has made it impossible to distinguish between these possibilities.

In an attempt to further delineate the 4G2dc1 epitope, a proteolytic digestion approach was adopted to identify a small fragment within DI-II containing this epitope (Fig 4.7). The regions of a molecule likely to be accessible to protease digestion are exposed loops and regions of the polypeptide chain that form inter-domain links. Due to the lack of structural information pertaining to the ectodomain of PfAMA1, regions of the polypeptide chain that might be accessible to proteolytic digestion were unknown. For this reason, a range of proteolytic enzymes was used and the digestion products were analysed by Western blot under non-reducing conditions for recognition by 4G2dc1.

4.4.1: Digestion of rPfAMA1 DI-III

4.4.1.1: Trypsin/Chymotrypsin

Within 40 minutes of digestion with trypsin, (Fig.4.8 A), only a 40kDa product was observed, suggesting that this part of the protein is fairly resistant to further digestion. However, after 4 hours of digestion some small fragments appeared. In the case of chymotrypsin, DI-III of rPfAMA1 was first digested to products of 40 – 43 kDa and then to fragments of 18 - 30kDa (Fig.4.8 B). In Western blot analysis none of the trypsin/chymotrypsin digestion products were recognized by 4G2dc1 (data not shown).

4.4.1.2: Subtilisin

At an enzyme:substrate ratio of 1:100, subtilisin degraded rPfAMA1 DI-III to a 40kDa product, similar to that seen with trypsin and chymotrypsin (data not shown). Increasing this ratio to 1:10 led to rapid (within 30 minutes) degradation of the protein to small fragments (Fig. 4.9 A). However, after 30 minutes of digestion, no fragments were detectable on Coomassie stained gels. When probed with 4G2dc1 on a Western blot, a 30 kDa fragment was the smallest detected (Fig. 4.9 B).

4.4.1.3: Pepsin and Papain

Pepsin degraded the full-length ectodomain almost immediately (Fig. 4.10 A), resulting in small fragments (<14kDa) showing no reactivity with 4G2dc1 in a Western blot (data not shown).

Papain digestion gave two products, the smallest of which (35kDa) appeared to be relatively stable over time (Fig. 4.10 B) and also reacted with 4G2dc1 in a Western blot (Fig 4.10 C).

4.4.2: Digests of rPfAMA1 DI /II alone

None of the enzymes described so far were able to generate sufficiently small fragments within DI-III that may have contained the 4G2dc1 epitope. The same approach was used with rPfAMA1 DI-II to try to achieve this.

4.4.2.1: Trypsin/Chymotrypsin

Recombinant PfAMA1 DI-II appeared initially to be resistant to trypsin and chymotrypsin digestion (Fig. 4.11 A and B respectively). However, in the presence of chymotrypsin, it eventually degraded (4 hours) and no small fragments appeared.

In order to enhance enzyme access to rPfAMA1 DI-II, trypsin and chymotrypsin digestion was repeated in the presence of 0.1% (w/v) SDS (Fig. 4.11 C and D respectively) and 1M urea (results not shown). Under both sets of conditions DI-II was completely degraded by trypsin and chymotrypsin, as shown by SDS PAGE analysis and confirmed in Western blots (data not shown). Again, no small fragments were recognized by 4G2dc1. This suggests that in the previous experiments, under non-denaturing conditions, the folding of DI-II may have delayed enzymatic digestion.

4.4.2.2: Pepsin

When digested with pepsin at enzyme:substrate ratios of 1:100 and 1:10, DI-II remained fairly stable (data not shown). In the latter case, when pepsin began to digest the molecule, no small fragments were detectable with Coomassie blue or in Western blot analysis with 4G2dc1.

As previously observed for rPfAMA1 DI-III, digestion of DI-II did not lead to the identification of small fragments retaining the 4G2dc1 epitope (data not shown).

4.4.3: Proteolytic digestion of the 4G2dc1 F(ab)$_2$/PfAMA1 DI/ II complex

The F(ab)$_2$ fragment of mAb 4G2dc1 was prepared by pepsin digestion of the intact antibody (section 2.4.5.2.2). This protease is relatively non-specific but will preferentially cleave the peptide chain after aromatic or other hydrophobic residues (at the P_1 position). Pepsin cleaves the IgG heavy chain immediately down-stream of the hinge region between F(ab)$_2$ and Fc

regions of the Ab. The F(ab)2 region of 4G2dc1 purified from the resulting mixture is relatively resistant to pepsin digestion. From the results obtained in the current study, rPfAMA1 DI-II is initially resistant to pepsin digestion; however, when pepsin does begin to digest the molecule it does so to completion, generating no stable intermediate products. Thus, a protection assay was carried out on rPfAMA1 DI-II complexed to 4G2dc1 $F(ab)_2$ fragment, in the presence of pepsin, to see if the enzyme would digest exposed regions of the molecule, while leaving the 4G2dc1 epitope intact. However, the digestion pattern for DI-II in the complex (Fig 4.12 A) was similar to that seen for DI-II on its own (Fig 4.12 B) and no small fragments were produced. This was confirmed in Western blot analysis probed with 4G2dc1 (Fig 4.12 C) and in the Western probed with the secondary Ab alone (Fig 4.12 D) in order to distinguish Ab fragments from rPfAMA1 DI-II digestion products.

In conclusion, proteolytic digestion of the rPfAMA1 ectodomain did not result in the isolation of a region significantly smaller than DI-II that could be shown to contain the 4G2dc1 epitope.

4.5: Site-directed mutagenesis of PfAMA1 DI and DII to disrupt 4G2dc1 recognition

Using proteolytic digestion to generate intact fragments of a molecule that may retain a certain structure or function is a fairly crude approach to analysing the properties of a protein. This approach did not produce any additional information regarding identification of the 4G2 epitope. For this reason, it was decided to use SDM, as this technique allows specific regions of the molecule to be targeted. Strategic modifications within DI-II may allow the identification of amino acid residues of which the epitope recognised by mAb 4G2dc1 is comprised.

4.5.1: Identification of the disulphide bonds (DBs) responsible for the reduction sensitivity of the 4G2dc1 epitope

The epitope recognise by mAb 4G2dc1 is reduction sensitive. For this reason, it was decided to sequentially disrupt the DBs in DI-II (outlined in Table 4.3) to differentially affect or reduce 4G2dc1 binding and thereby identify a region within the molecule that contains this epitope. Two approaches were used to target the disulphide bonds.

4.5.1.1: Mutagenesis of the first cysteine residue in each disulphide bond

Using construct pSec/sg'Pfama1 as a template, SDM was carried out to replace the first cysteine residue (in the PfAMA1 amino acid sequence) of each disulphide bond in DI-II with alanine. The resulting constructs (pSec/sg'PfaΔsDB1 - ΔsDB5) were expressed in COS-7 cells, giving rise to the mutants' ΔsDB1 - ΔsDB5. Western blot analysis and IFA were carried out on

the transgenic cells. Table 4.3 summarises the specific residues and mutations carried out to achieve this.

Western blot analysis of reduced samples using polyclonal serum R1 showed that each cysteine mutant was expressed (Fig 4.13 A). However, non-reduced samples probed with 4G2dc1 showed that only one mutant retained 4G2 recognition (Fig 4.13 B). In this mutant the third disulphide bond in domain I was disrupted (ΔsDB3). Moreover, when unfixed, transfected COS-7 cells were analysed by IFA using polyclonal serum N1, all cysteine mutants were expressed on the surface (Fig 4.14), though only ΔsDB3 (mutation in cysteine 4) showed expression at a level comparable to the wild type. When analysed in IFA using 4G2dc1 however, ΔsDB1 (mutation in cysteine 1) and ΔsDB4 (mutation in cysteine 7) exhibited no surface fluorescence, indicating loss of the 4G2dc1 epitope (Fig 4.15).

4.5.1.2: Mutagenesis of both cysteines in each disulphide bond

Disruption of a disulphide bond by mutagenising only one of the bonded cysteines leaves a free reactive sulphydryl group in the structure. It was possible that 4G2 recognition of the cysteine mutants in IFA might be due to loss of integrity of the overall fold resulting from the presence of these free reactive sulphydryl groups. To investigate this possibility, the remaining free cysteine from each DB was also mutated to alanine (in the constructs pSec/sg'PfaΔdDB1 - ΔdDB5), giving rise to the mutants ΔdDB1 - ΔdDB5. Table 4.3 summarises the details of the mutations carried out to achieve this. As predicted, by Western blot analysis with the polyclonal serum N1, the double cysteine mutants were all clearly expressed (Fig 4.16 A). Furthermore, all still retained 4G2dc1 recognition except ΔdDB1 (mutations in cysteines 1 and 6) and ΔdDB4 (mutations in cysteines 7 and 10) in Western blot (Fig 4.16 B). These findings are confirmed by IFA of unfixed and unpermeabilised COS-7 cells, with the polyclonal serum N1, in which all mutants were expressed on the cell surface (Fig 4.17). The mutant ΔdDB1 only shows a low level of surface fluorescence with this polyclonal serum. In addition, analysis by IFA using the mAb 4G2dc1 shows that all the mutants, with the exception of ΔdDB1 and ΔdDB4, retain the epitope recognised by this mAb (Fig 4.18). This suggests that the epitope recognised by this mAb is constrained by both of these disulphide bonds but not by any of the others. Disulphide bond 1 links the extreme termini of DI, thus disruption of this DB is likely to have a global effect on protein fold. This is reflected in the low level of surface localisation of ΔdDB1 detected with the polyclonal serum N1. In comparison, DB4 links the termini of DII (via cysteines 7 and 10), however, this DB is adjacent to DB5 (linking cysteines 8 and 9). Therefore, disruption of DB4 will have less effect on the global fold of the molecule due to the stabilising effect of DB5. This may explain the higher level of surface expression of DB4 than DB5 detected in IFA by the polyclonal serum N1.

4.5.2: SDM to target surface exposed residues in DI-II

Sequential disruption of the disulphide bonds in DI-II indicated that both domains are likely to be important for 4G2dc1 recognition. These results have not added any information as to the actual residues involved in this recognition event, nor have they reduced the target area within which these residues are located. The epitope recognised by an Ab to Pf AMA1 must be exposed on the surface of the molecule. For this reason, the sequence of PfAMA1 DI-II was analysed using the JNet (Cuff and Barton, 2000) and Emini (Emini et al., 1985) computer algorithms. These algorithms analyse the local (hexapeptide) environment of a particular amino acid in a protein sequence and determine its surface probability using the accessible surface probabilities defined by Janin *et al.* (1978). A value greater than 1 for a given hexapeptide indicates an increased probability of it being located on the surface of the protein. Thus, applied to the amino acid sequence of pfAMA1 DI-II, these algorithms could be used to predict potential amino acid residues that contribute to recognition by mAb 4G2dc1. These algorithms give the surface accessibility probabilities for peptides in the protein sequence, not for individual amino acids. A SDM approach was used to specifically replace groups of amino acids (triplets) within DI-II of PfAMA1 that were predicted using these algorithms to be located on the proteins surface. It was considered that mutating more than three consecutive amino acids simultaneously might affect the local conformation of the protein. Thus, any disruption of mAb 4G2dc1 recognition of this protein might be an indirect effect of loss of the local fold, rather than a direct effect of the loss of Ab-antigen interaction. Amino acid residues were mutated to either alanine, or where the residue was already alanine, to a residue present in the AMA1 sequence from another species of *Plasmodium* (Table 4.4.). Alanine was selected as it is a small, non-polar residue and is therefore unlikely to disrupt the protein fold. Mutations were introduced into the plasmid pSec/sg'Pfama1, used previously for expression of sgPfAMA1 in COS-7 cells and the resulting mutants were expressed in this cell line. Cell lysates were analysed by Western Blot analysis using the mAb 4G2dc1 and the polyclonal Ab sera R1 and AdsN1. The polyclonal serum R1 was raised against the reduced and alkylated rPfAMA1 ectodomain. This polyclonal serum recognised mutants expressed in this system, showing no preference for protein conformation as it recognised reduced and non-reduced proteins equally. As a result, this serum gave a measure of the total level of sgPfAMA1 expression. The polyclonal serum N1 was raised against the non-reduced (native conformation) rPfAMA1 ectodomain. This serum showed some recognition of linear epitopes in the rPfAMA1 ectodomain, as it recognised the reduced and alkylated rPfAMA1 ectodomain. For this reason, the polyclonal serum was adsorbed out against reduced and alkylated rPfAMA1 ectodomain, giving the serum AdsN1 that recognised only "native", conformational epitopes in the rPfAMA1 ectodomain, as confirmed in Western blot analysis of rPfAMA1 DI-II and DI-III under reducing or non-reducing conditions (Fig 4.19). Finally, the mAb 4G2 was used in Western blot analysis of SDMs, to determine whether the mutations introduced had any effect on 4G2dc1 recognition of the molecule. Using mAb 4G2dc1 in conjunction with AdsN1, allowed the distinction to be made between mutations affecting

protein conformation as well 4G2dc1 recognition and those that specifically disrupted 4G2dc1 recognition without altering the remainder of the molecule. In the case of a triplet mutation that specifically disrupted 4G2dc1 recognition, the individual mutations were subsequently made, replacing the amino acids one at a time and screening each of them against the same panel of Abs.

All the mutants were expressed at a high level, as indicated by strong recognition with the polyclonal serum R1 (Fig 4.20 A). In the first round of mutagenesis, mutants 110WTE/AAA, 115AKYD/EAAA, 233NYK/AAA, and 278PAK/AAA all affect the overall fold of the protein, as indicated by reduced recognition by polyclonal serum AdsN1 (Fig 4.20 B). Only three mutants (348DQP/AAA, 351KQY/AAA and 388DRY/AAA) were shown to have a specific effect on 4G2dc1 recognition (data not shown). To investigate these mutations further, the residues in each triplet were mutated individually to alanine and again analysed in Western blot with the three antibodies. Interestingly, none of the individual point mutations in isolation completely abrogated 4G2dc1 recognition, however, substitution of five residues (highlighted in bold in table 4.4) were found to significantly reduce the 4G2dc1 signal (Fig 4.20 C, lanes 9, 10, 11, 15 and 16). On the basis of these results it seems likely that these five residues are components of the epitope recognised by mAb 4G2dc1. None of the remaining point mutations generated from these three triplet mutants appeared to affect 4G2dc1 recognition. From these results it would appear that the epitope recognised by mAb 4G2dc1 may be localised exclusively within DII. Several mutations introduced into DI disrupted the overall conformation of the molecule. Thus, the effect on 4G2 recognition was not considered to be a specific effect on the epitope. The identification of components of the 4G2dc1 epitope within DII, suggests that these domains are interconnected and disruption of the "native" conformation in one region of the molecule can alter the conformation in distal regions. It is possible that residues within DI have a structural role within PfAMA1 and that altering these residues disrupts the stability of the molecule, detected in this study as a decrease in recognition by the polyclonal serum AdsN1 and loss of 4G2dc1 recognition.

As has been indicated, none of the point mutations identified as specifically disrupting 4G2dc1 recognition completely disrupted this recognition. The possibility therefore existed that this decrease in 4G2dc1 recognition was the result of a conformational change in the molecule, too subtle to be detected by the serum AdsN1. For this reason, two of these mutations (K351 and R389) were combined to determine whether these had an additive effect on 4G2dc1 recognition. In addition, it was anticipated that if the disruption of 4G2dc1 recognition was a result of an undetectable conformational change, combining the mutations might increase this to within detectable levels. Furthermore, these two residues were mutated to corresponding residues from the PvAMA1 sequence (K351/T and R389/N). Residues that are present at the equivalent position in the AMA1 sequence from *P. vivax* are unlikely to adversely affect the function or structure of the molecule, thus minimising the conformational disruption induced by

the double mutation. If the effect of the individual mutations was specific for 4G2dc1 recognition, this double mutation should generate a 4G2dc1 negative form of PfAMA1. As anticipated, the double mutant (K351/T and R389/N) was not recognised by 4G2dc1 in Western blot analysis (Fig 4.20 C, lane 18). However, recognition by both polyclonal sera R1 and AdsN1 was unaltered (Fig 4.20 A and B respectively, lane 18).

At the beginning of this analysis, no tertiary structure data was available for DI-II of AMA1 from any species of malaria parasite. However, the crystal structure of PvAMA1 has subsequently become available (Pizarro et al. 2005). Superimposing the residues apparently involved in 4G2dc1 recognition of PfAMA1 onto a model of PfAMA1 constructed by homology with the recently published structure of PvAMA1, indicates that the 4G2dc1 epitope lies within the base of a flexible or unstructured loop within DII. To investigate the possibility that other residues within this region of the molecule may contribute to 4G2dc1 recognition, a series of further SDMs (listed in Table 4.5) were analysed using the COS-7 expression system (Fig 4.21). As observed previously, no single point mutation resulted in complete abrogation of 4G2dc1 binding. However, the mutation F385/A (Fig 4.21 C, lane 9) significantly reduced 4G2dc1 recognition of sgPfAMA1.

No electron density was present for the forty amino acid stretch in DII corresponding to the DII loop. This region was therefore mobile or disordered. For this reason, structural algorithms were used to predict the secondary structural components within the loop, based on the primary sequence. These algorithms indicated the presence of two α-helices, helix 1: 353-YEQHLTDYEKIKEGFK-368 and helix 2: 373-DMIKS-377. To investigate the function of these putative helices in 4G2dc1 recognition of PfAMA1, two mutants were generated in which one or other of the helices was deleted from the sequence. Both of the mutant forms of sgPfAMA1 (Δhelix1 and Δhelix2) were expressed at levels equivalent to that of "wild type" sgPfAMA1, as shown in Western blot analysis with the polyclonal sera R1 and AdsN1 (Fig 4.21 A and B respectively, lanes 5 and 6). In addition, deletion of helix 2 had no effect on 4G2dc1 recognition (Fig 4.21 C, lane 6). By comparison, Δhelix1 showed complete abrogation of 4G2dc1 recognition (Fig 4.21 C, lane 5). A possible explanation for this effect was that the loss of helix 1 destabilised the DII loop, thus disrupting 4G2 recognition. For this reason, a mutant was constructed that lacked the entire stretch from 353Y-S377, thus removing both helices (Δhelix1/2). Despite being strongly expressed, as indicated in Western blot analysis with the polyclonal sera R1 and AdsN1 (Fig 4.21 A and B respectively, lane 7), this mutant was not recognised by mAb 4G2dc1 (Fig4.21 C, lane 7).

Based on the results from the helix deletions in the DII loop, it was considered likely that (a) residue(s) within helix 1 contributed directly to 4G2dc1 recognition. To assess this possibility, two mutants were produced in which proline substitutions were introduced into the loop sequence, at H356 or K364 (both in helix 1). As a result of conformational constraints placed

upon it by its pyrrolidine side chain, proline introduces a kink in the amino acid chain, so these substitutions might be expected to disrupt any downstream α-helical structure. If an amino acid residue downstream of the newly introduced proline participated in 4G2dc1 binding, it might be predicted that the substitution would result in loss of Ab recognition. Western blot analysis indicated that only the first substitution H356/P abrogated 4G2dc1 recognition (Fig 4.21 C, lane 3). This suggests that a residue between H356 and K364 contributed to the epitope recognised by 4G2dc1. Of this stretch of residues (356HLTDYEKI363) the only ones not previously investigated by substitution were L357, T358 and H356 itself. Substitution 357LT/AA had no effect on 4G2dc1 recognition (Fig 4.21 C, lane 4). By comparison, the substitution 354EQH/AAA resulted in complete abrogation of 4G2dc1 recognition (Fig 4.21 C, lane 2). This suggested that one of the latter residues (354E, 355Q or 356H) contributed to the epitope. However, when each of these residues was individually mutated to alanine they were highly expressed and recognised by both R1 and AdsN1 (data not shown) but none produced any observable disruption of 4G2dc1 recognition in Western blot analysis (Fig 4.21 D).

The above results indicated that residues 354EQH collectively affect 4G2dc1 binding, as does the mutation of 356H/P, whereas K364/P has no effect. Thus, it was considered possible that only the first part of helix 1 contributed to 4G2 binding. To investigate this possibility, two mutants were constructed in which sections of the second half of helix 1 were deleted (357LTDYEKIKEGFK368, or 361EKIKEGFK368). The only residue in this region still untested was E365, but as mutation K364/P had no effect on 4G2dc1 binding, it seemed unlikely that this residue contributed to Ab recognition. Both helix truncation mutants showed loss of 4G2dc1 binding (data not shown). Thus, although the individual residues within helix 1 did not appear to have an effect on the ability of the antibody to bind, complete disruption of the helix prevented binding. This finding was supported by the fact that the mutations Δhelix1 and Δhelix1/2 resulted in loss of 4G2 recognition (Fig 4.21 C, lane 5 and 7 respectively). In contrast, deletion of helix 2 had no effect on 4G2dc1 recognition of the molecule (Fig 4.21 C, lane 6). It is therefore possible that helix 1, but not helix 2, has a local stabilising role in the molecule, that influences 4G2 recognition and binding.

Figure 4.22 (A) shows the surface location of residues identified as contributing to the 4G2dc1 epitope in the ectodomain of PfAMA1. In addition, residues that lie in close proximity to this epitope are indicated for future analysis (Figure 4.22 B). The SDM approach used above relied on surface predictive algorithms. Residues were selected for mutagenesis according to their likelihood of being surface exposed as predicted by these algorithms. Such algorithms rely on calculations of the probability of an amino acid residue within a sequence being localised on the surface, based on the empirical calculations derived from other proteins with known structure. It is therefore possible that certain amino acid residues localised on the surface of PfAMA1 were not identified as such and as a result that potential components of the epitope recognised by mAb 4G2dc1 might have been overlooked. It was decided therefore to take a broader approach

to determine which amino acid residues are important for 4G2dc1 recognition of PfAMA1. Rather than targeting specific residues by SDM, a random mutagenic approach was devised to screen the entire DI-II sequence.

4.6: Random mutagenic screen to isolate 4G2dc1 negative (4G2dc1$^-$) forms of PfAMA1

A library of sg'PfAMA1 random mutants (sg'Pfa1RML, with mutations in DI-II) was generated using the plasmid pSec/sg'Pfama1 previously used for expression of sg'PfAMA1 in COS-7 cells. It was anticipated that transfection of COS-7 cells resulted in a single cell receiving on average a single plasmid. Thus, transfection of COS-7 cells with sg'Pfa1RML would result in different cells in the population expressing single mutant forms of sg'PfAMA1. As with previous use of this construct, expression of these mutants in COS-7 cells should have resulted in surface localisation of the protein. The resulting mixed cultures were screened for expression of mutant forms of PfAMA1 that retained the 4G2dc1 epitope and were therefore recognised by this mAb. In a negative selection step, these cells were extracted from the culture and discarded. Any cells remaining in the culture would be expressing 4G2dc1$^-$ mutant forms of sg'PfAMA1 but the culture would contain a mixture of cells. Some of these cells should express 4G2dc1$^-$ mutant forms of sg'PfAMA1, in which the overall protein conformation was correct (native$^+$) and others express 4G2dc1$^-$ mutant forms of sg'PfAMA1, in which the mutations had resulted in partial or full loss of protein conformation. In addition, some cells might not be expressing sg'PfAMA1, as transformants were not positively selected for (see below).

A positive selection step was used to isolate cells expressing 4G2dc1$^-$, native$^+$ mutant forms of sg'PfAMA1. Plasmid DNA was rescued from this cell sample, amplified in *E. coli* and the selection procedure repeated two further times. In this way, the number of mutant forms of sg'PfAMA1 that retained the 4G2dc1 epitope but escaped the negative selection step would be further diminished by repeated cycles of negative selection.

The selection steps relied on the use of anti-mouse IgG coupled to Dynabeads. The transfected COS-7 cells were pre-incubated with either the mAb 4G2dc1 (negative selection step) or the polyclonal serum N1 (positive selection step), followed by incubation with the Dynabeads. Thus, cells to which the primary antibody was bound would subsequently be bound by the anti-mouse IgG coupled to the Dynabeads. Cells that were bound to the Dynabeads were then isolated from the cell suspension using a Dynal magnet.

Random mutagenic PCR conditions were used to introduce mutations within the sequence encoding DI-II of the PfAMA1 ectodomain. These were incorporated back into the plasmid pSecΔ*Pst*I/sg'Pfa for expression in COS-7 cells. To enable screening for random mutants in which the 4G2dc1 epitope was disrupted, adherent transfected COS-7 cells were released into

single cell suspension using trypsin:EDTA. However, this treatment also removed much of the surface expressed sg'PfAMA1, rendering selection impossible. To overcome this, the trypsin inhibitors soyabean trypsin inhibitor and TLCK were used to inactivate the enzyme after suspension of the cells and also during the incubation steps.

Preliminary experiments were performed to test the efficiency of the above-described approach, using COS-7 cells transfected with constructs expressing either "wild type" sg'PfAMA1 (pSec/sg'Pfama1) or a mutant already shown to lack the 4G2 epitope, ΔdDB4 (construct pSec/sg'PfaΔdDB4 in which the disulphide bond in DII between Cys320 [C7] and Cys418 [C10] had been disrupted by replacement of both cysteines in the bond with alanine, see section 4.5.2). As previously described, IFA analysis using the polyclonal serum N1 had shown this mutant to be expressed on the surface of transfected cells. Cells transfected with each of these constructs were subjected to a single selection step either with or without one of the primary antibodies 4G2dc1 or N1. If selection was working efficiently it was expected that neither set of transfected COS-7 cells would bind Dynabeads in the absence of primary antibody. By contrast, both were predicted to bind in the presence of N1 and only the cells expressing wild type PfAMA1 were expected to bind in the presence of 4G2dc1. For each transfected culture, a sample was harvested immediately after treatment a trypsin. This gave a measure of the total amount of mutant and wild type sg'PfAMA1 present prior to the selection steps. The samples were analysed by Western blot, using the polyclonal sera R1 and N1 (Fig 4.23 i and ii) and the mAb 4G2dc1 (Fig 4.23 iii). In the following description of this result, B, UB and T, refer to bound unbound and trypsin treated respectively. As expected, neither set of transfected cells bound the Dynabeads in the absence of primary antibody (Fig 4.23 I and II, a, B). The ΔdDB4 mutant (Fig 4.23 II) appeared to bind to 4G2dc1 at a low level as indicated by a faint signal in Western blot analysis of the 4G2dc1 bound fraction (Fig 4.23 II, b, B). This mutant was 4G2dc1$^-$, so this result suggested that a small proportion of cells were able to bind non-specifically in the negative selection step of the screen. In addition, with N1 nearly all the ΔdDB4 mutant was found in the unbound fraction, as determined by Western blot analysis (Fig 4.23 II, c, UB). Some cells expressing the wild type sg'PfAMA1 were present in the unbound fraction from both antibodies (Fig 4.23 I, b and c, UB), though most was found in the bound fraction (Fig 4.23 I, b and c, B). The wild type sg'PfAMA1 appeared to be expressed at a higher level than the ΔdDB4 mutant (Fig 4.23 I and II respectively, T) therefore it was possible that insufficient 4G2dc1 was used in the negative selection step to bind efficiently to, and allow extraction of, all the wild type sg'PfAMA1 expressing cells. These results indicate that the selection process was efficient for wild type sg'PfAMA1 transfected COS-7 cells, but it appeared to be less specific for the DB 4 mutant.

Several experiments were carried out to assess the efficiency of the (double negative followed by positive) selection procedure (data not shown). In all of these, the second (positive) selection step appeared to be very inefficient, with most cells not binding to N1 even though they were

detected by N1 in Western blot analysis. By contrast nearly all cells expressing wild type PfAMA1 were found in the 4G2dc1 bound fraction, suggesting that although there was a small degree of non-specific binding in this step, the positive selection was almost absolute. This suggested that most cells expressing mutant forms of rPfAMA1, in which the 4G2dc1 epitope was still intact, were able to bind during this step and anything that did not bind here was likely to lack the epitope. For this reason it was decided to subject the random mutant library (sg'Pfa1RML) to three round of negative selection to enhance the population for 4G2dc1$^-$ mutants before using the positive selection step. At each round of negative selection two 4G2dc1 binding steps were performed. Between each round of selection the plasmid from the unbound fraction was recovered and amplified in *E. coli*, before being re-transfected back into COS-7 cells. After three round of negative selection the mutant library was transfected back into COS-7 cells and subjected to a further negative selection step, this time followed by a positive selection step with N1. Plasmid recovered from the N1 bound fraction was cloned in *E. coli* for sequencing and subsequent expression in COS-7 cells. The clones were transfected into COS-7 cells and expression analysed by Western blot with the polyclonal antibodies AdsN1 and R1 and the mAb 4G2dc1, for expression and the presence of the 4G2dc1 epitope respectively (as for the SDM screening above).

Despite screening over 100 mutant clones, only 10 mutants were identified that were 4G2dc1$^-$, but correctly folded (native$^+$) by the criteria described above (Fig 2.11). Many of the mutants screened retained the 4G2dc1 epitope (Fig 4.24, lanes 10, 14, 17, 19, 22, 28) and a number of others did not appear to express sg'PfAMA1 in any form (Fig 4.24, lanes 1, 2, 7, 9, 11, 15, 16, 17, 19, 21, 22, 25, 26, 29*). A small proportion of the clones screened expressed a truncated form of sg'PfAMA1 (Fig 4.23, lane 12). In one such case, the 4G2dc1 epitope remained intact. All twelve 4G2dc1$^-$/native$^+$ mutants were sequenced to determine the amino acids responsible for loss of 4G2dc1 recognition (Fig 4.25). In all cases between 5 and 10 amino acid substitutions were observed within DI-II (representing 342 amino acids), indicating a much higher level of mutation at the nucleotide level than that initially determined (5 per kb). The amino acid substitutions were found to be evenly distributed over DI-II and one of the mutations (Clone 5; Phe385/Cys) coincided with a residue identified by SDM as being a component of the 4G2dc1 epitope (Fig 4.25). An additional mutation present in one of these clones (clone 26 Phe379/Tyr) was found in one of the residues considered as a potential component of the 4G2dc1 epitope based on its proximity to the residues already identified.

4.7: Discussion

4.7.1. The invasion inhibitory activity of 4G2dc1-Fab

Erythrocyte invasion by *P. falciparum* merozoites can be inhibited by mAb 4G2dc1, which recognises a reduction sensitive, conformation dependent epitope in the PfAMA1 ectodomain

(Kocken et al. 1998). This suggests that the PfAMA1 ectodomain is important for invasion, thus identification of the 4G2dc1 epitope may reveal a functionally important or crucial region of the AMA1 ectodomain. In this study it has been shown that 4G2dc1-Fab fragments also block erythrocyte invasion, with a higher percentage inhibition, at much lower (nearly 10 fold) concentrations than the intact Ab. This finding was confirmed in a recently published work by Dutta et al. (2005). However, the level of inhibition (20% inhibition at 360 $\mu g\ ml^{-1}$) demonstrated by Dutta et al for intact IgG was lower than that observed in the current study. These finding are not without precedent, Thomas et al. (1984) demonstrated that $F(ab)_2$ and Fab fragments of the *P. knowlesi* AMA1 specific rat mAb R3/1C2 produced the same level of invasion-inhibition as intact IgG at a 10 fold lower concentration. As discussed earlier, only two thirds of the concentration of an intact IgG is contributed by Fab fragment. For this reason, in the current work, the concentration of the intact antibody was adjusted to represent the concentration of Fab present in the sample. Intact 4G2dc1 exhibited 44% invasion-inhibition at 0.47 mg ml^{-1} compared with 97% inhibition by 4G2dc1-Fab at 0.4 mg ml^{-1}. At higher concentrations, the level of inhibition was much closer with the intact Ab exhibiting 74% invasion-inhibition at 1.8 mg ml^{-1}, compared with 99% invasion-inhibition for 4G2dc1-Fab at 1.6 mg ml^{-1}. Interestingly, 4G2dc1-Fab mediated significant invasion-inhibition down to relatively low concentrations, showing 24% inhibition at 0.05 mg ml^{-1} (Fig 4.1 B). This represents a concentration of 4G2dc1-Fab fragment one fifth that found in the intact antibody assay, giving a percentage inhibition of 30%. Overall these results indicate that the 4G2dc1-Fab has a higher level of inhibition than the intact antibody at equivalent molar concentrations of the Fab fragment. This suggests that the inhibition mediated by this Ab is not one of steric hindrance. One possible explanation for this increased inhibition is a result of the Fab fragment being one third the size of the intact antibody

4.7.2: Interactions between the subdomains of PfAMA1

By Western blot analysis of different regions of the PfAMA1 ectodomain (DI, DI-II and DI-III) expressed in *P. pastoris*, the current study demonstrated that the mAb 4G2dc1 epitope lies within DI-II, confirming previous suggestions to this effect (Lalitha et al., 2004; Howell et al., 2001). Expression of rPfAMA1 DI on its own has previously been demonstrated using phage display (Coley et al., 2001; Lalitha et al., 2004), however, in the current study expression of this domain on its own in a correctly folded form was not possible in *P. pastoris* or in COS-7 cells.

The PvAMA1 X-ray crystal structure (Pizarro et al. 2005) highlights an interactive interface between DI and DII. Residue Lys280 (corresponding to Lys225 in PvAMA1), which is invariant in AMA1 throughout *Plasmodium*, is buried in the PvAMA1 structure and interacts via its amino group with an equally invariant Asn (Asn338 and 283 in PfAMA1 and PvAMA1 respectively). This study showed that substitution of this residue with alanine resulted in loss of mAb 4G2dc1 recognition (Fig 4.20 a, lane 7) but also reduced recognition by the conformation dependent polyclonal sera AdsN1 (Fig 4.20 b, lane). This suggests that the two domains are

interdependent and may not fold correctly in isolation. In the current study, digestion of rPfAMA1 DI-III with subtilisin, trypsin and chymotrypsin produced stable fragments about the same size as DI-II and still recognised by 4G2dc1. Confirmation that these fragments were likely to be DI-II came from the observation that DI-II was resistant to digestion with both trypsin and chymotrypsin. Furthermore, the presence of low levels of the denaturants SDS and urea were required for digestion of rPfAMA1 DI-II to occur. These results confirm the findings of Pizarr o et al. (2005) and suggest that DI and DII may be closely apposed in the intact molecule, rendering the inter-domain sequences inaccessible to these proteases. 4G2dc1 recognition of the molecule therefore probably requires the stable complex of both domains even though the epitope appears to be formed by residues that lie exclusively within DII. By comparison, the production of a DI-II sized fragment on digestion of DI-III and the stability of DI-II in the absence of denaturing agents, demonstrated in the current study, suggests that DIII is not so closely packed in the structure as DI-II. It is possible that DIII, which lies adjacent to the merozoite plasma membrane, provides the molecule with a degree of flexibility while the functionally important regions of the molecule (DI-II) retain a more rigid structure.

The findings and interpretations of this study are supported by the observations of Gupta *et al.* (2005), that the PfAMA1 ectodomain is fairly resistant to proteolytic digestion. This group identified four susceptible sites in a construct comprising the PfAMA1 ectodomain and prodomain when digested with elastase. The N-terminal prodomain and C-terminus of the ectodomain were digested by this enzyme at almost exactly the same positions as those observed during the normal processing events (Howell et al. 2001). A single cleavage at position Ile460 (Gupta et al. 2005) corresponds closely to the DIII nick, giving rise to the $PfAMA1_{44}$ form (Howell et al. 2003). Finally and perhaps of most interesting in relation to the current study, residues H356 to A384 were degraded (Gupta et al. 2005). The sequence delineated by these residues corresponds to the unstructured or flexible region identified during determination of the PvAMA1 structure i.e. the DII loop (Pizarro et al. 2005). Thus, unlike the rest of DI-II, the DII loop is less tightly packed within the tertiary structure, perhaps more mobile and therefore likely to be accessible to extramolecular interacitons.

In the current study it proved impossible to express any of the individual domains of the PfAMA1 ectodomain in isolation, with the exception of DI-II. Reports exist of expression of PfAMA1 ectodomains in isolation and in varying combination (Lalitha et al. 2004), but these have usually required refolding to obtain the disulphide bonded conformations necessary to induce growth inhibitory antibodies (Dutta et al., 2002). In addition, the solution structures of DII (Feng et al., 2005) and DIII (Nair et al., 2002), expressed in *E. coli* and refolded, showed the presence of some secondary structural element(s), however, in both cases the majority of the molecule was unstructured. These findings suggest that in the intact molecule these domains are stabilised by multiple interdomain interactions and that in isolation they are unable to adopt their native conformation.

In an attempt to protect the mAb 4G2dc1 epitope, rPfAMA1 DI-II was complexed to 4G2dc1 $F(ab)_2$ before digestion with pepsin. The complex was initially resistant to degradation by pepsin, although when digestion did commence it went to completion, a finding similar to that seen with DI-II alone. One interpretation of this finding is that even if the 4G2dc1 epitope is protected by 4G2dc1 $F(ab)_2$, when the digested complex is electrophoresed on SDS-PAGE in the absence of the remainder of the molecule the loops making up the epitope dissociate. While this approach has not helped in the elucidation of the 4G2dc1 epitope, it has given some structural information about the ectodomain of PfAMA1. This includes the observation that interactions exist between DI and DII, keeping them closely packed together in the intact PfAMA1 ectodomain. In addition, the apparent susceptibility of DIII to proteolytic digestion suggests that it is less tightly associated with DI-II. However, this latter finding is not substantiated by the findings of Gupta *et al.* (2005), who showed the whole ectodomain to be resistant to elastase digestion. In addition, the PvAMA1 X-ray crystal structure shows that the N-terminus of DI lies across the surface of DII and DIII, interacting extensively with them (Pizarro et al. 2005). In the present study, mutations of amino acid residues in the N-terminus of DI (110WTE/AAA, 115AKYD/EAAA and NYK/AAA) or truncations of DI (T1 and T2), affected protein fold as well as 4G2dc1 recognition, suggesting that interactions between these segments and DII stabilise the molecule and are required for correct folding. In combination, these finding suggest that there is a considerable amount of interconnection between all three subdomains of the AMA1 ectodomain.

4.7.3: Identification of amino acid residues involved in 4G2dc1 recognition of PfAMA1

Random mutagenesis of DI-II of the PfAMA1 ectodomain could be a powerful tool to identify the epitope recognised by the mAb 4G2dc1, as it allows screening of large numbers of mutants very rapidly. However, in this study the mutation rate that was originally calculated was much lower than that finally achieved. This resulted in large numbers of mutations per clone, many of which probably resulted in loss of protein fold rather than specific disruption of the 4G2dc1 epitope. Furthermore, there was a considerable degree of non-specificity in the selection steps in the Dynabead binding assay. Although the first selection step was very efficient in depleting the sample of $4G2dc1^+$ cells, depletion was incomplete and during subsequent recovery, amplification and selection steps the proportion of $4G2dc1^+$ cells did not appear to decrease. This may be a result of the delicate balance between treating the cells with trypsin for a time sufficient to obtain a single cell suspension without removing all the surface protein. Incomplete trypsin treatment may have resulted in clumping of the cells and consequently non-specific selection.

Site directed mutagenesis conclusively identified six amino acid residues that participate in 4G2dc1 recognition and binding (Asp348, lys351, Gln352, Phe385, Asp388 and Arg389). These

have all been shown to lie at the base of a flexible loop in DII. Figure 4.22 shows the position of these residues in the DII loop (A) and highlights several other residues that might be worth considering as potential candidates which contribute to 4G2dc1 recognition (B). In this structure Asp348 is not exposed on the surface, which might suggest that its disruption has an indirect effect on 4G2dc1 recognition. However, the observation that the DII loop is flexible and may take up several alternative conformations suggests that 4G2dc1 may bind when the loop is in a different conformation and Asp348 is exposed. The observation that disruption of DB4 (substitution of Cys320 and Cys418) disrupts 4G2dc1 recognition but DB5 (substitution of Cys337 and Cys409) does not is unexpected. From the primary amino acid sequence, the epitope lies in close proximity to DB5. For this reason, it would seem likely that disrupting this bond would destabilise the local structure of the molecule. DB4 on the other hand draws domains I, II and III together, therefore, loss of this interaction may have a more wide reaching influence on protein structure.

Proteins targeted for secretion enter the secretory pathway via the endoplasmic reticulum (ER). Quality control mechanisms prevent the exit of incorrectly folded proteins from the ER. Thus, only properly folded proteins reach the plasma membrane or are secreted. For this reason, secretion and surface localisation are usually good measures of protein folding. In the case of the ΔdDB4, a strong surface signal was obtained with the polyclonal Ab N1 in IFA, suggesting that the protein is secreted and therefore folded. By contrast, mutant ΔdDB1 (substitution of Cys149 and Cys302) gives weak surface fluorescence with the polyclonal Ab N1, indicating that most of the molecule does not fold sufficiently to be secreted. This is understandable, as the DB between these two cysteine residues draws together the extreme ends of the DI primary sequence, therefore this DB must have a significant stabilising influence on the whole molecule. By comparison, DB3 links a very small loop in the primary structure of PfAMA1. It is not surprising therefore that disruption of this disulphide bond had no effect on expression and folding of the molecule in transfected COS-7 cells, with 4G2dc1 recognition in Western and IFA at the level of wild type. PAN domains are typically stabilised by three disulphide bonds, however, in AMA1 only DB2 (Cys217-Cys247) in DI and DB5 (Cys337-Cys409) in DII conform to the PAN motif (Pizzaro *et al.* 2005). Clearly the DBs in AMA1 must have a stabilising effect on the tertiary structure of the molecule, but the analogies drawn between the role of the DBs in classical PAN motifs and those in AMA1 are limited.

4.7.4: Possible mechanisms of invasion inhibitory activity of 4G2dc1

Dutta *et al* (2005) suggested that 4G2dc1 and 4G2dc1-Fab, as well as other anti-AMA1 antibodies, inhibit erythrocyte invasion by blocking processing/shedding of PfAMA1, as has been observed with PfMSP1 (Blackman et al., 1994). In addition, rabbit anti-AMA1 immune serum has been shown to cross-link AMA1, preventing its relocalisation across the merozoite surface (Dutta et al. 2005). In invasion-inhibition assays, intact Abs from this rabbit antiserum

exhibited greater inhibitory activity than their Fab fragment or than that of 4G2dc1, except at high concentrations. The Fab fragments, being monovalent, are unable to cross-link protein molecules. Thus, the ability of some antibodies to block relocalisation of PfAMA1 across the merozoite surface may increase their potency. Relocalisation of PfAMA1 across the parasite surface may be essential for invasion. In addition, cross-linkage of PfAMA1 at the apical prominence may interfere with normal secretion of the apical organelles. Such a mechanism of inhibition would be extremely efficient as many proteins involved in the invasion process are released onto the merozoite surface from the micronemes and rhoptries via the apical prominence (Preiser et al., 2000; Dubremetz et al., 1998). The mAb 4G2dc1 does not exhibit this cross-linking activity.

The location of the 4G2dc1 epitope at the base of the flexible domain II loop suggests that this region of the molecule is functionally important. The PvAMA1 crystal structure has shown that DI and DII belong to the PAN module family, implicated in adhesion of protein or carbohydrate receptors. The domain II loop of PvAMA1 lies within the region connecting helix α7 (the PAN domain helix) and strand β15. This region is equivalent to the loop connecting the PAN domain helix and strand β3 of the Hepatocyte Growth Factor NK1. This loop in NK1 makes direct contact with its ligand heparin (Lietha et al., 2001). Comparison of the PAN domains of PvAMA1 with the PAN domain of NK1 complexed to its ligand suggests that the domain II loop of AMA1 replaces the NK1 loop, and may function by closing over its putative receptor once it is in place. Thus mobility of the domain II loop would be essential for AMA1 function. The mAb 4G2dc1 may directly interfere with PfAMA1 function by anchoring the domain II loop, thus preventing it from stabilising the ligand-receptor interaction or locking it over the receptor binding site.

In conclusion, residues identified in this study as contributing specifically to the recognition of PfAMA1 by the mAb 4G2dc1, lie at the base of the DII loop. This loop appears to be flexible and may adopt different conformations during the invasion process. Binding of 4G2dc1 to PfAMA1 may reduce the flexibility of the loop, which may be an essential property of the molecule for RBC binding during invasion by *P. falciparum* merozoites. It is possible that residues not yet identified are also involved in 4G2dc1 binding. These residues may also be in the DII loop, some of which (at the C-terminus of the loop) have not yet been mutated. Alternatively, they may be on the surface of AMA1 against which the loop rests. In this way, 4G2dc1 binding may anchor the loop against DI, thus reducing its flexibility. Future work will focus on identifying these residues.

Table 4.1: Percentage invasion-inhibition of the mAb 4G2dc1

(a) Comparison of 4G2dc1 IgG with its purified 4G2dc1-Fab fragment

Concentration	% Invasion-inhibition	
mg ml^{-1} (Fab binding sites)	Intact 4G2	4G2dc1-Fab
0.4 (0.27)	30	97
0.7 (0.47)	43	99
1.6 (1.1)	21	99
2.7 (1.8)	74	99

(b) Activity of the purified 4G2dc1 Fab fragment at low concentrations

Concentration (mg ml^{-1})	4G2dc1-Fab
0	0
0.03	18
0.05	24
0.11	50
0.27	62
0.43	68

Table 4.2: Recombinant PfAMA1 DI-III complexed to 4G2dc1-Fab reduces the merozoite invasion inhibitory activity of the Fab fragment

Concentration of 4G2dc1-Fab (mg ml^{-1})	% Invasion-inhibition	
	4G2dc1-Fab	4G2dc1-Fab + rPfAMA1 DI-III
0	0	32
0.03	18	11
0.05	24	17
0.11	50	43
0.16	14	4
0.27	62	38
0.43	68	75

Table 4.3: The disulphide bond (DB) linkage in DI-II and nomenclature of the disulphide bond mutants

DB	Cysteine in sequence	Cysteine numbering	Single mutants (ΔsDB)	Double mutants (ΔdDB)
DB1	C149-C302	C1-C6	C149 (C1) - ΔsDB1	C1+C6 - ΔdDB1
DB2	C217-C247	C2-C3	C217 (C2) - ΔsDB2	C2+C3 - ΔdDB2
DB3	C263-C275	C4-C5	C263 (C4) - ΔsDB3	C4+C5 - ΔdDB3
DB4	C320-C418	C7-C10	C320 (C7) - ΔsDB4	C7+C10 -ΔdDB4
DB5	C337-C409	C8-C9	C337 (C8) - ΔsDB5	C8+C9 - ΔdDB5

Table 4.4: Summary of SDMs generated on the basis of surface prediction and their recognition by Abs 4G2dc1, N1 and R1.

Mutations	4G2dc1	AdsN1	R1
102RSN/AAA	+	+	+
110WTE/AAA	-	+/-	+
115AKYD/EAAA	-	+/-	+
140TQYR/AQAA	+	+	+
160NSKT/AAKA	+	+	+
174QDL/AAA	+	+	+
224MNP/AAA	+	+	+
227DND/AAA	+	+	+
230KNS/AAA	+	+	+
233NYK/AAA	-	+/-	+
257NNG/AAA	+	+	+
266DQS/AQA	+	+	+
269KRN/AAA	+	+	+
278PA**K**/AAA	-	+/-	+
305KNL/AAA	+	+	+
348**D**QP/AAA	-	+	+
351**KQ**Y/AAA	-	+	+
359DYE/AAA	+	+	+
362KIK/AAA	+	+	+
366GFK/AAA	+	+	+
369NKN/AAA	+	+	+
388**DR**Y/AAA	-	+	+
403NRE/AAA	+	+	+

Table 4.5: The effect on Ab recognition of mutations introduced within or adjacent to the DII loop of PfAMA1

Mutation	4G2dc1	AdsN1	R1
E120/A	+	+	+
E121/A	+	+	+
G124/A	+	+	+
R277/A	+	+	+
R319/T	+	+	+
354EQH/AAA	-	+	+
EQH356/EQP	-	+	+
357LT/AA	+	+	+
Y353 - K368 deletion	-	+	+
D373 - S377 deletion	+	+	+
Y353 - S377 deletion	-	+	+
L357-K368 deletion	-	+	+
E361-K368 deletion	-	+	+
K368/P	+	+	+
L380/A	+	+	+
T382/A or T382/R	+	+	+
F385/A	+/-	+	+
K391/A	+	+	+
H393/A	+	+	+
K395/A	+	+	+

Figure 4.1: *P. falciparum* merozoite invasion-inhibition by mAb 4G2dc1: 4G2dc1-Fab is more potent than the intact Ab

(A) Assays were perfomed at 2% haematocrit and 10% parasitaemia in the presence of purified 4G2dc1-Fab (blue) or intact 4G2dc1 (pink). For each sample, counts were made of the number of rings per 10^4 RBCs. The 4G2dc1-Fab and 4G2dc1 concentrations (mg ml^{-1}) were calculated to represent the amount of Fab binding sites present. Results were expressed as a percentage of the mean parasitaemia observed in the absence of IgG (PBS only). The Fab shows a greater degree of invasion-inhibition than the intact Ab at equivalent concentrations of the Fab binding domain. **(B)** Assay repeated at lower concentrations of 4G2dc1-Fab where, even at relatively low concentrations, 4G2dc1-Fab fragment exhibit potent invasion-inhibition.

(A)

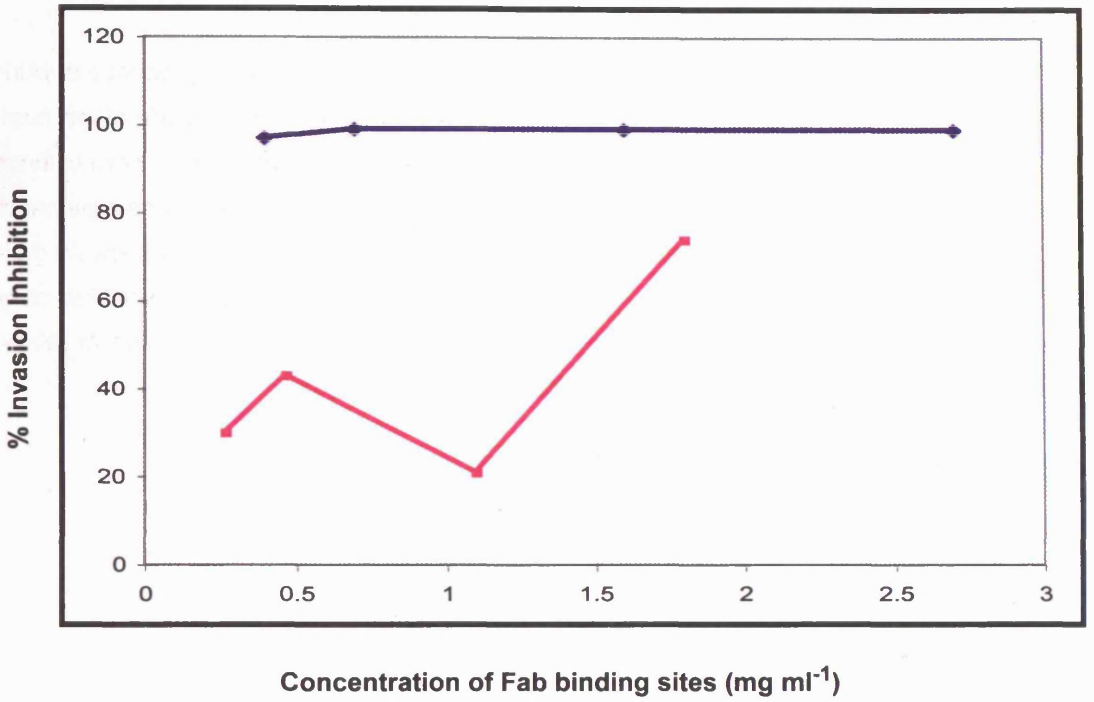
120
100
80
60
40
20
0
% Invasion Inhibition
0
0.5
1
1.5
2
2.5
3
Concentration of Fab binding sites (mg ml-1)

(B)

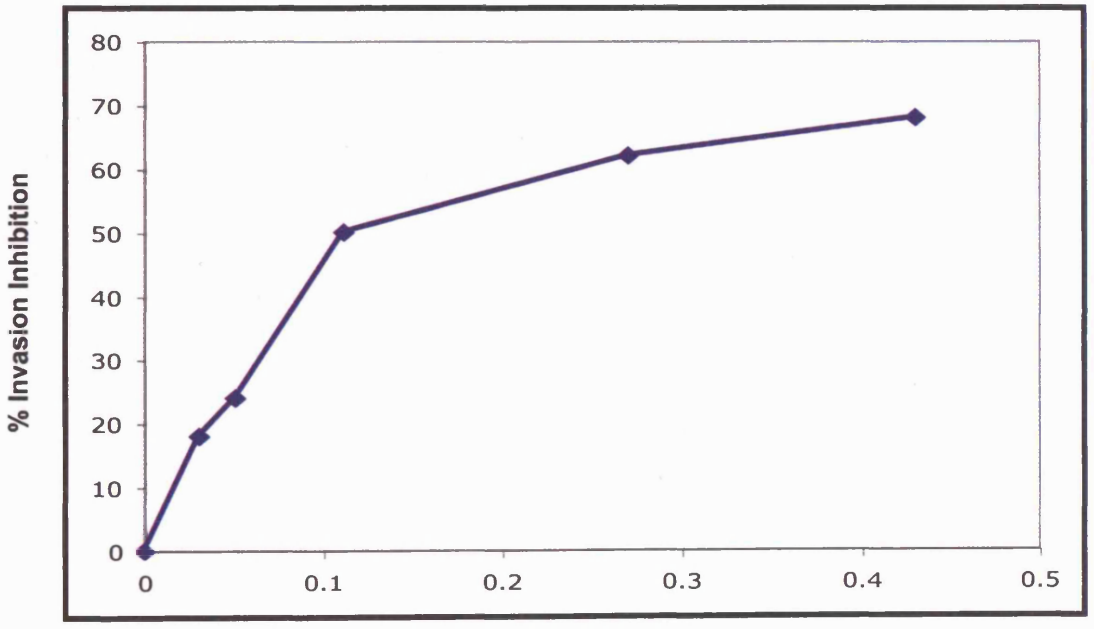
80
70
60
50
40
30
20
10
0
% Invasion Inhibition
0
0.1
0.2
0.3
0.4
0.5
Concentration of Fab binding sites (mg ml-1)
4G2dc1-Fab
4G2dc1

Figure 4.2: 4G2dc1-Fab forms a stable complex with rPfAMA1 DI-III

Purified 4G2dc1-Fab was incubated with an approximate 40 fold excess of rPfAMA1 DI-III to allow binding of Fab and antigen species. The mixture was then separated by HPLC gel filtration (yellow) to determine the proportion of 4G2dc1-Fab to rPfAMA1 DI-III in the complex. Identical amounts of 4G2dc1 (blue) and rPfAMA1dc1 (pink) were run separately to determine the elution points and absorbance peaks of the individual species. The slight reduction in height of the DI-III peak in the combined sample indicates some complex formation. This is confirmed by the presence of a new peak, eluting earlier from the column (and therefore of greater mass) than either of the individual species. The 4G2dc2-Fab peak is no longer visible however, slight broadening of one edge of the DI-III peak indicates that the monomeric species eluted close together due to their similar masses.

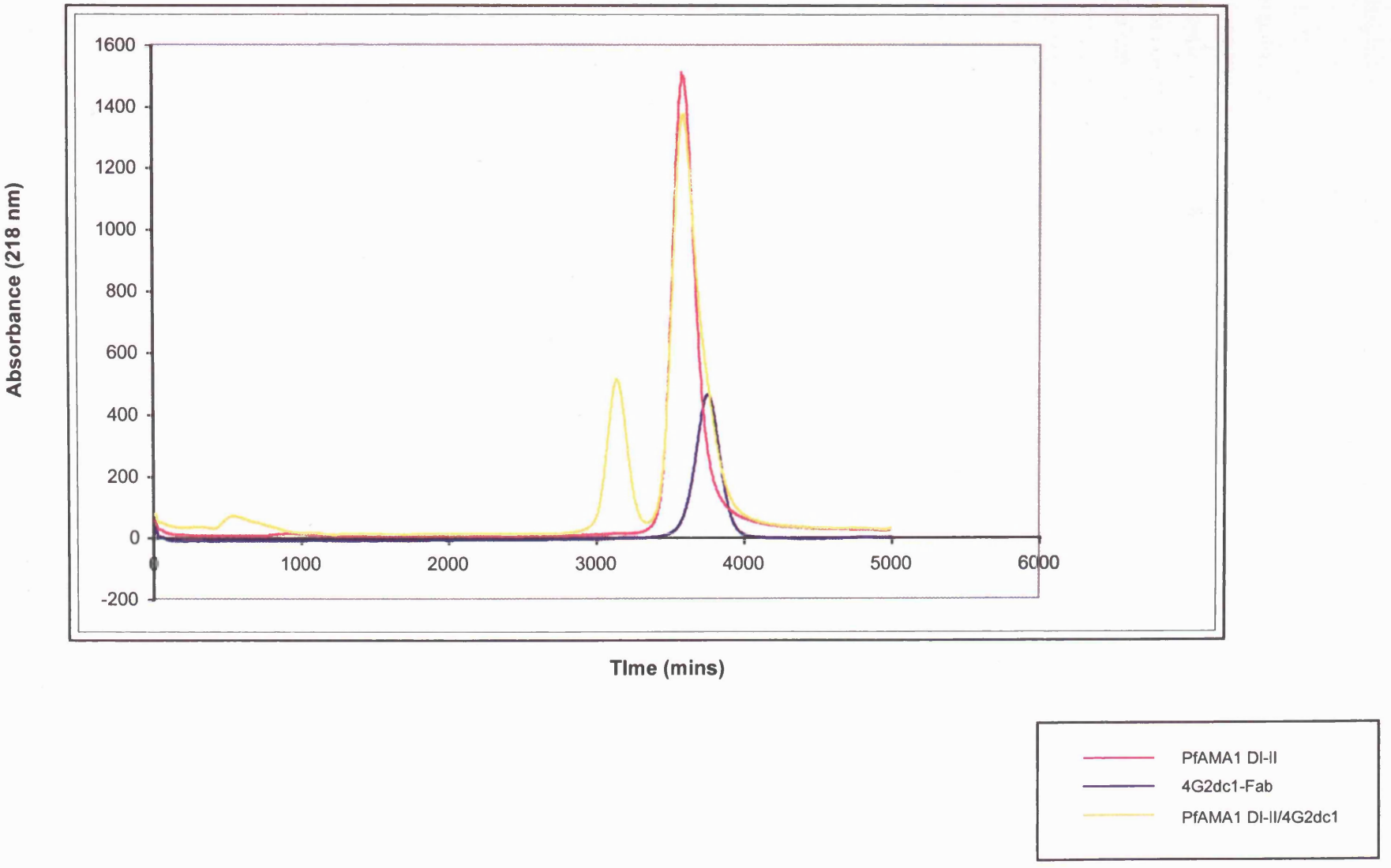
Absorbance (218 nm)
1600
1400
1200
1000
800
600
400
200
0
-200
0
1000
2000
3000
4000
5000
6000
TIme (mins)
PfAMA1 DI-II
4G2dc1-Fab
PfAMA1 DI-II/4G2dc1

Figure 4.3: *P. falciparum* merozoite invasion-inhibition by 4G2dc1 is not significantly reduced by pre-complexing with rPfAMA1

Purified rPfAMA1 DI-III (at a constant concentration) was incubated with varying concentrations of 4G2dc1-Fab prior to performing invasion-inhibition assay (red). At the highest Fab concentration there was a two fold excess of rPfAMA1 to 4G2dc1-Fab compared to a forty fold excess at the lowest 4G2dc1-Fab concentration, the latter ratio corresponding to that used in the Fab-antigen binding assay (section 4.2.1.1). As a control for invasion-inhibition, the assay was performed in parallel with Fab alone (blue).

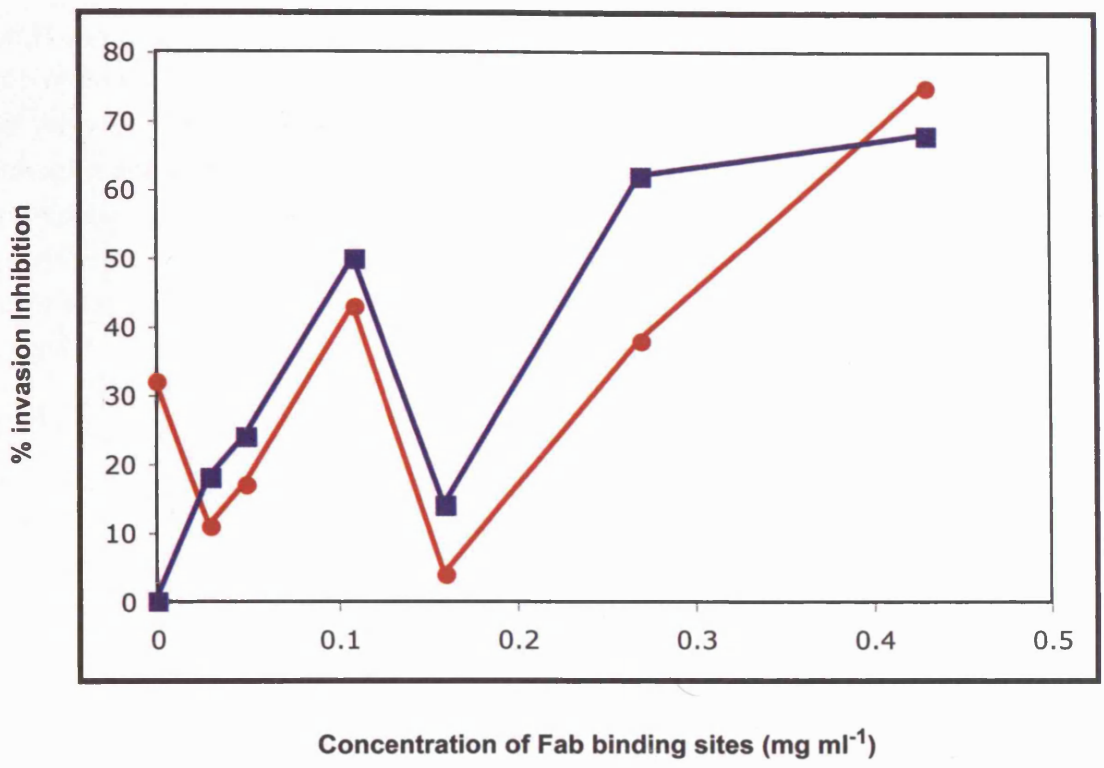
80
70
60
50
40
30
20
10
0
0
0.1
0.2
0.3
0.4
0.5
% invasion Inhibition
Concentration of Fab binding sites (mg ml-1)
4G2dc1-Fab + DI-III
4G2dc1-Fab

Figure 4.4: Expression of PfAMA1 subdomains in *P. pastoris*: confirmation that the epitope recognised by 4G2dc1 lies in DI-II

P. pastoris clones transfected with constructs for the expression of PfAMA1 subdomains DI, DI-II and DI-III were cultured as described. Culture supernatants were electrophoresed on 10% SDS-PAGE under non-reducing conditions, transferred to nitrocellulose and Western blot membranes probed with mAb 4G2dc1. Recombinant PfAMA1 DI was not detected by mAb 4G2dc1 (lanes **5 - 8**) or with the polyclonal sera R1 or AdsN1 (data not shown). Detection of recombinant PfAMA1 DI-II (lanes **2-4**) and DI-III (lane **9**) indicates the presence of the epitope within these two molecular forms of the ectodomain. Their positions are highlighted (black arrows) and their calculated masses indicated in kDa. It can therefore be concluded that the 4G2dc1 epitope lies within DI-II.


kDa
1
2
3
4
5
6
7
8
9
68 -
43 -
29 -
60 kDa
45 kDa

Figure 4.5: The subdomains of PfAMA1 are interconnected and in isolation from each other are unable to fold completely

Constructs were designed for expression of different regions of the sg'PfAMA1 ectodomain in COS-7 cells. A construct was designed for expression of DI on its own in soluble form (DI). Other expression constructs were designed in which either DII or DI was deleted (ΔDII and ΔDI, respectively). **(A)** Schematic representations of these constructs are compared with that of the construct for expression of full length sg'PfAMA1 (sg'). **(B)** Culture supernatant from DI transfected cells was run on 10% SDS-PAGE under non-reducing (n) and reducing (r) conditions, transferred to nitrocellulose and probed in Western blot with the polyclonal serum R1, to assess disulphide bond formation. A difference in migration of the two samples on SDS-PAGE was detected (black arrows) confirming some disulphide bond formation. This recombinant form of sg'PfAMA1 was only faintly detected with polyclonal serum AdsN1 and not at all with mAb 4G2dc1, suggesting an absence of native fold (data not shown).

COS-7 cells transfected with the constructs for expression of ΔDII (**C**) and ΔDI (**D**) were solubilised directly into SDS sample buffer (non-reducing) and electrophoresed on 10% SDS-PAGE. In Western blot analysis, the samples were probed with polyclonal sera; **(i)** R1 or **(ii)** N1, or **(iii)** mAb 4G2dc1. Expression of these modified recombinant forms was compared with that of sg'PfAMA1 as a positive control. In addition, COS-7 cells transfected with the construct for expression of DII were additionally compared in Western blot with untransfected COS-7 cells as a negative control. Expression of ΔDII, ΔDI (red and blue arrow heads) and sg'PfAMA1 (short black arrows) is indicated. The strong bands observed after Western blot membranes were probed with polyclonal serum R1 indicate that high levels of expression of both modified forms had occurred. However, reduced recognition with polyclonal serum AdsN1 indicated a loss of native fold. Neither form was recognised by mAb 4G2dc1.

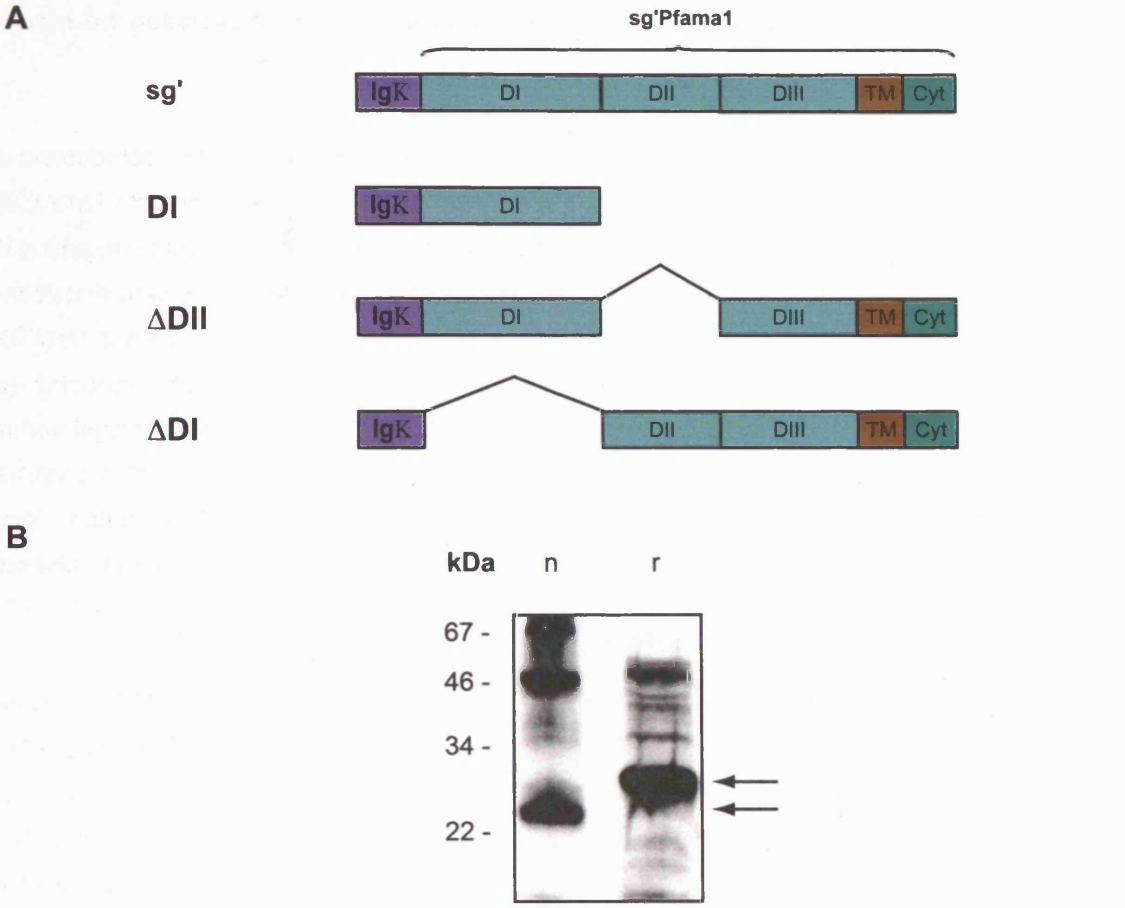
A
sg'Pfama1
sg'
IgK
DI
DII
DIII
TM
Cyt
DI
ΔDII
ΔDI
B
kDa
n
r
67 -
46 -
34 -
22 -
C
(i)
(ii)
(iii)
ΔDII
sg'
kDa
94 -
67 -
46 -
34 -
D
(i)
(ii)
(iii)
ΔDI
neg
sg'
kDa
94 -
67 -
46 -
34 -

Figure 4.6: PfAMA1 only adopts its native conformation when the N-terminus of PfAMA1 DI is present

Two constructs (T1 and T2) were designed for the expression of N-terminally truncated forms of PfAMA1. The constructs differed only in terms of the number of amino acid residues encoded prior to the first cysteine in DI (three in the case of T1 and eleven in T2). Both were expressed in COS-7 cells in membrane bound form and cell lysates analysed by Western blot under non-reducing conditions. Blots were probed with polyclonal sera R1 (**A** and **B**) and AdsN1 (**C** and **D**). T1 and T2 were both recognised strongly by R1 indicating that they were expressed at a high level (red and blue arrow heads). However, neither form was detected by AdsN1 indicating that the N-terminal truncations deleteriously affect the folding of the protein. Western blot analysis of COS-7 cells expressing sg'PfAMA1 gave a strong band with both Abs (black arrows). T1 was analysed by Western blot under reducing and non-reducing conditions to investigate disulphide bond formation in this truncated form **(E)**. A single reduced sample was run on SDS-PAGE, with non-reduced samples on either side. The presence of disulphide bonds in T1 would result in differential migration of the protein from the centre of the blot outwards due to diffusion of the reducing agent in the gel. Evidence of some disulphide bond formation was detected in Western blot analysis.

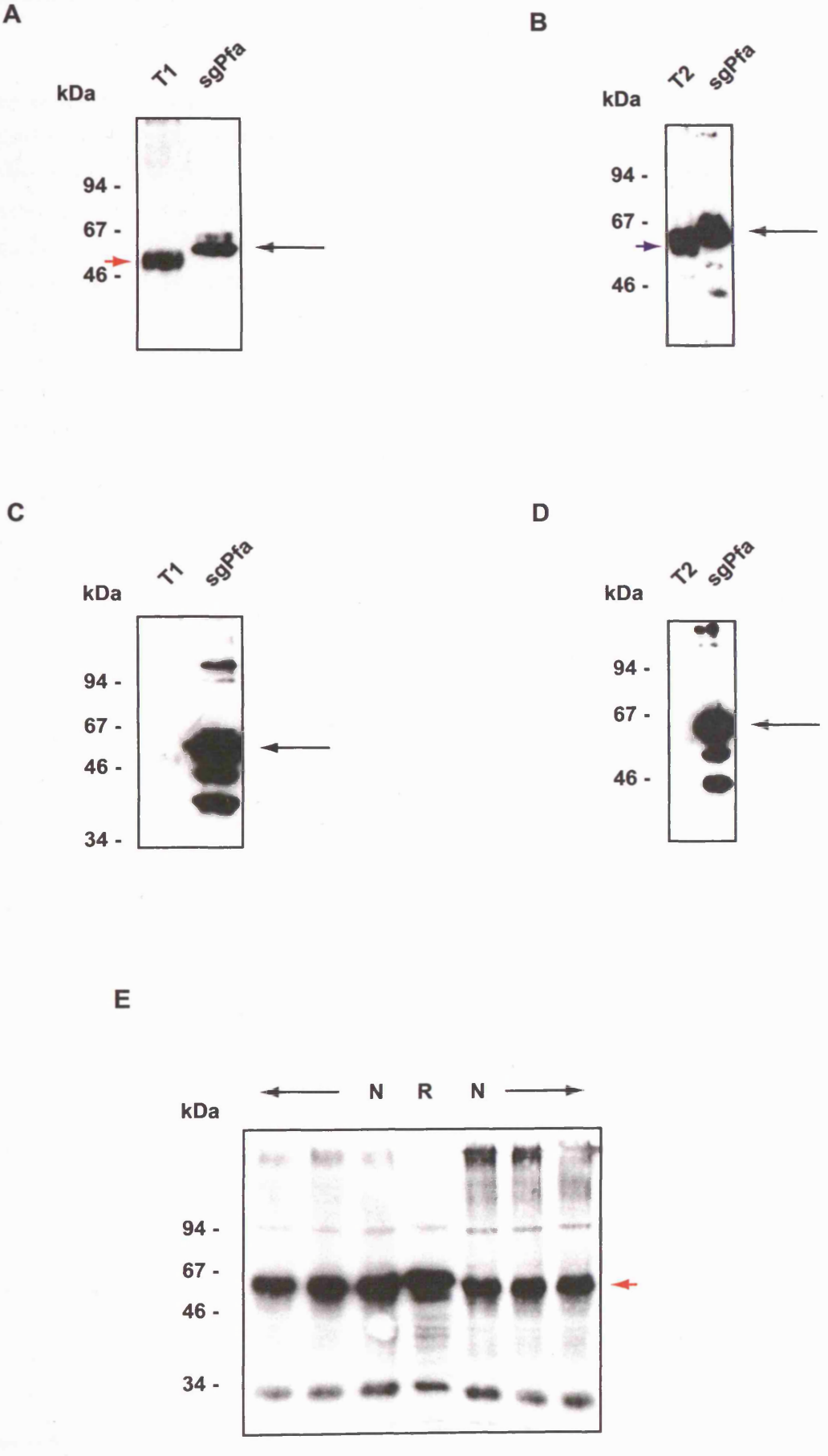
A
kDa
T1
sgPfa
94 -
67 -
46 -
B
kDa
T2
sgPfa
94 -
67 -
46 -
C
kDa
T1
sgPfa
94 -
67 -
46 -
34 -
D
kDa
T2
sgPfa
94 -
67 -
46 -
E
N
R
N
kDa
94 -
67 -
46 -
34 -

Figure 4.7: Can protease digestion of rPfAMA1 DI-III be used as a tool to map the epitope recognised by mAb 4G2dc1?

(1) Digestion of the rPfAMA1 ectodomain with different proteolytic enzymes generates different sized protein fragments. **(2)** The digested samples can then be separated by SDS-PAGE on 10% gels, transferred to nitrocellulose and Western blot membranes probed with mAb 4G2dc1. **(3)** Small fragments that retain recognition by the mAb can then be analysed by Mass spectroscopy. Comparing results from different proteolytic digestions may identify the fragment of the PfAMA1 ectodomain containing the epitope responsible for mAb 4G2dc1 binding.

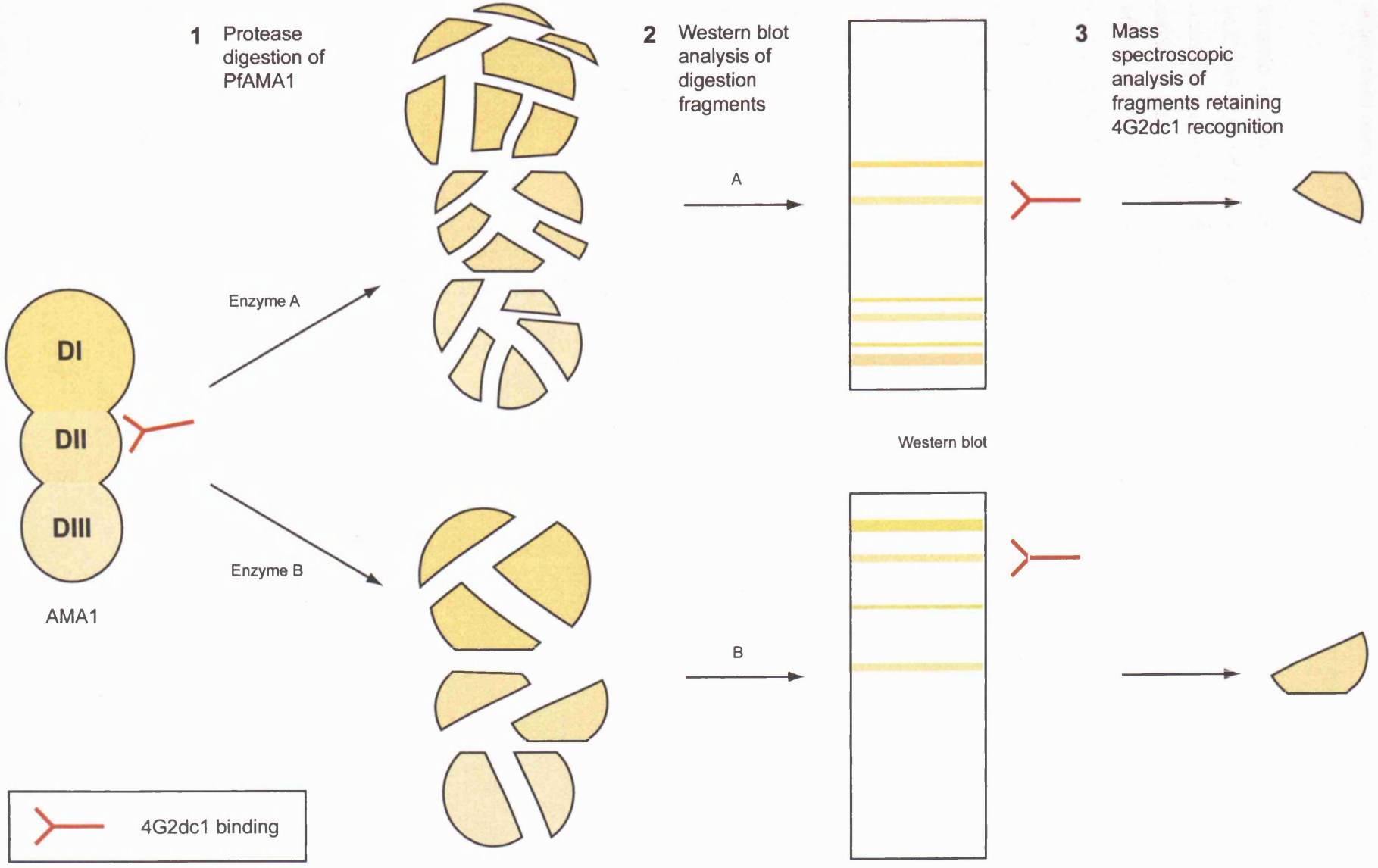
1 Protease digestion of PfAMA1
2 Western blot analysis of digestion fragments
3 Mass spectroscopic analysis of fragments retaining 4G2dc1 recognition
DI
DII
DIII
AMA1
Enzyme A
Enzyme B
A
B
Western blot
4G2dc1 binding

Figure 4.8: Trypsin and chymotrypsin digestion of rPfAMA1 DI-III generates stable DI-II sized (35 - 40 kDa) protein fragments

Purified rPfAMA1 DI-III was digested with trypsin or chymotrypsin at enzyme:substrate ratios of 1:10. Samples were removed at 0, 40, 60, 120 and 240 minutes after enzyme addition and added directly to Pefabloc (to a final concentration of 2 mM) to neutralise the enzyme. Digestion products were separated by SDS-PAGE on 12.5% gels and stained with Coomassie blue. The smallest major product following trypsin **(A)** or chymotrypsin **(B)** digestion are highlighted (blue and red arrows respectively) and their calculated masses indicated in kDa.

A

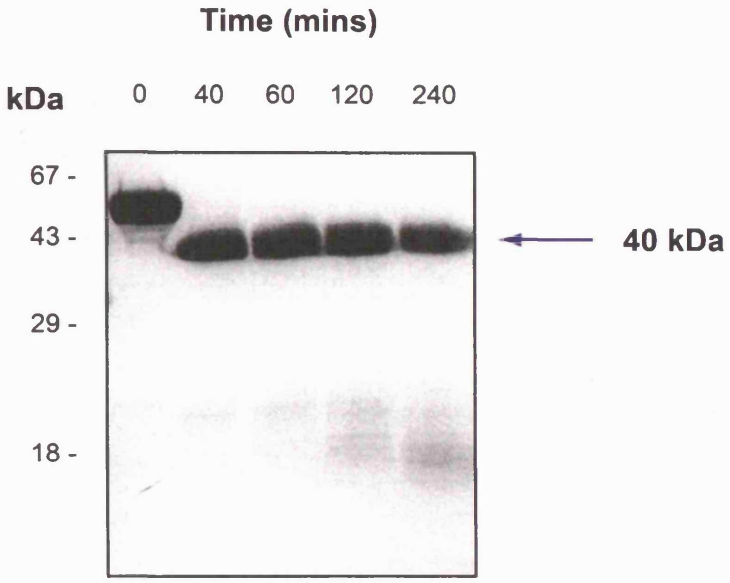
Time (mins)
kDa
0
40
60
120
240
67 -
43 -
29 -
18 -
40 kDa

B

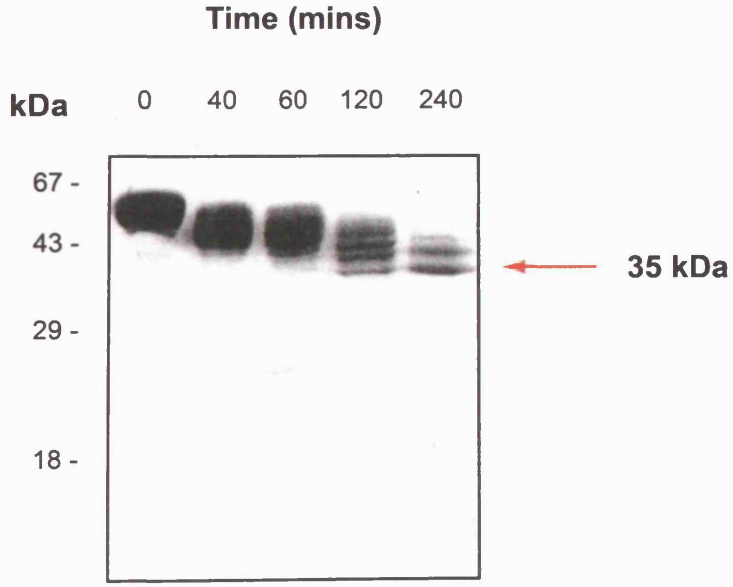
Time (mins)
kDa
0
40
60
120
240
67 -
43 -
29 -
18 -
35 kDa

Figure 4.9: Subtilisin digestion of rPfAMA1 DI-III generates a small fragment of (~8 kDa) fragment

Purified rPfAMA1 was digested with subtilisin at an enzyme substrate ratio of 1:10. Samples were removed at 0, 30, 70, 120, and 240 minutes and added directly to the protease inhibitor Pefabloc (at a final concentration of 2 mM). Digestion fragments were separated by SDS-PAGE on 12.5% gels and **(A)** stained with Coomassie blue or **(B)** transferred to nitrocellulose and probed with mAb 4G2dc1. Immediately after the addition of papain (at time 0), PfAMA1 DI-III was digested to produce several fragments, the smallest of which was approximately 8 kDa, all the fragments generated were rapidly degraded. The smallest fragment identified as retaining 4G2dc1 recognition by Western blot was of approximately 30 kDa. The major small digestion products identified by these methods are highlighted (red and blue arrows) and their calculated masses indicated in kDa.

A

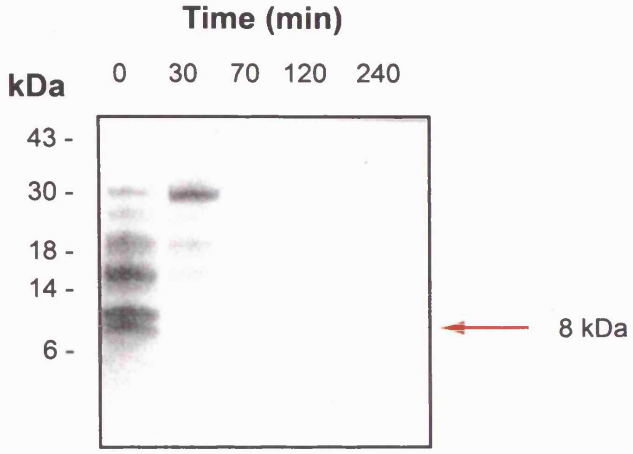
Time (min)
kDa
0
30
70
120
240
43 -
30 -
18 -
14 -
6 -
8 kDa

B

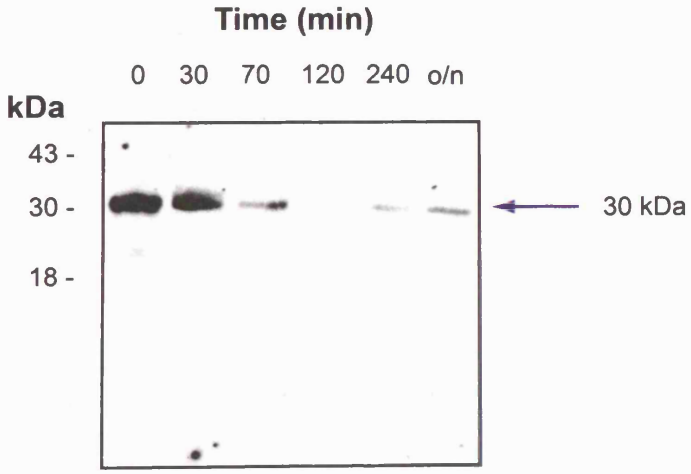
Time (min)
0
30
70
120
240
o/n
kDa
43 -
30 -
18 -
30 kDa

Figure 4.10: Pepsin and papain digestion of rPfAMA1 DI-III generates small unstable fragments that are not recognised in Western blot analysis by mAb 4G2dc1

Purified PfAMA1 was digested with pepsin and papain at an enzyme:substrate ratio of 1:10. Samples were removed at 10, 40, 60, 120 and 240 minutes after the addition of the enzyme and added directly to Tris-HCl, pH 8.0 (final concentration 0.5 M) and iodoacetamide (final concentration 10 mM) respectively, to inhibit enzyme activity. Digestion products were separated by SDS-PAGE and either stained with Coomassie blue or probed with mAb 4G2dc1 in Western blot. Digestion with pepsin **(A)** generated fragments of approximately 8 and 10 kDa, while papain **(B)** generated fragments of approximately 8 and 12 kDa detectable by Coomassie blue staining. However, probing papain digestion products with mAb 4G2dc1 in Western blot only resulted in the detection of fragments of approximately 35 and 40 kDa **(C)**. Major fragments are highlighted (black arrows) and their calculated masses indicated in kDa.

A

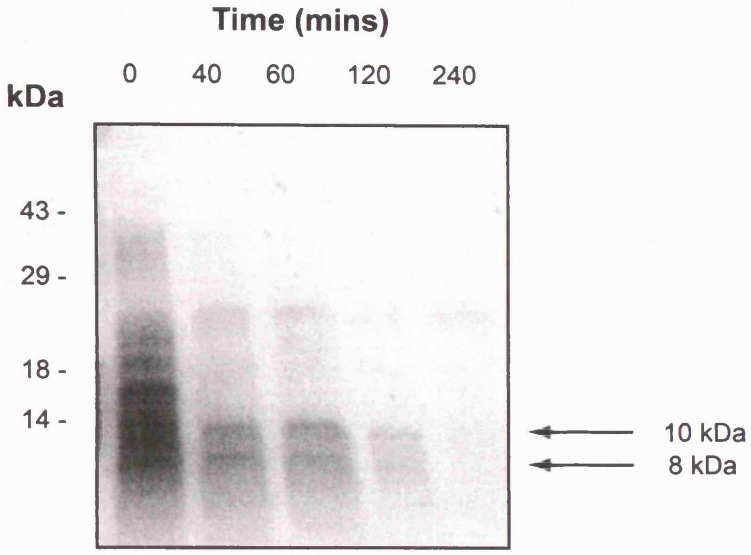
Time (mins)
0
40
60
120
240
kDa
43 -
29 -
18 -
14 -
10 kDa
8 kDa

B

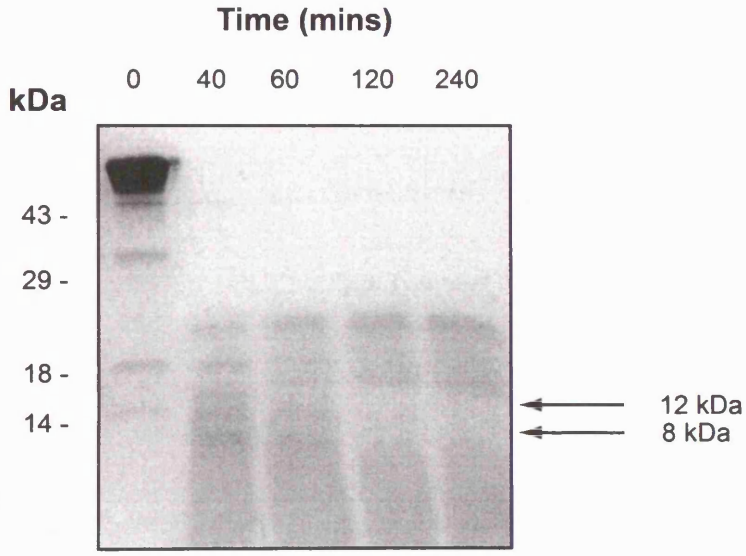
Time (mins)
0
40
60
120
240
kDa
43 -
29 -
18 -
14 -
12 kDa
8 kDa

C

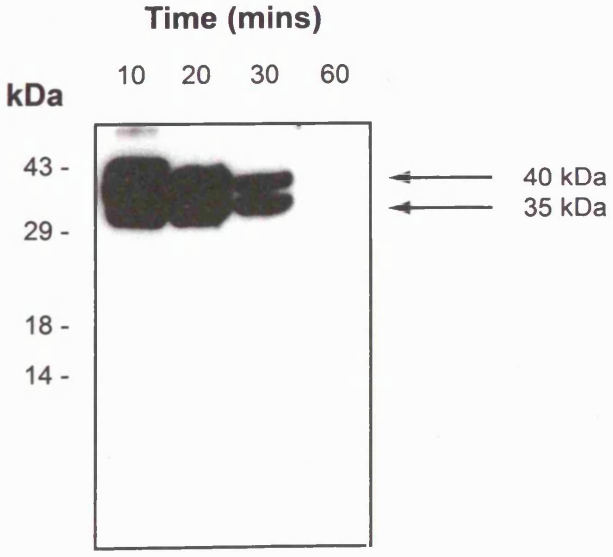
Time (mins)
10
20
30
60
kDa
43 -
29 -
18 -
14 -
40 kDa
35 kDa

Figure 4.11: Recombinant PfAMA1 DI-II is resistant to digestion with trypsin and chymotrypsin

Purified PfAMA1 DI-II was digested with trypsin or chymotrypsin at enzyme:substrate ratios of 1:10. Samples were taken at 30, 60, 120 and 240 minute time points after enzyme addition and added directly to pefabloc (2 mM final concentration) to inhibit enzyme activity. Digestion products were separated by SDS-PAGE on 10% gels and stained with Coomassie blue. The molecule was initially resistant to digestion by both enzymes. In the case of trypsin **(A)**, continued digestion resulted in no stable digestion products. With chymotrypsin **(B)** there was an initial intermediate product (red arrow head), migrating fractionally lower on SDS-PAGE than the intact molecule (black arrow), followed by complete degradation. In an attempt to increase accessibility of the molecule to digestion by these proteases, the digestions were repeated in the presence of 0.1% SDS. All other reaction conditions remained constant. Samples were taken at 0, 20, 40, 90, 120 and 240 minute time points after enzyme addition. Under these modified conditions neither trypsin **(C)** nor chymotrypsin **(D)** produced any stable digestion intermediates.

A

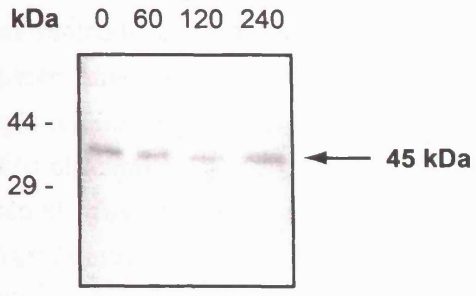
kDa 0 60 120 240
44 -
29 -
45 kDa

B

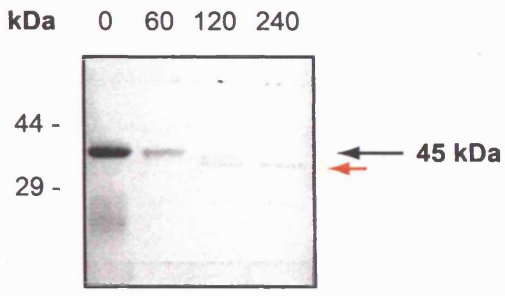
kDa 0 60 120 240
44 -
29 -
45 kDa

C

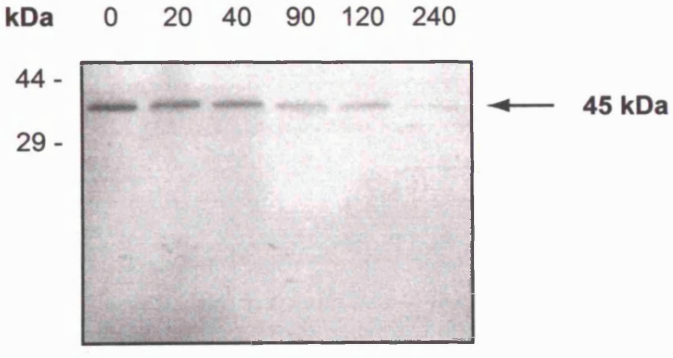
kDa 0 20 40 90 120 240
44 -
29 -
45 kDa

D

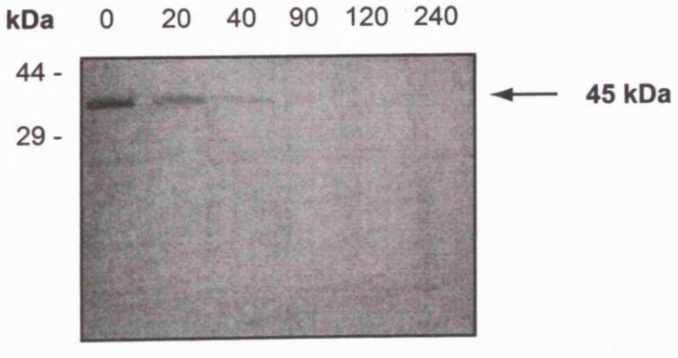
kDa 0 20 40 90 120 240
44 -
29 -
45 kDa

Figure 4.12: PfAMA1 DI-II complexed with 4G2dc1-F(ab)$_2$ is partially protected against degradation by pepsin

Recombinant PfAMA1 DI-II was incubated with 4G2dc1-F(ab)$_2$ to allow immune complex formation which was then purified by gel filtration. The complex was digested with pepsin (enzyme:substrate ratio 1:10), to determine whether this Ab fragment would specifically prevent degradation of the epitope to which it was bound, thus allowing identification of the PfAMA1 ectodomain fragment containing this epitope. Digestion products were separated by SDS-PAGE on 10% gels and either stained with Coomassie blue or transferred to nitrocellulose for analysis by Western blot. Coomassie stained gels of pepsin digestion of the complex **(A)** were compared with that of the antigen **(B)** under identical conditions. In the presence of F(ab)$_2$, PfAMA1 DI-II remained resistant to pepsin digestion, whereas in its absence it was gradually degraded although no stable intermediates were detected. Western blot membranes of pepsin digestion of the complex were probed with either **(C)** 4G2dc1 or **(D)** the secondary Ab only. Recombinant PfAMA1 DI-II was detected by 4G2dc1, but not by the secondary Ab. Western blot analysis confirms the potent protective activity of mAb 4G2dc1-F(ab)2 against PfAMA1 DI-II degradation. The band representing PfAMA1 DI-II is highlighted (black arrows) and its calculated molecular weight indicated in kDa.

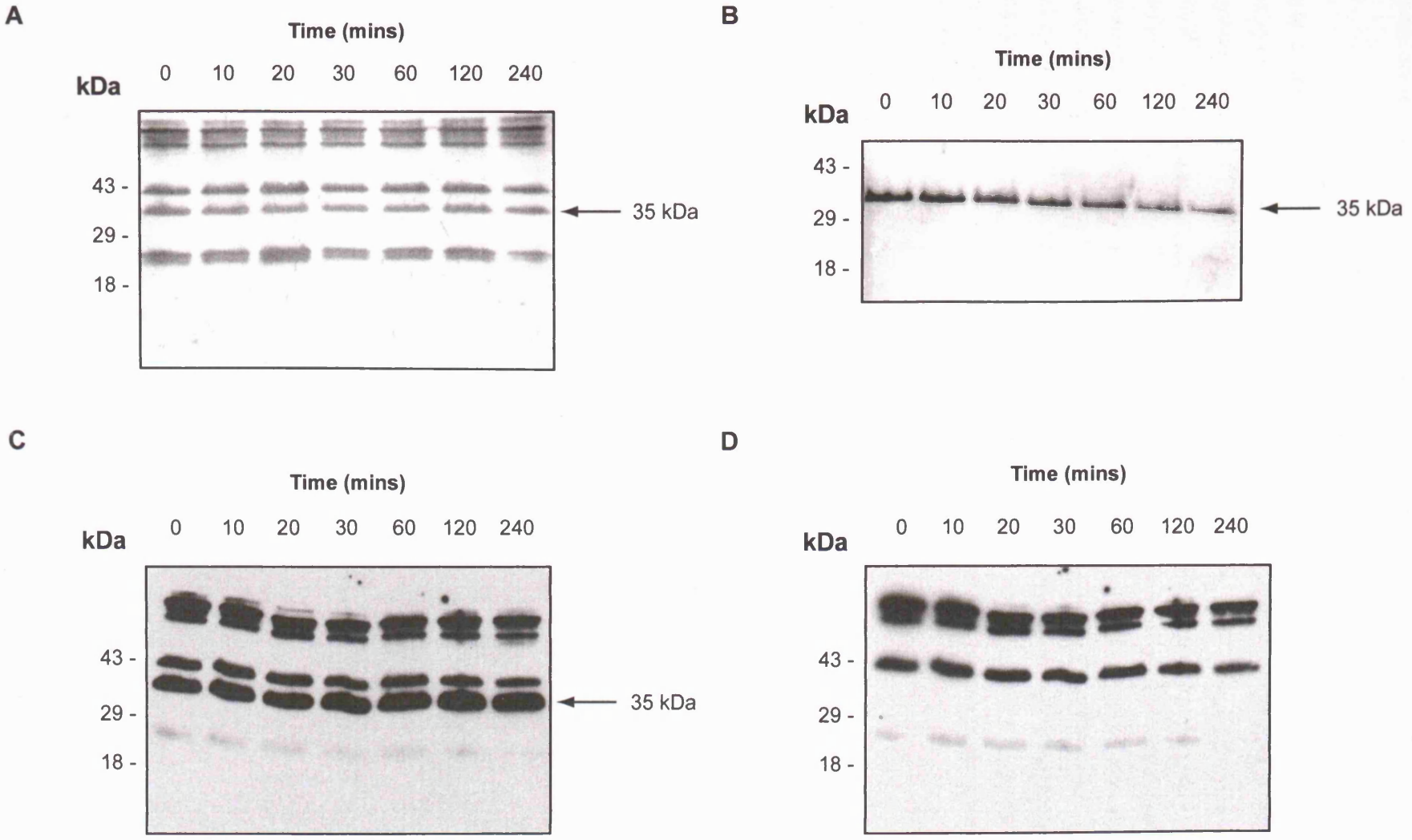
A
Time (mins)
kDa
0 10 20 30 60 120 240
43 -
29 -
18 -
35 kDa
B
Time (mins)
kDa
0 10 20 30 60 120 240
43 -
29 -
18 -
35 kDa
C
Time (mins)
kDa
0 10 20 30 60 120 240
43 -
29 -
18 -
35 kDa
D
Time (mins)
kDa
0 10 20 30 60 120 240
43 -
29 -
18 -

Figure 4.13: The disulphide bond between Cys263 and Cys275 (DB3) is not critical for the overall conformation of PfAMA1

Disulphide bond mutants of sg'PfAMA1 were generated by sequentially replacing a single cysteine residue from each of the five disulphide bonds in DI-II with alanine. The resulting disulphide bond mutants were denoted ΔsDB1 - ΔsDB5. COS-7 cells transfected with constructs for the expression of these mutants were solubilised directly in SDS sample buffer under non-reducing conditions, the extract run on 10% SDS-PAGE and transferred to nitrocellulose. Western blot membranes were probed with polyclonal serum R1 and mAb 4G2dc1. All DB mutant forms (labelled **1 - 5**) produced strong bands in Western blot analysis when probed with R1 **(A)** indicating high level expression. By comparison, only DB3 (linking Cys263 and Cys275) was recognised by 4G2dc1 **(B)**. The band representing the $PfAMA1_{66}$ form of the DB mutants is highlighted (black arrows) and the calculated mass indicated in kDa.

A

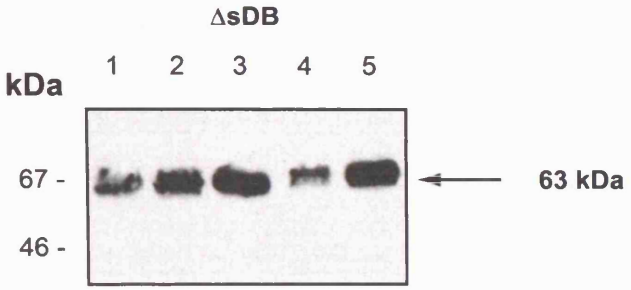

B

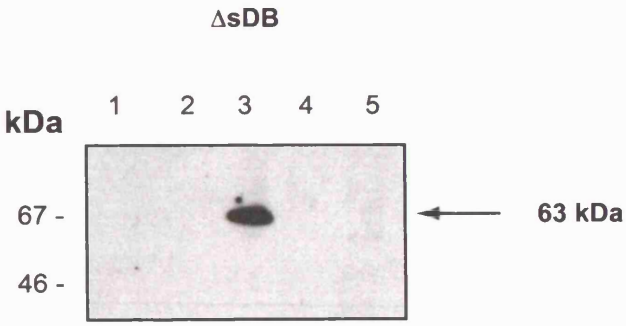

Figure 4.14: IFA with antisera to PfAMA1 confirms that single cysteine mutants of sgPfAMA1 are correctly localised on the surface of COS-7 cells

COS-7 cells were analysed unfixed and unpermeabilised to detect surface localised protein only. Antibody (polyclonal serum N1) binding was examined in cells transfected with constructs for expression of single cysteine mutants (ΔsDB1 - ΔsDB5, labelled **1 - 5**) and compared with those expressing wild type sg'PfAMA1 **(6)** as a positive control and untransfected cells **(7)** as a negative control. Polyclonal serum N1 was used at 1 in 100 dilution. The image is a composite of DAPI (blue), Evans blue (red) and FITC conjugate (green) images from fluorescence microscopy as described in the materials and methods (section 2.4.3).

1

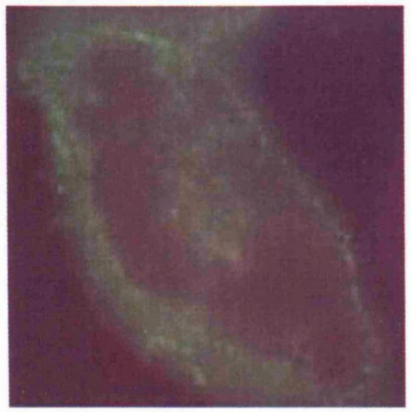

2

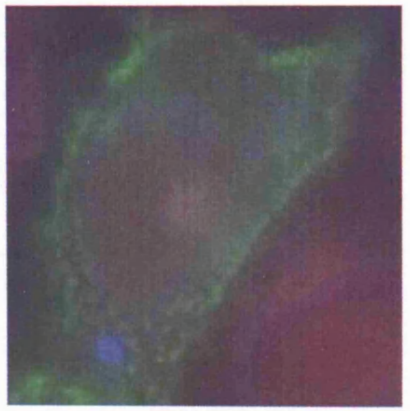

3

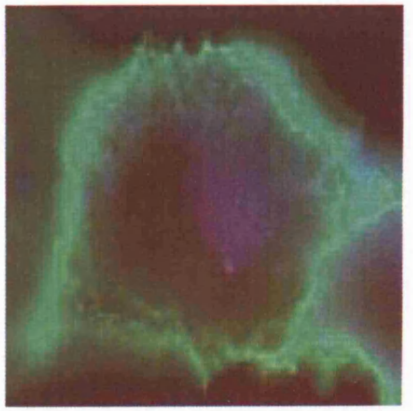

6

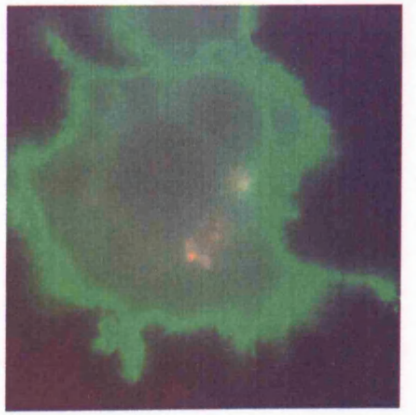

4

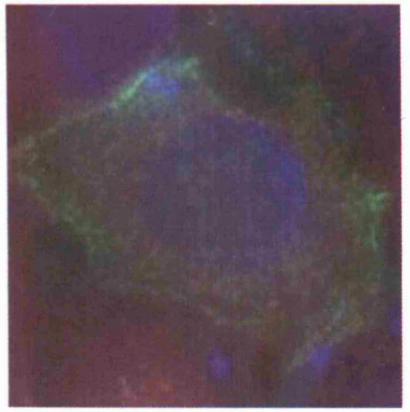

5

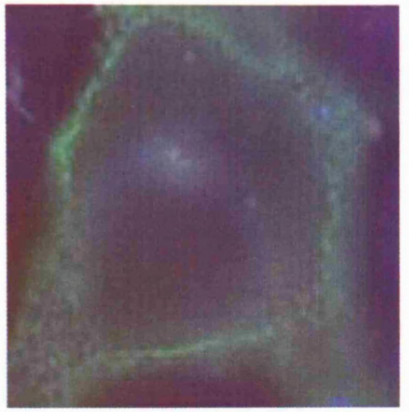

7

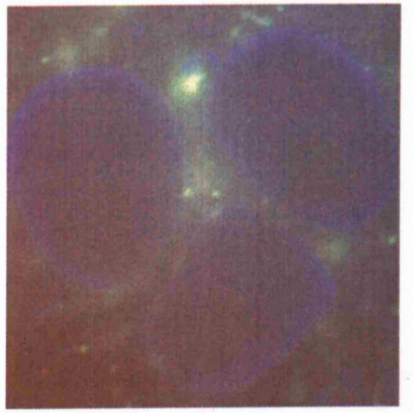

Figure 4.15: IFA reveals that two single cysteine sg'PfAMA1 mutants (ΔsDB1, between Cys149 and Cys302 and ΔsDB4, between Cys320 and Cys418) are no longer recognised by 4G2dc1

Monoclonal Ab 4G2dc1 binding was examined in COS-7 cells transfected with constructs for expression of single cysteine mutants (ΔsDB1 - ΔsDB5, labelled **1 - 5**) and compared with those expressing wild type sg'PfAMA1 **(6)** as a positive control and untransfected cells **(7)** as a negative control. Cells were incubated with mAb 4G2dc1 without prior fixation to determine surface localisation. The image is a composite of DAPI (blue), Evans blue (red) and FITC conjugate (green) images from fluorescence microscopy as described in materials and methods (section 2.4.3). Only ΔsDB3 retains 4G2dc1 recognition at an equivalent level to the wild type sg'PfAMA1.

1

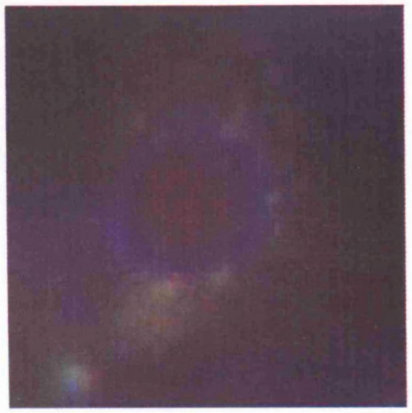

2

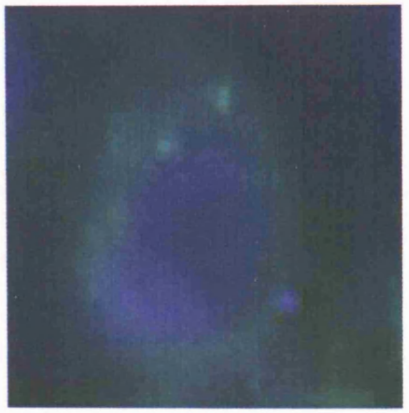

3

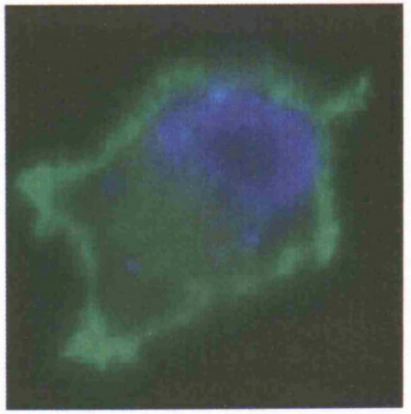

6

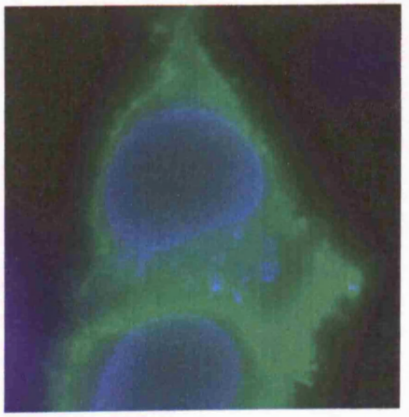

4

5

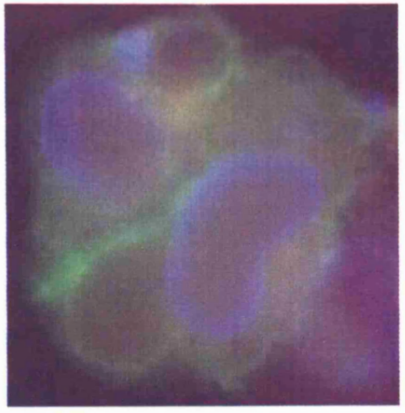

7

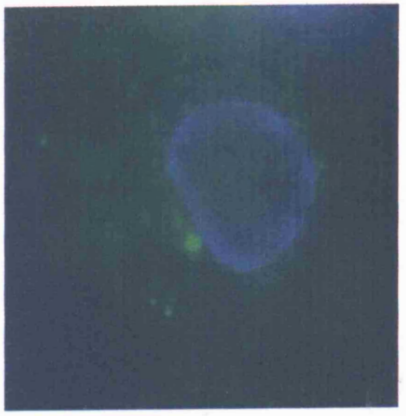

Figure 4.16: Western blot analysis confirms that disruption of DB1 (Cys149 and Cys302) and DB4 (Cys320 and Cys418) abrogates recognition by mAb 4G2dc1

Disulphide bond mutants of sg'PfAMA1 were generated by sequentially replacing both cysteine residues from each of the five disulphide bonds in DI-II with alanine. The resulting disulphide bond mutants were denoted ΔdDB1 - ΔdDB5. COS-7 cells transfected with constructs for the expression of these mutants were solubilised directly in SDS sample buffer (non-reducing) and the extract run on 10% SDS-PAGE and transferred to nitrocellulose. Western blot membranes were probed with polyclonal serum R1 and mAb 4G2dc1. All DB mutant forms of PfAMA1 produced strong bands in Western blot analysis when probed with R1 **(A)** indicating high level expression. 4G2dc1 recognition was completely disrupted in mutants ΔdDB1 and ΔdDB4, while all the remaining mutants retained some level of recognition by this mAb **(B)**. The band representing the DB mutant forms of $PfAMA1_{66}$ is highlighted (black arrows) and the calculated mass indicated in kDa.

A

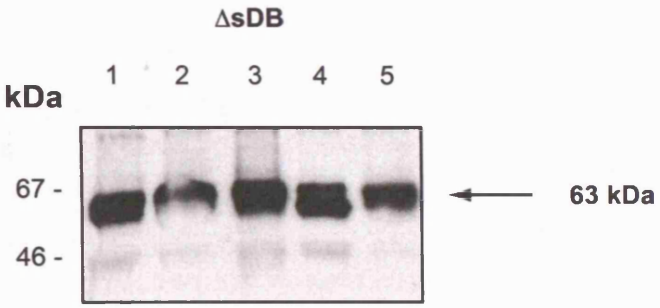

B

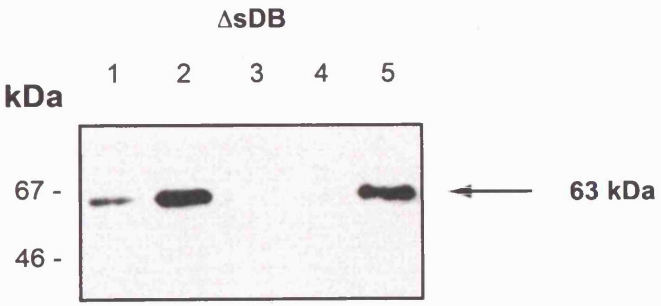

Figure 4.17: IFA with antisera to PfAMA1 confirms that all double cysteine mutants of sg'PfAMA1 are correctly localised on the surface of COS-7 cells

COS-7 cells were analysed unfixed and unpermeabilised to detect surface localised protein only. Antibody binding using polyclonal serum N1, was examined in cells transfected with constructs for expression of the double cysteine mutants (ΔdDB1 - ΔdDB5, labelled **1 - 5**) and compared with those expressing wild type sg'PfAMA1 **(6)** as a positive control and untransfected cells **(7)** as a negative control. N1 was used at 1 in 100 dilution. The image is a composite of DAPI (blue), Evans blue (red) and FITC conjugate (green) images from fluorescence microscopy as described in materials and methods (section 2.4.3).

1

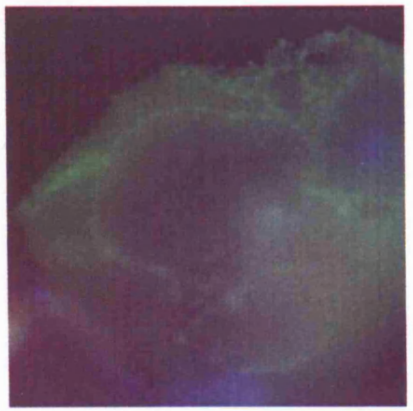

2

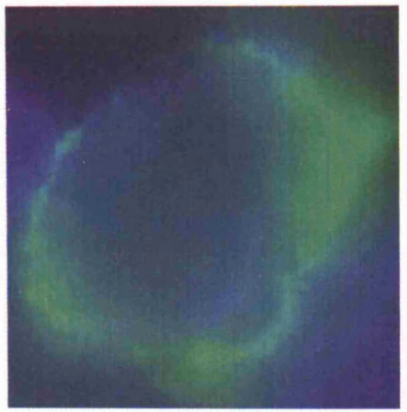

3

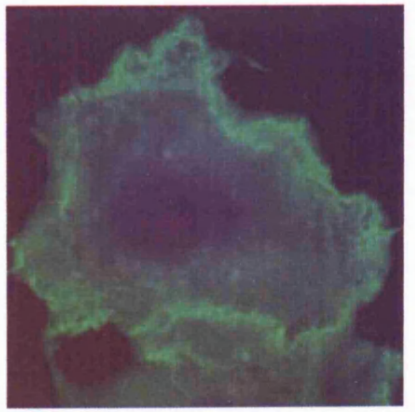

6

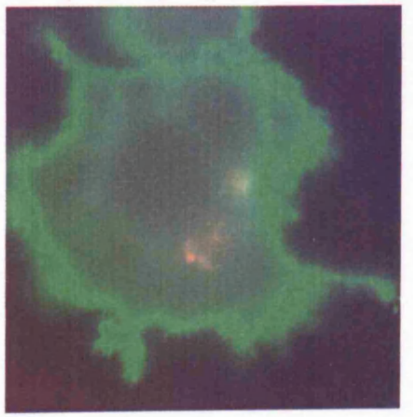

4

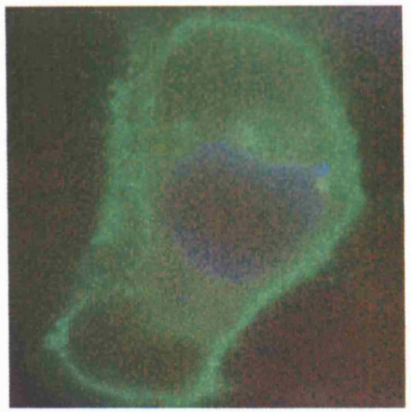

5

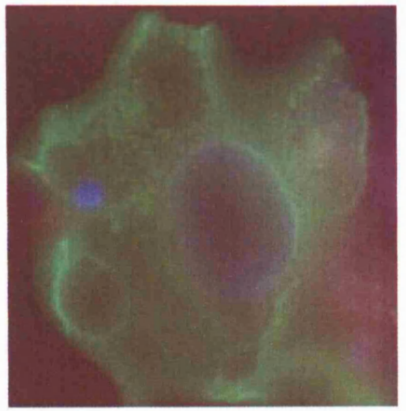

7

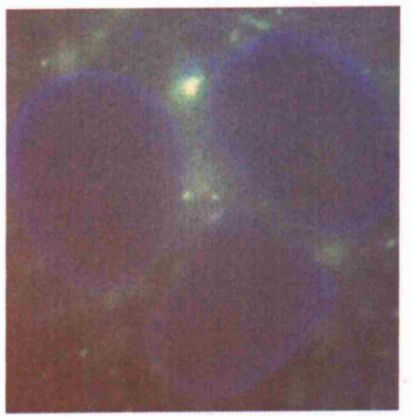

Figure 4.18: 4G2dc1 recognition of PfAMA1 is lost after disruption of DB1 and DB4

COS-7 cells were analysed unfixed and unpermeabilised to detect surface localised protein only. Monoclonal Ab 4G2dc1 binding was examined in cells transfected with constructs for expression of double cysteine mutants (ΔdDB1 - ΔdDB5, labelled **1 - 5**) were compared with those expressing wild type sg'PfAMA1 **(6)** as a positive control and untransfected cells **(7)** as a negative control. The image is a composite of DAPI (blue), Evans blue (red) and FITC conjugate (green) images from fluorescence microscopy as described in materials and methods (section 2.4.3).

1

2

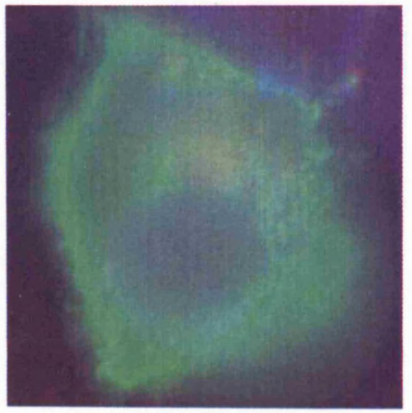

3

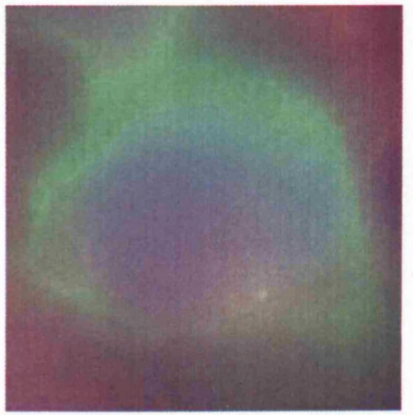

6

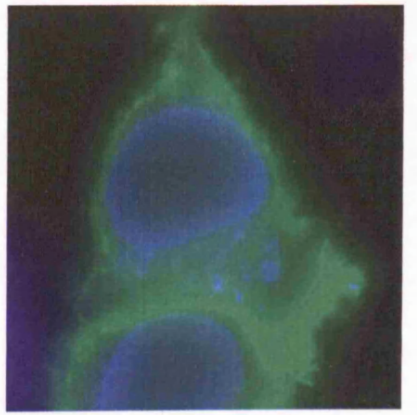

4

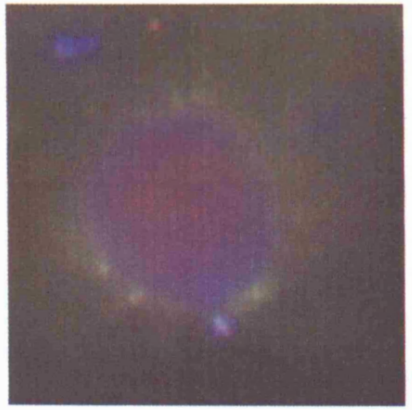

5

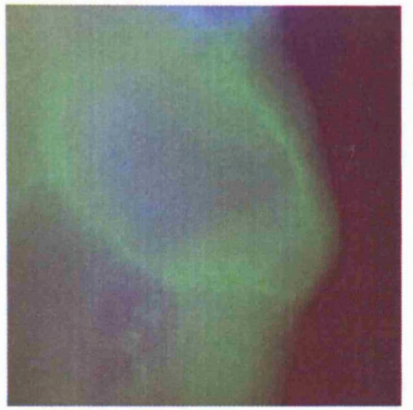

7

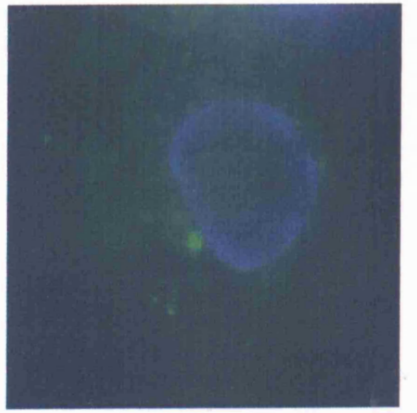

Figure 4.19: Western blot analysis confirms the specificity of the polyclonal sera Ads N1 and R1 and mAb 4G2 for non-reduced and reduced rPfAMA1 ectodomain

Purified samples of rPfAMA1 DI-III and DI-II were electrophoresed on 10% SDS-PAGE gels under **(A)** non-reducing or **(B)** reducing conditions and transferred to nitrocellulose for Western blot analysis using the polyclonal serum N1 **(i)** or R1 **(ii)**, or mAb 4G2dc1 **(iii)**. The position of DI-III and DI-II bands is indicated (red and blue arrow heads).

A

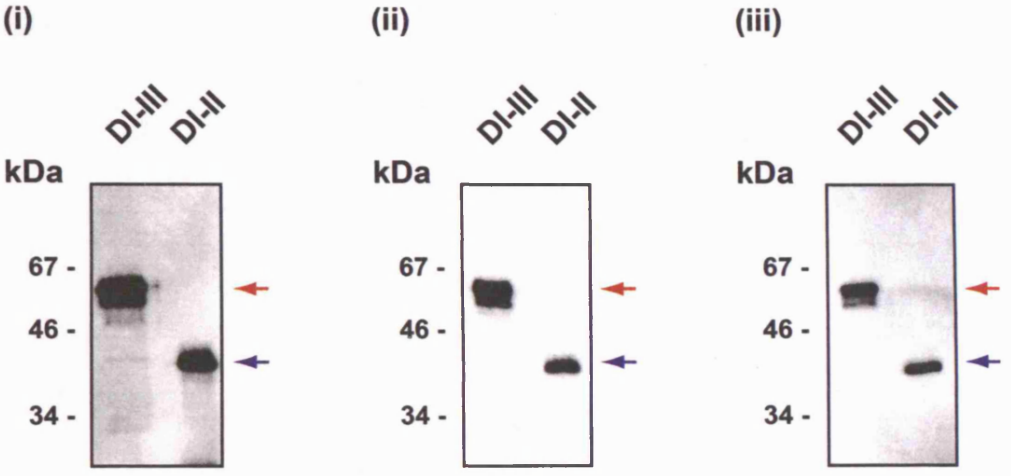

B

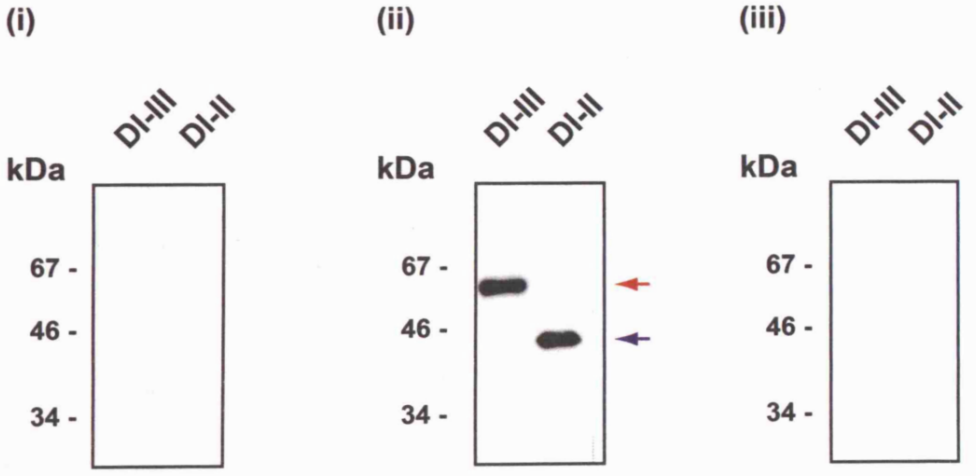

Figure 4.20: The PfAMA1 epitope recognised by mAb 4G2dc1 lies predominantly in DII

To map the 4G2dc1 epitope, amino acid residues within DI-II of PfAMA1 ectodomain with a high probability of being exposed at the surface of the molecule were mutated by SDM. Mutations were primarily to alanine, but in those cases where the residue was already alanine, the amino acid was mutated to one found at the corresponding position in the AMA1 sequence from another species of *Plasmodium*. Mutants were transfected into COS-7 cells and cell lysates analysed by Western blot to confirm expression and determine the effect on 4G2dc1 recognition. Western blot membranes were probed with polyclonal sera R1 **(A)** and N1 **(B)** and mAb 4G2dc1 **(C)**. Results for a selection of these mutants (numbered 1 to 18) are shown and the sg'PfAMA1 band indicated (black arrow). Mutations that abrogate 4G2dc1 recognition and those that affect overall protein conformation are highlighted (red and blue asterisks).

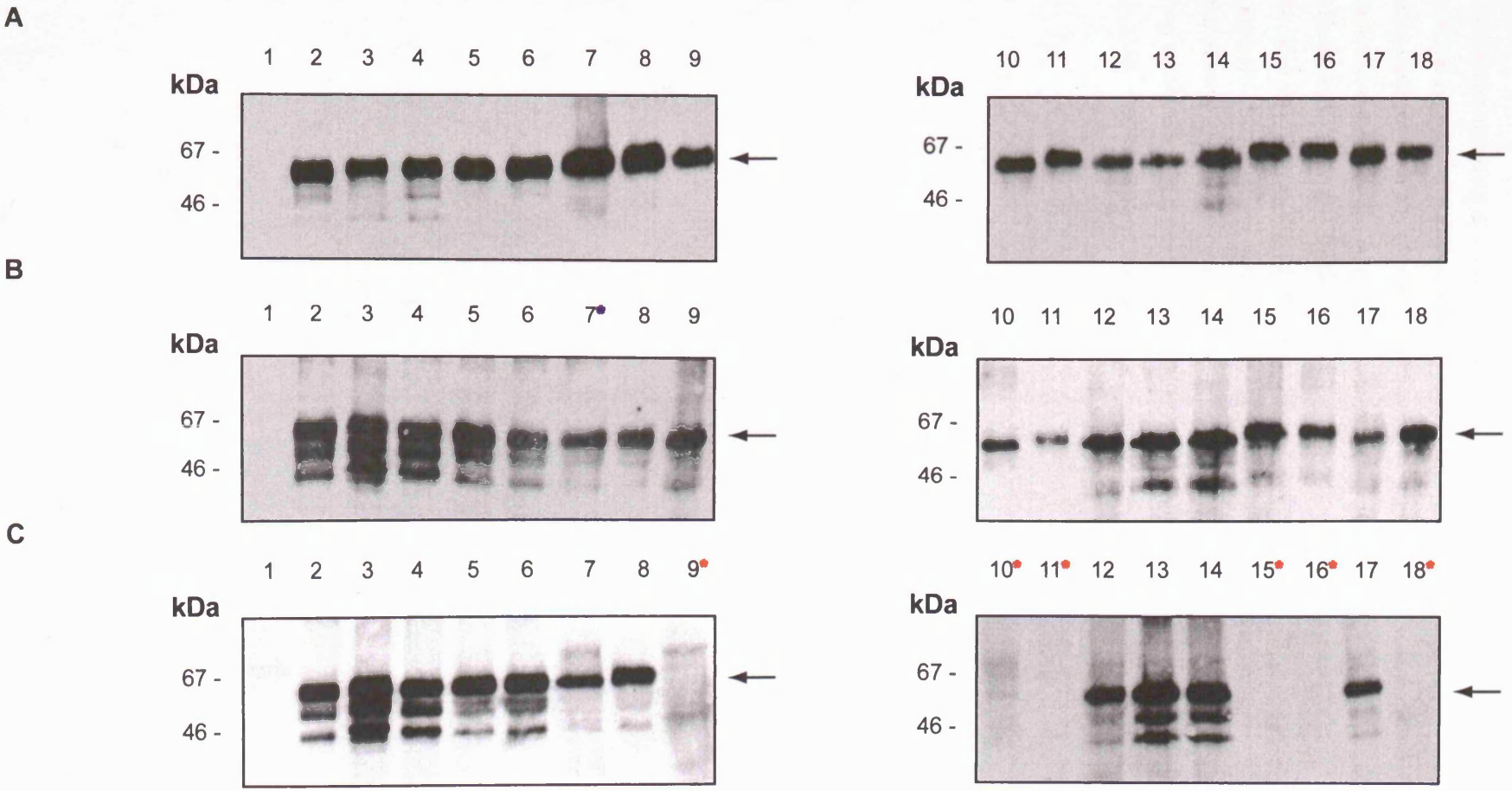

Site directed mutants

(1) neg	(4)140TQYR/AQAA	(7) 280K/A*	(10) 351K/A•	(13) 366GFK/AAA	(16) 389R/A•
(2) sg'	(5) 227DND/AAA	(8) 305JNK/AAA	(11) 352Q/A•	(14) 369NKN/AAA	(17) 403NRE/AAA
(3) 102RSN/AAA	(6) 266DQS/AAA	(9) 348D/A•	(12) 359DYE/AAA	(15) 388D/A•	(18) 351K/T + 389R/N•

Figure 4.21: The domain II loop plays a key role in 4G2dc1 recognition

Residues in the 4G2dc1 epitope lie at the base of the flexible DII loop. Amino acid residues in this loop were specifically targeted for mutagenesis to determine the role played by this structure in 4G2dc1 recognition. In addition, secondary structure predictions indicate the presence of two helices in the loop (353Y-K368 and 373D-S377), both were deleted (individually and together) to determine whether their presence was essential for 4G2dc1 binding. Constructs for the expression of mutant forms of sg'PfAMA1 were transfected into COS-7 cells and cell lysates analysed by Western blot to confirm expression and determine the effect on 4G2dc1 recognition. Western blot membranes were probed with polyclonal sera R1 **(A)** and N1 **(B)** and mAb 4G2dc1 **(C)**. Results for a selection of these mutants are shown and the presence of sg'PfAMA1 indicated (black arrow). Mutations that specifically abrogate 4G2dc1 recognition and those that indirectly affect binding are highlighted (red and blue asterisks).

A

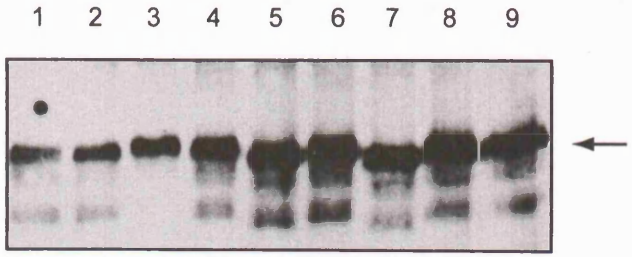

B

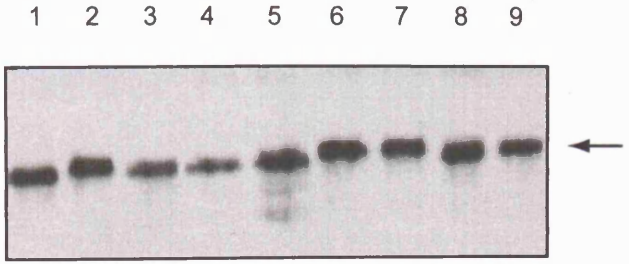

Site directed mutants

(1) sg'
(2) 354EQH/AAA
(3) 356H/P
(4) 357LT/AA
(5) del 353Y-K368
(6) del 373D-S377
(7) del 353Y-S377
(8) 364K/P
(9) 385F/A
(10) 354EQH/AQH
(11) 354EQH/EAH
(12) 354EQH/EQA

C

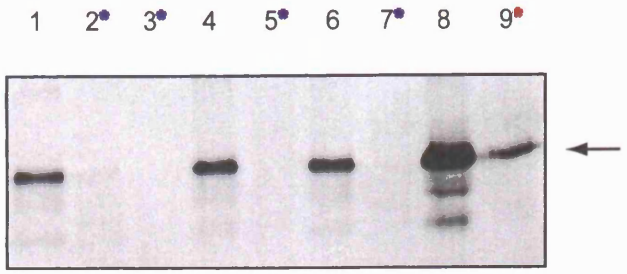

D

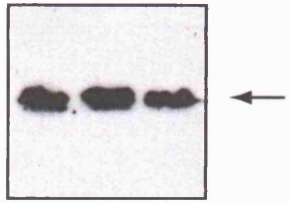

Figure 4.22: Surface structure of PfAMA1 DI-II, showing the position of 4G2dc1 epitope in the DII loop.

(A) The residues of which the 4G2dc1 epitope is comprised (black) are shown to cluster together in one region of the DII loop (shown in blue, as is the rest of DII) which itself extends across the surface of DI (orange). One residue (Phe 385, shown in black) lies in a four amino acid stretch that was not detected in the crystal structure. This stretch is depicted in this figure as a loop extending from the side of the DII loop where it is located in the primary sequence. **(B)** Several residues in the DII loop, some of which appear to lie in close proximity to the 4G2dc1 epitope, have not been mutated. These residues and additional residues from DI (all shown in pink) are potential components of this epitope.

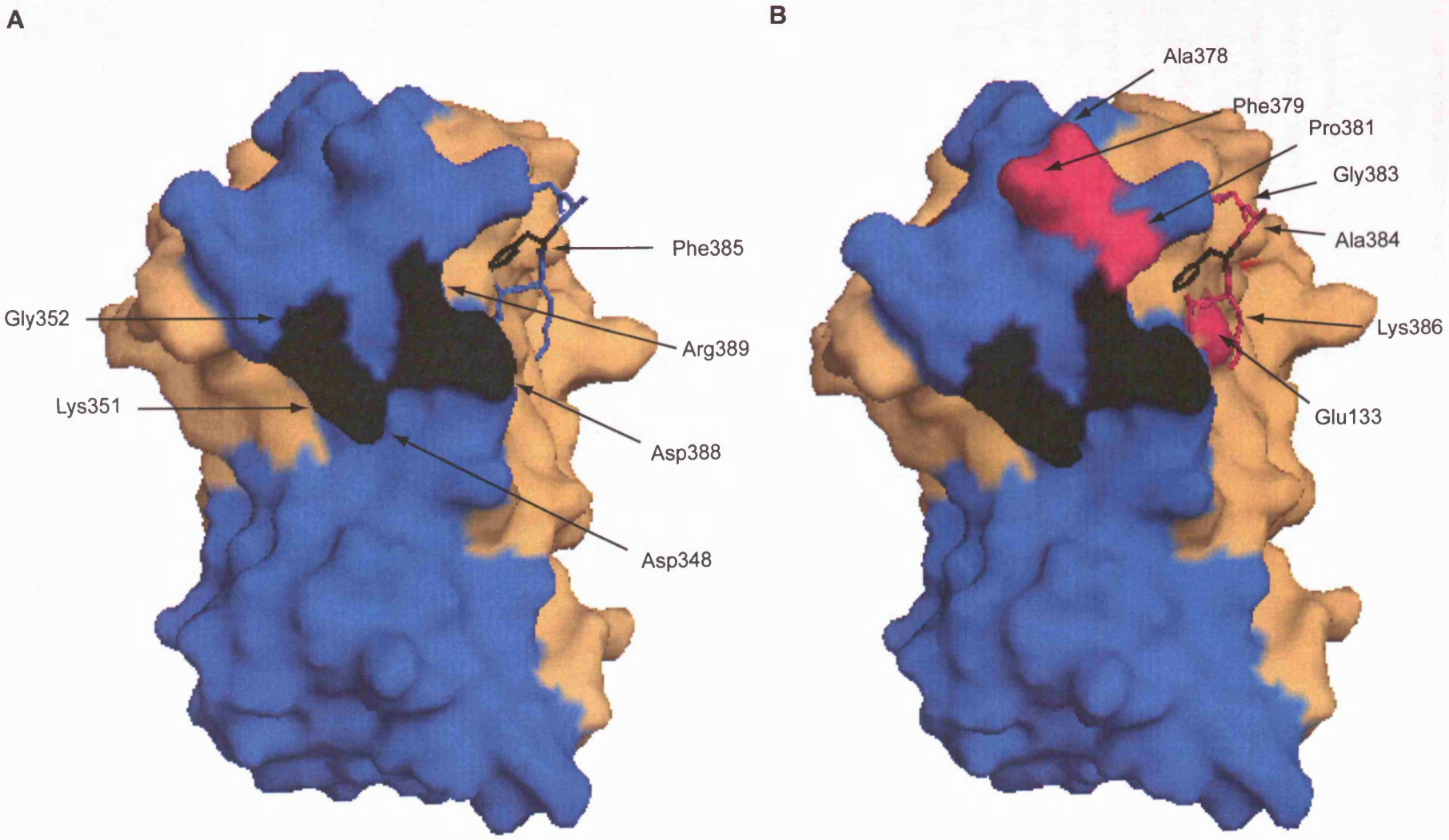
A
Phe385
Gly352
Arg389
Lys351
Asp388
Asp348
B
Ala378
Phe379
Pro381
Gly383
Ala384
Lys386
Glu133

Figure 4.23: The selection process to isolate 4G2dc1$^-$/native$^+$ random mutants: the negative selection step is very efficient, but the positive selection step is inefficient

To assess the efficiency of each step in the selection process for 4G2dc1$^-$/native$^+$ random mutants, COS-7 cells expressing either **(I)** non-mutated (4G2dc1$^+$/native$^+$) sg'PfAMA1 or **(II)** ΔdDB4 (4G2dc1$^-$/native$^+$) were subjected to a single round of selection using either **(a)** Dynabeads (coupled to anti-mouse IgG) alone, **(b)** mAb 4G2dc1 or **(c)** polyclonal serum N1. In the latter two cases, after incubation with the primary Ab, the cells were incubated with Dynabeads and then (for all three treatment conditions) the cells were separated using a Dynal magnet into Dynabead bound **(B)** and unbound **(UB)** fractions. For both transfected COS-7 cell lines, a sample was harvested by trypsin treatment **(T)** and not subjected to further selection to give an indication of the starting protein concentration. Cell fractions were solubilised directly into SDS sample buffer (non-reducing) the extract run on 10% SDS-PAGE gels and transferred to nitrocellulose. Western blot membranes were probed with either polyclonal sera **(i)** R1 or **(ii)** N1, or **(iii)** mAb 4G2dc1.

I

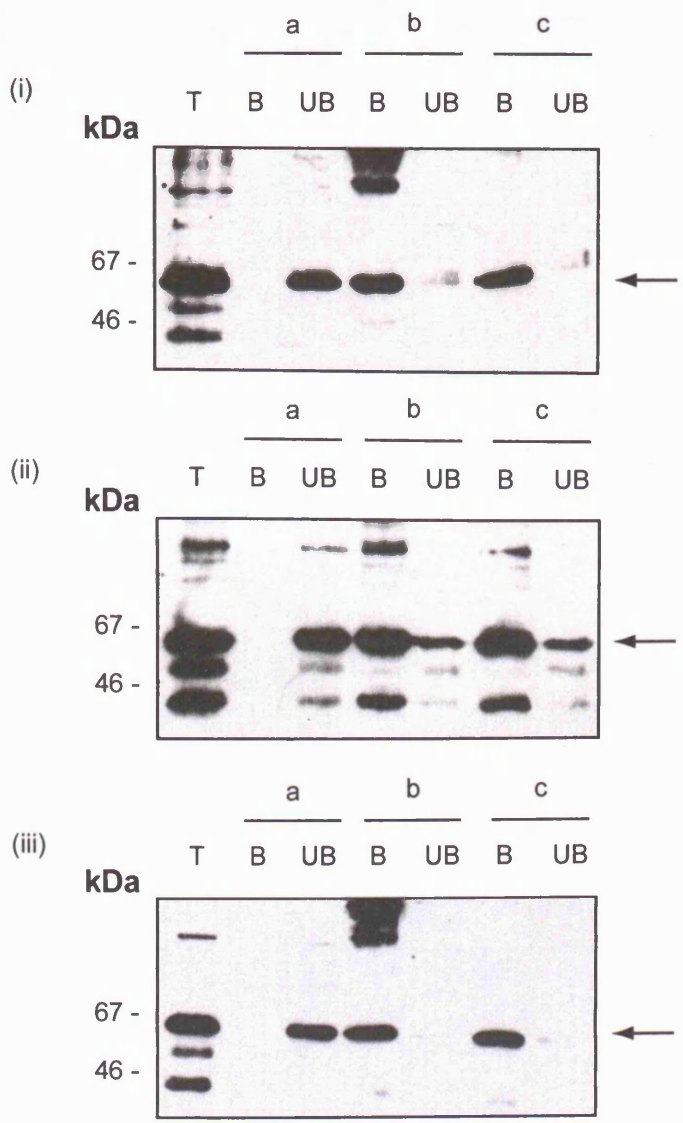

II

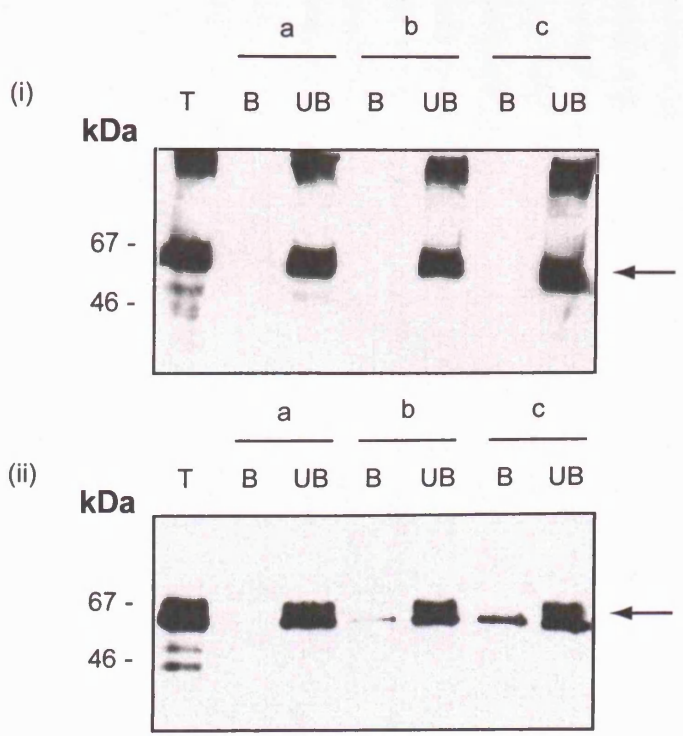

Figure 4.24: 4G2dc1$^-$/native$^+$ mutant forms of PfAMA1 are identified by screening the sg'PfAMA1 random mutant library

COS-7 cells were transfected with sg'Pfa1RML. The selection procedure involved three rounds of negative selection followed by a single round of positive selection as detailed in the materials and methods (section 4.6). At the final round of selection (positive) plasmid DNA was recovered from the isolated cells and transformed into *E. coli* for cloning, following which DNA was transfected into COS-7 cells for expression. Cells were harvested, solubilised into SDS-sample buffer (non-reducing), the extract run on 10% SDS-PAGE gels and transferred to nitrocellulose for analysis in Western blot. Western blot membranes were probed with polyclonal sera **(A)** R1 or **(B)** N1 or mAb **(C)** 4G2dc1. Mutants forms that were 4G2dc1$^-$/native$^+$ or 4G2dc1$^+$/native$^+$ are indicated (red and blue asterisks). COS-7 cells expressing non-mutated sg'PfAMA1 (sg') and untransfected COS-7 cells (neg) were used as positive and negative controls respectively.

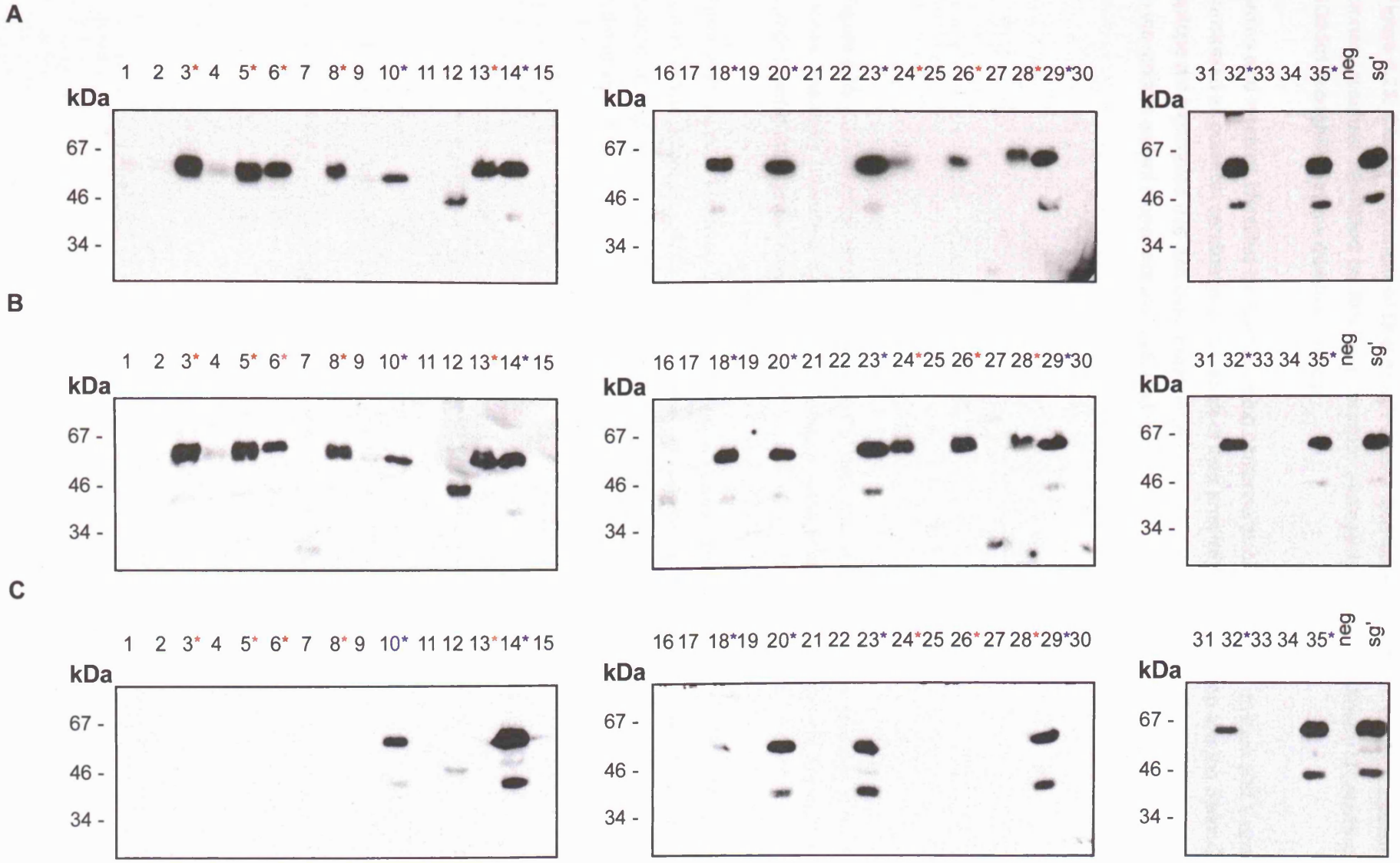
A
1 2 3* 4 5* 6* 7 8* 9 10* 11 12 13* 14* 15
kDa
67 -
46 -
34 -
16 17 18* 19 20* 21 22 23* 24* 25 26* 27 28* 29* 30
kDa
67 -
46 -
34 -
31 32* 33 34 35* neg sg'
kDa
67 -
46 -
34 -
B
1 2 3* 4 5* 6* 7 8* 9 10* 11 12 13* 14* 15
kDa
67 -
46 -
34 -
16 17 18* 19 20* 21 22 23* 24* 25 26* 27 28* 29* 30
kDa
67 -
46 -
34 -
31 32* 33 34 35* neg sg'
kDa
67 -
46 -
34 -
C
1 2 3* 4 5* 6* 7 8* 9 10* 11 12 13* 14* 15
kDa
67 -
46 -
34 -
16 17 18* 19 20* 21 22 23* 24* 25 26* 27 28* 29* 30
kDa
67 -
46 -
34 -
31 32* 33 34 35* neg sg'
kDa
67 -
46 -
34 -

Figure 4.25: Clustal alignment of DI-II of sg'PfAMA1 and 4G2dc1-/native+ random mutant clones: residues identified by SDM and random mutagenesis as specifically disrupting 4G2dc1 recognition show minimal overlap

Amino acid residues identified by SDM as being components of the 4G2dc1 epitope and those considered as potential candidates on the basis of their proximity to the DII loop and the defined epitope are highlighted (red and blue, respectively) in sg'PfAMA1. Residues found to be altered in the random mutant clones are also indicated (yellow).

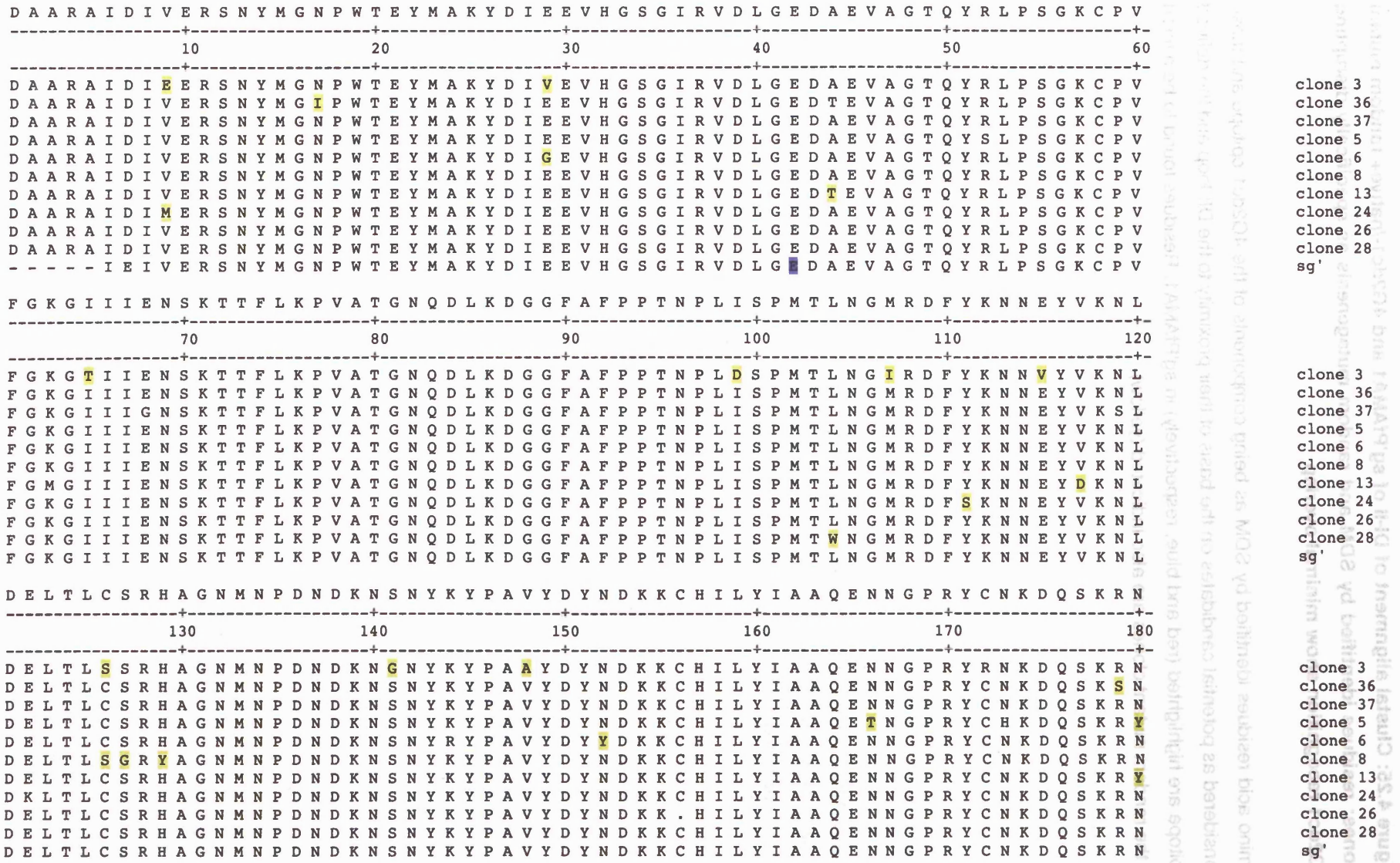
10 20 30 40 50 60
clone 3
clone 36
clone 37
clone 5
clone 6
clone 8
clone 13
clone 24
clone 26
clone 28
sg'
70 80 90 100 110 120
clone 3
clone 36
clone 37
clone 5
clone 6
clone 8
clone 13
clone 24
clone 26
clone 28
sg'
130 140 150 160 170 180
clone 3
clone 36
clone 37
clone 5
clone 6
clone 8
clone 13
clone 24
clone 26
clone 28
sg'

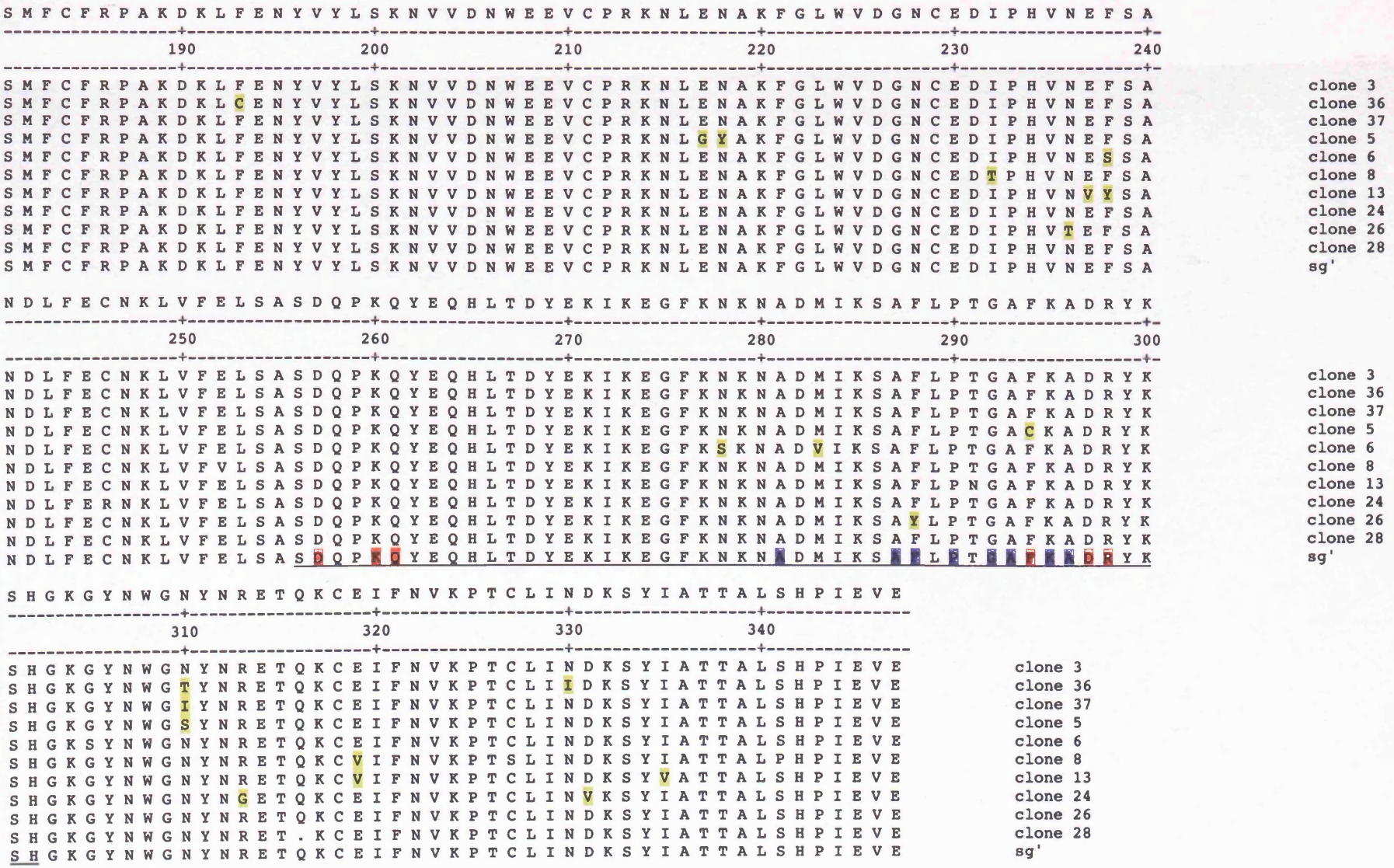
SMFCFRPAKDKLFENYVYLSKNVVDNWEEVCPRKNLENAKFGLWVDGNCEDIPHVNEFSA
190 200 210 220 230 240
clone 3
clone 36
clone 37
clone 5
clone 6
clone 8
clone 13
clone 24
clone 26
clone 28
sg'
NDLFECNKLVFELSASDQPKQYEQHLTDYEKIKEGFKNKNADMIKSAFLPTGAFKADRYK
250 260 270 280 290 300
clone 3
clone 36
clone 37
clone 5
clone 6
clone 8
clone 13
clone 24
clone 26
clone 28
sg'
SHGKGYNWGNYNRETQKCEIFNVKPTCLINDKSYIATTALSHPIEVE
310 320 330 340
clone 3
clone 36
clone 37
clone 5
clone 6
clone 8
clone 13
clone 24
clone 26
clone 28
sg'

Chapter 5

Function of PfAMA1 in signal transduction

5.1: Introduction

Living cells of both unicellular and multicellular organisms are faced with the requirement for sensing changes in their environment and the need for rapid adaptive responses to that environment. Eukaryotic cells have evolved several complex and highly conserved mechanisms for overcoming this problem.

Signals from the extracellular milieu are detected via a receptor embedded in the plasma membrane. Binding of the signalling molecule to the receptor initiates a downstream cascade of events, often involving phosphorylation of the receptor cytoplasmic domain and/or downstream effector molecules, the end result of which can be regulation of specific cytoplasmic machineries or of the activation of certain genes in the nucleus. Signalling pathways are tightly regulated to ensure the correct timing, duration and magnitude of the signal. To this end, the protein kinases (PK) and phosphatases (PP) that often regulate signalling are themselves tightly regulated. The addition of phosphate groups to protein substrates significantly affects their activity, stability, binding properties and subcellular localisation (Kappes et al., 1999).

5.1.1: Receptor molecules involved in signal transduction

Several major classes of cell surface receptor exist that are involved in signal transduction. These include the receptor tyrosine kinase family, cytokine receptors (type I and II), haematopoietic antigen receptors, protein serine/threonine kinase receptors, the tumour necrosis factor (TNF) receptor family and G-protein coupled receptors. These receptors have extracellular receptor domains. Ligand binding often induces receptor dimerisation. The cytoplasmic domains of signalling receptor molecules often allow transduction of the signal by mediating interactions between the receptor and downstream effector molecules. These domains include Src homology (SH) and pleckstrin homology (PH) domains and have been implicated in facilitating protein-protein and protein-lipid interactions, thus mediating the assembly of signalling complexes at the cytoplasmic face of the plasma membrane. In addition, some classes of receptors possess catalytic domains in their cytoplasmic tail that are capable of autophosphorylation. Residues in the SH domains of such receptors, that are required for protein-protein interaction, may be phosphorylated in this way.

Class I cytokine receptors and haematopoietic antigen receptors (e.g. T-cell antigen receptors, TCRs) appear to lack these homology domains and instead possess conserved amino acid

motifs that facilitate protein-protein interactions. For instance, the TCR is composed of two largely extracellular variable polypeptide chains ($\alpha\beta$ or $\gamma\delta$) capable of binding diverse ligands. These interact non-covalently via their short cytoplasmic tail with invariant polypeptide chains comprising the CD3 complex (γ, δ and two ε chains) and ζ-homodimer. The invariant chains contain a total of ten immunoreceptor tyrosine activation motifs (ITAMs; $YX_2(L/I)X_{6-8}YX_2(L/I)$) (Reth, 1991; Irving and Weiss, 1991; Irving et al., 1993). ITAM sequences are essential for the signalling capacity of the antigen receptor complex (Weiss et al., 1993; Burkhardt et al., 1994). Phosphorylation of tyrosine residues within the ITAM sequence, by Src-family kinases (Lck and Fyn) is thought to generate docking sites for downstream signalling molecules such as the cytosolic tyrosine kinase Zap-70. Binding of Zap-70 occurs via tandem SH2 domains (Chan et al., 1992). Thus receptor molecules interact directly or indirectly with downstream signalling molecules via conserved domains or motifs.

5.1.2: Signal transduction in apicomplexan parasites

Plasmodium is evolutionarily divergent from both yeast and higher eukaryotes. Identity between the catalytic domains of protozoan PKs and those of their putative homologues in other eukaryotes is typically only 40 - 60%, exceeding 60% only rarely (Doerig et al., 2002). This allows for considerable functional and structural divergence. Thus, functional predictions resulting from comparison-based analysis can be difficult and may prove misleading. Open reading frames (ORFs) have been identified from the genome of *P. falciparum* that encode polypeptides with clearly recognisable PK catalytic domains but, on the basis of identity alone, these cannot be consigned to a specific family. Furthermore, several enzymes have been identified in the *P. falciparum* kinome (the group of genes in the *P. falciparum* genome believed to encode for parasite protein kinases) having regions of homology to two distinct PK families (Bracchi-Ricard et al., 2000; Dorin et al., 2005; Ward et al., 2004).

While *Plasmodium* and other protozoan parasites share many of the classical components of signalling pathways, there are also apparent gaps in the signalling machinery. Members of the conventional protein tyrosine kinase family of PKs have not been identified in the *Plasmodium* genome (Doerig, 2004). However, tyrosine phosphorylation has been observed in *P. falciparum* (Sharma, 2000) and it has been postulated that this may be carried out by members of a dual-specificity PK family that phosphorylate serine or threonine as well as tyrosine residues (Doerig *et al.* 2002). Such dual-specificity PKs have been identified in budding yeast where typical tyrosine kinases also appear to be missing (Hunter and Plowman, 1997). The absence of the tyrosine kinase family has been observed in most single celled eukaryotes, so it is perhaps not surprising that it is also absent in the *Plasmodium* kinome (Shiu *et al.* 2004).

A further example of *Plasmodium* divergence from higher eukaryotes in terms of signal transduction pathways is the absence of a classical tripartite mitogen-activation protein kinase

(MAPK, also known as extracellular regulated kinases, ERKs) pathway. In mammalian systems MAPK pathways regulate responses to a wide variety of stimuli. These are activated by dual phosphorylation of Thr and Tyr in a conserved MAPK activation motif, TXY by a specific MAPK kinase (MAPKK). These are activated by phosphorylation of two Ser or Thr residues in the conserved motif SMANS by a MAPK kinase kinase (MAPKKK). Activation of MAPKKK occurs in response to a number of extracellular or intracellular stimuli. Two *P. falciparum* homologues of MAPKs have been identified to date; Pfmap-1 encodes a protein with a classical TXY activation motif (Doerig et al., 1996) whereas Pfmap-2 encodes a protein having an atypical TSH motif, in which both T and H are essential for kinase activity of recombinant Pfmap-2 (Dorin et al., 1999). However, no classical MAPKK or MAPKKK genes have been identified in the genome (Ward et al., 2004). The *P. falciparum* PK Pfnek-1 has an activation site with more similarity to that of MAPKKs than the never-in-mitosis/Aspergillus (NIMA) or NIMA-like (Nek) kinase family to which it displays more overall homology (Dorin et al., 2001). The putative activation site of Pfnek-1 possesses a SMAHS motif, rather than the activation sequence normally found in the active site of mammalian MAPKK enzymes. Pfnek-1 specifically phosphorylates recombinant Pfmap-2 but not Pfmap-1 or mammalian ERK2 *in vitro* and acts synergistically with Pfmap-2 in phosphorylation of the exogenous substrate myelin basic protein (MBP), consistent with a role in an atypical MAPK pathway. It remains to be seen whether Pfnek-1 functions as a MAPKK *in vivo*. Searches of the *P. falciparum* genome database led to the identification of a novel PK, PFPK7, having homology to MAPKK in its C-terminal lobe (subdomains VI and XI) (Dorin et al., 2005). However, it contains certain residues that are more similar to those found in protein kinase A (PKA). Recombinant PfPK7-GST fusion protein was capable of autophosphorylation, but was unable to phosphorylate recombinant Pfmap-1 or Pfmap-2 *in vitro*, suggesting the absence of MAPKK activity. Furthermore, inhibitors of PKA had no effect on phosphorylation of MBP by PfPK7 while only two MAPKK inhibitors had any effect and then only at high concentrations. However, it cannot be ruled out that *in vivo* this protein functions as a MAPKK via some atypical pathway. Despite the discovery of a G-protein α-subunit that may be involved in triggering the switch from asexual to sexual development, G-protein-coupled receptors are also apparently absent from the *Plasmodium* genome (Aravind *et al.* 2003). MAPK pathways are often activated in response to G-protein-coupled receptor activation (Doerig, 1997; Cobb *et al.* 1995).

A further area of disparity between the kinome of *Plasmodium* and that of vertebrates is the presence of members of the calcium dependent protein kinase (CDPK) family (Li and Cox, 2000; Zhao et al., 1993; Kappes et al., 1999; Ward et al., 2004). This family of PKs have only previously been identified in plants and some protozoan species, including the apicomplexan parasites *Eimeria tenella* and *E. maxima* (Dunn et al., 1996) where they are usually members of multigene families.

In contrast to the PKs that are apparently absent in the *P. falciparum* kinome, many have been identified that belong to "orphan" groups as they do not cluster with any of the established eukaryotic PK groups. In particular is the FIKK (motif) family (20 members in *P. falciparum*), members of which have only been identified to date in Apicomplexan parasites (Ward et al., 2004). These contain the vast majority of residues in the catalytic site thought to be important for kinase activity. In addition they possess several fully conserved amino acid "signature" motifs that are characteristic of the family, for instance, protein sequences of all FIKK family members have a conserved tryptophan in the motif [ILV][YF]W[NTS]XX[GC] about 100 amino acid residues upstream of the FIKK motif. The glycine triad (GXGXXG) normally present in subdomain I of PKs is incomplete in FIKK protein sequences, no family member having the full complement of glycines. Apart from the glycine triad, all residues required for phospho-transfer in PKs are present in the FIKK sequences, suggesting that these proteins are PKs. However, no experimental evidence exists to substantiate this claim. Some FIKK family members in *P. falciparum* contain putative signal peptides and/or transmembrane spanning domains N-terminal to the predicted catalytic domain. With these exceptions and the similarities in the predicted catalytic domain, this protein family possess no other previously characterised protein domains.

5.1.3: Signalling during host cell invasion by apicomplexan parasites

Invasion of host cells by apicomplexan parasites is a complex and tightly regulated process (see section 1.1.1.). The necessity for signal transduction for successful invasion by these parasites has been known for some time. Ward *et al.* (1994) showed that staurosporin, a serine/threonine PK inhibitor, arrests invasion at the point of tight junction formation and concluded that phosphorylation was essential for merozoite invasion of host erythrocytes. Dobrowolski *et al.* (1997) demonstrated that the protein kinase inhibitor KT5926 blocks *T. gondii* tachyzoite motility and attachment to host cells. Loss of these activities is likely to result directly from the observed loss of microneme, and therefore MIC2, secretion. Kieschnick *et al.* (2001) identified TgCDPK1 as the specific target of this inhibitor, implicating this PK in playing a role in microneme secretion and host cells attachment of *T. gondii* tachyzoites. Thus, it would appear that the activation of TgCDPK1 leads to phosphorylation of the parasite proteins involved in secretion of MIC2 and possibly other microneme proteins.

In *T. gondii*, ionophore induced elevation of intracellular calcium concentrations ($[Ca^{2+}]_i$) triggers microneme secretion (Carruthers et al., 1999a; Carruthers et al., 1999b; Carruthers and Sibley, 1999). Secretion of rhoptry and dense granule components did not occur under these conditions, suggesting that there is differential regulation of apical organelle secretion (Carruthers and Sibley, 1999). Additionally, Carruthers *et al.* (1999c) demonstrated that microneme discharge was regulated by a staurosporin sensitive kinase, essential for parasite invasion of host cells. The addition of the Ca^{2+} ionophore A23187, in the presence of high levels of extracellular Ca^{2+}, was unable to reverse the effects of staurosporin. Carruthers *et al.* (1999)

concluded that the calcium-dependent step in the signalling pathway triggering microneme secretion preceded the staurosporin-sensitive kinase step. Bumstead and Tomley (2000) demonstrated that microneme secretion in *E. tenella* sporozoites occurred in the presence of albumin *in vitro*. In the blood, albumin is believed to be crucial for regulating free calcium (Aguanno *et al.* 1982). For this reason, the group suggest that the presence of albumin in *in vitro* culture facilitates the uptake of calcium by Eimeria sporozoites, possibly triggering microneme secretion (Bumstead and Tomley, 2000). In *P. falciparum*, the requirement for Ca^{2+} in invasion of human erythrocytes was noted as early as 1982. Wasserman *et al.* (1982) showed that in the presence of the Ca^{2+} chelator EGTA, merozoites were unable to progress beyond cell attachment. Whether this effect was due to loss of microneme secretion, as indicated for *T. gondii*, was not determined but is none-the-less possible. Thus, signal transduction is necessary for microneme secretion and this signal can be induced in the absence of host cells. Furthermore, the signals required for microneme and rhoptry secretion appear to be distinct.

Thus, for successful invasion of host cells by apicomplexan parasites signals must be successfully transduced across the parasite plasma membrane. The receptor molecules responsible for induction of this signal remain to be identified.

5.1.4: Merozoite surface receptors involved in signal transduction

Despite many potential cytosolic signalling molecules having been identified in apicomplexan parasites, the signalling pathways within which they play a role have yet largely to be elucidated. Furthermore, no parasite signalling receptor molecules have been identified. For instance, while it appears likely that Ca^{2+} signalling plays a key role in microneme secretion during host cell invasion, the precise event that initiates this signal is unknown.

In the cell membrane, sphingolipids and cholesterol cluster together into moving platforms or rafts (Simons and Ikonen, 1997). These lipid rafts are plasma membrane microdomains rich in glycosphingolipids, sphingomyelin and cholesterol (Brown and London, 1998). Membrane associated proteins such as glycosylphosphatidylinositol (GPI) anchored proteins and dually acylated proteins as well as transmembrane proteins are all able to interact with the rafts. Simons *et al.* (1997) observed that cross-linking of GPI-anchored proteins led to raft formation and activation of lymphoid cells. In addition, it has been observed that several signalling molecules partition into detergent-insoluble glycolipid-enriched complexes (Anderson *et al.* 1993; Lisanti *et al.* 1994). Harder and Simons (1999) showed that cross-linking the ganglioside G_{M1} using cholera toxin B subunit led to an increase in cytosolic phosphotyrosine. They demonstrated that the phosphotyrosine signal was significantly reduced by incubation with PP1, a specific inhibitor of the tyrosine kinases Lck and Fyn that are implicated in TCR signalling. Both Lck and Fyn have been shown to localise to lipid rafts, association with the rafts being

mediated by the acyl modifications of these PKs (Kabouridis *et al.* 1997) . Upon activation of the TCR, the receptor itself is recruited to lipid rafts (Montixi et al., 1998; Xavier *et al.* 1999). GPI-anchored proteins and gangliosides do not span the plasma membrane. It is therefore difficult to anticipate how they could, on their own, transduce a signal across the membrane. Harder and Simons (1999) concluded that under physiological conditions the activated TCR might act synergistically with the raft-associated components in T-cell activation. GPI anchored proteins have also been implicate in signal transduction in haematopoietic cells (Peles et al., 1997), leading to stimulation of Src-family PKs, and in neurons (Robinson, 1991). At the time of *Plasmodium* schizont rupture the majority of proteins making up the merozoite surface coat are GPI-anchored (Dubremetz et al., 1998). As in the mammalian system, it is unlikely that in merozoites GPI-anchored proteins alone are responsible for signal transduction. It therefore seems likely that some transmembrane protein(s) participate in the signalling events that occur during the invasion process.

AMA1 is a type I integral membrane protein expressed in late schizogony when it is trafficked to the micronemes. Around the time of schizont rupture AMA1 is secreted from the micronemes and can be detected on the merozoite surface. With the exception of MAEBL, none of the DBLs have been detected on the surface of merozoites (Kappe et al., 1998a) suggesting that AMA1 and MAEBL may be the first transmembrane proteins to localise to the merozoite surface after schizont rupture. The cytoplasmic tail of EBA-175 does not play a role in protein trafficking to the micronemes (Gilberger et al., 2003a). For this reason, it seems unlikely that the cytoplasmic domain of AMA1 could be involved in microneme targeting if that of EBA-175 is not. Rather, it seems probable that the parasite uses a conserved mechanism for protein targeting to these organelles.

The high degree of conservation observed in the cytoplasmic tail of AMA1 (Fig 5.1.) across the phylum is suggestive of a conserved, essential function of this region of the molecule. Furthermore, there are several tyrosine, serine and threonine residues that are absolutely conserved in all *Plasmodium* AMA1 sequences identified to date. One of each of these residues is also conserved in the sequence of the *T. gondii* AMA1 homologue. Although the cytoplasmic tail of AMA1 does not contain any typical signalling motifs, the unusual nature of many of the signalling molecules already identified in *Plasmodium*, raises the possibility that these residues in AMA1 could be targets for kinase activity during signal transduction. This, together with its presence on the merozoite surface so early after schizont rupture, makes AMA1 an ideal candidate for a novel *Plasmodium* receptor for transducing a signal to the parasite cytosol at the time of "appropriate" host cell contact.

5.2: Analysis of the role of PfAMA1 as a signalling molecule

AMA1 is considered to be a valuable potential component of a subunit anti-malarial vaccine. As a signalling molecule it would also become a potential target for chemotherapeutic intervention. Because of the atypical nature of many *Plasmodium* signalling molecules, they are ideal candidates for drug design. In addition, some *Plasmodium* PKs share features found in PKs from other protozoans, such as *Trypanosoma brucei* and *Leishmania* that are not shared by other eukaryotes. Others share homology to PKs unique to plants and a few other protozoans (Li and Cox, 2000; Zhao et al., 1993; Kappes et al., 1999; Ward et al., 2004). These unique characteristics are valuable qualities in drug targets, as drugs that effectively inhibit their activity should be specific for the target species. As an essential gene product (Triglia et al., 2000; Hehl et al., 2000) chemotherapeutic agents that effectively prevent AMA1 participation in a signalling pathway would also prevent erythrocyte invasion by merozoites and thus disrupt parasite growth and development. To explore the possibility of a role for PfAMA1 in signal transduction, the phosphorylation status of this protein in purified merozoites extracts was analysed.

P. falciparum schizonts were synchronised on a 70% percoll cushion, returned to culture in the absence of fresh RBCs and allowed to rupture for 4 hours. Merozoites were collected and analysed under reducing conditions by Western blot using the polyclonal serum R1 and mAbs specifically recognising phosphoserine (p-Ser), phosphothreonine (p-Thr) and phosphotyrosine (p-Tyr).

In this study, the presence of $PfAMA1_{66}$ in merozoite lysates was confirmed using polyclonal serum R1, giving a clear band running just above the 67 kDa marker band (Fig 5.2, D). The anti-p-Thr mAb detected several bands, one of which migrated at a similar size to that detected by R1 (Fig 5.2, A). To determine whether this was also PfAMA1, each of the two blots was re-probed this time with the alternative antibody, i.e. the blot that had been probed with R1 was now probed with anti-p-Thr, and *vice versa*. In both cases a doublet was detected (Fig 5.2, E and F respectively) indicating the presence of the first band that had not been removed by stripping the blots, and a novel band detected by the second primary antibody. This confirmed that the two antibodies were detecting different proteins migrating at slightly different sizes. This result was confirmed by repeating the Western blot using larger gels to obtain better resolution. Once again probing a blot with the two different antibodies (polyclonal serum R1, Fig 5.3 A, and anti-phosphothreonine consecutively) produced a doublet (Fig 5.3, B).

The blot probed with anti-p-Ser mAb showed high background, with multiple bands (Fig 5.2, B). However there appeared to be a band at about 67 kDa, close to the size of PfAMA1. This result was not however reproducible. Probing with anti-p-Tyr mAb (4G10) produced several faint bands, none of which were at the correct size for PfAMA1 (Fig 5.2, C).

Results obtained from similar analysis of different preparations of merozoites gave variable results. However, none led to the detection of phosphorylation of any type in PfAMA1.

5.3: Discussion

5.3.1: Phosphorylation status of PfAMA1

Receptors that lack intrinsic kinase activity are often phosphorylated upon activation by associated kinases (Ihle, 1995; Taniguchi, 1995). For *Plasmodium* merozoites this receptor activation would occur when the parasite makes the initial attachment with the appropriate host cell and/or at some stage downstream of this event. In this study phosphorylation of PfAMA1 was not detected with any of the antibodies used. For this study, schizonts were isolated from cultures using a 70% percoll cushion. The schizonts floating on top of the cushion were washed and then returned to culture in the absence of fresh RBCs to complete their development and rupture. Schizonts purified in this way were about 95% pure, there being about 5% contamination with trophozoite stage parasites and some uninfected cells. Because of the low level of contamination it is unlikely that the released merozoites, harvested from these samples by centrifugation, would have encountered any uninfected RBCs. As a result, the conditions necessary for transducing the signal to initiate the chain of events leading to erythrocyte invasion would not have been met by these merozoites. However, some merozoites may have come into contact with RBC debris from ruptured schizonts although whether such membranes, which have been extensively modified (Berendt et al., 1994) by the parasite, are capable of triggering the necessary signals for parasite invasion is unknown. It is possible however, that some low level stimulation would occur under these conditions. Nevertheless, the degree of phosphorylation of PfAMA1 might have been insufficient for detection by these antibodies. To increase the likelihood of detecting low-level phosphorylation, PfAMA1 could first be purified by immunoprecipitation using a PfAMA1 specific antibody. Alternatively purification of all phosphorylated parasite proteins would have enhanced the small fraction of phosphorylated PfAMA1 protein present. Increasing the concentration of phosph-PfAMA1 by either of these methods would make detection by Western blot analysis easier. This approach will be considered in more detail in the future.

5.3.2: Regulation of receptor activation

Signal transduction can result in diverse, or diametrically apposed downstream effects, such as apoptosis and cell proliferation (Shiu *et al.*, 2004; Ward et al., 2004; Caraglia et al., 2005; Dailey et al., 2005). In order that these processes are kept in check, the receptors and PKs involved are tightly regulated. Regulation of PK activity can be achieved by phosphorylation and/or dephosphorylation of inhibitory sites outside the catalytic domain. For instance, members of the Src tyrosine kinase family have an inhibitory tyrosine phosphorylation site in the C-terminal tail

(Cooper and King, 1986) and stimulatory tyrosine phosphorylation sites in the catalytic domain. Regulation of Src activity involves interplay between these sites, activation requiring phosphorylation in the kinase domain and inhibition resulting from C-terminal phosphorylation (Kmiecik et al., 1988). Only a small energy barrier lies between the two states enabling the molecule to flip rapidly between them (Cooper *et al.* 1993). Thus, regulation of Src kinase activity requires the interplay of phosphatases and kinases in the cell (Okada and Nakagawa *et al.* 1989). Indeed, there appears to be a rapid turnover of phosphate at both sites.

The catalytic domains of most eukaryotic kinases are about 250 - 300 residues in length (Hanks and Quinn 1993). The cytoplasmic tail of PfAMA1 is only 54 amino acid residues long and is therefore unlikely to be a functional kinase domain unless it does so as an atypical protein kinase. If this were the case, the potential phosphorylation sites in the AMA1 cytoplasmic tail could function in receptor regulation as either inhibitory or stimulatory sites. If both types were present one might expect to see receptor phosphorylation regardless of whether the receptor was activated or not. The only difference might be in the nature and position of the residue phosphorylated. The absence of any detectable phosphorylation in PfAMA1 under the conditions used in this study, argues against the presence of inhibitory phosphorylation sites.

One further possibility for the lack of PfAMA1 phosphorylation found in this study is the absence of phosphatase inhibitors. Phosphorylation is usually a reversible and dynamic process, the phosphorylated residues being rapidly de-phosphorylated by phosphoprotein phosphatases to prevent over stimulation (Roskoski 2005). Phosphorylation of PfAMA1 might not have been observed due to rapid removal of the phosphate group by active protein phosphatase contamination present in the merozoite lysates.

5.3.3: PfAMA1 as a signalling receptor molecule

From the data discussed here, it would appear that PfAMA1 does not undergo phosphorylation. However, these results are only preliminary and a much more detailed analysis of signalling during invasion is required before PfAMA1 can be demonstrated conclusively to play a role in signalling or not. For a more thorough examination of AMA1's role as a signalling molecule it will be necessary to be able to dissect out and/or "freeze in time" different stages in the invasion process, i.e. the points of initial interaction, reorientation and tight junction formation and assess the phosphorylation status of AMA1 at each of these time points. This is particularly difficult in *Plasmodium* as the invasion process is extremely rapid (about 20 seconds) and the invasive half-life of merozoites is very short, in the order of 10-30 minutes at 23°C and 4-7 minutes at 37°C in *P. knowlesi* (Johnson et al., 1980). Cytochalasin B "freezes" parasites at the point of tight junction formation (Miller et al., 1979a) and merozoite attachment is stable at 0°C (Johnson et al., 1980). However this latter result was obtained using purified *P. knowlesi* merozoites. Viable *P. falciparum* merozoites have never been purified and it is debatable whether schizont

rupture could occur normally at 0°C. Isolation of *P. falciparum* merozoites attached to human erythrocytes may therefore not be possible. Isolation of merozoites at the point of reorientation, prior to tight junction formation may also be difficult. However, if these difficulties could be overcome, the progress of PfAMA1 could be followed through the invasion process and its phosphorylation status fully characterised.

The transport of PfAMA1 to the merozoite surface around the time of schizont rupture suggests that it plays a role in the early stages of invasion (Peterson et al., 1989). MAEBL is the only other integral membrane protein purported to be an erythrocyte binding protein that has been localised to the merozoite surface (Kappe et al., 1998a). This suggests that the role these two proteins play in invasion is distinct from that of the other erythrocyte binding antigens. Furthermore, if release of this second group of binding proteins from the micronemes is delayed, a signal is presumably necessary for their subsequent release. Whether a separate signal is required for AMA1 and MAEBL relocalisation is unclear. Their presence on the surface is detected so rapidly after schizont rupture, that if a signal is required it may be temporally linked to schizont rupture itself rather than to initial erythrocyte interaction. From previous studies in *T. gondii*, it is clear that microneme and rhoptry release are triggered by different stimuli (Carruthers et al., 1999a; Carruthers et al., 1999b; Carruthers and Sibley, 1999). Keischnick *et al.* (1998) suggest a role for *T. gondii* CDPK1 in microneme secretion. Dense granule secretion is also distinct from microneme release (Carruthers et al., 1999a).

5.3.4: Signal transduction and host cell invasion

Signal transduction plays a crucial role in host cell invasion by apicomplexan parasites. Several steps in the invasion process appear to require signals to allow the parasite to traverse to the next stage. A possible scenario for the interaction of signal transduction and host cell invasion by the malaria merozoite is as follows: Upon schizont rupture, daughter merozoites are released into the blood stream of the host. This triggers the first wave of microneme release, which sees the redistribution of AMA1 and MAEBL (possibly from the rhoptries) onto the merozoite surface. The parasite collides with host cells as it passes through the blood vessels and must rapidly be able to detect whether a cell is permissive to invasion or not. The parasite reorientates so its apical tip is in contact with the host cell membrane. At this stage, if an appropriate cell has been identified, a Ca^{2+} dependent signal triggers the second wave of microneme secretion and these proteins interact with host cell proteins to form the tight junction. This triggers release of the rhoptry proteins that participate in PV formation. The parasite enters the host cell and the PV membrane seals behind it, enclosing it in the PV. Release of the dense granules into the PV is triggered and parasite differentiation to the next developmental stage, the ring stage, must be stimulated. The signalling molecules and stimuli involved at each of these stages are unknown.

The unique nature of many of the *Plasmodium* signalling molecules identified so far makes them important potential drug targets. Furthermore, those involved in invasion are of particularly interest as inhibition of merozoite invasion would abolish infection and blood-stage replication. This area should clearly be a major focus for future study.

Figure 5.1: Clustal alignment shows a considerable degree of amino acid conservation in the sequences of the predicted cytoplasmic tail of AMA1 from different species of apicomplexan parasites

Dashes indicate gaps in the alignment. The residues in the cytoplasmic tail of AMA1 that are potentially involved in signal transduction are highlighted in red. Other highly conserved (or conservatively substituted) residues present in all the sequences are highlighted in blue, while those conserved only in other species of *Plasmodium* are highlighted in yellow. The complete sequence of *P. reichenowi* was not available. If this sequence corresponds to the rest of those from *Plasmodium*, the N-terminal 9 amino acids are missing. There is a large degree of conservation among sequences from *Plasmodium*. In addition, even those of *T. gondii* and *B. bovis* show a considerable degree of overall conservation. However, with respect to the amino acid residues potentially involved in signalling, these do not overlap strongly between phyla though the threonine at the position equivalent to 613 in *P. falciparum* is absolutely conserved. In addition, the 601SFW motif in *P. falciparum* is absolutely conserved in *Plasmodium* and *T. gondii*. This corresponds to YFW in *B. bovis*.

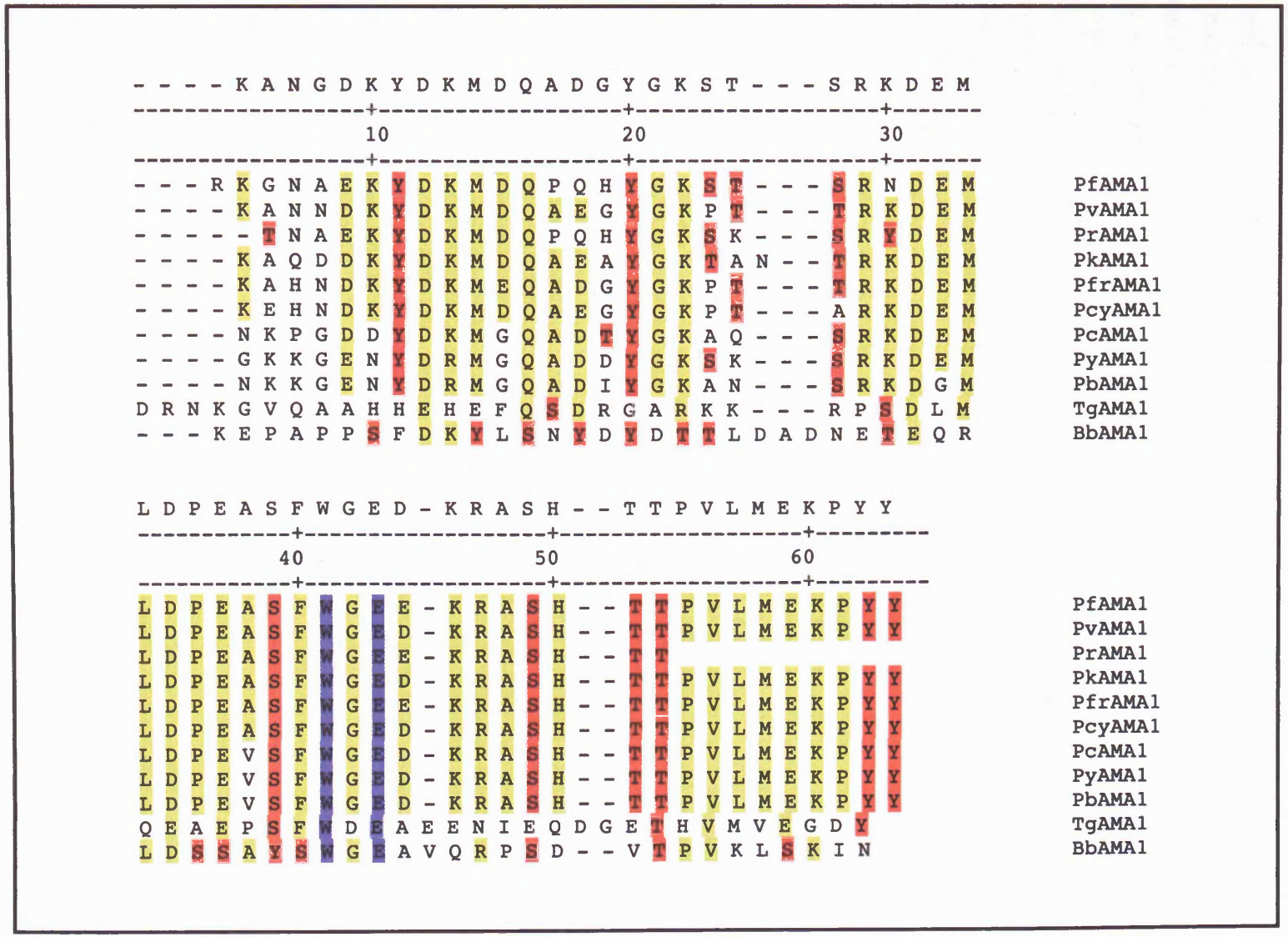
- - - - K A N G D K Y D K M D Q A D G Y G K S T - - - S R K D E M
10
20
30
- - - R K G N A E K Y D K M D Q P Q H Y G K S T - - - S R N D E M PfAMA1
- - - - K A N N D K Y D K M D Q A E G Y G K P T - - - T R K D E M PvAMA1
- - - - - T N A E K Y D K M D Q P Q H Y G K S K - - - S R Y D E M PrAMA1
- - - - K A Q D D K Y D K M D Q A E A Y G K T A N - - T R K D E M PkAMA1
- - - - K A H N D K Y D K M E Q A D G Y G K P T - - - T R K D E M PfrAMA1
- - - - K E H N D K Y D K M D Q A E G Y G K P T - - - A R K D E M PcyAMA1
- - - - N K P G D D Y D K M G Q A D T Y G K A Q - - - S R K D E M PcAMA1
- - - - G K K G E N Y D R M G Q A D D Y G K S K - - - S R K D E M PyAMA1
- - - - N K K G E N Y D R M G Q A D I Y G K A N - - - S R K D G M PbAMA1
D R N K G V Q A A H H E H E F Q S D R G A R K K - - - R P S D L M TgAMA1
- - - K E P A P P S F D K Y L S N Y D Y D T T L D A D N E T E Q R BbAMA1
L D P E A S F W G E D - K R A S H - - T T P V L M E K P Y Y
40
50
60
L D P E A S F W G E E - K R A S H - - T T P V L M E K P Y Y PfAMA1
L D P E A S F W G E D - K R A S H - - T T P V L M E K P Y Y PvAMA1
L D P E A S F W G E E - K R A S H - - T T PrAMA1
L D P E A S F W G E D - K R A S H - - T T P V L M E K P Y Y PkAMA1
L D P E A S F W G E E - K R A S H - - T T P V L M E K P Y Y PfrAMA1
L D P E A S F W G E D - K R A S H - - T T P V L M E K P Y Y PcyAMA1
L D P E V S F W G E D - K R A S H - - T T P V L M E K P Y Y PcAMA1
L D P E V S F W G E D - K R A S H - - T T P V L M E K P Y Y PyAMA1
L D P E V S F W G E D - K R A S H - - T T P V L M E K P Y Y PbAMA1
Q E A E P S F W D E A E E N I E Q D G E T H V M V E G D Y TgAMA1
L D S S A Y S W G E A V Q R P S D - - V T P V K L S K I N BbAMA1

Figure 5.2: Determination of the phosphorylation status of PfAMA1 in *P. falciparum* merozoites by Western blot analysis

Merozoite samples were solubilised directly into SDS sample buffer and the extract electrophoresed on 10% SDS-PAGE. The samples were analysed by Western blot to detect phosphorylated parasite proteins using; **(A)** anti-phosphothreonine (α-pThr), **(B)** anti-phosphoserine (α-pSer) or **(C)** anti-phosphotyrosine (4G10) Abs. To confirm the presence and location of PfAMA1 in the samples, the polyclonal serum R1 **(D)** was also used. The 66 kDa bands are indicated in A and D (black arrows). To determine the identity of the approximately 66 kDa band detected with the α-pThr Ab, Western blot membranes probed with the polyclonal serum R1 and α-pThr were reprobed with **(E)** α-pThr and **(F)** R1 respectively. The presence of $PfAMA1_{66}$ (black arrow) in the samples is indicated.

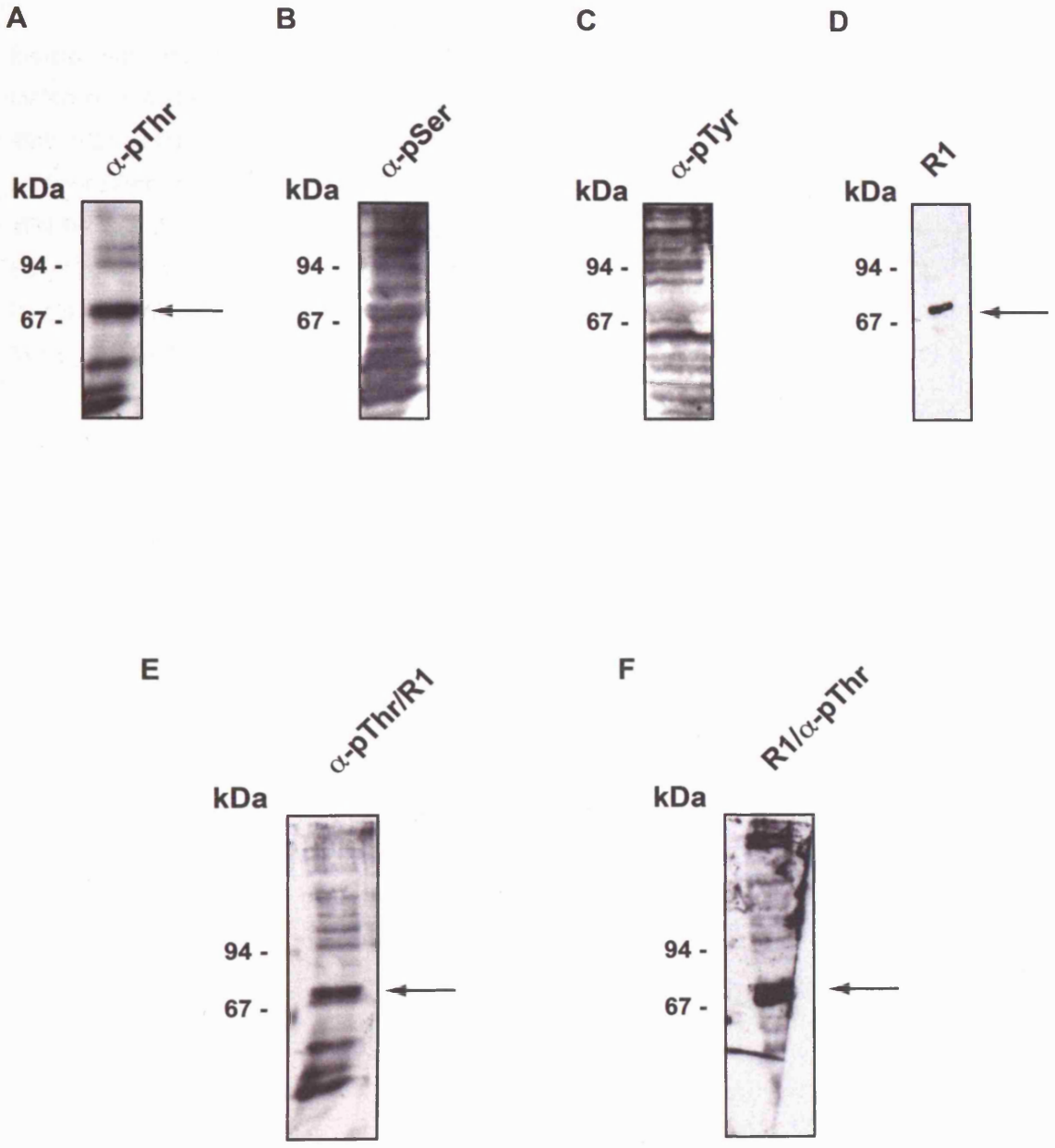
A
α-pThr
kDa
94 -
67 -
B
α-pSer
kDa
94 -
67 -
C
α-pTyr
kDa
94 -
67 -
D
R1
kDa
94 -
67 -
E
α-pThr/R1
kDa
94 -
67 -
F
R1/α-pThr
kDa
94 -
67 -

Figure 5.3: Merozoite-derived PfAMA1 is not recognised by an anti-phosphothreonine antibody.

P. falciparum merozoites were solubilised directly into SDS sample buffer (with reducing agent) and the extract electrophoresed on SDS-PAGE. Large gels were used for increased resolution. In Western blot analysis, the samples were probed first with polyclonal serum R1 **(A)** followed by the anti-phosphothreonine (α-pThr) Ab **(B)**. The location of $PfAMA1_{66}$ (black arrow) and the additional anti-phosphothreonine-specific band (red arrow) are indicated. Therefore, the proteins detected by these two antibodies appear to be distinct.

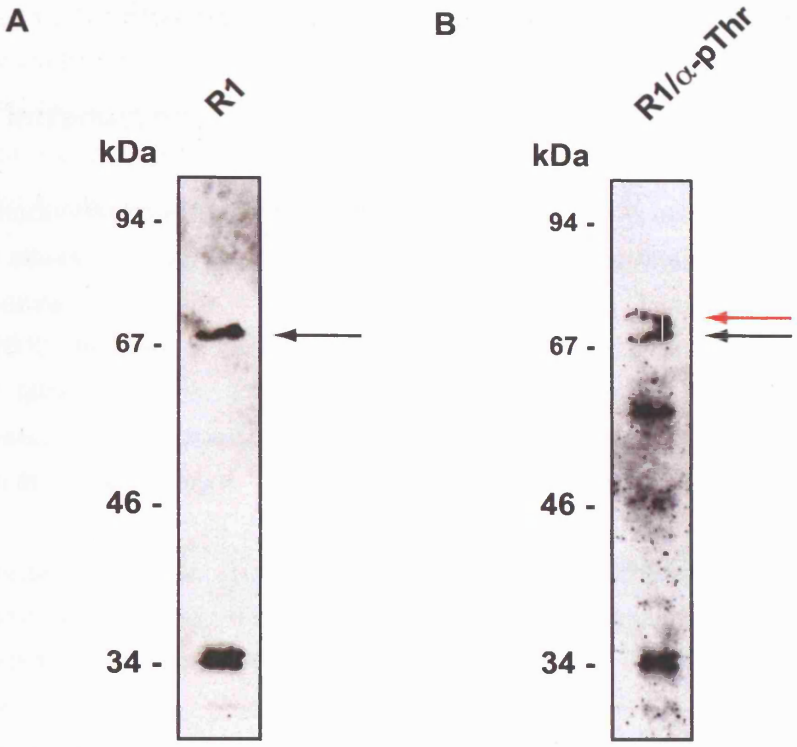
A
R1
kDa
94 -
67 -
46 -
34 -
B
R1/α-pThr
kDa
94 -
67 -
46 -
34 -

Chapter 6

Functionality of sgPfAMA1 in *P. falciparum*

6.1: Introduction

The nucleotide composition of the *P. falciparum* genome is extremely A+T-rich. For this reason, early attempts to express PfAMA1 in eukaryotic systems resulted in truncated products due to premature transcription termination (Kocken et al., 2002). To overcome this problem, Kocken et al. (2002) designed a synthetic *Pfama1* gene (*sgPfama1*), replacing the A+T-rich codon usage of *P. falciparum* strain FVO with that of the methylotrophic yeast *Pichia pastoris*. This gene sequence was used for the expression of rPfAMA1 protein in all the functional studies carried out in the current project.

P. falciparum exhibits low N-glycosylation capability. Furthermore, mass spectrometric peptide fingerprinting of schizont derived PfAMA1 ($PfAMA1_{83}$ and $PfAMA1_{66}$) showed that five of the potential N-glycosylation sites were not glycosylated (Howell et al., 2001). Howell et al. were unable to detect any peptide containing the sixth potential N-glycosylation site, N371, leaving open the possibility that this site is modified in the parasite. However, this site is not highly conserved in *Plasmodium* (Fig 6.1) perhaps suggesting that it has no functional/structural significance as an N-glycosylation site. Collectively, therefore, the evidence indicates that N-glycosylation is not a requirement for AMA1 function. On the other hand, the presence of inappropriate N-glycosylation may alter the structure and/or function of the molecule. Removal of the potential N-glycosylation sites eliminates this potential problem as well as the requirement for tunicamycin during heterologous expression. Tunicamycin prevents the addition of N-acetylglucosamine to dolichol phosphate, thus preventing the formation of the lipid-linked oligosaccharide precursor. This blanket inhibition of N-linked glycosylation can be detrimental to surrogate expression systems, as many eukaryotic proteins require N-glycosylation to function. In addition, N-glycosylation does not produce predetermined structures and non-homogeneous populations of glycoproteins can result. These potential problems were avoided by replacing all six sites. Thus, in addition to the codon usage adjustments described, the coding sequence of *sgPfama1* was altered to replace the six potential N-glycosylation sites (N-X-S/T) present in the AMA1 gene sequence of the *P. falciparum* FVO strain with the corresponding sequence from other species of *Plasmodium* (replacements made were: N162/K, T288/V, S373/D, N422/S, S423/K and N499/E).

Alterations to the amino acid sequence of a protein potentially alter its structure and/or function. That the rPfAMA1 expressed in the heterologous systems utilised in this study retains its native conformation has been confirmed by means of the mAb 4G2dc1 and the polyclonal serum

N1Ads. The mAb 4G2dc1 recognises a reduction sensitive, conformational epitope in DII of the PfAMA1 ectodomain (see Chapter 4), while N1Ads recognises only the "native" conformation of the PfAMA1 ectodomain. However, subtle alterations that might affect the proteins function in the parasite might pass undetected. It was therefore decided to attempt to assess the functionality of sgPfAMA1 in *P. falciparum*. To this end, *sgPfama1* was transfected into *P. falciparum* using constructs designed either to replace the endogenous gene with the synthetic gene (by homologous recombination) or for episomal expression of the synthetic gene product alongside that of the endogenous gene. In order to distinguish the sgPfAMA1 from the endogenous gene product (wtPfAMA1), a single HA epitope tag (YPYDVPDYA) was embedded in frame in the stub region of sgPfAMA1 (sgPfAMA1/HA). This was achieved by minimal modification of the amino acid sequence (Fig 6.2 A). The HA epitope tag can be detected using the mAb 3F10. All transfections were carried out using the *P. falciparum* clone 3D7. To ensure the correct timing of expression of sgPfAMA1, the synthetic gene was transfected under the control of the *Pfama1* promoter.

Stable transfection in *P. falciparum* is a relatively inefficient and technically demanding technology, sensitive to minor alterations in conditions (Cowman and Crabb, 2002). During transfection as few as 1 in 10^6 *P. falciparum* parasites take up plasmid (O'Donnell et al., 2002). Although transfection in other *Plasmodium* parasite species is carried out using purified mature schizonts (van Dijk et al., 1995; Waters et al., 1997), with *P. falciparum* the use of schizonts results in reduced transfection efficiency, possibly due to increased susceptibility of this stage to rupture during electroporation (Waterkeyn et al., 1999). As a result transfection of *P. falciparum* relies on the use of immature ring stage parasites. The inefficiency observed with *P. falciparum* transfection may in part be due to host cell damage during the transfection procedure. In addition, stable transfection of intracellular parasites necessitates the movement of transfected DNA across four membranes (the RBC plasma membrane, PVM as well as the parasite's plasma and nuclear membranes) further reducing the efficiency of transfection (Wu *et al.* 1995).

Attempts to induce stable transfection of *P. falciparum* can have several different outcomes. Furthermore, even successful integration results in a mixed parasite population in which some parasites retain episomally maintained plasmid while others have undergone integration. As the asexual stages of *Plasmodium* parasites are haploid, gene deletions or replacements that are lethal to the parasite result in the death of parasites in which integration has occurred (O'Donnell et al., 2000). The failure of a plasmid to integrate could result from the inability of the target sequence to undergo homologous recombination. In both these cases, parasites recovered after drug selection pressure will contain episomal plasmid only. Interpreting the cause of a failure to recover stable transfectants is therefore complex. In addition to lethal gene deletions or replacements are those that have a deleterious effect on parasite growth, replication or invasion. In mixed parasite cultures, these parasites may be outgrown by those in which integration has not occurred. Cycling of transfected parasites on and off drug selection

pressure should favour the isolation of integrants (Wu et al., 1996), as episomal plasmids are rapidly lost in the absence of drug pressure (O'Donnell et al., 2001; O'Donnell et al., 2002). However, parasite lines must eventually be cloned in order to fully analyse the phenotypic effects of integration. Not all gene deletions or modifications result in an identifiable phenotypic effect. One possible explanation for this is that the parasites may utilise an alternative pathway, thus side-stepping the loss or modification of function of a particular gene. For example, the loss of functional EBA-175 results in parasite utilisation of an EBA-175/sialic acid independent invasion pathway (Reed et al., 2000; Duraisingh et al., 2003a).

All plasmids used for transfection in this study contained the gene encoding the positive selectable marker human dihydrofolate reductase (hDHFR). This gene encodes the mutation L22/Y in the active site of the enzyme that confers resistance to the antifolate drug WR99210 (Fidock and Wellems 1997), so parasites lacking this gene are susceptible to WR99210. For plasmid integration by single cross-over, the plasmid pHH1 was used (Reed et al., 2000). Transfected parasites were subjected to repeated cycles of three weeks off drug pressure, followed by the addition of WR99210 to cultures until the parasites had re-established. For double integration transfection, the plasmid pHHT-TK, additionally containing the *Herpes simplex* virus gene encoding the negative selectable marker thymidine kinase (TK), was used (Duraisingh *et al.* 2002). Thymidine kinase converts nucleoside analogues into toxic metabolites. The nucleoside analogue ganciclovir was therefore used in conjunction with WR99210 at the point of parasite re-establishment after the reintroduction of WR99210. Thus, parasites that had undergone the second integration event, losing the *tk* gene whilst retaining the *hdhfr* gene, were selected for.

6.2: Analysis of sgPfAMA1/HA expression in COS-7 cells

The HA epitope tag was introduced into the stub region of PfAMA1 placing it between the bulk of the PfAMA1 ectodomain and the merozoite plasma membrane. Thus, it may be largely hidden from the extracellular milieu on surface-expressed protein. At the time of designing this tagged form of sgPfAMA1, the structure of AMA1 was unknown. For this reason, it was not possible to select a region of the PfAMA1 ectodomain that was know to be located on the surface of the molecule. Furthermore, as the mechanism of AMA1 function is unknown, the insertion of an epitope tag in an exposed region of the ectodomain, supposing such a region could be identified, would be risky as it might deleteriously affect the function of the protein. Because transfection in *P. falciparum* is a slow process, the plasmid pSec/sg'Pfama1/HA was transfected into COS-7 cells to more rapidly assess expression of sg'PfAMA1/HA and the accessibility of the HA tag for analysis. This plasmid contains the *sg'Pfama1* gene sequence that was used for COS-7 cell expression (Section 3.2.) with the addition of the sequence encoding the HA tag. In *P. falciparum,* processing of AMA1 to remove the prodomain appears to be necessary for its release from the micronemes (Narum and Thomas, 1994b). Thus, PfAMA1

found on the surface of merozoites lacks the prodomain. Processing of $PfAMA1_{83}$ to $PfAMA1_{66}$ may not occur successfully in COS-7 cells where, in addition, the presence of the prodomain may inhibit secretion of sgPfAMA1. For these reasons, the construct used in this study for COS-7 cell expression comprised a modified version of the synthetic gene, lacking the prodomain (*sg'Pfama1*).

In IFA of unfixed COS-7 cells (uIFA), sg'PfAMA1/HA was shown to be surface localised using the mAb 4G2dc1 (Fig 6.3 A) and the polyclonal serum N1 (Fig 6.3 B) both of which recognise epitopes in the PfAMA1 ectodomain (2.4.1). This suggested that in this system the HA epitope tag does not deleteriously affect the targeting of the protein to the secretory pathway. However, for detection of the HA tag using the mAb 3F10, acetone fixation (fIFA) was required (Fig 6.3 C). The gentle fixative paraformaldehyde was insufficient to allow detection of the tag in IFA. One interpretation of this result is that, on the surface of the cell, the epitope tag is buried beneath the bulky ectodomain of PfAMA1 and is therefore inaccessible to antibodies unless the cells are fixed and extensively permeabilised. The presence of AMA1 in transfected cells was confirmed in Western blot analysis with the polyclonal serum R1 (Fig 6.3 D) and mAb 4G2dc1 (Fig 6.3 E). Reducing condition were required in Western blot analysis for the detection of the HA tag in sg'PfAMA1/HA transfected cells with the Abs 12CA5 and 3F10 (Fig 6.3 F and G respectively). Similar conditions were therefore applied for analysis of parasite-derived material after transfection. The Ab 12CA5 binds non-specifically to an additional band in COS-7 cell lysates. This is confirmed by the presence of this band in samples from COS-7 cells transfected with "wild-type" sg'PfAMA1 and untransfected cells (Fig 6.4 F).

6.3. Episomal expression of sgPfAMA1 in *P. falciparum*

Selection of transiently transfected parasite lines is generally a relatively rapid process compared with selection of integrants. The parasite genome is unaltered by the presence of an episomally maintained plasmid. Transiently transfected parasites lines express the same repertoire of genes as wild type parasites with the additional expression of episomally encoded genes. For this reason, so long as the episomal gene product has no deleterious effects on parasite replication, the expression, localisation and processing of modified genes can be observed without threatening parasite survival.

In this study, to ensure that expression of sgPfAMA1 was possible in *P. falciparum*, the construct pHAM-sgPfa/HA was designed for episomal expression of the HA tagged synthetic gene product (Fig 2.8). In this construct, expression of the *sgPfama1* gene was under the control of the *Pfama1* promoter and the 3' termination sequence of the *P. berghei* DHFR-thymidylate synthase (DHFR-TS) gene (PbDT3'). This 3' UTR has previously been demonstrated to be functional in *P. falciparum* (Crabb et al., 1997; O'Donnell et al., 2000). The expression cassette described here was used in all subsequent transfection studies.

Demonstration of its functionality in the parasite was therefore important. It was considered a possibility, for example, that the presence of sgPfAMA1/HA might have a dominant negative effect, thus inhibiting the activity of wtPfAMA1. As PfAMA1 appears to be essential for parasite survival (Triglia et al., 2000) this would be lethal to the parasite and therefore transfected parasites would not be recovered. Provided that sgPfAMA1/HA did not behave in a dominant negative manner, it was predicted that episomal expression would allow localisation and processing of sgPfAMA1 to be ascertained without affecting parasite survival.

P. falciparum parasites transfected with pHAM-sgPfa/HA (referred to as 3D7-sgPfa/HA) were detected on day 28 post-transfection. The overall level of PfAMA1 expression in late schizont samples was determined by Western blot analysis using the polyclonal serum R1, PfAMA1 being expressed maximally late in this parasite stage. A lower level of PfAMA1 expression was detected in the transfected compared with the wild type parasite lines (Fig 6.4 A). This was probably a result of a lower parasite loading in this sample. Low levels of sgPfAMA1/HA were detected in schizonts by Western blot analysis with mAb 3F10 (Fig 6.4 B). Only the $PfAMA1_{66}$ form was detected, suggesting that the synthetic gene product was correctly processed. The absence of the $PfAMA1_{83}$ form, suggests that in these late stage parasites most of the processing had gone to completion. However, sgPfAMA1/HA expression was not observed in fIFA using the mAb 3F10. As was demonstrated for the COS-7 cell expression of sg'PfAMA1/HA, the mAb 3F10 was not as sensitive as the polyclonal serum N1 used here or as the mAb 4G2. This is probably partly due to the location of the single HA tag in the relatively inaccessible stub region of the PfAMA1 ectodomain. The only method of distinguishing between endogenous and synthetic gene products was the presence of the HA tag. It is also possible that the inability to detect sgPfAMA1 in IFA resulted from it being present at levels too low to be detected by mAb 3F10.

To investigate the possibility that expression of sgPfAMA1 from the episome was affected by plasmid rearrangement, plasmid recovery was performed on 3D7-sgPfa/HA and the resulting DNA analysed by restriction digestion. Genomic DNA was treated with *Dpn*I prior to transformation into *E. coli*. This restriction enzyme preferentially digests the sequence GATC in which the adenine residue is *dam* methylated. As *dam* methylation does not occur in *Plasmodium*, residual *E. coli* derived plasmid from the transfection step should be degraded by this treatment, leaving only plasmid, which has undergone replication within the parasite. This allowed the direct comparison between the original parent plasmid and that replicated in the parasite. To test the recovered plasmid for rearrangement, three different digestions were performed (Fig 6.5 A). Restriction digestion with *Afl*II (*Bfr*I) should linearise the plasmid (Fig 6.5 **D**), giving a single digestion product (9.0 kb). Digestion with *Xho*I should excise *sgPfama1* (Fig 6.5 C), cutting the plasmid into two fragments (1.9 kb and 7.2 kb). In contrast, there are two sites each for *Bam*HI and *Hind*III in the plasmid and therefore digestion with these enzymes in combination (Fig 6.5 D) should produce four digestion products (3.3 kb, 1.0 kb, 0.6 kb and 4.2

kb). When the recovered plasmid and the parent plasmid were subjected to these digestions, the same band patterns were observed on ethidium bromide stained agarose gels. The expected fragment sizes were observed with all digests (Fig 6.5 B, C and D). However, digestion with *Bam*HI and *Hind*III produced additional fragments. The reason for this is unclear, as neither enzyme is prone to star activity. As the parent plasmid gave the same pattern of digestion and this had previously been analysed by sequencing and digestion, the problem was not investigated further and the parasite-derived plasmid was assumed to be unaltered.

6.4: *Pfama1* 3' replacement

The introduction of the nine amino acid HA epitope tag into the stub region of sgPfAMA1 may have a deleterious effect on the function of this protein. To investigate this possibility, plasmid pHH1-Pfa/HA was designed to introduce the same HA epitope tag into the equivalent region of the endogenous *Pfama1* coding sequence (Fig 6.2 B) by single cross-over homologous recombination. In the event that this integration might be unsuccessful or deleterious, a similar plasmid (pHH1-3'Pfama1) was designed for direct 3' replacement. In this case the stub region consisted of endogenous gene sequence lacking the HA tag. Thus, upon integration the plasmid should reconstruct the endogenous *Pfama1* gene confirming that targeting to this region of the gene was possible. In both cases expression of the resulting gene product would be under the control of the endogenous gene promoter, and transcription termination controlled by the PbDT3' provided within the plasmid.

Parasites transfected with pHH1-3'Pfama1 and pHH1-Pfa/HA (3D7-3'Pfama1 and 3D7-Pfa/HA respectively) were detected on days 32 and 39 post-transfection respectively. Parasites were subjected to drug selection cycles using the antifolate WR99210 as described earlier. The predicted digestion pattern observed for DNA recovered from 3D7-3'Pfama1 and 3D7-Pfa/HA parasites is depicted in figure 6.6 A and B respectively. DNA loadings for Southern blot analysis were determined using ultraviolet illumination of ethidium bromide stained gels prior to transfer of DNA to Hybond N^+ membrane (Fig 6.7 A and B). After two cycles, integration was suggested from Southern blot analysis (Fig 6.7 C and D, respectively) by a decrease in the intensity of the plasmid and endogenous gene band (5.9 kb and 3.7 kb respectively for 3D7-3'Pfama1; Fig 6.6 A and 6.8 kb and 2.5 kb respectively for 3D7-Pfa/HA; Fig 6.6 B). In both cases the DNA loading for cycle 2 was greater than that for cycle 1 (Fig 6.7 A and B). This suggested that the decrease in intensity observed for the episome and endogenous gene bands was not the result of insufficient DNA in the samples. Integration of pHH1-3'Pfama1 was further confirmed by the presence of the smaller integration band (2.8 kb) after a longer exposure (Fig 6.7 C). The larger band (6.7 kb) was probably obscured by the persistent plasmid band (5.9 kb). Identification of the integration doublet in 3D7-Pfa/HA (3.8 and 4.8 kb) was more difficult. The endogenous gene band was clearly visible at 2.5 kb at cycle 0 (Fig 6.7 E) and clearly decreased in intensity from drug cycles 1 to 3 (Fig 6.7 E). However, for the 3D7 digestion there were two additional bands

present at 3.7 kb and 6 kb (Fig 6.7 E) probably resulting from incomplete digestion. The smaller of these bands was equivalent in size to the endogenous gene band observed in the *Nde*I digest of 3D7-3'Pfama1 (Fig 6.7 C and D). Digestion of DNA for the 3D7-Pfa/HA Southern blot analysis was carried out using *Nde*I and *Sna*BI. Therefore, the band at 3.7 kb probably resulted from digestion of the endogenous gene locus with *Nde*I only. In the event of successful integration, this band would be lost, as was indicated in cycle 2 (Fig 6.7 E) by loss of band intensity. By cycle 3 (Fig 6.7 E) the band appeared to run marginally higher and possibly represents the smaller (3.8 kb) integration band.

PfAMA1 was detected in 3D7-Pfa/HA by Western blot analysis using the polyclonal serum N1 (Fig 6.8 A). Furthermore, the HA tagged version of the endogenous gene product (PfAMA1/HA) was detected in 3D7-Pfa/HA by Western blot analysis in schizont stage parasites using the mAb 3F10 (Fig 6.8 B) confirming the presence of HA-tagged protein in this parasite line. However, the signal could not be detected by fIFA using the same Ab, perhaps due to the lower sensitivity of this detection method. This is consistent with the earlier finding for 3D7-sgPfa/HA parasites. However, these analyses were not carried out on a cloned parasite population. Hence, the proportion of parasites in which plasmid integration occurred upstream of the sequence encoding the HA tag may have been low, making their detection by IFA unlikely.

6.5: Functional complementation of PfAMA1

In order to formally test the functionality of the synthetic gene product, it was finally necessary to completely replace the *Pfama1* endogenous gene with the synthetic gene. Two approaches were taken to attempt this.

6.5.1: Single cross-over approach targeting the endogenous gene sequence

The construct pHH1-5'/sgPfa/HA was designed to target the PfAMA1 coding sequence (Fig 2.9). The synthetic gene expression cassette used for episomal expression of sgPfAMA1/HA (Section 2.1.4.10) was inserted into the plasmid downstream of the target sequence, a 5' region of the *Pfama1* coding sequence. Single cross-over integration would result in the insertion of the entire plasmid within the 5' region of the *Pfama1* coding sequence. A stop codon inserted in frame at the 3' end of the target sequence would result in synthesis of a truncated gene product of about 300 amino acid residues, comprising the prodomain and most of domain I. If this region of the molecule is expressed it is unlikely to be functional as it lacks the bulk of the PfAMA1 ectodomain and has no membrane association. Thus, disruption of the endogenous gene coding sequence as a result of integration at the targeted locus should be accompanied by expression of the synthetic gene product.

Viable parasites containing episomal plasmid were detected by day 21 after transfection with this construct. Figure 6.9 (A) shows the expected digestion pattern after *Sna*BI and *Pac*I digestion of DNA recovered from these transfected parasites (referred to as 3D7-5'/sgPfa/HA). Ultraviolet illumination of the ethidium bromide stained gel prior to DNA transfer for Southern blot analysis, indicated a slightly lower loading of DNA in cycle 4 than cycle 0 (Fig 6.9 B). Southern blot analysis (Fig 6.9 C) after 4 cycles of positive drug (WR99210) pressure indicated loss of intensity of the endogenous band (1.7 kb; Fig 6.9 A) suggesting integration of the plasmid into the endogenous gene locus. However, the predicted integration bands (2.4 and 10.2 kb; Fig 6.9 A) were not observed. The decrease in DNA loading observed in the ethidium bromide stained gel from cycles 0 to 4 (Fig 6.9 B) was probably not sufficient to account for the observed loss of the endogenous band. Expression of sgPfAMA1/HA was detected by Western blot analysis using the mAb 3F10 (Fig 6.10 A). The synthetic gene appeared to be successfully processed from the 83 kDa form ($sgPfAMA1_{83}$) to the 66 kDa form ($sgPfAMA1_{66}$). The processed form appeared to migrate slightly faster on the gel than the 3D7 endogenous gene product when probed with the polyclonal serum R1 (Fig 6.10 B), suggesting that the synthetic gene product has a slightly smaller mass. This may be due to the amino acid modifications introduced to remove the potential N-glycosylation sites. The $PfAMA1_{83}$ form was not detectable in the Western blot, but presumably this also has a slightly greater mass than $sgPfAMA1_{83}$. In fIFA with mAb 3F10, sgPfAMA1/HA exhibited an apical localisation, consistent with microneme association, in the merozoites of mature schizonts (data not shown). Thus, it would appear that the targeting of this gene product in developing merozoites is comparable to that of the wild type protein. The apical staining observed prior to schizont rupture was still present in free merozoites, but there was no detectable redistribution of sgPfAMA1/HA onto the merozoite surface. So far it has not been possible to determine whether shedding of the sgPfAMA1 ectodomain occurs normally. If this occurred and invasion proceeded normally, the HA tagged cytoplasmic tail would be present in ring stage parasites. This study has been unable to demonstrate this by either Western blot analysis or IFA due to time restrictions. This clearly requires further investigation.

It should be noted that expression of the synthetic gene product in 3D7-5'/sgPfa/HA parasites does not confirm integration of the plasmid. The presence of the entire synthetic gene expression cassette would allow expression from episomally maintained plasmid. To confirm integration further Southern blots must be carried out using different restriction enzymes. Nevertheless, results from the current study have conclusively shown that the synthetic gene product is expressed, localises to the apical tip of developing merozoites, presumable to the micronemes, and is correctly processed from $sgPfAMA1_{83}$ kDa to $sgPfAMA1_{66}$.

6.5.2: Double cross-over approach to excise the endogenous gene

The second approach taken was designed to replace the endogenous *Pfama1* gene entirely with the synthetic gene by double cross-over homologous recombination (Duraisingh et al., 2002)(Duraisingh *et al.* 2002). Plasmid pHTK-sgPfa/HA was designed to integrate into the genomic DNA sequence within both the 5' and 3' UTRs of the *Pfama1* endogenous gene, thus excising the endogenous gene and replacing it with the synthetic gene expression cassette (Fig 2.10). This transfection approach can result in four possible outcomes; namely that parasites maintain the plasmid episomally, that integration occurs by single cross-over at either the 5' or 3' UTR or finally that integration occurs by double cross-over. As with single cross-over homologous recombination, transfected parasites were subjected to cycles of positive drug selection using WR99210. The thymidine kinase (TK) gene present in the pHHT-TK plasmid confers ganciclovir susceptibility to the parasites providing an additional negative selection step to select for the double integration event. This is accompanied by loss of the TK cassette and excision of the intervening genomic DNA sequence (the *Pfama1* gene sequence in this case - see Fig 6.11).

There are several advantages to the double cross-over approach. Single cross-over recombination into the coding sequence of a gene can be used to disrupt the function of the gene (as described above). However, in the event that gene disruption or replacement is deleterious but non-lethal, parasites having undergone single cross-over recombination in this way could be outgrown by parasites retaining episomal plasmid copies even after growth in the absence of drug. The negative selection step inherent in the double cross-over recombination approach actively selects against parasites carrying the intact plasmid and the single cross-overs as these retain the *tk* gene and are therefore susceptible to ganciclovir. This means that parasites having undergone the double integration event should be recovered even if they exhibit growth defects, as they have a selection advantage in the presence of ganciclovir. In addition, plasmids integrated by single cross-over recombination can be lost from the genome by the same method resulting in regeneration of the endogenous gene. As integration by double cross-over homologous recombination results in excision of the endogenous gene, no subsequent recombination event can reverse this as the rest of the plasmid has been discarded in the recombination event. The resulting transgenic line is therefore stable even in the absence of drug pressure.

In the current analysis, parasites transfected with the plasmid pHTK-sgPfa/HA were detected 25 days post transfection. In recent studies (O'Donnell unpublished data) the concentration (4μM) of ganciclovir normally used for negative selection (Duraisingh et al., 2002) was insufficient to force/select for the second recombination event. In the current study negative selection was only applied after the third cycle of positive selection using elevated levels of ganciclovir (180 μM). This level was selected based on dose response assays using wild type 3D7 parasites and

transfected parasite lines and has been demonstrated to result in successful double recombination (O'Donnell unpublished data). In these cultures the parasitaemia increased to 5% within 6 days of the addition of ganciclovir, even though some cell death was initially observed after drug treatment. The expected digestion pattern after digestion with the restriction enzymes *Eco*RI and *Age*I for Southern blot analysis is depicted in figure 6.11. Illumination (UV) of ethidium bromide stained gels prior to DNA transfer (Southern blot) indicated considerably lower DNA loadings for cycles 2, 3 and 3G (Fig 6.12 A). Persistence of the (2.5 kb) endogenous gene band at was observed in Southern blot analysis after ganciclovir selection at cycle 3 (Fig 6.12 B). Bands presumed to represent digested plasmid were observed at about 7 kb and 8.2 kb. These were smaller than the 8.9 kb band expected for digested plasmid (Fig 6.11) and possibly represent incompletely linearised plasmid. These enzymes are not prone to star activity and so, these products should not be the result of aberrant digestion. An additional band of about 9 kb was present after one cycle of drug treatment (Fig 6.12 B) and this band, together with the larger plasmid band, was present in subsequent cycles. Integration by 3' cross-over was predicted to produce fragments of 2.5 kb (comparable to the endogenous gene band) and 10.3 kb. It is possible that in the agarose gel the DNA ran smaller than predicted and that the larger (9 kb) band, observed at cycle 1 and thereafter, represented the 10.3 kb band resulting from the 3' cross-over event. The persistence of the endogenous gene band would support this suggestion. The 5' cross-over was predicted to generate bands of 3.2 kb and 8.3 kb. The 8.3 kb band observed from cycle 2 onwards may represent the larger band of this cross-over event. However, the absence of a corresponding band at 3.2 kb suggests that the 5' integration event did not occur, in which case, the identity of the 8.3 kb band is unclear. Furthermore, the absence of the 3.2 kb band confirms that the double integration event did not occur successfully, unless at undetectable levels. From these results it would appear that, at most, a 3' integration event may have occurred. Time restraints prevented further analysis of this line, but the use of alternative restriction enzymes in Southern blot analysis may go some way to clarifying these results in future work.

6.6: Discussion

6.6.1. Functionality of the sgPfAMA1 expression cassette

Plasmid pHAM-sgPfa/HA contains the synthetic gene expression cassette, comprising *sgPfama1* under the control of the *Pfama1* 5' promoter and the PbDT3' UTR. The simplest method to assess the functionality of the expression cassette was by stable episomal expression of this plasmid in *P. falciparum* parasites. Healer *et al.* (2004) demonstrated that episomal expression of PfAMA1 resulted in an overall level of protein roughly equivalent to that observed in wild type parasites although the episomally encoded gene product dominated. Healer *et al* used equal numbers of segmented transfected or wild type schizonts in Western blot analysis and the resulting band intensities were comparable. This suggests the existence of

inhibitory regulation of endogenous gene expression to prevent over-expression of PfAMA1. Extrapolating this result to the current study, it might expect that a predominance of synthetic gene product over wtPfAMA1 would be seen. However, the low level of PfAMA1 expression detected in 3D7-sgPfa/HA parasite samples, made it impossible to draw any conclusions about the relative levels of endogenous versus episomal gene expression. In both studies, episomal expression was under the control of the *Pfama1* 5' promoter (with the PbDT3'). If this region contributes to regulation of expression then the two studies would be expected to give similar results, namely a higher level of expression of episomally encoded than endogenous gene product. The low level of PfAMA1 detected in this transfected parasite line compared to wild type 3D7 parasites, may result from differential loadings of parasite extract and/or low levels of mature schizonts present in the samples. The synthetic gene product detected here may reflect the lack of sensitivity of detection methods based on the mAb 3F10 rather than the level of protein expression from this expression cassette. Thus, Western blot analysis using this antibody may not be a reliable method to determine the relative expression levels of these gene products.

Kocken *et al.* (1998) previously demonstrated in transgenic *P. berghei* parasites that the timing of expression of $PfAMA1_{83}$ was critical for its correct localisation. In the current study, the use of the *Pfama1* promoter should have ensured that expression of sgPfAMA1/HA occurred at the correct time in late schizogony. Localisation of sgPfAMA1/HA by IFA (using the mAb 3F10) to the apical complex of developing merozoites transfected with pHH1-5'/sgPfa/HA confirmed that this timing was correct. This work demonstrates that the synthetic gene expression cassette is functional in *P. falciparum*, a finding that validates the use of this cassette in all of the current work described.

6.6.2: Analysis of the HA epitope tag integrated into PfAMA1

Green *et al.* (1982) demonstrated that antibodies raised against peptides from the influenza virus antigen haemagglutinin, were able to recognise the whole protein. Subsequently, a nine amino acid fragment of one of the peptides (HA1 residues 75-110) used by Green *et al.* (1982) was demonstrated to comprise the complete antigenic determinant of that peptide (Wilson *et al.* 1984). This nine amino acid sequence has since been successfully used as a fusion peptide for affinity purification purposes (Field et al., 1988). The amino acid sequence of the endogenous and synthetic gene products is not sufficiently different ordinarily to allow them to be easily distinguished, so in order to be able to distinguish between them it was necessary to introduce a tag into the synthetic gene coding sequence. Normal tagging procedure suggests that a tag be incorporated at either the N- or the C-terminus of the protein. However, AMA1 is N-terminally processed so a tag could not be fused at this end. In addition, it has been suggested that the cytoplasmic tail of AMA1 is involved in signal transduction, so addition of a tag at the carboxy-terminus was considered likely to interfere with its function (although this has not been formally

tested). For this reason the decision was made to introduce the HA epitope tag into the coding sequence of the mature protein, by minimal substitution, in a position that might not be expected to affect the function of the protein. The stub-region of the PfAMA1 ectodomain contains the site at which the proteolytic processing occurs and which results in shedding of the molecule from the parasite surface. Insertion of the tag in this region may therefore interfere with this processing step. As the normal shedding site is 17 residues N-terminal to the first residue in the inserted HA-tag, it was anticipated that inhibition of shedding would not occur. The function of AMA1 is unknown and at the time of designing these constructs no structure was available for the PfAMA1 ectodomain, thus it was impossible to accurately determine which regions of the ectodomain could be altered without deleteriously affecting the structure and/or function of the molecule. The safest strategy was therefore to alter the amino acid sequence within the stub region to incorporate this tag. However, it was necessary to determine that the tag itself had no deleterious effect on AMA1 function. For this reason, as a control, the sequence encoding this HA-epitope tag was also introduced into the endogenous PfAMA1 coding sequence.

The integration-targeting sequence in the pHH1-Pfa/HA plasmid consisted of the *P. falciparum* T9/96 PfAMA1 coding sequence from 46 bp downstream of the start site to the end of the cytoplasmic tail. The sequence encoding the HA epitope tag was embedded in the coding sequence for the stub region. Nearly 1.5 kb of coding sequence lay upstream of the HA tag sequence, compared to about 230 bp downstream of it. Therefore, integration upstream of the HA epitope tag was over six times more likely than downstream. From Southern blot analysis, it appeared that integration had occurred (Fig 6.7). Detection of the HA epitope tagged protein in Western blot analysis using the mAb 3F10 (Fig 6.8 B) confirmed that, in at least some parasites, integration had occurred upstream of the tag encoding sequence. Furthermore, the intensity of the signal in Western blot analysis using this mAb suggests that in this parasite population, a large proportion of integration events had occurred upstream of the tag encoding sequence.

Analysis of the parasite line 3D7-5'/sgPfa/HA demonstrated expression of sgPfAMA1/HA, as previously mentioned. Furthermore, in IFA the HA-tagged synthetic gene product appeared to localise correctly, at least as far as the apical tip of the parasites. This suggests that the presence of the HA epitope tag in the stub-region of the PfAMA1 ectodomain did not affect targeting of the molecule to the secretory pathway and from there to an apical compartment consistent with a microneme localisation. However, and despite several attempts, the tagged protein could not be detected on the surface of free merozoites and in ring stage parasites. One possible explanation for this is that the presence of the tag in these parasites has some effect on relocalisation of the protein onto the merozoite surface and on the final processing step during RBC invasion by merozoites. As this is likely to affect erythrocyte invasion, it is more likely that the inability to detect the HA tag in free merozoites and ring stage parasites results from the more diffuse distribution of the protein. This, coupled with the low sensitivity of the mAb 3F10 has made detection increasingly difficult. Several studies have been carried out in which

multiple consecutive copies of the HA-epitope tag have been used to tag proteins and increase the sensitivity of the detection method (Tyers et al., 1992; Krawchuk and Wahls, 1999; Harris *et al.* submitted, O'Donnell *et al.* unpublished). These studies have relied on terminally fused tags but this approach, as mentioned earlier, was not possible with this protein, Furthermore, embedding multiple tags into the ectodomain would have increased the likelihood of disrupting the proteins function. It is worth noting that the existence now of high resolution structural determinations of both PfAMA1 and PvAMA1 should aid the placement of epitope tags in future work.

The HA epitope tag was embedded in endogenous and synthetic genes to ensure minimal modification of the amino acid sequence in the stub region of these proteins. It is nevertheless possible that key residues in the PfAMA1 ectodomain have been altered. Modification of the amino acid sequence in this region of the protein is clearly not lethal to the parasite, as 3D7-Pfa/HA parasites having integrated the plasmid pHH1-Pfa/HA upstream of the HA tag encoding sequence survive. While these modifications do not abrogate the function of the protein, it is possible that they diminish its functionality. To assess the effect of the HA epitope tag in this position of the PfAMA1 ectodomain on the function of the protein 3D7-Pfa/HA parasites should be cloned. Growth rate assays (and invasion rate assays) should then be carried out to determine whether the tag confers any growth defect on the parasite. This should be a focus of future work in this area.

Plasmid pHH1-5'/sgPfa/HA was designed for integration into the PfAMA1 endogenous gene coding sequence. Integration in this position is predicted to result in disruption of the endogenous gene, replacing it with the synthetic gene sequence that has been further modified to include the coding sequence for the HA-epitope tag. Southern blot analysis suggests that this construct may have integrated into the endogenous gene locus, thus disrupting expression of wtPfAMA1. This further supports the finding that the amino acid mutations generated during introduction of the HA epitope tag into the stub region of the sgPfAMA1 ectodomain did not abrogate the function of this protein in the parasite. Integration of this construct needs to be confirmed by Southern blot analysis after digestion with alternative restriction enzymes.

In addition, integration of the HA epitope tag into the stub region of the PfAMA1 ectodomain does not appear to affect the correct processing of the wtPfAMA1 from $PfAMA1_{83}$ to $PfAMA1_{66}$. Western blot analysis of 3D7-5'/sgPfa/HA (Fig 6.10 B lane 2) shows that the synthetic gene product also undergoes this processing event. Narum and Thomas (1994) demonstrated that the full-length 83 kDa and 66 kDa forms of AMA1 differentially localise to the micronemes and merozoite surface respectively. This suggests that processing between these two forms is a prerequisite for microneme secretion of this protein. The observation that processing occurs in the presence of the HA-epitope tag suggests that, barring some other tag-induced functional defect, the processed (66 kDa) form of PfAMA1/HA should be relocalised onto the parasite

surface. This further supports the notion that the inability to detect tagged forms of PfAMA1 on the surface of free merozoites, or in ring stage parasites, by IFA reflects a lack of sensitivity in the detection method rather than the absence of the protein in these parasite stages.

6.6.3: Analysis of sgPfAMA1 functionality in *P. falciparum*

Gene replacement by homologous recombination has been used extensively to assess functional complementation of *Plasmodium* proteins. (Triglia et al., 2000) demonstrated using this technique that not only could PcAMA1 partially complement the function of PfAMA1 in *P. falciparum* parasites but that these transfected parasites demonstrated increased invasiveness of murine erythrocytes. Healer *et al.* (2005) took this finding one step further, by assessing the degree of complementation conveyed by the different sub-domains within the AMA1 ectodomain. Constructs were designed for the expression of chimeras of AMA1, comprising mixtures of the PfAMA1 and PcAMA1 domains, for transfection into *P. falciparum*. The group determined that DI-II of PcAMA1 in conjunction with the prodomain and DIII of PfAMA1, was processed normally and partially complemented the function of PfAMA1, though to a lesser extent than intact PcAMA1. However, processing of the 83 kDa form of the chimeric protein containing the PfAMA1 prodomain and DI-II and PcAMA1 DIII to the 66 kDa form did not occur and the protein was unable to redistribute onto the surface of the parasite. As a result, this chimeric protein was unable to complement PfAMA1 function. In an analogous study with a different merozoite protein, O'Donnell *et al.* (2000) demonstrated that the C-terminal 19 kDa fragment of *P. falciparum* MSP1 could be complemented in function with the corresponding sequence from *P. chabaudi* MSP1. This region of PcMSP1 diverges significantly in sequence from that of PfMSP1, indicating that the role of this fragment in erythrocyte invasion is conserved across the genus.

As was observed in chapter 4, single point mutations (for example K280/A) can disrupt the overall architecture of a protein. Confirmation that the mutations introduced into the PfAMA1 synthetic gene to replace the potential N-glycosylation sites did not affect protein folding and function was therefore necessary. For this reason, complementation studies were carried out using *sgPfama1*.

In plasmid pHH1-5'/sgPfa/HA the synthetic gene expression cassette lies downstream of the PfAMA1 5' coding sequence. The presence of this coding sequence should target the construct for integration into the *Pfama1* gene sequence and result in the disruption of the endogenous gene. In the event that integration does not occur, expression of the synthetic gene product should still take place from the episomally maintained plasmid. Southern blot analysis suggests that this plasmid may have integrated (Fig 6.9 C). However, the absence of the predicted integration bands suggests that caution is required in drawing conclusions from this. If the decrease in the endogenous gene band intensity is a genuine indication of integration, this

suggests that most of the parasites present have integrated the plasmid. In addition, it would indicate that the synthetic gene product can indeed complement the function of the endogenous gene. To ascertain whether this gene replacement has produced any phenotypic effect, growth and invasion rate assays should be carried out using cloned parasite lines.

Integration by double cross-over using the TK selection cassette is a slow and unreliable process. The inability to isolate any double integrants in the current study does not necessarily suggest that this gene locus cannot be targeted for double cross-over. It may suggest that the conditions required for this integration have not yet been identified. Integration into non-coding sequence in *P. falciparum* is less favourable than integration into coding sequence (Wu *et al.* 1996), possibly due to the increased A+T content in intragenic regions (Aravind et al., 2003). It follows therefore that double integration into non-coding sequence is an extremely rare event. If replacement of the endogenous gene with the synthetic gene product by targeting the endogenous gene coding sequence has occurred, this would suggest that the lack of gene replacement by the double cross-over method results from methodological problems rather than the inability of the synthetic gene product to complement the function of the wtPfAMA1.

If the integration of pHH1-5'/sgPfa/HA into the endogenous *Pfama1* gene can be validated it would suggest functional complementation of the endogenous gene product. To confirm conclusively the level of complementation, transfected parasite lines in which the endogenous gene has been replaced with the synthetic gene must be cloned and compared in growth and invasion rate assays with wild type 3D7 parasites. To distinguish between growth defects conferred by the HA epitope tag and the synthetic gene product itself, these parasites should also be compared with parasites in which the endogenous gene has been tagged (3D7-Pfa/HA parasites).

In conclusion, the ability to target the 3' region of *Pfama1* by single cross-over homologous recombination has been confirmed using the plasmids pHH1-3'Pfama1 and pHH1-Pfa/HA. In addition, Western blot analysis and IFA have confirmed that embedding the HA-epitope tag into the stub-region of the PfAMA1 ectodomain is not lethal to the parasite. It has yet to be confirmed that the HA-tagged protein can be redistributed onto the parasite surface at the time of schizont rupture and that the tag does not interfere with the final shedding of the protein from the merozoite surface. Use of a triple-HA tag may overcome the sensitivity problems encountered with 3F10, but this raises additional problems of where to locate such a tag. Expression of the synthetic gene product and correct targeting to the apical organelles has been confirmed in Western blot analysis and IFA of 3D7-5'/sgPfa/HA parasites, respectively. It remains to be conclusively demonstrated that the HA-tagged synthetic gene product can complement the function of the native protein. This will clearly be the focus of future work in this area. Not only will this justify the use of the synthetic gene in further reverse genetics studies

designed to investigate the function of AMA1, it will also validate the use of the synthetic gene product in functional studies of PfAMA1.

Fig 6.1: Clustal alignment of *Plasmodium* AMA1 amino acid sequences shows a lack of sequence homology at the putative N-glycosylation site at position 371 in the PfAMA1 ectodomain

The position of N371 is highlighted in red. Residues corresponding to the third position of the glycosylation motif (N-X-S/T) are indicated in blue. This sequence alignment shows that the asparagine is highly conserved at the equivalent position in other species of *Plasmodium*, deviating only (to aspartic acid) in *P. fragile*. By comparison, the third amino acid in the motif (S) is only conserved in *P. reichenowi* and *P. cynomolgi*.

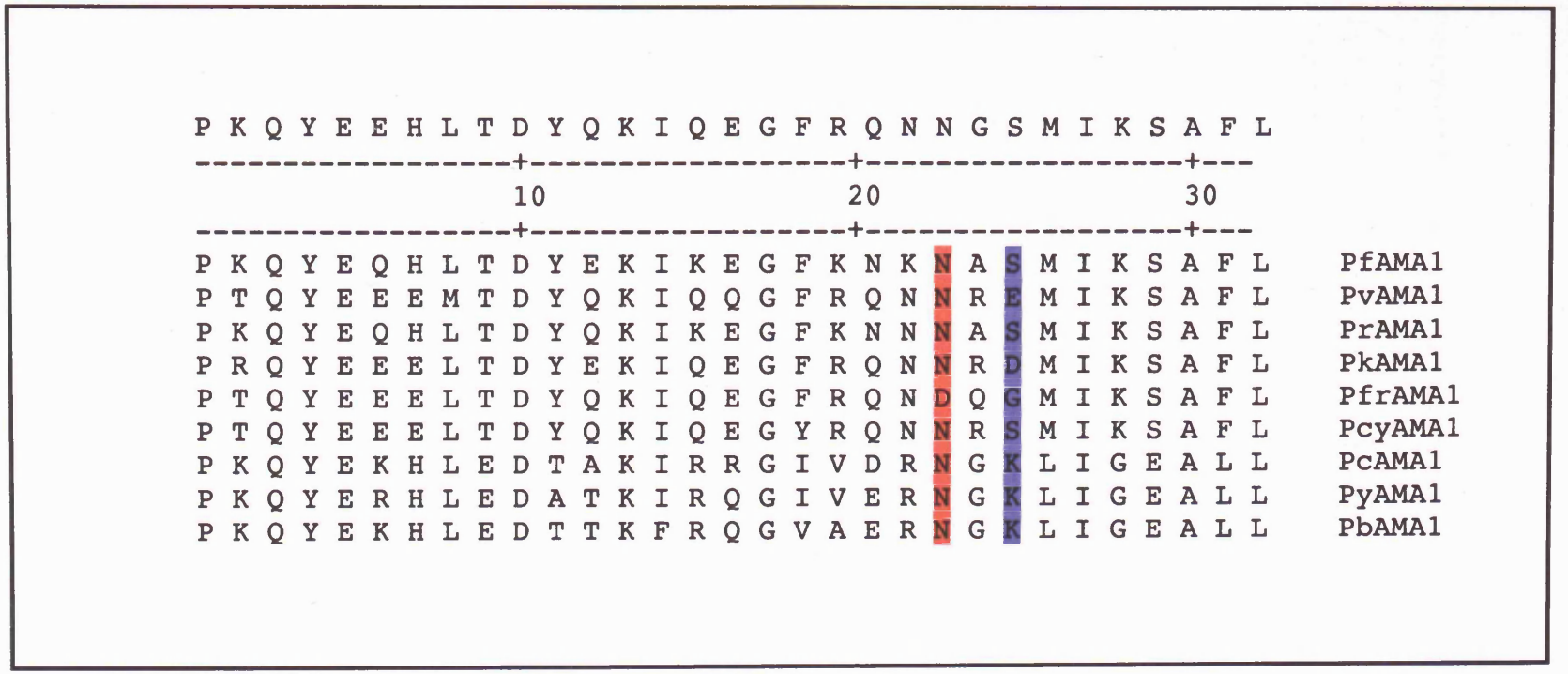
P K Q Y E E H L T D Y Q K I Q E G F R Q N N G S M I K S A F L
10
20
30
P K Q Y E Q H L T D Y E K I K E G F K N K N A S M I K S A F L PfAMA1
P T Q Y E E E M T D Y Q K I Q Q G F R Q N N R E M I K S A F L PvAMA1
P K Q Y E Q H L T D Y Q K I K E G F K N N N A S M I K S A F L PrAMA1
P R Q Y E E E L T D Y E K I Q E G F R Q N N R D M I K S A F L PkAMA1
P T Q Y E E E L T D Y Q K I Q E G F R Q N D Q G M I K S A F L PfrAMA1
P T Q Y E E E L T D Y Q K I Q E G Y R Q N N R S M I K S A F L PcyAMA1
P K Q Y E K H L E D T A K I R R G I V D R N G K L I G E A L L PcAMA1
P K Q Y E R H L E D A T K I R Q G I V E R N G K L I G E A L L PyAMA1
P K Q Y E K H L E D T T K F R Q G V A E R N G K L I G E A L L PbAMA1

Figure 6.2: Integrating the HA Tag into the PfAMA1 ectodomain.

The nucleotide and amino acid modifications required in order to embed the HA epitope tag into the stub region of the PfAMA1 ectodomain of **(A)** the synthetic and **(B)** the endogenous 3D7 gene sequences. Nucleotide modifications are shown in red. Amino acid modifications are highlighted in blue.

A

	I	P	E	H	K	P	T	Y	D
Synthetic gene sequence	ATT	CCA	GAG	CAT	AAG	CCT	ACG	TAC	GAT

HA tag sequence	TAT	CCA	TAC	GAT	GTG	CCT	GAC	TAT	GCT
	Y	P	Y	D	V	P	D	Y	A

B

	I	P	E	H	K	P	T	Y	D
Endogenous gene sequence	ATT	CCT	GAA	CAT	AAG	CCA	ACT	TAT	GAT

HA tag sequence	TAT	CCT	TAC	GAT	GTG	CCA	GAT	TAT	GCT
	Y	P	Y	D	V	P	D	Y	A

Figure 6.3: IFA and Western blot analysis confirm expression of sg'PfAMA1/HA in COS-7 cells

IFA was carried out on acetone fixed COS-7 cells expressing sg'PfAMA1/HA, using the polyclonal serum N1 **(A)** and the mAbs 4G2dc1 **(B)** and 3F10 **(C)**. The cells were additionally stained with DAPI (blue) and Evans blue (red). Western blot analysis was carried out on COS-7 cell lysates from lines expressing sg'PfAMA1/HA **(1)** or sg'PfAMA1 **(3)** or on untransfected COS-7 cells as a negative control **(3)**. The polyclonal serum R1 **(D)** and the anti-HA Abs 12CA5 **(F)** and 3F10 **(G)** were used to probe samples prepared under reducing conditions, whereas the mAb 4G2dc1 **(E)** was used to analyse samples under non-reducing conditions. The non-specific band recognised in COS-7 cell lysate by 12CA5 is indicated (arrow).

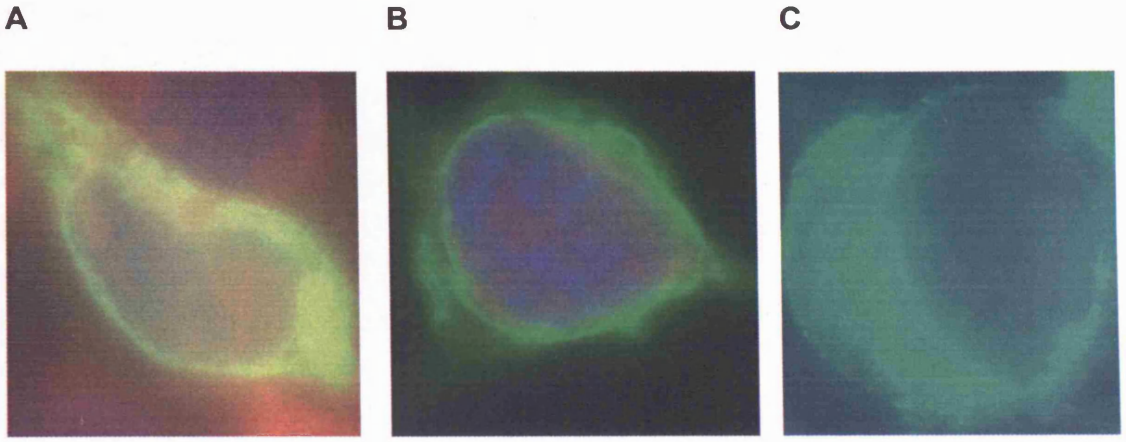
A
B
C

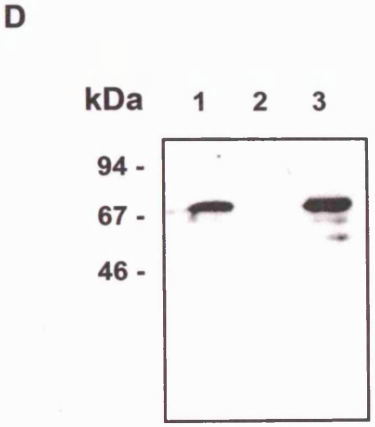
D
kDa
1
2
3
94 -
67 -
46 -

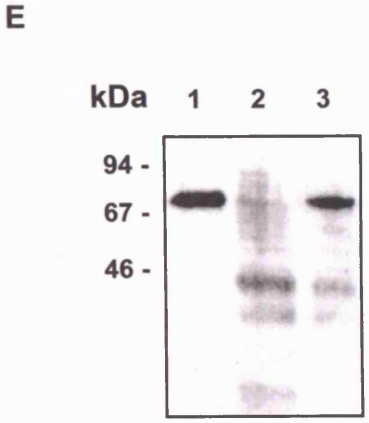
E
kDa
1
2
3
94 -
67 -
46 -

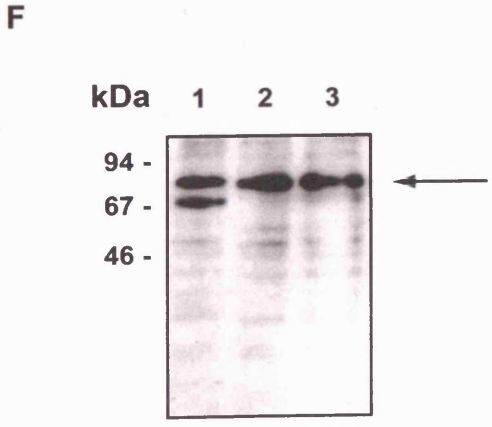
F
kDa
1
2
3
94 -
67 -
46 -

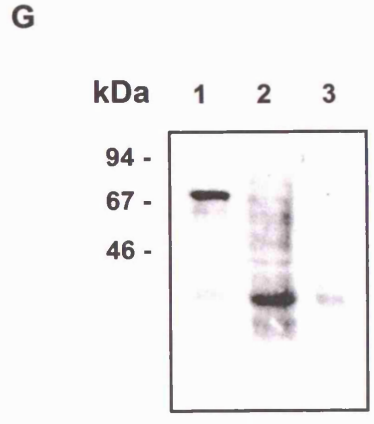
G
kDa
1
2
3
94 -
67 -
46 -

Figure 6.4: Western blot analysis indicates low level expression of sgPfAMA1/HA from the sgPfAMA1 expression cassette in 3D7 parasites

Lysates from wild type 3D7 and 3D7-sgPfa/HA schizont stage parasites were electrophoresed under reducing conditions and analysed by Western blot with the polyclonal serum R1 **(A)** and the mAb 3F10 **(B)**. The 83 and 66 kDa fragments of PfAMA1 are indicated (arrows). The HA-tagged form of sgPfAMA1 is also indicated (**B**, arrow).

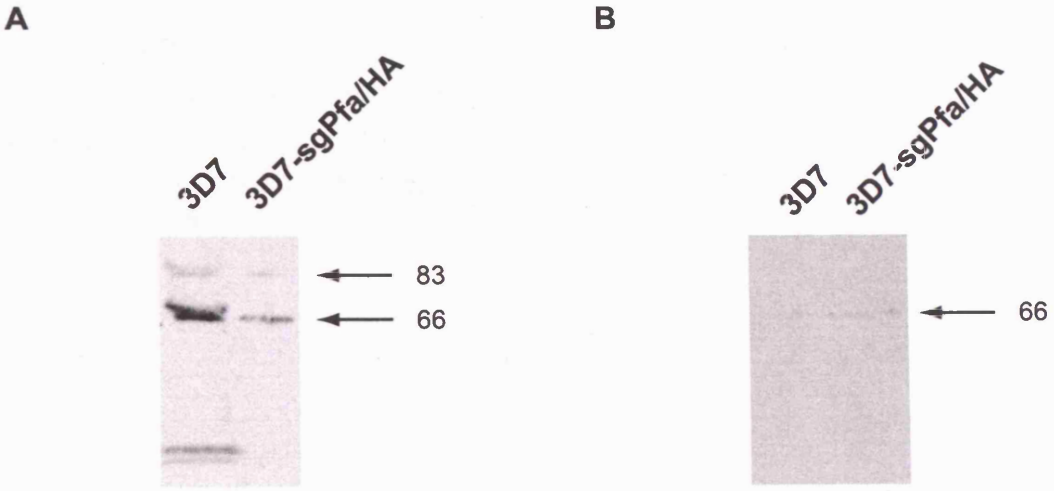
A
3D7
3D7-sgPfa/HA
83
66
B
3D7
3D7-sgPfa/HA
66

Figure 6.5: Confirmation of the fidelity of the plasmid pHAM-sgPfa/HA by plasmid rescue

Plasmid DNA was recovered from the transfected parasite line 3D7-sgPfa/HA, after treatment with *Dpn*I to destroy any remaining parent plasmid, and cloned in *E. coli*. Five bacterial clones were selected, the plasmid purified and analysed by restriction digestion with *Bam*HI and *Hind*III **(B)**, *Xho*I **(C)** and *Afl*II **(D)**. The positions of the restriction sites in the plasmid are indicated **(A)**. Expected plasmid sizes are also indicated. Digestion products of the five clones (lanes **2 - 6**) were run along side those of the parent plasmid (lane **1**).

A

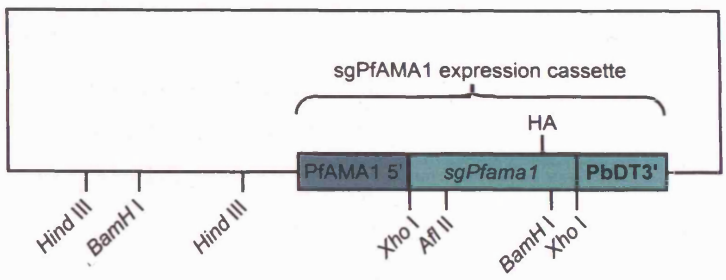

pHAM-sgPfa/HA

B

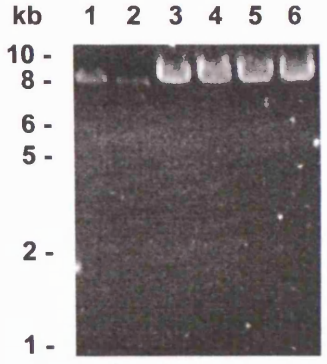

C

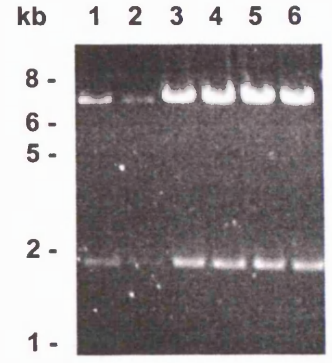

D

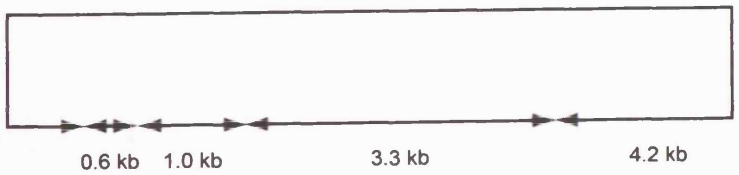

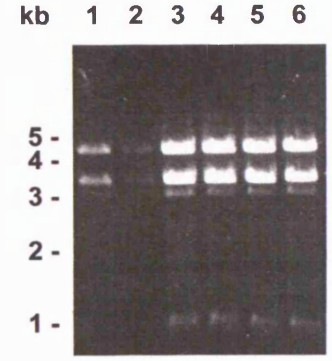

Figure 6.6: Plasmids used and potential integration events following transfection of *P. falciparum* parasites

The 3' replacement plasmids pHH1-3'Pfama1 and pHH1-Pfa/HA were constructed by ligating the target DNA fragment into unique BglII and XhoI sites in the vector pHH1. The target DNA consisted of a 0.9 kb 3' region (**A**, yellow) and the entire *Pfama1* sequence (**B**, pink) minus that encoding the N-terminal 46 amino acids and modified by the addition of the sequence encoding the HA-epitope tag, respectively. Both sequences extended to include the 3' stop codon. The predicted structures of the *ama1* gene loci after plasmid integration are shown below. The location of the restriction enzyme sites (*Nde*I and *Sna*BI) used to map these loci is indicated. The predicted sizes are not drawn to scale.

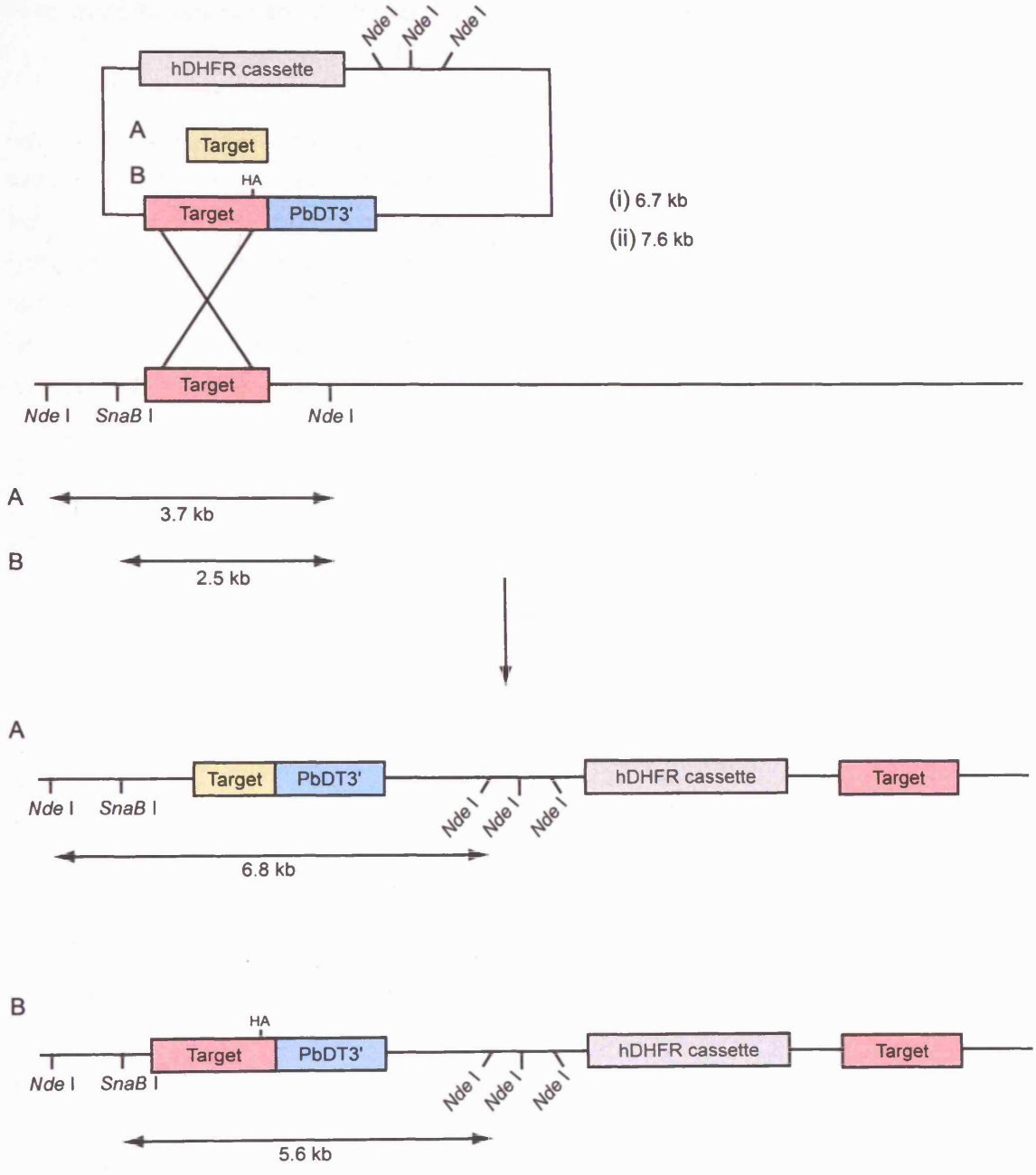
Nde I
Nde I
Nde I
hDHFR cassette
A
Target
B
HA
Target
PbDT3'
(i) 6.7 kb
(ii) 7.6 kb
Target
Nde I
SnaB I
Nde I
A
3.7 kb
B
2.5 kb
A
Target
PbDT3'
hDHFR cassette
Target
Nde I
SnaB I
Nde I
Nde I
Nde I
6.8 kb
B
HA
Target
PbDT3'
hDHFR cassette
Target
Nde I
SnaB I
Nde I
Nde I
Nde I
5.6 kb

Figure 6.7: Southern blot analysis of genomic DNA from transfected *P.falciparum* parasites indicating integration of pHH1-3'Pfama1 and pHH1-Pfa/HA

UV gels to confirm the DNA loading used in the Southern blots shows greater loading for cycles 0 and 2 for pHH1-3'Pfama1 **(A)** and cycle 2 for pHH1Pfa/HA **(B)** than for other cycles. In order to compare the restriction profile of these transfected parasite lines with that of 3D7 wild type parasites, DNA from 3D7-3'Pfama1 parasites was restriction digested with the enzyme NdeI, while 3D7-Pfa/HA DNA was digested with NdeI and *Sna*BI. A 0.5 kb fragment from within the 3' target region of the plasmid was used to probe these blots. The restriction profile for these transfected parasite lines was compared with that of 3D7 wild type parasites as a control. Integration was indicated for both 3D7-3'Pfama1 **(C)** and 3D7-Pfa/HA **(D)** parasites, by a decrease in intensity of the endogenous gene band (3.7 and 2.5 kb respectively) by cycle 2. This was accompanied in both cases by a decrease in the plasmid band (5.9 and 6.8 kb respectively). Concomitant with this for 3D7-3'Pfama1 parasites was the appearance of the integration band (2.9 kb). The larger integration band (6.8 kb) is probably obscured by the plasmid band. Integration bands were not apparent for parasite line 3D7-Pfa/HA but this may have been due to incomplete digestion by *Sna*BI. The digestion band at about 3.7 kb, present at all cycles, corresponded to the endogenous gene band digested with NdeI alone **(D)**.

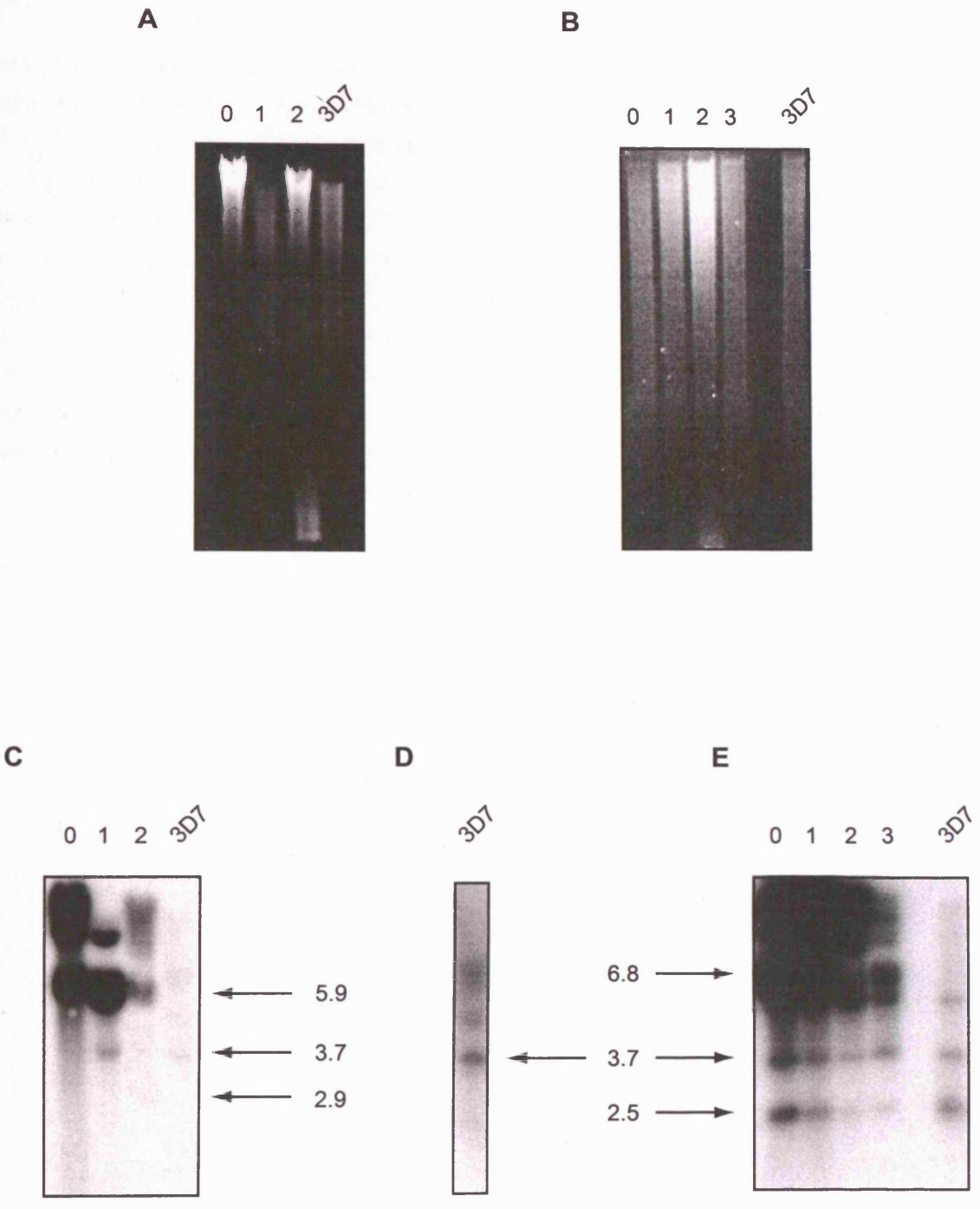
A
0 1 2 3D7
B
0 1 2 3 3D7
C
0 1 2 3D7
5.9
3.7
2.9
D
3D7
6.8
3.7
2.5
E
0 1 2 3 3D7

Figure 6.8: Western blot analysis confirms expression of HA tagged PfAMA1 in 3D7-Pfa/HA parasites

Schizont stage parasites were analysed under reducing conditions in Western blot, using the polyclonal serum R1 **(A)** and mAb 3F10 **(B)**. In each case wild type 3D7 parasites were used as a positive control. The PfAMA1 83 and 66 kDa forms are indicated (arrows).

A

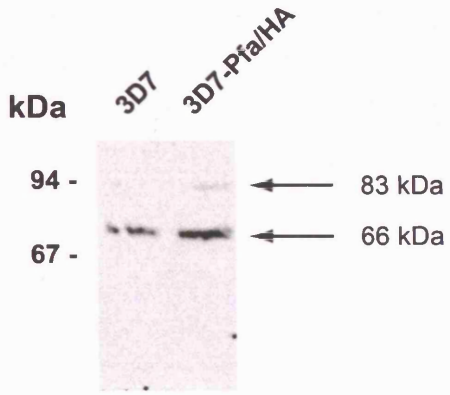
kDa
3D7
3D7-Pfa/HA
94 -
67 -
83 kDa
66 kDa

B

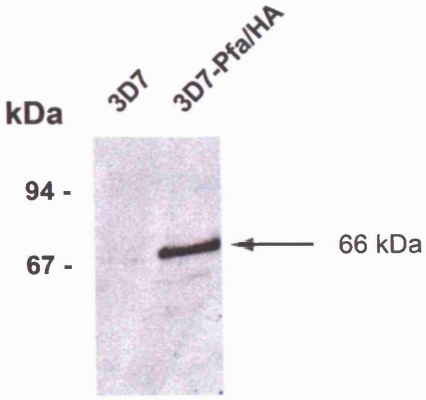
kDa
3D7
3D7-Pfa/HA
94 -
67 -
66 kDa

Figure 6.9: Plasmids used and potential integration events following transfection of *P. falciparum* parasites with pHH1-sgPfa/HA

(A) The gene replacement vector was constructed by ligating the PfAMA1 synthetic gene expression cassette (green) downstream of the target sequence, 0.9 kb of the PfAMA1 5' coding sequence (purple). The selectable marker (hDHFR) cassette is shown. The predicted structure of the AMA1 locus following integration is depicted below. The position of *Sna*BI and *Pac*I restriction sites for mapping these loci is indicated. Map sizes were not drawn to scale. **(B)** UV gel image, taken prior to the transfer of DNA to nitrocellulose for the Southern, indicated that the loadings were approximately equivalent. **(C)** Southern blot analysis of 3D7-5'/sgPfa/HA parasite genomic DNA followed drug selection cycles 0 and 4. A 0.5 kb 5' fragment of endogenous *Pfama1* was used to probe the membrane. Wild type 3D7 parasites were used as a positive control. Endogenous gene and plasmid bands are indicated (1.7 and 10.9 kb, respectively). No integration bands are evident, however at cycle 4 the endogenous gene band is reduced.

A

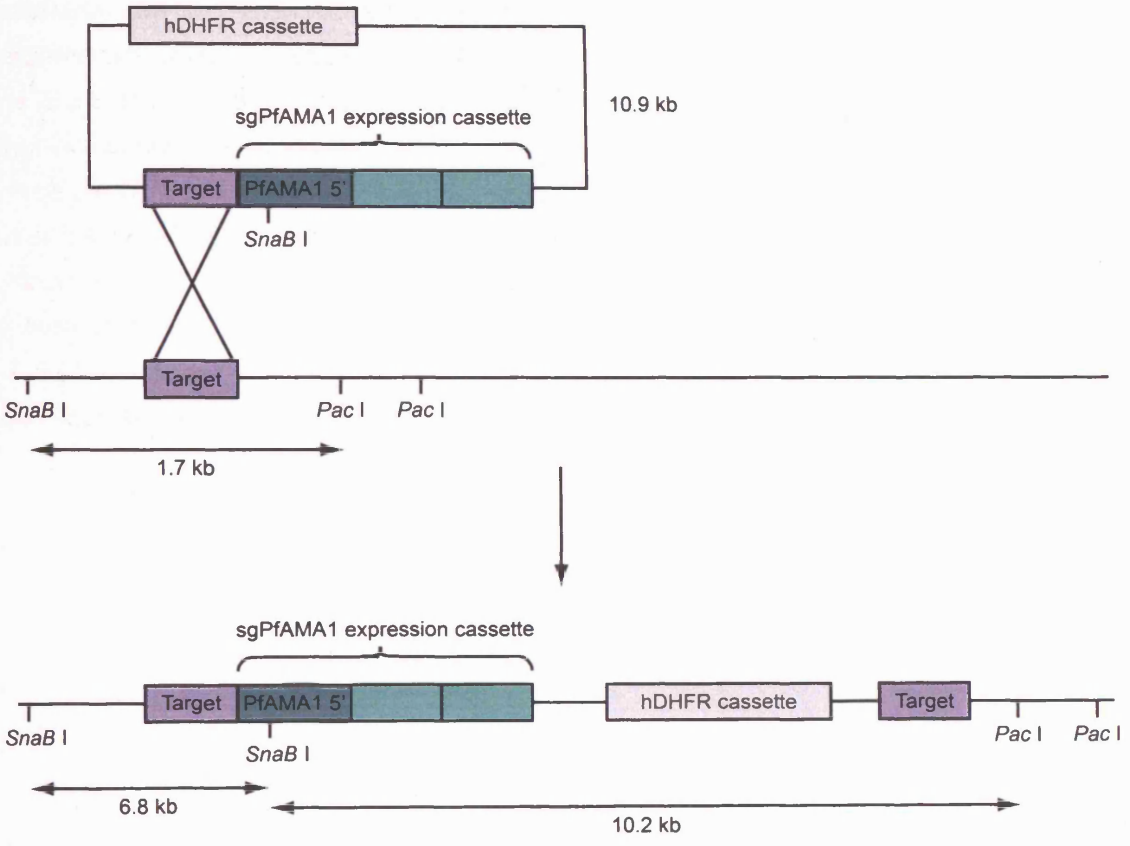
hDHFR cassette
10.9 kb
sgPfAMA1 expression cassette
Target
PfAMA1 5'
SnaB I
Target
SnaB I
Pac I
Pac I
1.7 kb
sgPfAMA1 expression cassette
Target
PfAMA1 5'
hDHFR cassette
Target
SnaB I
SnaB I
Pac I
Pac I
6.8 kb
10.2 kb

B

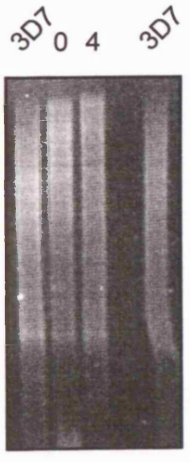
3D7
0
4
3D7

C

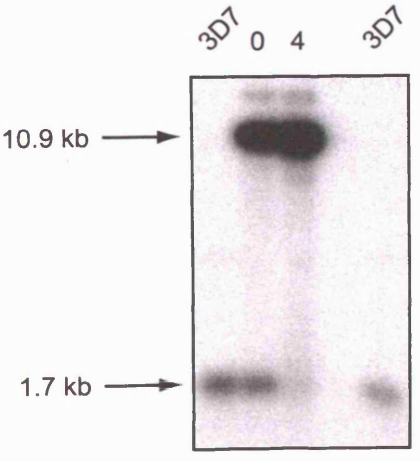
3D7
0
4
3D7
10.9 kb
1.7 kb

Figure 6.10: IFA and Western blot analysis indicate correct expression of sgPfAMA1/HA in *P. falciparum* parasites.

Protein extracts from schizont enriched 3D7-5'/sgPfa/HA wild type 3D7 parasites were analysed under reducing conditions in Western blot, using the mAb 3F10 **(A)** and polyclonal serum R1 **(B)**. Both $PfAMA1_{83}$ and $PfAMA1_{66}$ forms were detected by mAb 3F10 indicating the correct processing of this product.

A

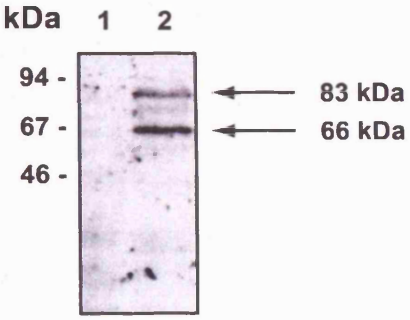

B

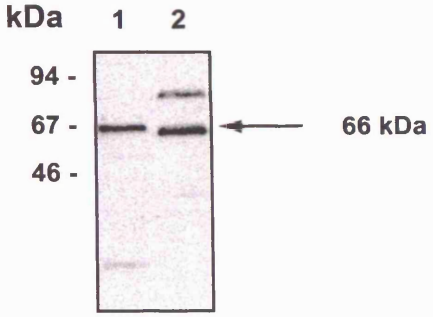

Figure 6.11: Schematic representation of the plasmid and potential integration events following transfection of *P.falciparum* with pHTK-sgPfa/HA

(A) The vector designed for gene replacement by double cross-over was constructed by ligating the synthetic gene expression cassette (green) as well as a 0.9 kb sequences from the 3' UTR (brown) of *Pfama1* into the pHHT-TK plasmid. The two selectable marker cassettes (hDHFR and TK) are shown. The integration target sequence were the 0.9 kb 3' UTR and the 1.4 kb 5' promoter region of *Pfama1* (dark green) present in the synthetic gene expression cassette. The predicted structures of the *ama1* locus after integration are shown below (**B, C, and D**). The location of *Eco*RI and *Age*I restriction sites used to map these loci are indicated and their calculated masses indicated in kb. The sizes of the predicted maps are not drawn to scale.

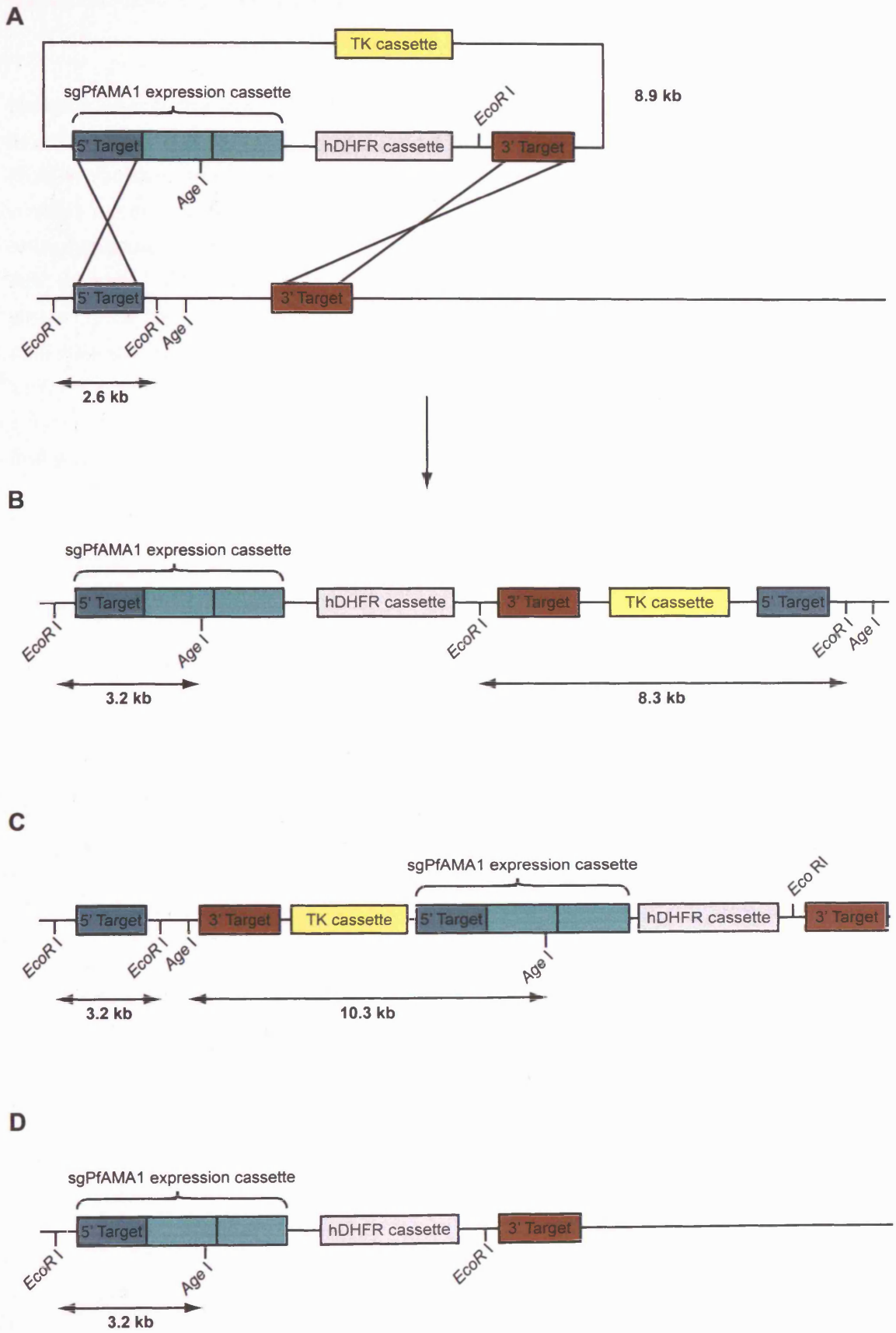
A
TK cassette
sgPfAMA1 expression cassette
8.9 kb
EcoR I
5' Target
hDHFR cassette
3' Target
Age I
5' Target
3' Target
EcoR I
EcoR I
Age I
2.6 kb
B
sgPfAMA1 expression cassette
5' Target
hDHFR cassette
3' Target
TK cassette
5' Target
EcoR I
Age I
EcoR I
EcoR I
Age I
3.2 kb
8.3 kb
C
sgPfAMA1 expression cassette
Eco RI
5' Target
3' Target
TK cassette
5' Target
hDHFR cassette
3' Target
EcoR I
EcoR I
Age I
Age I
3.2 kb
10.3 kb
D
sgPfAMA1 expression cassette
5' Target
hDHFR cassette
3' Target
EcoR I
Age I
EcoR I
3.2 kb

Figure 6.12: Southern blot analysis of pHTK-sgPfa/HA transfected parasite and parent 3D7 genomic DNA

(A) The UV image of restriction enzyme digested samples for Southern blot analysis indicated that drug cycles 0 and 1 have the highest DNA loading. Southern blot analysis was carried out on genomic DNA extracted after cycles 0, 1, 2 and 3 and on drug cycle 3 after growth of parasites in the presence of ganciclovir (3G). After electrophoretic transfer of the DNA to nitrocellulose, the membranes were probed with a 0.4 kb fragment from the 5' promoter region (5' target sequence) in the synthetic gene expression cassette **(B)** Parental 3D7 genomic DNA was used as a control. The presence of endogenous gene (2.6 kb) and plasmid (8.9 kb) bands is indicated as is the predicted large 3' integration band (10.2 kb) that is possibly present from cycle 2 onwards. There is no indication of the presence of the band corresponding to the 3' or double integration fragments (3.2 kb), although the larger fragment (8.3 kb) corresponding to the 3' integration could be masked by the plasmid band, the absence of the smaller fragment refutes this.

A

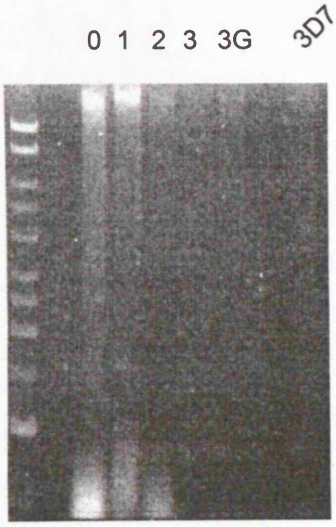

B

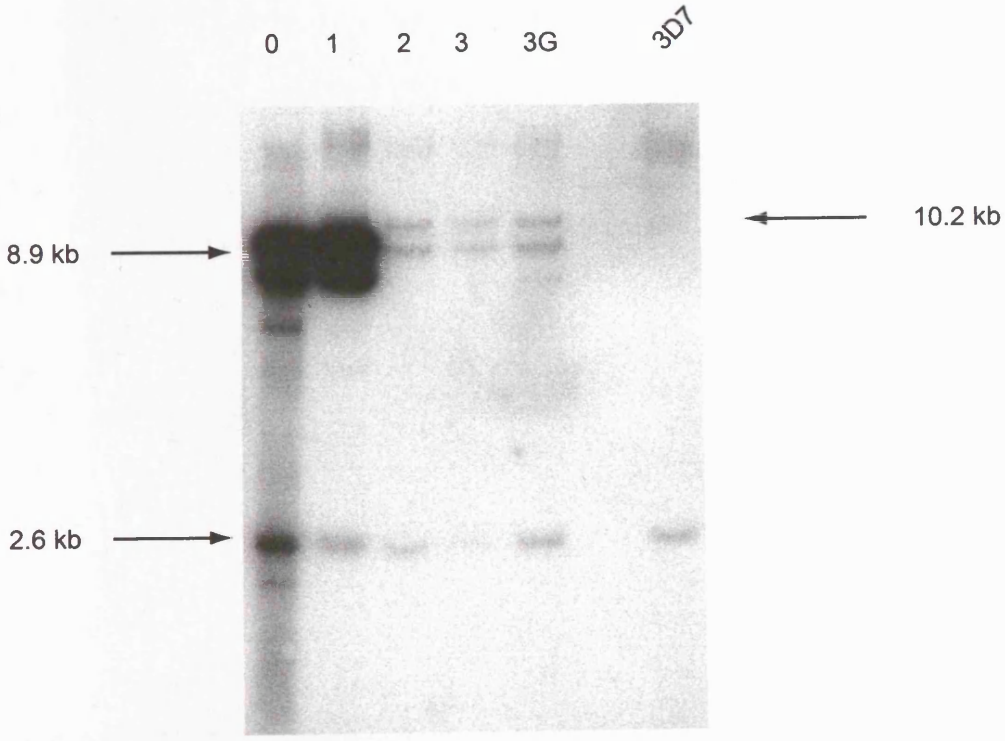

Chapter 7

Discussion

7.1: AMA1 as an erythrocyte binding molecule

AMA1 plays an essential role in host cell invasion by apicomplexan parasites. For this reason, a considerable amount of effort has gone into understanding the immunogenicity, structure and function of the molecule. The structure of both PvAMA1 DI-III and PfAMA1 DI-II have provided significant insight into understanding the immune selection pressure that this conserved molecule is under and the structural and possibly functional constraints placed upon it (Pizarro *et al.* 2005; Bai *et al.* 2005). In addition an increasing body of evidence implicates this antigen as having a role in RBC binding during invasion. The functional and immunogenic importance of AMAI have resulted in its being one of the leading candidates for inclusion in an asexual stage vaccine against *P. falciparum* malaria.

The existence of mAbs against AMA1 that block merozoite invasion of erythrocytes by preventing the formation of a close interaction between the two cells, suggests that AMA1 participates in host cell invasion by interacting with an erythrocyte receptor molecule (Deans et al., 1982; Mitchell et al., 2004). This is further supported by the observation that expression of PcAMA1 in *P. falciparum* allows this parasite species to invade murine erythrocytes, albeit inefficiently (Triglia et al., 2000). The absolute requirement by the parasite for AMA1 together with its integral involvement in the invasion process and apparent host-cell specificity, support the idea that AMA1 plays a role in merozoite adhesion to the RBC surface. The identification of two PAN modules (one in each of DI and DII) in PvAMA1 and PfAMA1, together with the evidence from other systems that PAN modules facilitate protein-protein and/or protein-carbohydrate interactions (Tordai et al., 1999) suggests an adhesive role for these domains in the AMA1 ectodomain (Pizarro et al., 2005). Furthermore, the identification of PAN or Apple domains in many microneme proteins from different apicomplexan parasites and the perceived role for microneme proteins in host cell attachment during invasion, raises the possibility that apicomplexan parasites exploit the PAN domain fold to overcome the problem of host cell recognition and receptor binding (Klein et al., 1996; Brown et al., 2000; Brown et al., 2001; Brecht et al., 2001). Fraser *et al.* (2001), demonstrated that DI-II of PyAMA1, but not the full-length ectodomain, bound murine erythrocytes, whereas Kato *et al.* (2005), demonstrated binding of PfAMA1 DIII to human erythrocytes. This raises the possibility that in different species of *Plasmodium* AMA1 utilises different domains to facilitate erythrocyte binding. The degree of structural similarity observed in the crystal structures obtained from PvAMA1 and PfAMA1, argues against this possibility. Several attempts to demonstrate erythrocyte binding using the PfAMA1 ectodomain shed from the parasite surface have proven unsuccessful (Howell *et al.*

2001; E. knuepfer, personal communication). However, the loss of binding capabilities as a result of proteolytic shedding from the parasite surface is not without precedent, as the full-length cellular form of *T. gondii* MIC2 binds host cells, while the proteolytically shed form does not (Carruthers *et al.* 1999c).

The present study has failed to demonstrate any erythrocyte binding activity for the full-length ectodomain of PfAMA1 or for DIII on its own when expressed on the surface of COS-7 cells. Erythrocyte binding was, however, easily observed with region II of the PvDBP, used in this study as a positive control. The ability of PvDBP to support erythrocyte binding under the same conditions, suggests that the inability to demonstrate erythrocyte binding with PfAMA1 was because of the choice of antigen, not because of the system. The question therefore remains; why was sgPfAMA1 unable to support erythrocyte binding activity if this is a genuine property of the molecule? The study further failed to demonstrate erythrocyte binding with DI-III of sgPfAMA1 expressed in *P. pastoris*, in a solid phase assay system, suggesting that the local concentration of sgPfAMA1 on the COS-7 cell surface was not a limiting factor in the former assay. The ability noted by the other workers, referred to above, of PyAMA1 DI-II, and to a lesser extent DI-III, to bind murine erythrocytes in the same expression system could result from parasite species differences in AMA1. Alternatively, chimeric expression of PyAMA1 DI-II in association with the HSVgD1 transmembrane domain may have resulted in the presentation of PyAMA1 on the COS-7 surface in a conformation not normally observed in AMA1 on the parasite surface (or when shed from the surface). The ability of DI-II to bind with higher efficiency than DI-III, suggests that even in *P. yoelii* the full-length ectodomain is not immediately accessible in a conformation likely to favour erythrocyte-binding. The current study has argued for the existence of a partner protein, which may act in conjunction with AMA1 at the parasite surface. One possible explanation for the apparent inconsistency between these two sets of results is that AMA1 undergoes some conformational change when it encounters such a putative partner protein on the parasite surface. This conformational change may expose a region of the AMA1 that is otherwise concealed, but that was exposed when PyAMA1 DI-II was expressed on its own in COS-7 cells in the study of Fraser *et al.* (2001). The revealed domain may then be able to interact with its receptor on the erythrocyte surface. If this were the case, using 4G2dc1 recognition in this assay as a measure of native fold may be inappropriate. This mAb recognises the shed fragments of PfAMA1, which do not support erythrocyte binding. Furthermore, 4G2dc1 results in the immunoprecipitation of PfAMA1 in isolation from any putative partner protein which, as it has just been argued may be required for induction of the conformational change necessary for erythrocyte binding. Thus, while this mAb is a useful tool in confirming disulphide bond formation and the correct overall architecture of the PfAMA1 ectodomain, it may not be sensitive enough to distinguish between functionally active and inactive conformations. The method of action by this mAb in invasion-inhibition may be to actively block the binding of PfAMA1 to its partner on the merozoite surface. Alternatively, it may prevent the conformational change required for PfAMA1 to interact with its erythrocyte receptor.

7.2: Characterisation of the AMA1 epitope recognised by the invasion inhibitory mAb 4G2dc1

The mAb 4G2dc1 inhibits invasion of erythrocytes by *P. falciparum* and *P. reichenowi* merozoites (Kocken et al., 1998b; Kocken et al., 2000). Thus, the epitope recognised by this mAb is of considerable interest for understanding the function of this molecule during this parasite stage and for vaccine development. Results described in the current study and reported elsewhere (Pizarro *et al.* 2005) have for the first time identified amino acid residues in the PfAMA1 ectodomain that are specifically responsible for recognition of the molecule by this important mAb. These residues lie within a region of the molecule now termed the domain II loop (Pizarro *et al.* 2005). This loop displayed no electron density in the crystal structure of PvAMA1, suggesting that this region of the molecule adopts a flexible conformation that extends from the molecule (Pizarro *et al.* 2005). The accessibility of the loop to tryptic digestion is in agreement with this hypothesis (Gupta *et al.* 2005). The flexible nature of this loop is also supported by work on the PfAMA1 DI-II crystal structure; although in the published structure the majority of the loop was structured, with the exception of four residues located in the C-terminus of the loop (Bai *et al.* 2005), two further structures of these domains solved by the same group gave different results for the DII loop region. In one, the loop took up an alternative conformation while in the other it was unstructured as for the *P. vivax* structure (A. Batchelor, personal communication). Locating the 4G2dc1 epitope at the base of the DII loop, as described in the current study, raises the possibility that this mAb interferes with the essential flexibility of this region and identifies an important functional region of the PfAMA1 ectodomain.

In support of these findings, Urquiza *et al.* (2001) identified four peptides from AMA1 that bound human erythrocytes *in vitro* and which blocked merozoite invasion. The peptide exhibiting the highest percentage invasion-inhibition (peptide 4325-MIKSAFLPTGAFKADRYKSH) derives from the DII loop (Urquiza *et al.* 2001; Cubillos *et al.* 2003). Peptide 4337, deriving from the cytoplasmic tail of PfAMA1, also exhibited a high degree of invasion-inhibition in this assay (Urquiza *et al.* 2001; Salazar *et al.* 2002). The location of this latter peptide in the cytoplasmic tail of PfAMA1 calls into question its ability to bind to RBCs and inhibit merozoite invasion. If this is the case, this also calls into question the validity of the result observed for the peptide derived from the DII loop, as it suggests there is non-specific interaction occurring in the assay. However, if the erythrocyte binding/invasion-inhibition activity of the peptide derived from the DII loop is indeed physiologically significant, this could suggest that the DII loop and the hydrophobic trough with which it interacts are specifically involved in erythrocyte binding. This suggestion seems increasingly likely when considering the invasion inhibitory properties of 4G2dc1 and the conserved nature of the residues in the hydrophobic trough. The enhanced inhibition observed in the current study and elsewhere (Dutta *et al.* 2005) by the 4G2dc1 Fab fragment, compared to that mediated by the intact antibody, suggests that inhibition by this mAb is specific to the function of the protein rather than some non-specific steric effect. The DII loop-

hydrophobic trough interaction could either result in the formation of an erythrocyte binding pocket in the PfAMA1 ectodomain, or in the concealment of that pocket. Without the structure of the 4G2dc1-PfAMA1 complex and with the information available at present, it is impossible to state which of these possibilities is the more likely. These questions clearly require further consideration.

7.3: Validation of the use of the PfAMA1 synthetic gene product

The possibility that the synthetic gene product used in the binding assays in this study was not functionally active was assessed by reverse genetics approaches in *P. falciparum* parasites. Thus, it was possible to demonstrate expression of sgPfAMA1 in these parasites and locate this gene product to the apical complex (probably micronemes) of developing merozoites. The ability of this synthetic gene product to complement the function of that of the endogenous gene remains to be confirmed.

7.4: Interaction of AMA1 with a putative partner protein at the RBC surface

Despite the inability of this study to demonstrate erythrocyte binding activity for PfAMA1, the weight of evidence supporting such a function is extremely persuasive. As has already been suggested, one mechanism by which PfAMA1 interacts with the erythrocyte receptor is by means of a conformational change induced by interaction with a putative partner protein on the parasite surface. In this study, PfAMA1 was not shown to interact with any parasite partner proteins during schizont and merozoite stages of parasite development. However, in *T. gondii*, TgAMA1 interaction with a rhoptry protein at the time of tight junction formation has been reported. To re-assess this possibility in PfAMA1, it would be necessary to halt invasion after the formation of the tight junction and immunoprecipitate AMA1 from the parasite lysate. It is possible that this could be achieved using cytochalasin B, which blocks the invasion process after tight junction formation. Furthermore, certain signalling molecules are brought together with their partner molecule only after the interaction of one of them with their ligand. For instance, the transforming growth factor β (TGF-β) receptor is composed of two subunits, TβR-I and TβR-II, both of which are required for signal transduction (Anders *et al.* 1998) TβR-II can bind in the absence of TβR-I, but signal transduction only occurs if TβR-I then binds. TβR-I cannot bind in the absence of TβR-II. It is possible that the AMA1 partner protein must bind its erythrocyte receptor first, thus allowing AMA1 to complex with both partner protein on the parasite surface and receptor molecule on the erythrocyte surface. Thus, the erythrocyte binding capability of AMA1 may only be observed in the context of its parasite partner protein already interacting with the host erythrocyte. Such an interaction would not have been observed in the current study, where PfAMA1 was expressed in COS-7 cells in isolation from any other parasite molecule. This may also explain the inability of other studies to demonstrate erythrocyte binding of the parasite derived soluble forms, $PfAMA1_{48}$ and $PfAMA1_{44}$.

The position in PvAMA1 corresponding to the proteolytic processing or shedding site identified in PfAMA1 (Thr517-Ser518) (Howell et al., 2003b) appears to be inaccessible to proteases in the crystal structure (Chesne-Seck *et al.* submitted). Domain III of PvAMA1 and PfAMA1 show least sequence homology (33%) of the three sub-domains (Chesne-Seck *et al.* submitted). It is therefore possible that these domains also exhibit the least structural homology, perhaps reflecting host-cell specificity. It has been suggested that proteolytic shedding of PfAMA1 is required for host cell invasion by *P. falciparum* merozoites (Dutta *et al.* 2003; Dutta *et al.* 2005). Thus, if the processing site were inaccessible in PfAMA1, a conformational change would be required to allow access to the site for the sheddase and protein release from the parasite surface. AMA1 binding to its receptor on the erythrocyte surface or to its putative partner protein on the merozoite surface may be responsible for inducing such an alteration of conformation. As the process of invasion is very rapid, these two steps (erythrocyte binding and AMA1 shedding) are likely to be tightly coupled. The binding of PfAMA1 by its putative partner protein may be the single event required to couple these two essential processes.

7.5: Could AMA1 play a role in signal transduction?

The inability of this study to demonstrate phosphorylation of schizont or merozoite derived PfAMA1 does not rule out its participation in a signalling cascade during the invasion process. Phosphorylation is a dynamic process. Many signalling molecules are only transiently phosphorylated, the phosphate group being rapidly removed by protein phosphatases. Protein phosphatase inhibitors were not used in this study. For this reason, contaminating protein phosphatases present in the assay could have reversed any phosphorylation of the PfAMA1 cytoplasmic tail in these parasite stages. In addition, cytoplasmic phosphorylation of PfAMA1 may require interaction with its erythrocyte receptor, which in turn may require the interaction of a putative parasite partner protein. Thus, phosphorylation might only be observed at the time of erythrocyte binding. This possibility was not tested here and therefore requires further investigation. The involvement of AMA1 in signalling during host cell invasion is suggested by the observation that in *T. gondii*, rhoptry secretion is inhibited by the loss of AMA1 (Mital et al., 2005). This indicates that AMA1 directly or indirectly activates a signalling pathway that results in secretion from these apical organelles. The development of a conditional system for gene expression in *P. falciparum* (Meissner et al., 2005) will allow a thorough investigation of AMA1 function in this parasite.

7.6: A proposed mechanism for AMA1 function in merozoite invasion of erythrocytes

A mechanism for AMA1 function in erythrocyte invasion is thus proposed (Fig 7.1.). AMA1 is released from the micronemes around the time of schizont rupture. Thus, when the merozoite contacts a host cell there is a concentration gradient of AMA1 across the surface of the merozoite, decreasing from anterior to posterior. The initial interaction between the merozoite and erythrocyte membranes is mediated by a parasite resident surface protein, such as MSP1, allowing attachment in any orientation. Following this long-range interaction, AMA1 interacts with its ligand on the erythrocyte surface. This interaction may be initiated by the AMA1 partner protein binding to the receptor on the erythrocyte surface, thus enhancing the affinity of AMA1 for both its partner protein and the receptor. Alternatively, erythrocyte binding mediated by AMA1 may require multiple AMA1 molecules, possibly interacting with each other in the form of a homo-multimer. Individually the molecules of this complex might have a low affinity for the erythrocyte receptor, but collectively they may have an additive effect on the AMA1-receptor binding affinity. In addition, the concentration of AMA1 on the surface may correlate with this binding affinity. Thus, weaker interactions in regions of low AMA1 concentration will be abandoned in favour of higher affinity binding in regions of higher AMA1 concentration. This will induce the reorientation of the merozoite until the apical tip is in contact with the erythrocyte surface. At this point tight junction formation ensues, mediated by other components of the invasion pathway. Furthermore, AMA1-receptor binding may result in a conformational change in the molecule that allows it to interact with parasite kinases in the parasite cytosol thus inducing phosphorylation of amino acid residues within its cytoplasmic tail. The signal transduced initiates a cascade of events resulting in the secretion of the rhoptry contents. These proteins induce deformation of the erythrocyte membrane and PV formation. AMA1-partner protein or -receptor binding also induces a conformational change in the C-terminal region of the AMA1 ectodomain, allowing access of MESH (SUB2) to the cleavage site within DIII. SUB2 is translocated by the actomyosin motor from anterior to posterior (Harris *et al.* submitted) forming a zone or ring of shedding around the parasite as it cleaves MSP1 and AMA1 in its path.

7.7: Conclusion

This study has helped identify a region of the PfAMA1 ectodomain that may play a critical role in erythrocyte binding and invasion by the malaria parasite *P. falciparum*. In addition, results from this study suggest that PfAMA1 is unable to bind its erythrocyte receptor, if such a receptor exists, in isolation, requiring interaction with a partner protein on the parasite surface and perhaps a conformational change, exposing regions of the molecule otherwise concealed. It would also appear likely that any possible role PfAMA1 plays in signal transduction is only detectable at the time of parasite-host cell binding.

Figure 7.1: A hypothetical role for AMA1 in erythrocyte invasion by *Plasmodium* merozoites

A merozoite released from a mature schizont **(1)** has a coating of surface proteins that it utilises to make the initial weak interaction with the (target) erythrocyte surface **(2).** Around this time, AMA1 (red) is released from the (anterior) apical complex onto the surface of the merozoite and forms a decreasing concentration gradient towards the posterior end of the merozoite. The hypothetical AMA1 parasite partner protein, binds to an erythrocyte receptor which may be the same as that of AMA1 **(3)** thus enabling AMA1 to interact with partner and receptor **(4)**. This key event results in a signal being transduced across the merozoite plasmalemma, possibly as a result of phosphorylation of the AMA1 cytoplasmic tail. The signal triggers rhoptry secretion **(5)**, which results in the perturbation of the erythrocyte membrane, leading to PV formation **(6)** and parasite internalisation (**7** and **8**).

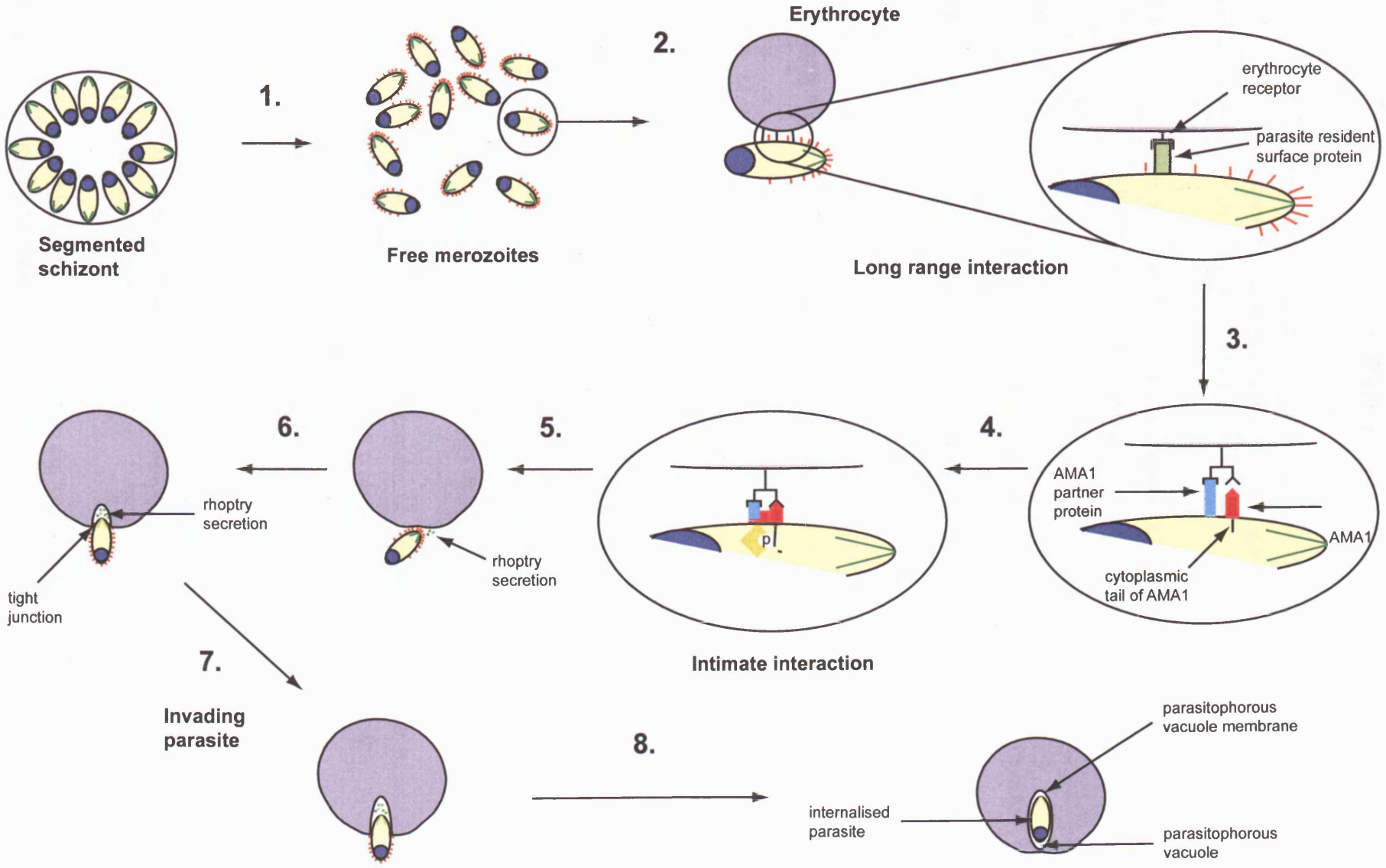
Segmented schizont
1.
Free merozoites
2.
Erythrocyte
erythrocyte receptor
parasite resident surface protein
Long range interaction
3.
4.
AMA1 partner protein
AMA1
cytoplasmic tail of AMA1
5.
Intimate interaction
6.
rhoptry secretion
rhoptry secretion
tight junction
7.
Invading parasite
8.
internalised parasite
parasitophorous vacuole membrane
parasitophorous vacuole

Bibliography

Adams, J. H., Hudson, D. E., Torii, M., Ward, G. E., Wellems, T. E., Aikawa, M., and Miller, L. H. (1990). The Duffy receptor family of Plasmodium knowlesi is located within the micronemes of invasive malaria merozoites. Cell *63*, 141-153.

Adams, J. H., Sim, B. K., Dolan, S. A., Fang, X., Kaslow, D. C., and Miller, L. H. (1992a). A family of erythrocyte binding proteins of malaria parasites. Proc Natl Acad Sci U S A *89*, 7085-7089.

Aguanno, J. J., Ladenson, J. H. (1982). Influence of fatty acids on the binding of calcium to human albumin. Correlation of binding and conformation strudies and evidence for distinct differences between unsaturated fatty acids and saturated fatty acids. J Biol Chem 257, 8745-8748.

Aikawa, M., Miller, L. H., Johnson, J., and Rabbege, J. (1978). Erythrocyte entry by malarial parasites. A moving junction between erythrocyte and parasite. J Cell Biol *77*, 72-82.

Aikawa, M., Miller, L. H., Rabbege, J. R., and Epstein, N. (1981). Freeze-fracture study on the erythrocyte membrane during malarial parasite invasion. J Cell Biol *91*, 55-62.

Alon, R., Chen, S., Puri, K. D., Finger, E. B., and Springer, T. A. (1997). The kinetics of L-selectin tethers and the mechanics of selectin-mediated rolling. J Cell Biol *138*, 1169-1180.

Amante, F. H., Crewther, P. E., Anders, R. F., and Good, M. F. (1997). A cryptic T cell epitope on the apical membrane antigen 1 of Plasmodium chabaudi adami can prime for an anamnestic antibody response: implications for malaria vaccine design. J Immunol *159*, 5535-5544.

Anders, R. F., Crewther, P. E., Edwards, S., Margetts, M., Matthew, M. L., Pollock, B., and Pye, D. (1998). Immunisation with recombinant AMA-1 protects mice against infection with Plasmodium chabaudi. Vaccine *16*, 240-247.

Aravind, L., Iyer, L. M., Wellems, T. E., and Miller, L. H. (2003). Plasmodium biology: genomic gleanings. Cell *115*, 771-785.

Atkinson, C. T., and Aikawa, M. (1990). Ultrastructure of malaria-infected erythrocytes [see comments]. Blood Cells *16*, 351-368.

Baglia, F. A., and Walsh, P. N. (1996). A binding site for thrombin in the apple 1 domain of factor XI. J Biol Chem *271*, 3652-3658.

Bai, T., Becker, M., Gupta, A., Strike, P., Murphy, V. J., Anders, R. F., and Batchelor, A. H. (2005). Structure of AMA1 from Plasmodium falciparum reveals a clustering of polymorphisms that surround a conserved hydrophobic pocket. Proc Natl Acad Sci U S A.

Baldi, D. L., Andrews, K. T., Waller, R. F., Roos, D. S., Howard, R. F., Crabb, B. S., and Cowman, A. F. (2000). RAP1 controls rhoptry targeting of RAP2 in the malaria parasite Plasmodium falciparum. Embo J *19*, 2435-2443.

Ballou, W. R., Arevalo-Herrera, M., Carucci, D., Richie, T. L., Corradin, G., Diggs, C., Druilhe, P., Giersing, B. K., Saul, A., Heppner, D. G., *et al.* (2004). Update on the clinical development of candidate malaria vaccines. Am J Trop Med Hyg *71*, 239-247.

Bannister, L., and Mitchell, G. (2003). The ins, outs and roundabouts of malaria. Trends Parasitol *19*, 209-213.

Bannister, L. H., Hopkins, J. M., Dluzewski, A. R., Margos, G., Williams, I. T., Blackman, M. J., Kocken, C. H., Thomas, A. W., and Mitchell, G. H. (2003). Plasmodium falciparum apical membrane antigen 1 (PfAMA-1) is translocated within micronemes along subpellicular microtubules during merozoite development. J Cell Sci *116*, 3825-3834.

Bannister, L. H., Hopkins, J. M., Fowler, R. E., Krishna, S., and Mitchell, G. H. (2000a). A brief illustrated guide to the ultrastructure of Plasmodium falciparum asexual blood stages. Parasitol Today *16*, 427-433.

Bannister, L. H., Hopkins, J. M., Fowler, R. E., Krishna, S., and Mitchell, G. H. (2000b). Ultrastructure of rhoptry development in Plasmodium falciparum erythrocytic schizonts. Parasitology *121 (Pt 3)*, 273-287.

Barale, J. C., Blisnick, T., Fujioka, H., Alzari, P. M., Aikawa, M., Braun-Breton, C., and Langsley, G. (1999). Plasmodium falciparum subtilisin-like protease 2, a merozoite candidate for the merozoite surface protein 1-42 maturase. Proc Natl Acad Sci U S A *96*, 6445-6450.

Berendt, A. R., Ferguson, D. J., Gardner, J., Turner, G., Rowe, A., McCormick, C., Roberts, D., Craig, A., Pinches, R., Elford, B. C., and al., e. (1994). Molecular mechanisms of sequestration in malaria. Parasitology *108 Suppl*, S19-28.

Bjorkman, A., and Bhattarai, A. (2005). Public health impact of drug resistant Plasmodium falciparum malaria. Acta Trop *94*, 163-169.

Blackman, M. J. (1994). Purification of Plasmodium falciparum merozoites for analysis of the processing of merozoite surface protein-1. Methods Cell Biol *45*, 213-220.

Blackman, M. J., and Bannister, L. H. (2001). Apical organelles of Apicomplexa: biology and isolation by subcellular fractionation. Mol Biochem Parasitol *117*, 11-25.

Blackman, M. J., Dennis, E. D., Hirst, E. M., Kocken, C. H., Scott-Finnigan, T. J., and Thomas, A. W. (1996). Plasmodium knowlesi: secondary processing of the malaria merozoite surface protein-1. Exp Parasitol *83*, 229-239.

Blackman, M. J., Fujioka, H., Stafford, W. H., Sajid, M., Clough, B., Fleck, S. L., Aikawa, M., Grainger, M., and Hackett, F. (1998). A subtilisin-like protein in secretory organelles of Plasmodium falciparum merozoites. J Biol Chem *273*, 23398-23409.

Blackman, M. J., Heidrich, H. G., Donachie, S., McBride, J. S., and Holder, A. A. (1990). A single fragment of a malaria merozoite surface protein remains on the parasite during red cell invasion and is the target of invasion-inhibiting antibodies. J Exp Med *172*, 379-382.

Blackman, M. J., Ling, I. T., Nicholls, S. C., and Holder, A. A. (1991a). Proteolytic processing of the Plasmodium falciparum merozoite surface protein-1 produces a membrane-bound fragment containing two epidermal growth factor-like domains. Mol Biochem Parasitol *49*, 29-33.

Blackman, M. J., Scott-Finnigan, T. J., Shai, S., and Holder, A. A. (1994). Antibodies inhibit the protease-mediated processing of a malaria merozoite surface protein. J Exp Med *180*, 389-393.

Blackman, M. J., Whittle, H., and Holder, A. A. (1991b). Processing of the Plasmodium falciparum major merozoite surface protein- 1: identification of a 33-kilodalton secondary processing product which is shed prior to erythrocyte invasion. Mol Biochem Parasitol *49*, 35-44.

Blair, P. L., Kappe, S. H., Maciel, J. E., Balu, B., and Adams, J. H. (2002). Plasmodium falciparum MAEBL is a unique member of the ebl family. Mol Biochem Parasitol *122*, 35-44.

Bojang, K. A., Milligan, P. J., Pinder, M., Vigneron, L., Alloueche, A., Kester, K. E., Ballou, W. R., Conway, D. J., Reece, W. H., Gothard, P., *et al.* (2001). Efficacy of RTS,S/AS02 malaria vaccine against Plasmodium falciparum infection in semi-immune adult men in The Gambia: a randomised trial. Lancet *358*, 1927-1934.

Bracchi-Ricard, V., Barik, S., Delvecchio, C., Doerig, C., Chakrabarti, R., and Chakrabarti, D. (2000). PfPK6, a novel cyclin-dependent kinase/mitogen-activated protein kinase-related protein kinase from Plasmodium falciparum. Biochem J *347 Pt 1*, 255-263.

Brecht, S., Carruthers, V. B., Ferguson, D. J., Giddings, O. K., Wang, G., Jakle, U., Harper, J. M., Sibley, L. D., and Soldati, D. (2001). The toxoplasma micronemal protein MIC4 is an adhesin composed of six conserved apple domains. J Biol Chem *276*, 4119-4127.

Brossier, F., Jewett, T. J., Lovett, J. L., and Sibley, L. D. (2003). C-terminal processing of the toxoplasma protein MIC2 is essential for invasion into host cells. J Biol Chem *278*, 6229-6234.

Brown, D. A., and London, E. (1998). Functions of lipid rafts in biological membranes. Annu Rev Cell Dev Biol *14*, 111-136.

Brown, P. J., Billington, K. J., Bumstead, J. M., Clark, J. D., and Tomley, F. M. (2000). A microneme protein from Eimeria tenella with homology to the Apple domains of coagulation factor XI and plasma pre-kallikrein. Mol Biochem Parasitol *107*, 91-102.

Brown, P. J., Gill, A. C., Nugent, P. G., McVey, J. H., and Tomley, F. M. (2001). Domains of invasion organelle proteins from apicomplexan parasites are homologous with the Apple domains of blood coagulation factor XI and plasma pre-kallikrein and are members of the PAN module superfamily. FEBS Lett *497*, 31-38.

Buffet, P. A., Gamain, B., Scheidig, C., Baruch, D., Smith, J. D., Hernandez-Rivas, R., Pouvelle, B., Oishi, S., Fujii, N., Fusai, T., *et al.* (1999). Plasmodium falciparum domain mediating adhesion to chondroitin sulfate A: a receptor for human placental infection. Proc Natl Acad Sci U S A *96*, 12743-12748.

Bumstead, J., and Tomley, F. (2000). Induction of secretion and surface capping of microneme proteins in Eimeria tenella. Mol Biochem Parasitol *110*, 311-321.

Burkhardt, A. L., Costa, T., Misulovin, Z., Stealy, B., Bolen, J. B., and Nussenzweig, M. C. (1994). Ig alpha and Ig beta are functionally homologous to the signaling proteins of the T-cell receptor. Mol Cell Biol *14*, 1095-1103.

Burns, J. M., Jr., Flaherty, P. R., Nanavati, P., and Weidanz, W. P. (2004). Protection against Plasmodium chabaudi malaria induced by immunization with apical membrane antigen 1 and merozoite surface protein 1 in the absence of gamma interferon or interleukin-4. Infect Immun *72*, 5605-5612.

Camus, D., and Hadley, T. J. (1985). A Plasmodium falciparum antigen that binds to host erythrocytes and merozoites. Science *230*, 553-556.

Caraglia, M., Marra, M., Pelaia, G., Maselli, R., Caputi, M., Marsico, S. A., and Abbruzzese, A. (2005). Alpha-interferon and its effects on signal transduction pathways. J Cell Physiol *202*, 323-335.

Carruthers, V. B., Giddings, O. K., and Sibley, L. D. (1999a). Secretion of micronemal proteins is associated with toxoplasma invasion of host cells. Cell Microbiol *1*, 225-235.

Carruthers, V. B., Moreno, S. N., and Sibley, L. D. (1999b). Ethanol and acetaldehyde elevate intracellular [Ca2+] and stimulate microneme discharge in Toxoplasma gondii. Biochem J *342 (Pt 2)*, 379-386.

Carruthers, V. B., and Sibley, L. D. (1997). Sequential protein secretion from three distinct organelles of Toxoplasma gondii accompanies invasion of human fibroblasts. Eur J Cell Biol *73*, 114-123.

Carruthers, V. B., and Sibley, L. D. (1999). Mobilization of intracellular calcium stimulates microneme discharge in Toxoplasma gondii. Mol Microbiol *31*, 421-428.

Carvalho, L. J., Daniel-Ribeiro, C. T., and Goto, H. (2002). Malaria vaccine: candidate antigens, mechanisms, constraints and prospects. Scand J Immunol *56*, 327-343.

Casey, J. L., Coley, A. M., Anders, R. F., Murphy, V. J., Humberstone, K. S., Thomas, A. W., and Foley, M. (2004). Antibodies to malaria peptide mimics inhibit Plasmodium falciparum invasion of erythrocytes. Infect Immun *72*, 1126-1134.

Cavanagh, D. R., Elhassan, I. M., Roper, C., Robinson, V. J., Giha, H., Holder, A. A., Hviid, L., Theander, T. G., Arnot, D. E., and McBride, J. S. (1998). A longitudinal study of type-specific antibody responses to Plasmodium falciparum merozoite surface protein-1 in an area of unstable malaria in Sudan. J Immunol *161*, 347-359.

Cerede, O., Dubremetz, J. F., Bout, D., and Lebrun, M. (2002). The Toxoplasma gondii protein MIC3 requires pro-peptide cleavage and dimerization to function as adhesin. Embo J *21*, 2526-2536.

Chan, A. C., Iwashima, M., Turck, C. W., and Weiss, A. (1992). ZAP-70: a 70 kd protein-tyrosine kinase that associates with the TCR zeta chain. Cell *71*, 649-662.

Chang, S. P., Gibson, H. L., Lee-Ng, C. T., Barr, P. J., and Hui, G. S. (1992). A carboxyl-terminal fragment of Plasmodium falciparum gp195 expressed by a recombinant baculovirus induces antibodies that completely inhibit parasite growth. J Immunol *149*, 548-555.

Chen, Q., Barragan, A., Fernandez, V., Sundstrom, A., Schlichtherle, M., Sahlen, A., Carlson, J., Datta, S., and Wahlgren, M. (1998). Identification of Plasmodium falciparum erythrocyte membrane protein 1 (PfEMP1) as the rosetting ligand of the malaria parasite P. falciparum. J Exp Med *187*, 15-23.

Chen, Q., Heddini, A., Barragan, A., Fernandez, V., Pearce, S. F., and Wahlgren, M. (2000). The semiconserved head structure of Plasmodium falciparum erythrocyte membrane protein 1 mediates binding to multiple independent host receptors. J Exp Med *192*, 1-10.

Chen, S., and Springer, T. A. (2001). Selectin receptor-ligand bonds: Formation limited by shear rate and dissociation governed by the Bell model. Proc Natl Acad Sci U S A *98*, 950-955.

Cheng, Q., and Saul, A. (1994). Sequence analysis of the apical membrane antigen I (AMA-1) of Plasmodium vivax. Mol Biochem Parasitol *65*, 183-187.

Chitarra, V., Holm, I., Bentley, G. A., Petres, S., and Longacre, S. (1999). The crystal structure of C-terminal merozoite surface protein 1 at 1.8 A resolution, a highly protective malaria vaccine candidate. Mol Cell *3*, 457-464.

Chitnis, C. E., and Blackman, M. J. (2000). Host cell invasion by malaria parasites. Parasitol Today *16*, 411-415.

Chitnis, C. E., and Miller, L. H. (1994). Identification of the erythrocyte binding domains of Plasmodium vivax and Plasmodium knowlesi proteins involved in erythrocyte invasion. J Exp Med *180*, 497-506.

Clyde, D. F. (1975). Immunization of man against falciparum and vivax malaria by use of attenuated sporozoites. Am J Trop Med Hyg *24*, 397-401.

Coley, A. M., Campanale, N. V., Casey, J. L., Hodder, A. N., Crewther, P. E., Anders, R. F., Tilley, L. M., and Foley, M. (2001). Rapid and precise epitope mapping of monoclonal antibodies against Plasmodium falciparum AMA1 by combined phage display of fragments and random peptides. Protein Eng *14*, 691-698.

Collins, W. E., Pye, D., Crewther, P. E., Vandenberg, K. L., Galland, G. G., Sulzer, A. J., Kemp, D. J., Edwards, S. J., Coppel, R. L., Sullivan, J. S., and al., e. (1994). Protective immunity

induced in squirrel monkeys with recombinant apical membrane antigen-1 of Plasmodium fragile. Am J Trop Med Hyg *51*, 711-719.

Cooper J. A. and Howell, B. (1993). The when and how of Src regulation. Cell 73, 1051-1054.

Cooper, J. A., and King, C. S. (1986). Dephosphorylation or antibody binding to the carboxy terminus stimulates pp60c-src. Mol Cell Biol *6*, 4467-4477.

Cortes, A., Mellombo, M., Masciantonio, R., Murphy, V. J., Reeder, J. C., and Anders, R. F. (2005). Allele specificity of naturally acquired antibody responses against Plasmodium falciparum apical membrane antigen 1. Infect Immun *73*, 422-430.

Cortes, A., Mellombo, M., Mueller, I., Benet, A., Reeder, J. C., and Anders, R. F. (2003). Geographical structure of diversity and differences between symptomatic and asymptomatic infections for Plasmodium falciparum vaccine candidate AMA1. Infect Immun *71*, 1416-1426.

Cowman, A. F., and Crabb, B. S. (2002). The Plasmodium falciparum genome--a blueprint for erythrocyte invasion. Science *298*, 126-128.

Crabb, B. S., and Cowman, A. F. (1996). Characterization of promoters and stable transfection by homologous and nonhomologous recombination in Plasmodium falciparum. Proc Natl Acad Sci U S A *93*, 7289-7294.

Crabb, B. S., Triglia, T., Waterkeyn, J. G., and Cowman, A. F. (1997). Stable transgene expression in Plasmodium falciparum. Mol Biochem Parasitol *90*, 131-144.

Crewther, P. E., Matthew, M. L., Flegg, R. H., and Anders, R. F. (1996). Protective immune responses to apical membrane antigen 1 of Plasmodium chabaudi involve recognition of strain-specific epitopes. Infect Immun *64*, 3310-3317.

Cubillos, M., Salazar, L. M., Torres, L., and Patarroyo, M. E. (2002). Protection against experimental P. falciparum malaria is associated with short AMA-1 peptide analogue alpha-helical structures. Biochimie *84*, 1181-1188.

Cuff, J. A., and Barton, G. J. (2000). Application of multiple sequence alignment profiles to improve protein secondary structure prediction. Proteins *40*, 502-511.

Culvenor, J. G., Day, K. P., and Anders, R. F. (1991). Plasmodium falciparum ring-infected erythrocyte surface antigen is released from merozoite dense granules after erythrocyte invasion. Infect Immun *59*, 1183-1187.

Da Silva, E., Foley, M., Dluzewski, A. R., Murray, L. J., Anders, R. F., and Tilley, L. (1994). The Plasmodium falciparum protein RESA interacts with the erythrocyte cytoskeleton and modifies erythrocyte thermal stability. Mol Biochem Parasitol *66*, 59-69.

Dailey, L., Ambrosetti, D., Mansukhani, A., and Basilico, C. (2005). Mechanisms underlying differential responses to FGF signaling. Cytokine Growth Factor Rev *16*, 233-247.

D'Alessandro, U., Leach, A., Drakeley, C. J., Bennett, S., Olaleye, B. O., Fegan, G. W., Jawara, M., Langerock, P., George, M. O., Targett, G. A., and et al. (1995). Efficacy trial of malaria vaccine SPf66 in Gambian infants [see comments]. Lancet *346*, 462-467.

de Koning-Ward, T. F., O'Donnell, R. A., Drew, D. R., Thomson, R., Speed, T. P., and Crabb, B. S. (2003). A new rodent model to assess blood stage immunity to the Plasmodium falciparum antigen merozoite surface protein 119 reveals a protective role for invasion inhibitory antibodies. J Exp Med *198*, 869-875.

Deans, J. A. (1984). Protective antigens of bloodstage Plasmodium knowlesi parasites. Philos Trans R Soc Lond B Biol Sci *307*, 159-169.

Deans, J. A., Alderson, T., Thomas, A. W., Mitchell, G. H., Lennox, E. S., and Cohen, S. (1982). Rat monoclonal antibodies which inhibit the in vitro multiplication of Plasmodium knowlesi. Clin Exp Immunol *49*, 297-309.

Deans, J. A., Knight, A. M., Jean, W. C., Waters, A. P., Cohen, S., and Mitchell, G. H. (1988). Vaccination trials in rhesus monkeys with a minor, invariant, Plasmodium knowlesi 66 kD merozoite antigen. Parasite Immunol *10*, 535-552.

Dieckmann-Schuppert, A., Bender, S., Odenthal-Schnittler, M., Bause, E., and Schwarz, R. T. (1992). Apparent lack of N-glycosylation in the asexual intraerythrocytic stage of Plasmodium falciparum. Eur J Biochem *205*, 815-825.

Dluzewski, A. R., Rangachari, K., Wilson, R. J., and Gratzer, W. B. (1986). Plasmodium falciparum: protease inhibitors and inhibition of erythrocyte invasion. Exp Parasitol *62*, 416-422.

Dobrowolski, J. M., Carruthers, V. B., and Sibley, L. D. (1997). Participation of myosin in gliding motility and host cell invasion by Toxoplasma gondii. Mol Microbiol *26*, 163-173.

Doerig, C. (2004). Protein kinases as targets for anti-parasitic chemotherapy. Biochim Biophys Acta *1697*, 155-168.

Doerig, C., Meijer, L., and Mottram, J. C. (2002). Protein kinases as drug targets in parasitic protozoa. Trends Parasitol *18*, 366-371.

Doerig, C. D. (1997). Signal transduction in malaria parasites. Parasitol Today *13*, 307-313.
Doerig, C. M., Parzy, D., Langsley, G., Horrocks, P., Carter, R., and Doerig, C. D. (1996). A MAP kinase homologue from the human malaria parasite, Plasmodium falciparum. Gene *177*, 1-6.

Dolan, S. A., Miller, L. H., and Wellems, T. E. (1990). Evidence for a switching mechanism in the invasion of erythrocytes by Plasmodium falciparum. J Clin Invest *86*, 618-624.

Dolan, S. A., Proctor, J. L., Alling, D. W., Okubo, Y., Wellems, T. E., and Miller, L. H. (1994). Glycophorin B as an EBA-175 independent Plasmodium falciparum receptor of human erythrocytes. Mol Biochem Parasitol *64*, 55-63.

Donahue, C. G., Carruthers, V. B., Gilk, S. D., and Ward, G. E. (2000). The toxoplasma homolog of plasmodium apical membrane antigen-1 (AMA-1) is a microneme protein secreted in response to elevated intracellular calcium levels. Mol Biochem Parasitol *111*, 15-30.

Doolan, D. L., Hedstrom, R. C., Wang, R., Sedegah, M., Scheller, L. F., Hobart, P., Norman, J. A., and Hoffman, S. L. (1997). DNA vaccines for malaria: the past, the present, & the future. Indian J Med Res *106*, 109-119.

Dorfman, J. R., Bejon, P., Ndungu, F. M., Langhorne, J., Kortok, M. M., Lowe, B. S., Mwangi, T. W., Williams, T. N., and Marsh, K. (2005). B cell memory to 3 Plasmodium falciparum blood-stage antigens in a malaria-endemic area. J Infect Dis *191*, 1623-1630.

Dorin, D., Alano, P., Boccaccio, I., Ciceron, L., Doerig, C., Sulpice, R., and Parzy, D. (1999). An atypical mitogen-activated protein kinase (MAPK) homologue expressed in gametocytes of the human malaria parasite Plasmodium falciparum. Identification of a MAPK signature. J Biol Chem *274*, 29912-29920.

Dorin, D., Le Roch, K., Sallicandro, P., Alano, P., Parzy, D., Poullet, P., Meijer, L., and Doerig, C. (2001). Pfnek-1, a NIMA-related kinase from the human malaria parasite Plasmodium falciparum Biochemical properties and possible involvement in MAPK regulation. Eur J Biochem *268*, 2600-2608.

Dorin, D., Semblat, J. P., Poullet, P., Alano, P., Goldring, J. P., Whittle, C., Patterson, S., Chakrabarti, D., and Doerig, C. (2005). PfPK7, an atypical MEK-related protein kinase, reflects

the absence of classical three-component MAPK pathways in the human malaria parasite Plasmodium falciparum. Mol Microbiol *55*, 184-196.

Doury, J. C., Goasdoue, J. L., Tolou, H., Martelloni, M., Bonnefoy, S., and Mercereau-Puijalon, O. (1997). Characterisation of the binding sites of monoclonal antibodies reacting with the Plasmodium falciparum rhoptry protein RhopH3. Mol Biochem Parasitol *85*, 149-159.

Dubremetz, J. F., Garcia-Reguet, N., Conseil, V., and Fourmaux, M. N. (1998). Apical organelles and host-cell invasion by Apicomplexa. Int J Parasitol *28*, 1007-1013.

Dunn, P. P., Bumstead, J. M., and Tomley, F. M. (1996). Sequence, expression and localization of calmodulin-domain protein kinases in Eimeria tenella and Eimeria maxima. Parasitology *113 (Pt 5)*, 439-448.

Duraisingh, M. T., Maier, A. G., Triglia, T., and Cowman, A. F. (2003a). Erythrocyte-binding antigen 175 mediates invasion in Plasmodium falciparum utilizing sialic acid-dependent and -independent pathways. Proc Natl Acad Sci U S A *100*, 4796-4801.

Duraisingh, M. T., Triglia, T., and Cowman, A. F. (2002). Negative selection of Plasmodium falciparum reveals targeted gene deletion by double crossover recombination. Int J Parasitol *32*, 81-89.

Duraisingh, M. T., Triglia, T., Ralph, S. A., Rayner, J. C., Barnwell, J. W., McFadden, G. I., and Cowman, A. F. (2003b). Phenotypic variation of Plasmodium falciparum merozoite proteins directs receptor targeting for invasion of human erythrocytes. Embo J *22*, 1047-1057.

Dutta, S., Haynes, J. D., Barbosa, A., Ware, L. A., Snavely, J. D., Moch, J. K., Thomas, A. W., and Lanar, D. E. (2005). Mode of action of invasion-inhibitory antibodies directed against apical membrane antigen 1 of Plasmodium falciparum. Infect Immun *73*, 2116-2122.

Dutta, S., Haynes, J. D., Moch, J. K., Barbosa, A., and Lanar, D. E. (2003). Invasion-inhibitory antibodies inhibit proteolytic processing of apical membrane antigen 1 of Plasmodium falciparum merozoites. Proc Natl Acad Sci U S A *100*, 12295-12300.

Dutta, S., Lalitha, P. V., Ware, L. A., Barbosa, A., Moch, J. K., Vassell, M. A., Fileta, B. B., Kitov, S., Kolodny, N., Heppner, D. G., *et al.* (2002). Purification, characterization, and immunogenicity of the refolded ectodomain of the Plasmodium falciparum apical membrane antigen 1 expressed in Escherichia coli. Infect Immun *70*, 3101-3110.

Dutta, S., Malhotra, P., and Chauhan, V. S. (1995). Sequence analysis of apical membrane antigen 1 (AMA-1) of Plasmodium cynomolgi bastianelli. Mol Biochem Parasitol *73*, 267-270.

Dvorak, J. A., Miller, L. H., Whitehouse, W. C., and Shiroishi, T. (1975). Invasion of erythrocytes by malaria merozoites. Science *187*, 748-750.

Egan, A. F., Chappel, J. A., Burghaus, P. A., Morris, J. S., McBride, J. S., Holder, A. A., Kaslow, D. C., and Riley, E. M. (1995). Serum antibodies from malaria-exposed people recognize conserved epitopes formed by the two epidermal growth factor motifs of MSP1(19), the carboxy-terminal fragment of the major merozoite surface protein of Plasmodium falciparum. Infect Immun *63*, 456-466.

Egan, A. F., Morris, J., Barnish, G., Allen, S., Greenwood, B. M., Kaslow, D. C., Holder, A. A., and Riley, E. M. (1996). Clinical immunity to Plasmodium falciparum malaria is associated with serum antibodies to the 19-kDa C-terminal fragment of the merozoite surface antigen, PfMSP-1. J Infect Dis *173*, 765-769.

Eisen, D. P., Marshall, V. M., Billman-Jacobe, H., and Coppel, R. L. (1999). A Plasmodium falciparum apical membrane antigen-1 (AMA-1) gene apparently generated by intragenic recombination. Mol Biochem Parasitol *100*, 243-246.

Ekvall, H. (2003). Malaria and anemia. Curr Opin Hematol *10*, 108-114.

Emini, E. A., Hughes, J. V., Perlow, D. S., and Boger, J. (1985). Induction of hepatitis A virus-neutralizing antibody by a virus-specific synthetic peptide. J Virol *55*, 836-839.

Escalante, A. A., Freeland, D. E., Collins, W. E., and Lal, A. A. (1998a). The evolution of primate malaria parasites based on the gene encoding cytochrome b from the linear mitochondrial genome. Proc Natl Acad Sci U S A *95*, 8124-8129.

Escalante, A. A., Grebert, H. M., Chaiyaroj, S. C., Magris, M., Biswas, S., Nahlen, B. L., and Lal, A. A. (2001). Polymorphism in the gene encoding the apical membrane antigen-1 (AMA-1) of Plasmodium falciparum. X. Asembo Bay Cohort Project. Mol Biochem Parasitol *113*, 279-287.

Escalante, A. A., Lal, A. A., and Ayala, F. J. (1998b). Genetic polymorphism and natural selection in the malaria parasite Plasmodium falciparum. Genetics *149*, 189-202.

Fang, X. D., Kaslow, D. C., Adams, J. H., and Miller, L. H. (1991). Cloning of the Plasmodium vivax Duffy receptor. Mol Biochem Parasitol *44*, 125-132.

Feinberg, A. P., and Vogelstein, B. (1983). A technique for radiolabeling DNA restriction endonuclease fragments to high specific activity. Anal Biochem *132*, 6-13.

Feng, Z. P., Keizer, D. W., Stevenson, R. A., Yao, S., Babon, J. J., Murphy, V. J., Anders, R. F., and Norton, R. S. (2005). Structure and inter-domain interactions of domain II from the blood-stage malarial protein, apical membrane antigen 1. J Mol Biol *350*, 641-656.

Fidock, D. A., and Wellems, T. E. (1997). Transformation with human dihydrofolate reductase renders malaria parasites insensitive to WR99210 but does not affect the intrinsic activity of proguanil. Proc Natl Acad Sci U S A *94*, 10931-10936.

Field, J., Nikawa, J., Broek, D., MacDonald, B., Rodgers, L., Wilson, I. A., Lerner, R. A., and Wigler, M. (1988). Purification of a RAS-responsive adenylyl cyclase complex from Saccharomyces cerevisiae by use of an epitope addition method. Mol Cell Biol *8*, 2159-2165.

Finger, E. B., Puri, K. D., Alon, R., Lawrence, M. B., von Andrian, U. H., and Springer, T. A. (1996). Adhesion through L-selectin requires a threshold hydrodynamic shear. Nature *379*, 266-269.

Foley, M., Tilley, L., Sawyer, W. H., and Anders, R. F. (1991). The ring-infected erythrocyte surface antigen of Plasmodium falciparum associates with spectrin in the erythrocyte membrane. Mol Biochem Parasitol *46*, 137-147.

Fraser, T. S., Kappe, S. H., Narum, D. L., VanBuskirk, K. M., and Adams, J. H. (2001). Erythrocyte-binding activity of Plasmodium yoelii apical membrane antigen-1 expressed on the surface of transfected COS-7 cells. Mol Biochem Parasitol *117*, 49-59.

Fu, J., Saenz, F. E., Reed, M. B., Balu, B., Singh, N., Blair, P. L., Cowman, A. F., and Adams, J. H. (2005). Targeted disruption of maebl in Plasmodium falciparum. Mol Biochem Parasitol *141*, 113-117.

Gaffar, F. R., Yatsuda, A. P., Franssen, F. F., and de Vries, E. (2004). Erythrocyte invasion by Babesia bovis merozoites is inhibited by polyclonal antisera directed against peptides derived from a homologue of Plasmodium falciparum apical membrane antigen 1. Infect Immun *72*, 2947-2955.

Garcia-Reguet, N., Lebrun, M., Fourmaux, M. N., Mercereau-Puijalon, O., Mann, T., Beckers, C. J., Samyn, B., Van Beeumen, J., Bout, D., and Dubremetz, J. F. (2000). The microneme protein MIC3 of Toxoplasma gondii is a secretory adhesin that binds to both the surface of the host cells and the surface of the parasite. Cell Microbiol *2*, 353-364.

Garnham, P. C. C. (1966). Malaria parasites and other haemosporidia. Blackwell, Oxford.

Ghai, M., Dutta, S., Hall, T., Freilich, D., and Ockenhouse, C. F. (2002). Identification, expression, and functional characterization of MAEBL, a sporozoite and asexual blood stage chimeric erythrocyte-binding protein of Plasmodium falciparum. Mol Biochem Parasitol *123*, 35-45.

Giha, H. A., Staalsoe, T., Dodoo, D., Elhassan, I. M., Roper, C., Satti, G. M., Arnot, D. E., Theander, T. G., and Hviid, L. (1999). Nine-year longitudinal study of antibodies to variant antigens on the surface of Plasmodium falciparum-infected erythrocytes. Infect Immun *67*, 4092-4098.

Gilberger, T. W., Thompson, J. K., Reed, M. B., Good, R. T., and Cowman, A. F. (2003a). The cytoplasmic domain of the Plasmodium falciparum ligand EBA-175 is essential for invasion but not protein trafficking. J Cell Biol *162*, 317-327.

Gilberger, T. W., Thompson, J. K., Triglia, T., Good, R. T., Duraisingh, M. T., and Cowman, A. F. (2003b). A novel erythrocyte binding antigen-175 paralogue from Plasmodium falciparum defines a new trypsin-resistant receptor on human erythrocytes. J Biol Chem *278*, 14480-14486.

Goel, V. K., Li, X., Chen, H., Liu, S. C., Chishti, A. H., and Oh, S. S. (2003). Band 3 is a host receptor binding merozoite surface protein 1 during the Plasmodium falciparum invasion of erythrocytes. Proc Natl Acad Sci U S A *100*, 5164-5169.

Gowda, D. C., and Davidson, E. A. (1999). Protein glycosylation in the malaria parasite. Parasitol Today *15*, 147-152.

Gowda, D. C., Gupta, P., and Davidson, E. A. (1997). Glycosylphosphatidylinositol anchors represent the major carbohydrate modification in proteins of intraerythrocytic stage Plasmodium falciparum. J Biol Chem *272*, 6428-6439.

Green, N., Alexander, H., Olson, A., Alexander, S., Shinnick, T. M., Sutcliffe, J. G., and Lerner, R. A. (1982). Immunogenic structure of the influenza virus hemagglutinin. Cell *28*, 477-487.

Gupta, A., Bai, T., Murphy, V., Strike, P., Anders, R. F., and Batchelor, A. H. (2005). Refolding, purification, and crystallization of apical membrane antigen 1 from Plasmodium falciparum. Protein Expr Purif *41*, 186-198.

Hackett, F., Sajid, M., Withers-Martinez, C., Grainger, M., and Blackman, M. J. (1999). PfSUB-2: a second subtilisin-like protein in Plasmodium falciparum merozoites. Mol Biochem Parasitol *103*, 183-195.

Hall, R., Hyde, J. E., Goman, M., Simmons, D. L., Hope, I. A., Mackay, M., Scaife, J., Merkli, B., Richle, R., and Stocker, J. (1984). Major surface antigen gene of a human malaria parasite cloned and expressed in bacteria. Nature *311*, 379-382.

Hanks, S. K., Quinn, A. M. (1991) Protein kinase catalytic domain sequences database: Identification of conserved features of primary structures and classification of family members. Methods in Enzymology 200, 38-62.

Harder, T. and Simons, K. (1999). Clusters of glycolipid and glycosylphosphatidylinositol-anchored proteins in lymphoid cells: accumulation of actin regulated by local tyrosine phosphorylation. Eur J Immunol 29, 556-562.

Hay, S. I., Guerra, C. A., Tatem, A. J., Noor, A. M., and Snow, R. W. (2004). The global distribution and population at risk of malaria: past, present, and future. Lancet Infect Dis *4*, 327-336.

Haynes, J. D., Dalton, J. P., Klotz, F. W., McGinniss, M. H., Hadley, T. J., Hudson, D. E., and Miller, L. H. (1988). Receptor-like specificity of a Plasmodium knowlesi malarial protein that binds to Duffy antigen ligands on erythrocytes. J Exp Med *167*, 1873-1881.

Healer, J., Crawford, S., Ralph, S., McFadden, G., and Cowman, A. F. (2002). Independent translocation of two micronemal proteins in developing Plasmodium falciparum merozoites. Infect Immun *70*, 5751-5758.

Healer, J., Murphy, V., Hodder, A. N., Masciantonio, R., Gemmill, A. W., Anders, R. F., Cowman, A. F., and Batchelor, A. (2004). Allelic polymorphisms in apical membrane antigen-1 are responsible for evasion of antibody-mediated inhibition in Plasmodium falciparum. Mol Microbiol *52*, 159-168.

Healer, J., Triglia, T., Hodder, A. N., Gemmill, A. W., and Cowman, A. F. (2005). Functional analysis of Plasmodium falciparum apical membrane antigen 1 utilizing interspecies domains. Infect Immun *73*, 2444-2451.

Hehl, A. B., Lekutis, C., Grigg, M. E., Bradley, P. J., Dubremetz, J. F., Ortega-Barria, E., and Boothroyd, J. C. (2000). Toxoplasma gondii homologue of plasmodium apical membrane antigen 1 is involved in invasion of host cells. Infect Immun *68*, 7078-7086.

Heppner, D. G., Jr., Kester, K. E., Ockenhouse, C. F., Tornieporth, N., Ofori, O., Lyon, J. A., Stewart, V. A., Dubois, P., Lanar, D. E., Krzych, U., *et al.* (2005). Towards an RTS,S-based, multi-stage, multi-antigen vaccine against falciparum malaria: progress at the Walter Reed Army Institute of Research. Vaccine *23*, 2243-2250.

Ho, D. H., Badellino, K., Baglia, F. A., and Walsh, P. N. (1998). A binding site for heparin in the apple 3 domain of factor XI. J Biol Chem *273*, 16382-16390.

Hodder, A. N., Crewther, P. E., and Anders, R. F. (2001). Specificity of the protective antibody response to apical membrane antigen 1. Infect Immun *69*, 3286-3294.

Hodder, A. N., Crewther, P. E., Matthew, M. L., Reid, G. E., Moritz, R. L., Simpson, R. J., and Anders, R. F. (1996). The disulfide bond structure of Plasmodium apical membrane antigen-1. J Biol Chem *271*, 29446-29452.

Hoffman, S. L., Goh, L. M., Luke, T. C., Schneider, I., Le, T. P., Doolan, D. L., Sacci, J., de la Vega, P., Dowler, M., Paul, C., *et al.* (2002). Protection of humans against malaria by immunization with radiation-attenuated Plasmodium falciparum sporozoites. J Infect Dis *185*, 1155-1164.

Holder, A. A., and Freeman, R. R. (1982). Biosynthesis and processing of a Plasmodium falciparum schizont antigen recognized by immune serum and a monoclonal antibody. J Exp Med *156*, 1528-1538.

Holder, A. A., and Freeman, R. R. (1984). Characterization of a high molecular weight protective antigen of Plasmodium yoelii. Parasitology *88*, 211-219.

Horuk, R., Chitnis, C. E., Darbonne, W. C., Colby, T. J., Rybicki, A., Hadley, T. J., and Miller, L. H. (1993). A receptor for the malarial parasite Plasmodium vivax: the erythrocyte chemokine receptor. Science *261*, 1182-1184.

Howard, R. F., Jacobson, K. C., Rickel, E., and Thurman, J. (1998). Analysis of inhibitory epitopes in the Plasmodium falciparum rhoptry protein RAP-1 including identification of a second inhibitory epitope. Infect Immun *66*, 380-386.

Howell, S. A., Hackett, F., Jongco, A. M., Withers-Martinez, C., Kim, K., Carruthers, V. B., and Blackman, M. J. (2005). Distinct mechanisms govern proteolytic shedding of a key invasion protein in apicomplexan pathogens. Mol Microbiol *57*, 1342-1356.

Howell, S. A., Well, I., Fleck, S. L., Kettleborough, C., Collins, C. R., and Blackman, M. J. (2003). A single malaria merozoite serine protease mediates shedding of multiple surface proteins by juxtamembrane cleavage. J Biol Chem *278*, 23890-23898.

Howell, S. A., Withers-Martinez, C., Kocken, C. H., Thomas, A. W., and Blackman, M. J. (2001). Proteolytic processing and primary structure of Plasmodium falciparum apical membrane antigen-1. J Biol Chem *276*, 31311-31320.

Hughes, M. K., and Hughes, A. L. (1995). Natural selection on Plasmodium surface proteins. Mol Biochem Parasitol *71*, 99-113.

Hunter, T., and Plowman, G. D. (1997). The protein kinases of budding yeast: six score and more. Trends Biochem Sci *22*, 18-22.

Ihle, J. N. (1995). Cytokine receptor signalling. Nature *377*, 591-594.

Irving, B. A., Chan, A. C., and Weiss, A. (1993). Functional characterization of a signal transducing motif present in the T cell antigen receptor zeta chain. J Exp Med *177*, 1093-1103.

Irving, B. A., and Weiss, A. (1991). The cytoplasmic domain of the T cell receptor zeta chain is sufficient to couple to receptor-associated signal transduction pathways. Cell *64*, 891-901.

Janin, J. and Chothia, C. (1978). Conformation of amino acid side chains in proteins. J Mol Biol 125, 357-386

Jean, L., Hackett, F., Martin, S. R., and Blackman, M. J. (2003). Functional characterisation of the propeptide of Plasmodium falciparum subtilisin-like protease-1. J Biol Chem.

Johnson, J. G., Epstein, N., Shiroishi, T., and Miller, L. H. (1980). Factors affecting the ability of isolated Plasmodium knowlesi merozoites to attach to and invade erythrocytes. Parasitology *80*, 539-550.

Jones, T. R., Stroncek, D. F., Gozalo, A. S., Obaldia, N., 3rd, Andersen, E. M., Lucas, C., Narum, D. L., Magill, A. J., Sim, B. K., and Hoffman, S. L. (2002). Anemia in parasite- and recombinant protein-immunized aotus monkeys infected with Plasmodium falciparum. Am J Trop Med Hyg *66*, 672-679.

Kabouridis, P. S., Magee, A. I. (1997). S-acylation of LCK protein tyrosine kinase is essential for its signalling function in T-lymphocytes. EMBO 16, 4983-4998.

Kaneko, O., Fidock, D. A., Schwartz, O. M., and Miller, L. H. (2000). Disruption of the C-terminal region of EBA-175 in the Dd2/Nm clone of Plasmodium falciparum does not affect erythrocyte invasion. Mol Biochem Parasitol *110*, 135-146.

Kappe, S., Bruderer, T., Gantt, S., Fujioka, H., Nussenzweig, V., and Menard, R. (1999). Conservation of a gliding motility and cell invasion machinery in Apicomplexan parasites. J Cell Biol *147*, 937-944.

Kappe, S. H., and Adams, J. H. (1996). Sequence analysis of the apical membrane antigen-1 genes (ama-1) of Plasmodium yoelii yoelii and Plasmodium berghei. Mol Biochem Parasitol *78*, 279-283.

Kappe, S. H., Curley, G. P., Noe, A. R., Dalton, J. P., and Adams, J. H. (1997). Erythrocyte binding protein homologues of rodent malaria parasites. Mol Biochem Parasitol *89*, 137-148.

Kappe, S. H., Noe, A. R., Fraser, T. S., Blair, P. L., and Adams, J. H. (1998). A family of chimeric erythrocyte binding proteins of malaria parasites. Proc Natl Acad Sci U S A *95*, 1230-1235.

Kappes, B., Doerig, C. D., and Graeser, R. (1999). An overview of Plasmodium protein kinases. Parasitol Today *15*, 449-454.

Kato, K., Mayer, D. C., Singh, S., Reid, M., and Miller, L. H. (2005). Domain III of Plasmodium falciparum apical membrane antigen 1 binds to the erythrocyte membrane protein Kx. Proc Natl Acad Sci U S A *102*, 5552-5557.

Keizer, D. W., Miles, L. A., Li, F., Nair, M., Anders, R. F., Coley, A. M., Foley, M., and Norton, R. S. (2003). Structures of phage-display peptides that bind to the malarial surface protein, apical membrane antigen 1, and block erythrocyte invasion. Biochemistry *42*, 9915-9923.

Kennedy, M. C., Wang, J., Zhang, Y., Miles, A. P., Chitsaz, F., Saul, A., Long, C. A., Miller, L. H., and Stowers, A. W. (2002). In vitro studies with recombinant Plasmodium falciparum apical membrane antigen 1 (AMA1): production and activity of an AMA1 vaccine and generation of a multiallelic response. Infect Immun *70*, 6948-6960.

Kieschnick, H., Wakefield, T., Narducci, C. A., and Beckers, C. (2001). Toxoplasma gondii attachment to host cells is regulated by a calmodulin-like domain protein kinase. J Biol Chem *276*, 12369-12377.

Klein, H., Mehlhorn, H., and Ruger, W. (1996). Characterization of genomic clones encoding two microneme antigens of Sarcocystis muris (Apicomplexa). Parasitol Res *82*, 230-237.

Kmiecik, T. E., Johnson, P. J., and Shalloway, D. (1988). Regulation by the autophosphorylation site in overexpressed pp60c-src. Mol Cell Biol *8*, 4541-4546.

Kocken, C. H., Hundt, E., Knapp, B., Brazel, D., Enders, B., Narum, D. L., Wubben, J. A., and Thomas, A. W. (1998a). Immunization of Aotus monkeys with recombinant Plasmodium falciparum hybrid proteins does not reproducibly result in protection from malaria infection. Infect Immun *66*, 373-375.

Kocken, C. H., Narum, D. L., Massougbodji, A., Ayivi, B., Dubbeld, M. A., van der Wel, A., Conway, D. J., Sanni, A., and Thomas, A. W. (2000). Molecular characterisation of Plasmodium reichenowi apical membrane antigen-1 (AMA-1), comparison with P. falciparum AMA-1, and antibody-mediated inhibition of red cell invasion. Mol Biochem Parasitol *109*, 147-156.

Kocken, C. H., van der Wel, A. M., Dubbeld, M. A., Narum, D. L., van de Rijke, F. M., van Gemert, G. J., van der Linde, X., Bannister, L. H., Janse, C., Waters, A. P., and Thomas, A. W. (1998b). Precise timing of expression of a Plasmodium falciparum-derived transgene in Plasmodium berghei is a critical determinant of subsequent subcellular localization. J Biol Chem *273*, 15119-15124.

Kocken, C. H., Withers-Martinez, C., Dubbeld, M. A., van der Wel, A., Hackett, F., Valderrama, A., Blackman, M. J., and Thomas, A. W. (2002). High-level expression of the malaria blood-stage vaccine candidate Plasmodium falciparum apical membrane antigen 1 and induction of antibodies that inhibit erythrocyte invasion. Infect Immun *70*, 4471-4476.

Korenromp, E. L., Williams, B. G., Gouws, E., Dye, C., and Snow, R. W. (2003). Measurement of trends in childhood malaria mortality in Africa: an assessment of progress toward targets based on verbal autopsy. Lancet Infect Dis *3*, 349-358.

Krawchuk, M. D., and Wahls, W. P. (1999). High-efficiency gene targeting in Schizosaccharomyces pombe using a modular, PCR-based approach with long tracts of flanking homology. Yeast *15*, 1419-1427.

Lackritz, E. M. (1998). Prevention of HIV transmission by blood transfusion in the developing world: achievements and continuing challenges. Aids *12 Suppl A*, S81-86.

Lal, A. A., Hughes, M. A., Oliveira, D. A., Nelson, C., Bloland, P. B., Oloo, A. J., Hawley, W. E., Hightower, A. W., Nahlen, B. L., and Udhayakumar, V. (1996). Identification of T-cell

determinants in natural immune responses to the Plasmodium falciparum apical membrane antigen (AMA-1) in an adult population exposed to malaria. Infect Immun *64*, 1054-1059.

Lalitha, P. V., Ware, L. A., Barbosa, A., Dutta, S., Moch, J. K., Haynes, J. D., Fileta, B. B., White, C. E., and Lanar, D. E. (2004). Production of the subdomains of the Plasmodium falciparum apical membrane antigen 1 ectodomain and analysis of the immune response. Infect Immun *72*, 4464-4470.

Lambros, C., and Vanderberg, J. P. (1979). Synchronization of Plasmodium falciparum erythrocytic stages in culture. J Parasitol *65*, 418-420.

Lanar, D. E., Tine, J. A., de-Taisne, C., Seguin, M. C., Cox, W. I., Winslow, J. P., Ware, L. A., Kauffman, E. B., Gordon, D., Ballou, W. R., *et al.* (1996). Attenuated vaccinia virus-circumsporozoite protein recombinants confer protection against rodent malaria. Infect Immun *64*, 1666-1671.

Lawrence, M. B., Kansas, G. S., Kunkel, E. J., and Ley, K. (1997). Threshold levels of fluid shear promote leukocyte adhesion through selectins (CD62L,P,E). J Cell Biol *136*, 717-727.

Leech, J. H., Aley, S. B., Miller, L. H., and Howard, R. J. (1984). Plasmodium falciparum malaria: cytoadherence of infected erythrocytes to endothelial cells and associated changes in the erythrocyte membrane. Prog Clin Biol Res *155*, 63-77.

Li, F., Dluzewski, A., Coley, A. M., Thomas, A., Tilley, L., Anders, R. F., and Foley, M. (2002). Phage-displayed peptides bind to the malarial protein apical membrane antigen-1 and inhibit the merozoite invasion of host erythrocytes. J Biol Chem *277*, 50303-50310.

Li, J., and Cox, L. S. (2000). Isolation and characterisation of a cAMP-dependent protein kinase catalytic subunit gene from Plasmodium falciparum. Mol Biochem Parasitol *109*, 157-163.

Li, X., Chen, H., Oo, T. H., Daly, T. M., Bergman, L. W., Liu, S. C., Chishti, A. H., and Oh, S. S. (2004a). A co-ligand complex anchors Plasmodium falciparum merozoites to the erythrocyte invasion receptor band 3. J Biol Chem *279*, 5765-5771.

Li, X., Miao, J., Lei, J. C., Xue, C. F., Wang, X. F., Liu, Z. X., and Li, S. M. (2004b). [Modulation of immune response to Plasmodium falciparum apical membrane antigen 1 DNA vaccine by cytokine plasmids]. Zhongguo Ji Sheng Chong Xue Yu Ji Sheng Chong Bing Za Zhi *22*, 136-138.

Lietha, D., Chirgadze, D. Y., Mulloy, B., Blundell, T. L., and Gherardi, E. (2001). Crystal structures of NK1-heparin complexes reveal the basis for NK1 activity and enable engineering of potent agonists of the MET receptor. Embo J *20*, 5543-5555.

Lisanti, M. P., Scherer, P. E., Vidugiriene, J., Tang, Z., Hermanowske-Vosatka, A., Tu, Y. H., Cook, R. F., Sargiacomo, M. (1994). Characterisation of cavolin-rich membrane domains isolated from an endothelial rich source: implications for human disease. J Cell Biol 126, 111-126

Luke, T. C., and Hoffman, S. L. (2003). Rationale and plans for developing a non-replicating, metabolically active, radiation-attenuated Plasmodium falciparum sporozoite vaccine. J Exp Biol *206*, 3803-3808.

Lyon, J. A., Haynes, J. D., Diggs, C. L., Chulay, J. D., and Pratt-Rossiter, J. M. (1986). Plasmodium falciparum antigens synthesized by schizonts and stabilized at the merozoite surface by antibodies when schizonts mature in the presence of growth inhibitory immune serum. J Immunol *136*, 2252-2258.

Maier, A. G., Duraisingh, M. T., Reeder, J. C., Patel, S. S., Kazura, J. W., Zimmerman, P. A., and Cowman, A. F. (2003). Plasmodium falciparum erythrocyte invasion through glycophorin C and selection for Gerbich negativity in human populations. Nat Med *9*, 87-92.

Malkin, E. M., Diemert, D. J., McArthur, J. H., Perreault, J. R., Miles, A. P., Giersing, B. K., Mullen, G. E., Orcutt, A., Muratova, O., Awkal, M., *et al.* (2005). Phase 1 clinical trial of apical membrane antigen 1: an asexual blood-stage vaccine for Plasmodium falciparum malaria. Infect Immun *73*, 3677-3685.

Margos, G., Bannister, L. H., Dluzewski, A. R., Hopkins, J., Williams, I. T., and Mitchell, G. H. (2004). Correlation of structural development and differential expression of invasion-related molecules in schizonts of Plasmodium falciparum. Parasitology *129*, 273-287.

Marshall, V. M., Peterson, M. G., Lew, A. M., and Kemp, D. J. (1989). Structure of the apical membrane antigen I (AMA-1) of Plasmodium chabaudi. Mol Biochem Parasitol *37*, 281-283.

Marshall, V. M., Zhang, L., Anders, R. F., and Coppel, R. L. (1996). Diversity of the vaccine candidate AMA-1 of Plasmodium falciparum. Mol Biochem Parasitol *77*, 109-113.

Matuschewski, K., Nunes, A. C., Nussenzweig, V., and Menard, R. (2002). Plasmodium sporozoite invasion into insect and mammalian cells is directed by the same dual binding system. Embo J *21*, 1597-1606.

Mayer, D. C., Kaneko, O., Hudson-Taylor, D. E., Reid, M. E., and Miller, L. H. (2001). Characterization of a Plasmodium falciparum erythrocyte-binding protein paralogous to EBA-175. Proc Natl Acad Sci U S A *98*, 5222-5227.

Mayer, D. C., Mu, J. B., Feng, X., Su, X. Z., and Miller, L. H. (2002). Polymorphism in a Plasmodium falciparum erythrocyte-binding ligand changes its receptor specificity. J Exp Med *196*, 1523-1528.

Mayer, D. C., Mu, J. B., Kaneko, O., Duan, J., Su, X. Z., and Miller, L. H. (2004). Polymorphism in the Plasmodium falciparum erythrocyte-binding ligand JESEBL/EBA-181 alters its receptor specificity. Proc Natl Acad Sci U S A *101*, 2518-2523.

McBride, J. S., and Heidrich, H. G. (1987). Fragments of the polymorphic Mr 185,000 glycoprotein from the surface of isolated Plasmodium falciparum merozoites form an antigenic complex. Mol Biochem Parasitol *23*, 71-84.

McCarthy, V. C., and Clyde, D. F. (1977). Plasmodium vivax: correlation of circumsporozoite precipitation (CSP) reaction with sporozoite-induced protective immunity in man. Exp Parasitol *41*, 167-171.

McConkey, S. J., Reece, W. H., Moorthy, V. S., Webster, D., Dunachie, S., Butcher, G., Vuola, J. M., Blanchard, T. J., Gothard, P., Watkins, K., *et al.* (2003). Enhanced T-cell immunogenicity of plasmid DNA vaccines boosted by recombinant modified vaccinia virus Ankara in humans. Nat Med *9*, 729-735.

Medical Parasitology (1999) 8th edition

Meissner, M., Krejany, E., Gilson, P. R., de Koning-Ward, T. F., Soldati, D., and Crabb, B. S. (2005). Tetracycline analogue-regulated transgene expression in Plasmodium falciparum blood stages using Toxoplasma gondii transactivators. Proc Natl Acad Sci U S A *102*, 2980-2985.

Meissner, M., and Soldati, D. (2005). The transcription machinery and the molecular toolbox to control gene expression in Toxoplasma gondii and other protozoan parasites. Microbes Infect.

Michon, P., Stevens, J. R., Kaneko, O., and Adams, J. H. (2002). Evolutionary relationships of conserved cysteine-rich motifs in adhesive molecules of malaria parasites. Mol Biol Evol *19*, 1128-1142.

Miller, L. H., Aikawa, M., Johnson, J. G., and Shiroishi, T. (1979a). Interaction between cytochalasin B-treated malarial parasites and erythrocytes. Attachment and junction formation. J Exp Med *149*, 172-184.

Miller, L. H., and Carter, R. (1976). A review. Innate resistance in malaria. Exp Parasitol *40*, 132-146.

Miller, L. H., Haynes, J. D., McAuliffe, F. M., Shiroishi, T., Durocher, J. R., and McGinniss, M. H. (1977). Evidence for differences in erythrocyte surface receptors for the malarial parasites, Plasmodium falciparum and Plasmodium knowlesi. J Exp Med *146*, 277-281.

Miller, L. H., Mason, S. J., Clyde, D. F., and McGinniss, M. H. (1976). The resistance factor to Plasmodium vivax in blacks. The Duffy-blood-group genotype, FyFy. N Engl J Med *295*, 302-304.

Miller, L. H., Mason, S. J., Dvorak, J. A., McGinniss, M. H., and Rothman, I. K. (1975). Erythrocyte receptors for (Plasmodium knowlesi) malaria: Duffy blood group determinants. Science *189*, 561-563.

Miller, L. H., McAuliffe, F. M., and Johnson, J. G. (1979b). Invasion of erythrocytes by malaria merozoites. Prog Clin Biol Res *30*, 497-502.

Miller, L. H., Roberts, T., Shahabuddin, M., and McCutchan, T. F. (1993). Analysis of sequence diversity in the Plasmodium falciparum merozoite surface protein-1 (MSP-1). Mol Biochem Parasitol *59*, 1-14.

Mital, J., Meissner, M., Soldati, D., and Ward, G. E. (2005). Conditional Expression of Toxoplasma gondii Apical Membrane Antigen-1 (TgAMA1) Demonstrates That TgAMA1 Plays a Critical Role in Host Cell Invasion. Mol Biol Cell.

Mitchell, G. H., Hadley, T. J., McGinniss, M. H., Klotz, F. W., and Miller, L. H. (1986). Invasion of erythrocytes by Plasmodium falciparum malaria parasites: evidence for receptor heterogeneity and two receptors. Blood *67*, 1519-1521.

Mitchell, G. H., Thomas, A. W., Margos, G., Dluzewski, A. R., and Bannister, L. H. (2004). Apical membrane antigen 1, a major malaria vaccine candidate, mediates the close attachment of invasive merozoites to host red blood cells. Infect Immun *72*, 154-158.

Montixi, C., Langlet, C., Bernard, A. M., Thimonier, J., Dubois, C., Wurbel, M. A., Chauvin, J. P., Pierres, M., and He, H. T. (1998). Engagement of T cell receptor triggers its recruitment to low-density detergent-insoluble membrane domains. Embo J *17*, 5334-5348.

Morgan, W. D., Birdsall, B., Frenkiel, T. A., Gradwell, M. G., Burghaus, P. A., Syed, S. E., Uthaipibull, C., Holder, A. A., and Feeney, J. (1999). Solution structure of an EGF module pair from the Plasmodium falciparum merozoite surface protein 1. J Mol Biol *289*, 113-122.

Mueller, M. S., Renard, A., Boato, F., Vogel, D., Naegeli, M., Zurbriggen, R., Robinson, J. A., and Pluschke, G. (2003). Induction of Parasite Growth-Inhibitory Antibodies by a Virosomal Formulation of a Peptidomimetic of Loop I from Domain III of Plasmodium falciparum Apical Membrane Antigen 1. Infect Immun *71*, 4749-4758.

Nair, M., Hinds, M. G., Coley, A. M., Hodder, A. N., Foley, M., Anders, R. F., and Norton, R. S. (2002). Structure of domain III of the blood-stage malaria vaccine candidate, Plasmodium falciparum apical membrane antigen 1 (AMA1). J Mol Biol *322*, 741-753.

Narum, D. L., Fuhrmann, S. R., Luu, T., and Sim, B. K. (2002). A novel Plasmodium falciparum erythrocyte binding protein-2 (EBP2/BAEBL) involved in erythrocyte receptor binding. Mol Biochem Parasitol *119*, 159-168.

Narum, D. L., Haynes, J. D., Fuhrmann, S., Moch, K., Liang, H., Hoffman, S. L., and Sim, B. K. (2000). Antibodies against the Plasmodium falciparum receptor binding domain of EBA-175 block invasion pathways that do not involve sialic acids. Infect Immun *68*, 1964-1966.

Narum, D. L., and Thomas, A. W. (1994a). Differential localization of full-length and processed forms of PF83/AMA-1 an apical membrane antigen of Plasmodium falciparum merozoites. Mol Biochem Parasitol *67*, 59-68.

Ndengele, M. M., Messineo, D. G., Sam-Yellowe, T., and Harwalkar, J. A. (1995). Plasmodium falciparum: effects of membrane modulating agents on direct binding of rhoptry proteins to human erythrocytes. Exp Parasitol *81*, 191-201.

Nikodem, D., and Davidson, E. (2000). Identification of a novel antigenic domain of Plasmodium falciparum merozoite surface protein-1 that specifically binds to human erythrocytes and inhibits parasite invasion, in vitro. Mol Biochem Parasitol *108*, 79-91.

Noe, A. R., and Adams, J. H. (1998). Plasmodium yoelii YM MAEBL protein is coexpressed and colocalizes with rhoptry proteins. Mol Biochem Parasitol *96*, 27-35.

Noe, A. R., Fishkind, D. J., and Adams, J. H. (2000). Spatial and temporal dynamics of the secretory pathway during differentiation of the Plasmodium yoelii schizont. Mol Biochem Parasitol *108*, 169-185.

Nosten, F. (1994). Artemisinin: large community studies. Trans R Soc Trop Med Hyg *88 Suppl 1*, S45-46.

Nussenzweig, R. S., Vanderberg, J., Most, H., and Orton, C. (1967). Protective immunity produced by the injection of x-irradiated sporozoites of plasmodium berghei. Nature *216*, 160-162.

Nwuba, R. I., Sodeinde, O., Anumudu, C. I., Omosun, Y. O., Odaibo, A. B., Holder, A. A., and Nwagwu, M. (2002). The human immune response to Plasmodium falciparum includes both antibodies that inhibit merozoite surface protein 1 secondary processing and blocking antibodies. Infect Immun *70*, 5328-5331.

O'Donnell, R., Preiser, P. R., Williamson, D. H., Moore, P. W., Cowman, A. F., and Crabb, B. S. (2001). An alteration in concatameric structure is associated with efficient segregation of plasmids in transfected Plasmodium falciparum parasites. Nucleic Acids Res *29*, 716-724.

O'Donnell, R. A., Freitas-Junior, L. H., Preiser, P. R., Williamson, D. H., Duraisingh, M., McElwain, T. F., Scherf, A., Cowman, A. F., and Crabb, B. S. (2002). A genetic screen for improved plasmid segregation reveals a role for Rep20 in the interaction of Plasmodium falciparum chromosomes. Embo J *21*, 1231-1239.

O'Donnell, R. A., Saul, A., Cowman, A. F., and Crabb, B. S. (2000). Functional conservation of the malaria vaccine antigen MSP-119across distantly related Plasmodium species. Nat Med *6*, 91-95.

Oka, M., Aikawa, M., Freeman, R. R., Holder, A. A., and Fine, E. (1984). Ultrastructural localization of protective antigens of Plasmodium yoelii merozoites by the use of monoclonal antibodies and ultrathin cryomicrotomy. Am J Trop Med Hyg *33*, 342-346.

Okada, M. and Nakagawa, H. (1989). A protein tyrosine kinase involved in regulation of pp60c-src function. J Biol Chem 264, 20886-20893

Oliveira, D. A., Udhayakumar, V., Bloland, P., Shi, Y. P., Nahlen, B. L., Oloo, A. J., Hawley, W. E., and Lal, A. A. (1996). Genetic conservation of the Plasmodium falciparum apical membrane antigen-1 (AMA-1). Mol Biochem Parasitol *76*, 333-336.

Orlandi, P. A., Klotz, F. W., and Haynes, J. D. (1992). A malaria invasion receptor, the 175-kilodalton erythrocyte binding antigen of Plasmodium falciparum recognizes the terminal Neu5Ac(alpha 2-3)Gal- sequences of glycophorin A. J Cell Biol *116*, 901-909.

Pan, W., Huang, D., Zhang, Q., Qu, L., Zhang, D., Zhang, X., Xue, X., and Qian, F. (2004). Fusion of two malaria vaccine candidate antigens enhances product yield, immunogenicity, and antibody-mediated inhibition of parasite growth in vitro. J Immunol *172*, 6167-6174.

Pasloske, B. L., Baruch, D. I., Ma, C., Taraschi, T. F., Gormley, J. A., and Howard, R. J. (1994). PfEMP3 and HRP1: co-expressed genes localized to chromosome 2 of Plasmodium falciparum. Gene *144*, 131-136.

Peles, E., Nativ, M., Lustig, M., Grumet, M., Schilling, J., Martinez, R., Plowman, G. D., and Schlessinger, J. (1997). Identification of a novel contactin-associated transmembrane receptor with multiple domains implicated in protein-protein interactions. Embo J *16*, 978-988.

Perkins, M. E., and Holt, E. H. (1988). Erythrocyte receptor recognition varies in Plasmodium falciparum isolates. Mol Biochem Parasitol *27*, 23-34.

Perkins, M. E., Wu, T. W., and Le Blancq, S. M. (1998). Cyclosporin analogs inhibit in vitro growth of Cryptosporidium parvum. Antimicrob Agents Chemother *42*, 843-848.

Peterson, M. G., Marshall, V. M., Smythe, J. A., Crewther, P. E., Lew, A., Silva, A., Anders, R. F., and Kemp, D. J. (1989). Integral membrane protein located in the apical complex of Plasmodium falciparum. Mol Cell Biol *9*, 3151-3154.

Peterson, M. G., Nguyen-Dinh, P., Marshall, V. M., Elliott, J. F., Collins, W. E., Anders, R. F., and Kemp, D. J. (1990). Apical membrane antigen of Plasmodium fragile. Mol Biochem Parasitol *39*, 279-283.

Pinder, J., Fowler, R., Bannister, L., Dluzewski, A., and Mitchell, G. H. (2000). Motile systems in malaria merozoites: how is the red blood cell invaded? Parasitol Today *16*, 240-245.

Pinder, J. C., Fowler, R. E., Dluzewski, A. R., Bannister, L. H., Lavin, F. M., Mitchell, G. H., Wilson, R. J., and Gratzer, W. B. (1998). Actomyosin motor in the merozoite of the malaria parasite, Plasmodium falciparum: implications for red cell invasion. J Cell Sci *111*, 1831-1839.

Pizarro, J. C., Vulliez-Le Normand, B., Chesne-Seck, M. L., Collins, C. R., Withers-Martinez, C., Hackett, F., Blackman, M. J., Faber, B. W., Remarque, E. J., Kocken, C. H., *et al.* (2005).

Crystal structure of the malaria vaccine candidate apical membrane antigen 1. Science *308*, 408-411.

Polley, S. D., Chokejindachai, W., and Conway, D. J. (2003). Allele frequency-based analyses robustly map sequence sites under balancing selection in a malaria vaccine candidate antigen. Genetics *165*, 555-561.

Polley, S. D., and Conway, D. J. (2001). Strong diversifying selection on domains of the Plasmodium falciparum apical membrane antigen 1 gene. Genetics *158*, 1505-1512.

Polley, S. D., Mwangi, T., Kocken, C. H., Thomas, A. W., Dutta, S., Lanar, D. E., Remarque, E., Ross, A., Williams, T. N., Mwambingu, G., *et al.* (2004). Human antibodies to recombinant protein constructs of Plasmodium falciparum Apical Membrane Antigen 1 (AMA1) and their associations with protection from malaria. Vaccine *23*, 718-728.

Pombo, D. J., Lawrence, G., Hirunpetcharat, C., Rzepczyk, C., Bryden, M., Cloonan, N., Anderson, K., Mahakunkijcharoen, Y., Martin, L. B., Wilson, D., *et al.* (2002). Immunity to malaria after administration of ultra-low doses of red cells infected with Plasmodium falciparum. Lancet *360*, 610-617.

Prasad, C. D., Prasad Singh, A., Chitnis, C. E., and Sharma, A. (2003). A Plasmodium yoelii yoelii erythrocyte binding protein that uses Duffy binding-like domain for invasion: a rodent model for studying erythrocyte invasion. Mol Biochem Parasitol *128*, 101-105.

Preiser, P., Kaviratne, M., Khan, S., Bannister, L., and Jarra, W. (2000). The apical organelles of malaria merozoites: host cell selection, invasion, host immunity and immune evasion. Microbes Infect *2*, 1461-1477.

Preiser, P. R., Khan, S., Costa, F. T., Jarra, W., Belnoue, E., Ogun, S., Holder, A. A., Voza, T., Landau, I., Snounou, G., and Renia, L. (2002). Stage-specific transcription of distinct repertoires of a multigene family during Plasmodium life cycle. Science *295*, 342-345.

Price, R. N., Nosten, F., Luxemburger, C., ter-Kuile, F. O., Paiphun, L., Chongsuphajaisiddhi, T., and White, N. J. (1996). Effects of artemisinin derivatives on malaria transmissibility. Lancet *347*, 1654-1658.

Ranjan, A., and Chitnis, C. E. (1999). Mapping regions containing binding residues within functional domains of Plasmodium vivax and Plasmodium knowlesi erythrocyte-binding proteins. Proc Natl Acad Sci U S A *96*, 14067-14072.

Reed, M. B., Caruana, S. R., Batchelor, A. H., Thompson, J. K., Crabb, B. S., and Cowman, A. F. (2000). Targeted disruption of an erythrocyte binding antigen in Plasmodium falciparum is associated with a switch toward a sialic acid-independent pathway of invasion. Proc Natl Acad Sci U S A *97*, 7509-7514.

Reth, M. (1991). Signal transduction in B cells. Curr Opin Immunol *3*, 340-344.

Rivadeneira, E. M., Wasserman, M., and Espinal, C. T. (1983). Separation and concentration of schizonts of Plasmodium falciparum by Percoll gradients. J Protozool *30*, 367-370.

Robinson, P. J. (1991). Dephosphin, a 96,000 Da substrate of protein kinase C in synaptosomal cytosol, is phosphorylated in intact synaptosomes. FEBS Lett *282*, 388-392.

Rodrigues, M. H., Rodrigues, K. M., Oliveira, T. R., Comodo, A. N., Rodrigues, M. M., Kocken, C. H., Thomas, A. W., and Soares, I. S. (2005). Antibody response of naturally infected individuals to recombinant Plasmodium vivax apical membrane antigen-1. Int J Parasitol *35*, 185-192.

Rodriguez, L. E., Urquiza, M., Ocampo, M., Curtidor, H., Suarez, J., Garcia, J., Vera, R., Puentes, A., Lopez, R., Pinto, M., *et al.* (2002). Plasmodium vivax MSP-1 peptides have high specific binding activity to human reticulocytes. Vaccine *20*, 1331-1339.

Rogers, W. O., Baird, J. K., Kumar, A., Tine, J. A., Weiss, W., Aguiar, J. C., Gowda, K., Gwadz, R., Kumar, S., Gold, M., and Hoffman, S. L. (2001). Multistage multiantigen heterologous prime boost vaccine for Plasmodium knowlesi malaria provides partial protection in rhesus macaques. Infect Immun *69*, 5565-5572.

Rogers, W. O., Gowda, K., and Hoffman, S. L. (1999). Construction and immunogenicity of DNA vaccine plasmids encoding four Plasmodium vivax candidate vaccine antigens [In Process Citation]. Vaccine *17*, 3136-3144.

Roper, C., Pearce, R., Bredenkamp, B., Gumede, J., Drakeley, C., Mosha, F., Chandramohan, D., and Sharp, B. (2003). Antifolate antimalarial resistance in southeast Africa: a population-based analysis. Lancet *361*, 1174-1181.

Roskoski Jr. R., (2005). Src kinase regulation by phosphorylation and dephosphorylation. Biochem Biophys Res Comm 331, 1-14.

Rowe, J. A., Moulds, J. M., Newbold, C. I., and Miller, L. H. (1997). P. falciparum rosetting mediated by a parasite-variant erythrocyte membrane protein and complement-receptor 1. Nature *388*, 292-295.

Sajid, M., Withers-Martinez, C., and Blackman, M. J. (2000). Maturation and specificity of Plasmodium falciparum subtilisin-like protease-1, a malaria merozoite subtilisin-like serine protease. J Biol Chem *275*, 631-641.

Salazar, L. M., Alba, M. P., Torres, M. H., Pinto, M., Cortes, X., Torres, L., and Patarroyo, M. E. (2002). Protection against experimental malaria associated with AMA-1 peptide analogue structures. FEBS Lett *527*, 95-100.

Salmon, B. L., Oksman, A., and Goldberg, D. E. (2001). Malaria parasite exit from the host erythrocyte: a two-step process requiring extraerythrocytic proteolysis. Proc Natl Acad Sci U S A *98*, 271-276.

Salvatore, D., Hodder, A. N., Zeng, W., Brown, L. E., Anders, R. F., and Jackson, D. C. (2002). Identification of antigenically active tryptic fragments of apical membrane antigen-1 (AMA1) of Plasmodium chabaudi malaria: strategies for assembly of immunologically active peptides. Vaccine *20*, 3477-3484.

Sambrook, J., Fritsch, E. F., Maniatis, T. (1989). Molecular cloning: a laboratory manual. Cold Spring Harbour Laboratory Press, Cold Spring Harbour, NY.

Sam-Yellowe, T. Y., Florens, L., Wang, T., Raine, J. D., Carucci, D. J., Sinden, R., and Yates, J. R., 3rd (2004). Proteome analysis of rhoptry-enriched fractions isolated from Plasmodium merozoites. J Proteome Res *3*, 995-1001.

Sam-Yellowe, T. Y., and Perkins, M. E. (1991). Interaction of the 140/130/110 kDa rhoptry protein complex of Plasmodium falciparum with the erythrocyte membrane and liposomes. Exp Parasitol *73*, 161-171.

Sam-Yellowe, T. Y., Shio, H., and Perkins, M. E. (1988). Secretion of Plasmodium falciparum rhoptry protein into the plasma membrane of host erythrocytes. J Cell Biol *106*, 1507-1513.

Saul, A., Lawrence, G., Allworth, A., Elliott, S., Anderson, K., Rzepczyk, C., Martin, L. B., Taylor, D., Eisen, D. P., Irving, D. O., *et al.* (2005). A human phase 1 vaccine clinical trial of the Plasmodium falciparum malaria vaccine candidate apical membrane antigen 1 in Montanide ISA720 adjuvant. Vaccine *23*, 3076-3083.

Schwager, S. L., Chubb, A. J., Woodman, Z. L., Yan, L., Mentele, R., Ehlers, M. R., and Sturrock, E. D. (2001). Cleavage of disulfide-bridged stalk domains during shedding of angiotensin-converting enzyme occurs at multiple juxtamembrane sites. Biochemistry *40*, 15624-15630.

Shahabuddin, M., Fields, I., Bulet, P., Hoffmann, J. A., and Miller, L. H. (1998). Plasmodium gallinaceum: differential killing of some mosquito stages of the parasite by insect defensin. Exp Parasitol *89*, 103-112.

Sharma, A. (2000). Protein tyrosine kinase activity in human malaria parasite Plasmodium falciparum. Indian J Exp Biol *38*, 1222-1226.

Shiu, S., Li, W. (2004). Origins, lineage-specific expansions, and multiple losses of tyrosine kinases in eukaryotes. Mol Biol Evol 21, 828-840.

Sim, B. K., Carter, J. M., Deal, C. D., Holland, C., Haynes, J. D., and Gross, M. (1994a). Plasmodium falciparum: further characterization of a functionally active region of the merozoite invasion ligand EBA-175. Exp Parasitol *78*, 259-268.

Sim, B. K., Chitnis, C. E., Wasniowska, K., Hadley, T. J., and Miller, L. H. (1994b). Receptor and ligand domains for invasion of erythrocytes by Plasmodium falciparum. Science *264*, 1941-1944.

Sim, B. K., Orlandi, P. A., Haynes, J. D., Klotz, F. W., Carter, J. M., Camus, D., Zegans, M. E., and Chulay, J. D. (1990). Primary structure of the 175K Plasmodium falciparum erythrocyte binding antigen and identification of a peptide which elicits antibodies that inhibit malaria merozoite invasion. J Cell Biol *111*, 1877-1884.

Simons, K., and Ikonen, E. (1997). Functional rafts in cell membranes. Nature *387*, 569-572.
Singh, K., Wester, W. C., and Trenholme, G. M. (2003). Problems in the therapy for imported malaria in the United States. Arch Intern Med *163*, 2027-2030.

Sinnis, P., and Sim, B. K. (1997). Cell invasion by the vertebrate stages of Plasmodium. Trends Microbiol *5*, 52-58.

Smith, J. D., Chitnis, C. E., Craig, A. G., Roberts, D. J., Hudson-Taylor, D. E., Peterson, D. S., Pinches, R., Newbold, C. I., and Miller, L. H. (1995). Switches in expression of Plasmodium falciparum var genes correlate with changes in antigenic and cytoadherent phenotypes of infected erythrocytes [see comments]. Cell *82*, 101-110.

Smith, J. E. (1995). A ubiquitous intracellular parasite: the cellular biology of Toxoplasma gondii. Int J Parasitol *25*, 1301-1309.

Snow, R. W., Korenromp, E. L., and Gouws, E. (2004). Pediatric mortality in Africa: plasmodium falciparum malaria as a cause or risk? Am J Trop Med Hyg *71*, 16-24.

Soldati, D., Foth, B. J., and Cowman, A. F. (2004). Molecular and functional aspects of parasite invasion. Trends Parasitol *20*, 567-574.

Spencer Valero, L. M., Ogun, S. A., Fleck, S. L., Ling, I. T., Scott-Finnigan, T. J., Blackman, M. J., and Holder, A. A. (1998). Passive immunization with antibodies against three distinct epitopes on Plasmodium yoelii merozoite surface protein 1 suppresses parasitemia. Infect Immun *66*, 3925-3930.

Stoute, J. A., Slaoui, M., Heppner, D. G., Momin, P., Kester, K. E., Desmons, P., Wellde, B. T., Garcon, N., Krzych, U., and Marchand, M. (1997). A preliminary evaluation of a recombinant circumsporozoite protein vaccine against Plasmodium falciparum malaria. RTS,S Malaria Vaccine Evaluation Group [see comments]. N Engl J Med *336*, 86-91.

Stowers, A. W., Kennedy, M. C., Keegan, B. P., Saul, A., Long, C. A., and Miller, L. H. (2002). Vaccination of monkeys with recombinant Plasmodium falciparum apical membrane antigen 1 confers protection against blood-stage malaria. Infect Immun *70*, 6961-6967.

Struik, S. S., and Riley, E. M. (2004). Does malaria suffer from lack of memory? Immunol Rev *201*, 268-290.

Takechi, M., Matsuo, M., Ziba, C., MacHeso, A., Butao, D., Zungu, I. L., Chakanika, I., and Bustos, M. D. (2001). Therapeutic efficacy of sulphadoxine/pyrimethamine and susceptibility in vitro of P. falciparum isolates to sulphadoxine-pyremethamine and other antimalarial drugs in Malawian children. Trop Med Int Health *6*, 429-434.

Taniguchi, T. (1995). Cytokine signaling through nonreceptor protein tyrosine kinases. Science *268*, 251-255.

Thomas, A. W., Bannister, L. H., and Waters, A. P. (1990). Sixty-six kilodalton-related antigens of Plasmodium knowlesi are merozoite surface antigens associated with the apical prominence. Parasite Immunol *12*, 105-113.

Thomas, A. W., Deans, J. A., Mitchell, G. H., Alderson, T., and Cohen, S. (1984). The Fab fragments of monoclonal IgG to a merozoite surface antigen inhibit Plasmodium knowlesi invasion of erythrocytes. Mol Biochem Parasitol *13*, 187-199.

Thomas, A. W., Trape, J. F., Rogier, C., Goncalves, A., Rosario, V. E., and Narum, D. L. (1994). High prevalence of natural antibodies against Plasmodium falciparum 83-kilodalton apical membrane antigen (PF83/AMA-1) as detected by capture-enzyme-linked immunosorbent assay using full-length baculovirus recombinant PF83/AMA-1. Am J Trop Med Hyg *51*, 730-740.

Thompson, J., Cooke, R. E., Moore, S., Anderson, L. F., Janse, C. J., and Waters, A. P. (2004). PTRAMP; a conserved Plasmodium thrombospondin-related apical merozoite protein. Mol Biochem Parasitol *134*, 225-232.

Thompson, J., Janse, C. J., and Waters, A. P. (2001). Comparative genomics in Plasmodium: a tool for the identification of genes and functional analysis. Mol Biochem Parasitol *118*, 147-154.

Tine, J. A., Lanar, D. E., Smith, D. M., Wellde, B. T., Schultheiss, P., Ware, L. A., Kauffman, E. B., Wirtz, R. A., De Taisne, C., Hui, G. S., *et al.* (1996). NYVAC-Pf7: a poxvirus-vectored, multiantigen, multistage vaccine candidate for Plasmodium falciparum malaria. Infect Immun *64*, 3833-3844.

Tolia, N. H., Enemark, E. J., Sim, B. K., and Joshua-Tor, L. (2005). Structural basis for the EBA-175 erythrocyte invasion pathway of the malaria parasite Plasmodium falciparum. Cell *122*, 183-193.

Tordai, H., Banyai, L., and Patthy, L. (1999). The PAN module: the N-terminal domains of plasminogen and hepatocyte growth factor are homologous with the apple domains of the prekallikrein family and with a novel domain found in numerous nematode proteins. FEBS Lett *461*, 63-67.

Torii, M., Adams, J. H., Miller, L. H., and Aikawa, M. (1989). Release of merozoite dense granules during erythrocyte invasion by Plasmodium knowlesi. Infect Immun *57*, 3230-3233.
Trager, W., and Jensen, J. B. (1976). Human malaria parasites in continuous culture. Science *193*, 673-675.

Triglia, T., Healer, J., Caruana, S. R., Hodder, A. N., Anders, R. F., Crabb, B. S., and Cowman, A. F. (2000). Apical membrane antigen 1 plays a central role in erythrocyte invasion by Plasmodium species. Mol Microbiol *38*, 706-718.

Tsuboi, T., Kaneko, O., Eitoku, C., Suwanabun, N., Sattabongkot, J., Vinetz, J. M., and Torii, M. (2003). Gene structure and ookinete expression of the chitinase genes of Plasmodium vivax and Plasmodium yoelii. Mol Biochem Parasitol *130*, 51-54.

Tyers, M., Tokiwa, G., Nash, R., and Futcher, B. (1992). The Cln3-Cdc28 kinase complex of S. cerevisiae is regulated by proteolysis and phosphorylation. Embo J *11*, 1773-1784.

Urquiza, M., Suarez, J. E., Cardenas, C., Lopez, R., Puentes, A., Chavez, F., Calvo, J. C., and Patarroyo, M. E. (2000). Plasmodium falciparum AMA-1 erythrocyte binding peptides implicate AMA-1 as erythrocyte binding protein. Vaccine *19*, 508-513.

van Dijk, M. R., Waters, A. P., and Janse, C. J. (1995). Stable transfection of malaria parasite blood stages. Science *268*, 1358-1362.

Verra, F., and Hughes, A. L. (2000). Evidence for ancient balanced polymorphism at the Apical Membrane Antigen-1 (AMA-1) locus of Plasmodium falciparum. Mol Biochem Parasitol *105*, 149-153.

Ward, G. E., Fujioka, H., Aikawa, M., and Miller, L. H. (1994). Staurosporine inhibits invasion of erythrocytes by malarial merozoites. Exp Parasitol *79*, 480-487.

Ward, P., Equinet, L., Packer, J., and Doerig, C. (2004). Protein kinases of the human malaria parasite Plasmodium falciparum: the kinome of a divergent eukaryote. BMC Genomics *5*, 79.

Wasserman, M., Alarcon, C., and Mendoza, P. M. (1982). Effects of Ca++ depletion on the asexual cell cycle of Plasmodium falciparum. Am J Trop Med Hyg *31*, 711-717.

Waterkeyn, J. G., Crabb, B. S., and Cowman, A. F. (1999). Transfection of the human malaria parasite Plasmodium falciparum. Int J Parasitol *29*, 945-955.

Waters, A. P., Thomas, A. W., Deans, J. A., Mitchell, G. H., Hudson, D. E., Miller, L. H., McCutchan, T. F., and Cohen, S. (1990). A merozoite receptor protein from Plasmodium knowlesi is highly conserved and distributed throughout Plasmodium. J Biol Chem *265*, 17974-17979.

Waters, A. P., Thomas, A. W., Mitchell, G. H., and McCutchan, T. F. (1991). Intra-generic conservation and limited inter-strain variation in a protective minor surface antigen of Plasmodium knowlesi merozoites. Mol Biochem Parasitol *44*, 141-144.

Waters, A. P., Thomas, A. W., van Dijk, M. R., and Janse, C. J. (1997). Transfection of malaria parasites. Methods *13*, 134-147.

Weiss, W. R., Sedegah, M., Berzofsky, J. A., and Hoffman, S. L. (1993). The role of CD4+ T cells in immunity to malaria sporozoites. J Immunol *151*, 2690-2698.

Wertheimer, S. P., and Barnwell, J. W. (1989). Plasmodium vivax interaction with the human Duffy blood group glycoprotein: identification of a parasite receptor-like protein. Exp Parasitol *69*, 340-350.

White, N. (1999). Antimalarial drug resistance and mortality in falciparum malaria [editorial]. Trop Med Int Health *4*, 469-470.

White, N. J. (2004). Antimalarial drug resistance. J Clin Invest *113*, 1084-1092.

Wickham, M. E., Culvenor, J. G., and Cowman, A. F. (2003). Selective inhibition of a two-step egress of malaria parasites from the host erythrocyte. J Biol Chem *278*, 37658-37663.

Williamson, K. C., Fujioka, H., Aikawa, M., and Kaslow, D. C. (1996). Stage-specific processing of Pfs230, a Plasmodium falciparum transmission- blocking vaccine candidate. Mol Biochem Parasitol *78*, 161-169.

Withers-Martinez, C., Carpenter, E. P., Hackett, F., Ely, B., Sajid, M., Grainger, M., and Blackman, M. J. (1999). PCR-based gene synthesis as an efficient approach for expression of the A+T-rich malaria genome. Protein Eng *12*, 1113-1120.

Wu, Y., Kirkman, L. A., and Wellems, T. E. (1996). Transformation of Plasmodium falciparum malaria parasites by homologous integration of plasmids that confer resistance to pyrimethamine. Proc Natl Acad Sci U S A *93*, 1130-1134.

Wu, Y., Sifri, C. D., Lei, H. H., Su, X. Z., and Wellems, T. E. (1995). Transfection of Plasmodium falciparum within human red blood cells. Proc Natl Acad Sci U S A *92*, 973-977.

Xavier, R., and Seed, B. (1999). Membrane compartmentation and the response to antigen. Curr Opin Immunol 11, 265-269.

Xu, H., Hodder, A. N., Yan, H., Crewther, P. E., Anders, R. F., and Good, M. F. (2000). CD4+ T cells acting independently of antibody contribute to protective immunity to Plasmodium chabaudi infection after apical membrane antigen 1 immunization. J Immunol *165*, 389-396.

Yeung, S., Pongtavornpinyo, W., Hastings, I. M., Mills, A. J., and White, N. J. (2004). Antimalarial drug resistance, artemisinin-based combination therapy, and the contribution of modeling to elucidating policy choices. Am J Trop Med Hyg *71*, 179-186.

Zhao, Y., Kappes, B., and Franklin, R. M. (1993). Gene structure and expression of an unusual protein kinase from Plasmodium falciparum homologous at its carboxyl terminus with the EF hand calcium-binding proteins. J Biol Chem *268*, 4347-4354.